

October 2017

Identifying New Treatment Options and Risk Factors for Type 2 Diabetes: The Potential Role of Thymoquinone and Persistent Organic Pollutants

Shpetim Karandrea

University of South Florida, skarandr@health.usf.edu

Follow this and additional works at: <http://scholarcommons.usf.edu/etd>

 Part of the [Endocrinology Commons](#), and the [Pharmacology Commons](#)

Scholar Commons Citation

Karandrea, Shpetim, "Identifying New Treatment Options and Risk Factors for Type 2 Diabetes: The Potential Role of Thymoquinone and Persistent Organic Pollutants" (2017). *Graduate Theses and Dissertations*.
<http://scholarcommons.usf.edu/etd/7042>

This Dissertation is brought to you for free and open access by the Graduate School at Scholar Commons. It has been accepted for inclusion in Graduate Theses and Dissertations by an authorized administrator of Scholar Commons. For more information, please contact scholarcommons@usf.edu.

Identifying New Treatment Options and Risk Factors for Type 2 Diabetes: The Potential Role of
Thymoquinone and Persistent Organic Pollutants

by

Shpetim Karandrea

A dissertation submitted in partial fulfillment
of the requirements for the degree of
Doctor of Philosophy in Medical Sciences
with a Concentration in Molecular Pharmacology and Physiology
Department of Molecular Pharmacology and Physiology
College of Medicine
University of South Florida

Major Professor: Javier Cuevas, Ph.D.
Jerome Breslin, Ph.D.
Vrushank Dave, Ph.D.
Thomas Taylor-Clark, Ph.D.

Date of Approval:
October 16, 2017

Keywords: BDE-47, BDE-85, GSIS, Type 2 Diabetes, Thymoquinone

Copyright © 2017, Shpetim Karandrea

DEDICATION

This dissertation is dedicated to the memory of my late parents, Josif and Milika Karandrea. Thank you for sacrificing everything you had to fulfill my dreams and make me happy, for your unconditional love and support throughout the years. You created the perfect environment for me to grow and learn, always believed in me, and let me pursue my dreams, and you are the reason I am here today. I know that I can face any challenge because you will always be with me.

This dissertation is also dedicated to my wife, Dr. Alexis Karandrea, who has been my rock, my sounding board, and my light during this whole process. You are the most amazing person I know, and I feel extremely lucky to have you. Thank you for your love, for believing in me, for encouraging me at the most difficult moments, and for celebrating even the smallest of accomplishments. And thank you also for your amazing meal preps, without which I wouldn't have been able to complete this dissertation.

A special dedication goes to my mother and father-in-law, Drs. Robert and Roberta Killeen and brother-in-law Jonathan Killeen. I feel your love every time I come to visit, and you never hesitate to help me with anything I need. Thank you for welcoming me into your family and treating me like a son. Thank you to Jon for being a great friend and for your amazing sense of humor, which comes out when the least expected, and makes our family gatherings extra special.

ACKNOWLEDGEMENTS

First, I would like to thank my mentor Dr. Emma Heart for providing immeasurable support towards my scientific, professional, and personal goals. Your dedication, drive, and mentorship created the perfect environment for me to succeed and grow as a scientist and as a person and I will be forever thankful to you. I would like to thank my co-mentor Dr. Javier Cuevas for his help in guiding me through my dissertation defense and input on my presentation. I would like to thank the lab members Dr. Xiaomei Liang and Dr. Huquan Yin for their continued support and input on my projects and for working as part of the team to overcome all challenges; I wouldn't have been here today without you.

I would like to thank my committee members, Dr. Jerome Breslin, Dr. Javier Cuevas, Dr. Vrushank Dave, and Dr. Thomas Taylor-Clark for their input, valuable insight, and guiding me in the right direction throughout this process. I would like to thank my external chair, Dr. Ernesto Bernal-Mizrachi for his time and attention. Special thanks go to Dr. Eric Bennett, who was one of the main reasons I got accepted into the Ph.D. program and believed in my scientific abilities from the beginning. I would like to thank my friends Mario Buda, Dr. Stephanie Davis, Dr. Perna Malaney, Dr. Jaymin Kathiriya, Isaac Raplee, Natascha Alves and my cousin Anastas Sinjari; thank you for always being there for me and giving your unconditional support.

TABLE OF CONTENTS

List of Tables.....	iv
List of Figures.....	v
List of Abbreviations.....	vii
Abstract.....	ix
Chapter One: Introduction	1
1.1 Defining Persistent Organic Pollutants.....	1
1.2 Polybrominated Diphenyl Ethers BDE-47 and BDE-85	2
1.3 Perfluorinated Compounds PFOS and PFNA.....	4
1.4 The Potential Role of POPs in the Development of Metabolic Diseases	5
1.5 An Introduction to Thyroid Hormone and Implications in Type 2 Diabetes	7
1.6 The Role of the PI3K-Akt Pathway in Pancreatic β -cell Function.....	8
1.7 INS-1 832/13 Cell Line as a Pancreatic β -cell Model	9
1.8 Introduction to Thymoquinone and its Anti-Diabetic Potential	11
1.9 Objective, Hypotheses, and Aims	14
1.10 Significance and Impact	16
1.11 References.....	16
1.12 Tables and Figures.....	24
Chapter Two: Effects of Selected POPs on Insulin Secretion	25
2.1 The Importance of Identifying Potential Agents that Contribute to β -cell Dysfunction	25
2.2 Hypothesis	26
2.3 Methods	26
2.3.1 INS-1 832/13 Cell Culture and Maintenance	26
2.3.2 Glucose-stimulated Insulin Secretion (GSIS).....	26
2.3.3 Cell Viability	27
2.3.4 Chemicals	27
2.3.5 Statistical Analysis	28
2.4 Results	28
2.4.1 Concentration-response Curves for Cell Viability After 48-Hour Exposure to PFOS, PFNA, BDE-47, or BDE-85.....	28
2.4.2 PFOS Does Not Affect GSIS During Chronic Pre-Treatment and Acute Exposure	29
2.4.3 PFNA Does Not Affect GSIS During Chronic Pre-Treatment and Acute Exposure	29
2.4.4 BDE-47 Does Not Affect GSIS During Chronic Pre-Treatment; Increases Acute GSIS	29
2.4.5 BDE-85 Does Not Affect GSIS During Chronic Pre-Treatment; Increases Acute GSIS	30
2.5 Discussion.....	30

2.6 References.....	32
2.7 Tables and Figures.....	34
Chapter Three: Potential Mechanisms for BDE-47 and BDE-85-Mediated Increase in GSIS	41
3.1 Polybrominated Diphenyl Ethers and Thyroid Hormone Receptor	41
3.2 Polybrominated Diphenyl Ethers and Akt Activation.....	43
3.3 Hypothesis	44
3.4 Methods	44
3.4.1 INS-1 832/13 Cell Culture and Maintenance	44
3.4.2 Chemicals	45
3.4.3 Glucose-stimulated Insulin Secretion.....	45
3.4.4 Western Blot Analysis.....	46
3.4.5 Reverse Transcription and Quantitative Real-Time RT-PCR (qRT-PCR).....	46
3.4.6 Statistical Analysis	47
3.5 Results	47
3.5.1 BDE-47 and BDE-85 Do Not Affect TR Expression.....	47
3.5.2 Thyroid Hormone Increases GSIS	48
3.5.3 Combined Effects of Thyroid Hormone and BDE-47/85 on GSIS	49
3.5.4 Thyroid Receptor Antagonist Decreases T3-Mediated GSIS Potentiation	49
3.5.5 BDE-47 and BDE-85 Effect on GSIS is Mediated by TR	50
3.5.6 BDE-47 and BDE-85 Activate Akt in INS-1 832/13 Cells	50
3.5.7 Effect of BDE-47 and BDE-85 on GSIS is Dependent on Akt Activation	51
3.6 Discussion.....	51
3.7 References.....	53
3.8 Tables and Figures	58
Chapter Four: Anti-Diabetic Effects of Thymoquinone in the Diet-Induced Obesity (DIO) Mouse Model of Type 2 Diabetes	64
4.1 Prevalence and Overall Impact of Type 2 Diabetes	64
4.2 Current Treatments for Type 2 Diabetes.....	65
4.3 Diet-Induced Obesity (DIO) Mouse Model of Type 2 Diabetes	67
4.4 Hypothesis	68
4.5 Methods	69
4.5.1 Mouse Colony Maintenance and Ethical Statement.....	69
4.5.2 HepG2 Cell Culture and Treatment.....	69
4.5.3 Chemicals	70
4.5.4 Oral Glucose Tolerance Tests (OGTT) and Insulin Tolerance Tests (ITT)	70
4.5.5 Serum Collection	70
4.5.6 Tissue Collection and Storage	71
4.5.7 Serum Cholesterol Content Measurement.....	71
4.5.8 Serum Measurements of Insulin, Resistin, and MCP-1	71
4.5.9 Western Blot Analysis.....	71
4.5.10 Reverse Transcription and Quantitative Real-time RT-PCR (qRT-PCR).....	72

4.4.11 Metabolomics Analysis (GC/MS).....	72
4.5.12 Tissue Triglyceride Content Measurements	73
4.4.13 Tissue NADH/NAD ⁺ Measurement.....	73
4.5.14 Statistical Analysis	73
4.6 Results	73
4.6.1 C57/BL6J Mice Became Diabetic and Obese Following High Fat Diet Administration	73
4.6.2 Thymoquinone Ameliorates Weight Gain and Lowers Fasting Blood Glucose in DIO mice	74
4.6.3 Thymoquinone Ameliorates Hyperinsulinemia, Improves Glucose Tolerance and Insulin Sensitivity in DIO mice	74
4.6.4 Thymoquinone Lowers Serum Levels of Resistin and MCP-1 in DIO Mice	75
4.6.5 Thymoquinone Normalizes Lipid Profile in DIO Mice	75
4.6.6 Thymoquinone Activates SIRT-1 and AMPK α in Insulin-sensitive Tissues	76
4.6.7 Thymoquinone Lowers NADH/NAD ⁺ Ratio in Liver and Soleus Muscle	76
4.6.8 Thymoquinone Improves Insulin Resistance via SIRT-1 Activation in HepG2 Cells.....	77
4.6.9 Thymoquinone Does Not Induce Oxidative Stress	78
4.6.10 Thymoquinone Lowers Levels of TCA Cycle Anaplerotic Intermediates in INS-1 832/13 Cells but Not in the DIO Mice	78
4.7 Discussion.....	79
4.8 References.....	84
4.9 Tables and Figures	89
Chapter Five: Conclusions.....	103
5.1 Adverse Effects of Selected POPs on Pancreatic β -cell Function	103
5.2 Effects of Thymoquinone in the DIO Mouse Model of Type 2 Diabetes.....	104
5.3 Future Directions.....	105
5.4 References.....	107
5.5 Tables and Figures	109
Appendix A: IACUC Approval for Animal Research.....	110
Appendix B: Copyright Permissions	112
Appendix C: Published Manuscripts.....	115

LIST OF TABLES

Table 4.1: Effect of TQ on serum glycerol and fatty acids	93
Table 4.2: TQ decreased the levels of anaplerotic TCA cycle metabolites in INS-1 832/13 cells exposed to high glucose	101
Table 4.3: Effect of TQ on TCA cycle intermediates in liver	101
Table 4.4: Effect of TQ on TCA cycle intermediates in soleus muscle	102

LIST OF FIGURES

Figure 1.1: Illustration of chemical structures.....	24
Figure 2.1: Experimental design workflow to test the effects of selected POPs on GSIS	34
Figure 2.2: PFOS, PFNA, BDE-47, and BDE-85 affect INS-1 832/13 cell viability	35
Figure 2.3: Chronic pre-treatment and acute exposure to PFOS does not affect GSIS	36
Figure 2.4: Chronic pre-treatment and acute exposure to PFNA does not affect GSIS	37
Figure 2.5: BDE-47 potentiates GSIS during acute exposure but not during chronic pre-treatment	38
Figure 2.6: BDE-85 potentiates GSIS during acute exposure but not during chronic pre-treatment	39
Figure 2.7: High concentrations of BDE-47 and BDE-85 potentiate acute GSIS	40
Figure 3.1: BDE-47 and BDE-85 do not affect thyroid receptor α expression.....	58
Figure 3.2: Thyroid hormone increases GSIS during chronic pre-treatment and acute exposure	59
Figure 3.3: Co-treatment with BDE-47 or BDE-85 and thyroid hormone potentiates GSIS compared to single treatment.....	60
Figure 3.4: Thyroid receptor antagonist 1-850 decreases GSIS potentiation by T3	61
Figure 3.5: Thyroid receptor antagonist 1-850 decreases GSIS potentiation by BDE-47 and BDE-85	61
Figure 3.6: BDE-47 and BDE-85 activate Akt during an acute exposure	62
Figure 3.7: Wortmannin inhibits BDE-47 and BDE-85-mediated Akt activation	62
Figure 3.8: Effect of PI3K inhibitor wortmannin on BDE-47 and BDE-85-mediated GSIS potentiation	63
Figure 4.1: TQ ameliorates weight gain, lowers fasting blood glucose and insulin in DIO mice	89

Figure 4.2: TQ improves glucose tolerance and insulin sensitivity	90
Figure 4.3: Effects of TQ on serum resistin and MCP-1	91
Figure 4.4: Effects of TQ on triglyceride content in liver and muscle	92
Figure 4.5: Effects of TQ on serum cholesterol.....	94
Figure 4.6: TQ decreases NADH/NAD ⁺ ratio in liver and soleus muscle	95
Figure 4.7: TQ activates SIRT-1 in liver and soleus muscle	96
Figure 4.8: TQ activates Akt and AMPK α in liver.....	97
Figure 4.9: TQ improves insulin sensitivity in HepG2 cells via a SIRT-1 dependent mechanism	98
Figure 4.10: Effects of TQ on SIRT-1 and AMPK α activation in HepG2 cells.....	99
Figure 4.11: Effects of TQ on NQO1 expression	100
Figure 5.1: Proposed mechanism for potentiation of GSIS by BDE-47 and BDE-85.....	109
Figure 5.2: Proposed mechanism for anti-diabetic actions of TQ.....	109

LIST OF ABBREVIATIONS

AIC	AICAR
AMPK α	AMP-Activated Protein Kinase alpha
BDE-47	2,2',4,4'-tetra-bromodipheyl ether
BDE-85.....	2,2',3,4,4'-penta-bromodiphenyl ether
C.....	Compound C
DIO	Diet-Induced Obesity
G.....	Glucose
GAPDH	Glyceraldehyde 3-phosphpate dehydrogenase
GSIS.....	Glucose-Stimulated Insulin Secretion
GTT	Glucose Tolerance Test
HDL	High Density Lipoprotein
HFD.....	High Fat Diet
ITT	Insulin Tolerance Test
KRB.....	Krebs Ringer Buffer
LDL.....	Low Density Lipoprotein
LFD.....	Low Fat Diet
MCP-1	Monocyte Chemoattractant Protein-1
NAD ⁺	Nicotinamide Adenine Dinucleotide (Oxidized)
NADH	Nicotinamide Adenine Dinucleotide (Reduced)
NIC	Nicotinamide
NQO1	NAD(P)H Dehydrogenase Quinone 1
OGTT	Oral Glucose Tolerance Test

PBDE.....	Poly Brominated Diphenyl Ether
PFC	Per-Fluorinated Compound
PFNA.....	Per-Fluoro-Nonanoic Acid
PFOS.....	Per-Fluoro-Octane-Sulfonate
PI3K.....	Phosphoinositide 3-Kinase
PKA	Protein Kinase A
PKC.....	Protein Kinase C
POP.....	Persistent Organic Pollutant
PPAR γ	Peroxisome Proliferator-Activated Receptor Gamma
R.....	Resveratrol
SIRT-1	Sirtuin 1
SOD.....	Superoxide Dismutase
STZ.....	Streptozotocin
T2D.....	Type 2 Diabetes
T2DM.....	Type 2 Diabetes Mellitus
T3	Triiodothyronine
T4	Thyroxine
TQ	Thymoquinone
TR.....	Thyroid Receptor
TR α	Thyroid Receptor alpha
TR β	Thyroid Receptor beta
TZD	Thiazolidinedione
VLDL	Very Low-Density Lipoprotein
W.....	Wortmannin

ABSTRACT

Type 2 Diabetes Mellitus (T2DM) is a metabolic disorder characterized by chronic hyperglycemia, which develops as a consequence of peripheral insulin resistance and defective insulin secretion from pancreatic β -cells. A high calorie diet coupled with physical inactivity are known risk factors for the development of T2DM; however, these alone fail to account for the rapid rise of the disease. Recent attention has turned to the role of environmental pollutants in the development of metabolic diseases. PBDEs (polybrominated diphenyl ethers) are environmental pollutants that have been linked to the development of type 2 diabetes (T2D), however, the precise mechanisms are not clear. In particular, their direct effect on insulin secretion is unknown. In this study, we show that two PBDE congeners, BDE-47 and BDE-85, potentiate glucose-stimulated insulin secretion (GSIS) in INS-1 832/13 cells. This effect of BDE-47 and BDE-85 on GSIS was dependent on thyroid receptor (TR). Both BDE-47 and BDE-85 (10 μ M) activated Akt during an acute exposure. The activation of Akt by BDE-47 and BDE-85 plays a role in their potentiation of GSIS, as pharmacological inhibition of PI3K, an upstream activator of Akt, significantly lowers GSIS compared to compounds alone. This study suggests that BDE-47 and BDE-85 directly act on pancreatic β -cells to stimulate GSIS, and that this effect is mediated by the thyroid receptor (TR) and Akt activation. This can cause the β -cells to oversecrete insulin, potentially leading to hyperinsulinemia, insulin resistance, and high blood glucose. In contrast to the potential diabetogenic effects of POPs, there are several naturally-derived compounds which accomplish just the opposite, exerting sensitizing effect on the peripheral tissues and sparing effect on β -cells. TQ, a natural occurring quinone and the main bioactive component of plant *Nigella sativa*, undergoes intracellular redox cycling and re-oxidizes NADH to NAD⁺. TQ administration (20 mg/kg/bw/day) to the Diet-Induced Obesity (DIO) mice reduced their diabetic

phenotype by decreasing fasting blood glucose and fasting insulin levels, and improved glucose tolerance and insulin sensitivity as evaluated by oral glucose and insulin tolerance tests (OGTT and ITT). Furthermore, TQ decreased serum cholesterol levels and liver triglycerides, increased protein expression of phosphorylated Akt, decreased serum levels of inflammatory markers resistin and MCP-1, and decreased the NADH/NAD⁺ ratio. These changes were paralleled by an increase in phosphorylated SIRT-1 and AMPK α in liver and phosphorylated SIRT-1 in skeletal muscle. TQ also increased insulin sensitivity in insulin-resistant HepG2 cells via a SIRT-1-dependent mechanism. These findings are consistent with the TQ-dependent re-oxidation of NADH to NAD⁺, which stimulates glucose and fatty acid oxidation and activation of SIRT-1-dependent pathways. Taken together, these results demonstrate that TQ ameliorates the diabetic phenotype in the DIO mouse model of type 2 diabetes.

CHAPTER ONE:

INTRODUCTION

1.1 Defining Persistent Organic Pollutants

Persistent organic pollutants (POPs), as their name suggests, are organic compounds that do not easily degrade in nature and therefore can accumulate in the environment (Manzetti et al., 2014). They are man-made chemicals that are used in various industrial processes, such as food packaging, fire-retardant foam, textiles, carpets, plastics, electronic equipment, and fire extinguishers among others (Manzetti et al., 2014). The accumulation of these pollutants in the environment is a direct effect and a byproduct of human industrial activity. POPs can accumulate in the oceans, sediments, and air, ultimately making their way up the food chain and into our diets. Indeed, diet is one of the main exposure routes by which POPs enter our bodies. The harmful effects of POPs can thus be exacerbated due to accumulation in various tissues. POPs have been reported to cause liver, thyroid, and neurodevelopmental toxicity and can accumulate in liver, breast milk, and adipose tissue (Manzetti et al., 2014). Recognizing the harmful effects of POPs, the Stockholm Convention was created in 2001 and implemented in 2004 with the goal to decrease and prevent the effects of POPs on human health, wildlife, and the environment. The Convention, signed by 152 countries to date, calls for elimination and restriction of certain POPs, as well as supports additional research and monitoring to aid in developing successful strategies to decrease their impacts. Initially, the convention characterized 12 POPs divided into three categories: pesticides, industrial chemicals, and byproducts and made specific recommendations to eliminate, restrict the production, or reduce the unintentional release of such chemicals into the environment (Xu et al., 2013). Among the initial chemicals listed are well-studied POPs, such as DDT and polychlorinated biphenyls (PCBs). In 2009, 9 more chemicals were added to the list,

which included tetra and pentabromodiphenyl ether in the polybrominated diphenyl ethers (PBDEs class), as well as perfluorooctanesulfonic acid (PFOS) and related compounds (Xu et al., 2013). The particular effects of POPs on glucose homeostasis and their role in the development of type 2 diabetes and metabolic diseases has only recently received attention. Particularly, their effect on pancreatic β -cell function remains underassessed. To address the potential role of these environmental pollutants, this project focuses on the role of two major categories of POPs: polybrominated diphenyl ethers (PBDEs) and perfluorinated compounds (PFCs) on pancreatic β -cell function.

1.2 Polybrominated Diphenyl Ethers BDE-47 and BDE-85

BDE-47 (2,2',4,4'-tetrabromodiphenyl ether) is the major PBDE congener found in tissue samples and in the environment (Shea et al., 2012). The structure of BDE-47 consists of two benzene rings connected by an ester bond, with four bromines located at the 2,2',4,4' positions (Figure 1.1 A). BDE-85 (2,2',3,4,4'-pentabromodiphenyl ether) is a PBDE congener and its structure consists of two benzene rings connected by an ester bond, with five bromines located at the 2,2',3,4,4' positions (Figure 1.1 B). The main route of exposure to PBDEs comes from dietary intake, with the consumption of fish products being estimated as the highest in PBDE content (Schechter et al., 2010). In United States, dietary intake of PBDEs is estimated at 50 ng/day (Schechter et al., 2010). PBDEs are present in house dust, as a result of their release from household products into the air and also as by-products of combustion (Manzetti et al., 2014; Linares et al., 2015). In addition to the dietary exposure, human exposure to PBDEs can be by ingestion and inhalation of house dust, which poses a risk particularly for children (Betts, 2008; Linares et al., 2015). Due to their lipophilicity, PBDEs have the tendency to accumulate in lipid-abundant tissues. A study from Shea et al. reported that the concentration of BDE-47 in breast adipose samples ranged from 7-196 ng/g of lipid weight (lw) (Shea et al., 2012). In another study, mean levels of BDE-47 and BDE-85 were 132 and 6.9 ng/g lw respectively in samples collected from patients after liposuction surgery (Johnson-Restrepo et al., 2005).

In addition to adipose tissue, PBDEs can accumulate in other tissues. A study from Belgium reported a mean liver concentration of 0.95 ng/g lw for BDE-47, which was similar to the concentration in adipose tissue in the same study (Covaci et al., 2008). In a study of 5 subjects in Sweden, levels of different PBDEs were measured; with mean liver BDE-47 concentration of around 3 ng/g lw and a much lower BDE-85 concentration (around 0.1 ng/g lw) (Gruenewald et al., 2001).

Relatively high levels of PBDEs have been reported in human milk, with mean concentrations for BDE-47 and BDE-85 of 40.8 ng/g lw and 1.15 ng/g lw (Schechter et al., 2003). A later study reported similar concentrations for these two compounds in human milk (She et al., 2007).

In addition to accumulating in various tissues, PBDEs have also been detected in plasma and serum. A study from Sjödin et al. measured the serum levels of several PBDE congeners in a sample of a US population from 1985-2002, and reported that BDE-47 levels increased from 5.4 ng/g lw (approx. 10nM) in 1985 to 34 ng/g lw (approx. 64 nM) in 2002, while serum levels of BDE-85 did not significantly fluctuate, with a concentration of 0.5-0.7 ng/g lw (approx. 0.8 – 1.1 nM) during the same period (Sjödin et al., 2004). A study evaluating occupational exposure to PBDEs found high serum levels of PBDEs and most notably BDE-47 compared to control group among foam recyclers and carpet installers in the US (Stapleton et al., 2008). In this study, median BDE-47 serum concentrations were 77.8 (approx. 147 nM) and 100 ng/g lw (approx. 190 nM) for foam workers and carpet layers respectively, while the concentration in the control group was 7.9 ng/g lw (approx. 15 nM); also, median PBDE concentrations were higher compared to the general population, derived from the National Health and Nutrition Examination Survey (NHANES) (Stapleton et al., 2008).

PBDEs have been reported to cause neurodevelopmental toxicity, possibly by affecting thyroid hormone signaling pathways, which are important in growth and development (Manzetti et al., 2014). Due to their hazardous effects, the persistence in the environment and potential to

bioaccumulate, the United States Environmental Protection Agency (EPA) has implemented policies to monitor the levels of PBDEs. In 2004, all commercial penta- (which contains BDE-47 and BDE-85 among other congeners) and octa-BDE compounds were phased out the manufacturing and importing industries in the United States, however levels of various PBDEs are still being detected in the environment and human samples (US EPA Fact Sheet, 2014).

1.3 Perfluorinated Compounds PFOS and PFNA

Perfluorooctanesulfonic acid (PFOS) is a fluorinated organic compound containing an eight-carbon backbone and a sulfonate functional group (Figure 1.1 C). Perfluorononanoic acid (PFNA), also a fluorinated organic compound, has a structure consisting of a nine-carbon backbone and a carboxylic acid functional group (Figure 1.1 D). Due to their strong carbon-fluorine bonds, perfluorinated compounds (PFCs) are very stable and not easily biodegradable, for this reason they have the potential to bioaccumulate (Manzetti et al., 2014). The main route of exposure to PFOS comes from dietary and contaminated water sources; with house dust also playing an important role in the exposure to PFOS among children (Egeghy and Lorber, 2011). In United States, estimated daily intake of PFOS is 160 ng/day for adults and 50 ng/day for children (Egeghy and Lorber, 2011). PFCs can also accumulate in various tissues inside the human body. PFOS has been detected in the liver at concentrations ranging from 13.6 to 26.6 ng/g of tissue (Maestri et al., 2006; Kärroman et al., 2010), while PFNA has been detected at lower concentrations (<1 ng/g) (Kärroman et al., 2010). PFOS and PFNA have been detected in serum of people from different countries (Kannan et al., 2004), as well as in breast milk (Kärroman et al., 2010; Tao et al., 2008; Tao et al., 2008). In the United States, serum concentrations of PFOS between 11 – 20.75 ng/mL (22-41 nM) have been reported from NHANES studies (Calafat et al., 2006; Calafat et al., 2007; Gleason et al., 2015; Olsen et al., 2003); with much higher concentrations in occupationally exposed populations, ranging from 74-799 ng/mL (147-1597 nM) (Olsen et al., 2007; Rotander et al., 2015). Serum concentrations of PFNA have been reported around 1 ng/mL (2.15 nM) (Calafat et al., 2006; Calafat et al., 2007; Gleason et al., 2015; Rotander

et al., 2015). Since PFCs can cross the placental barrier, they have been associated with developmental defects (Stein et al., 2009), cancer (Gilliland and Mandel, 1993), and shown to disrupt thyroid hormone signaling (Bloom et al., 2010). Due to these potential harmful effects in humans, 3M, the leading international manufacturer of PFOS, began a voluntary phasing-out of the chemical, which was completed in 2003. However, although the usage of PFOS and other PFCs has decreased worldwide, the usage of such chemicals in some big industrial countries such as in China has increased (Han, 2009) and can contribute to the persistent worldwide problem of bioaccumulation and hazardous effects on human health from PFC exposure.

1.4 The Potential Role of POPs in the Development of Metabolic Diseases

Type 2 diabetes prevalence has increased exponentially in the last two decades in the United States (CDC, 2016). Although most risks associated with the development of type 2 diabetes involve diet, physical activity, and genetic predisposition, these factors alone cannot fully explain the increase in prevalence. It is imperative to not only find new therapies for T2D, but also to identify potential causative factors and agents in an effort to control the rise of the disease. Recently there is an increased interest in the role of several persistent organic pollutants (POPs) as causative agents for type 2 diabetes. Perfluorinated compounds (PFCs) and brominated flame retardants (BFRs) represent two different classes of POPs and are heavily used in various industrial processes. The case for POPs as metabolic disruptors and their link with obesity and diabetes is supported by several epidemiological studies. Clinical studies have shown that exposure to POPs is associated with type 2 diabetes (Airaksinen et al., 2011), higher insulin concentration and insulin resistance in children (Timmermann et al., 2014), as well as in adolescents and adults (Lin *et al.*, 2009). In an analysis of the National Health Examination and Nutrition Survey (NHANES), Lee et al. showed that serum concentrations of six different POPs are associated with type 2 diabetes prevalence. A study analyzing serum concentrations from a US population, found that PFOS and PFNA concentrations were correlated with higher total cholesterol and non-HDL cholesterol (Nelson et al., 2010); and PFOS was positively associated

with higher total cholesterol in a Danish population (Eriksen et al., 2013). In addition, it was reported that exposure to PFOS can change expression of genes involved in cholesterol metabolism and may cause hypercholesterolemia (Fletcher et al., 2013). PFNA was linked to diabetes in a study of seniors in Sweden (Lind et al., 2014); as well as with hyperglycemia in adolescents and adults from the NHANES survey (Lin et al., 2009). PFOS is associated with increased blood insulin, insulin resistance, and increased pancreatic β -cell function, measured by indirect methods calculated from fasting plasma glucose and insulin (Lin et al., 2009; Timmerman et al., 2014). PFOS is also associated with higher total triglycerides in overweight children (Timmerman et al., 2014). Although some studies have found association of PFCs with glucose homeostasis parameters, other studies report the opposite (Fisher et al., 2012; Nelson et al., 2010, Karnes et al., 2013). In contrast to PFOS and PFNA, the association of PBDEs (particularly BDE-47 and BDE-85) with glucose homeostasis parameters and diabetes has not been widely studied, although PBDEs have been previously reported not to be associated with diabetes except for BDE-153 (Lim et al., 2008). Recently, due to the increased levels of PBDEs in the environment, attention has turned to their role in diabetes, with BDE-47 shown to be associated with increased diabetes prevalence (Zhang et al., 2016).

Studies in rodent models have shown that prolonged exposure to POPs has the capacity to influence insulin signaling and glucose homeostasis. A 14-day exposure to PFNA caused liver insulin resistance and hyperglycemia in Sprague-Dawley (SD) rats (Fang et al., 2012). Additionally, an 8-week exposure to BDE-47 increased fasting blood glucose and decreased fasting insulin in SD rats (Zhang et al., 2016). Perinatal exposure to BDE-99 decreased phosphorylated Akt, a key component in insulin signaling, in rat pup livers (Blanco et al., 2013); and similar PFOS exposure caused impaired glucose tolerance, hyperinsulinemia and insulin resistance in exposed rats in adulthood (Lv et al., 2013). A PBDE mixture, DE-71 (which contains BDE-85), increased liver lipids in Wistar rats, but did not affect fasting blood glucose and insulin levels compared to controls (Nash et al., 2013).

In vitro studies have shown that exposure to POPs can affect lipid metabolism. Exposure of 3T3-L1 pre-adipocytes to a commercial PBDE mixture (containing BDE-47) as well as to BDE-47 alone, increased the differentiation of these cells to mature adipocytes (Tung et al., 2014), while the same effect has been observed with PFCs (Yamamoto et al., 2015). This could imply that these POPs can increase adipocyte formation, which can have implications in obesity and diabetes. Taken together, these findings suggest that exposure to the selected POPs can lead to insulin resistance, hyperglycemia, and altered pancreatic β -cell function.

1.5 An Introduction to Thyroid Hormone and Implications in Type 2 Diabetes

Thyroid hormone is a hormone produced by the thyroid gland and has important implications in growth and metabolism (Shoemaker et al., 2012). The thyroid gland produces mainly the inactive form of the hormone, thyroxine (T4), which is then converted to the active triiodothyronine (T3) by deiodination in target tissues (Shoemaker et al., 2012). Thyroid hormones (as T4 and T3 are referenced) are transported to their target tissues by binding to several transport proteins, more importantly thyroxine-binding globulin (TBG), transthyretin (TTR), and to a lesser extent, albumin (Schussler, 2000). Thyroid hormone acts by binding to the thyroid receptor, a nuclear receptor expressed in most tissues, including heart, lung, liver, kidney, brain, and pancreas, with different isoforms being predominant in different tissues (Harvey and Williams, 2002). Thyroid receptors belong to type II nuclear receptors, which are found primarily in the nucleus, and after being activated by ligand binding, act as transcription factors to initiate the transcription of target genes (Ren and Guo, 2013). Some of the main functions of thyroid hormone include growth and development of various tissues, as well as several metabolic effects, such as increased metabolic rate, stimulation of lipolysis, and stimulation of fatty acid oxidation (Mullur et al., 2014).

Since thyroid receptor is expressed in pancreas and also in the pancreatic β -cells (Shoemaker et al., 2012), researchers have looked into the potential role of thyroid hormone signaling in glucose homeostasis and β -cell function. Some of the early research has evidenced

that patients with hyperthyroidism (excess production of thyroid hormone) have reduced glucose tolerance and insulin action, suggesting that excess thyroid hormone may contribute in the development of type 2 diabetes (Shoemaker et al., 2012). However, since thyroid hormone also increases the metabolic rate, this could lead to weight reduction and increase insulin sensitivity, which has been shown in rodent studies (Amorim et al., 2009; Erion et al., 2007). In the β -cell, thyroid hormone signaling is important in growth and function (Mullur et al., 2014), but there is controversy surrounding whether thyroid hormone has direct effects on GSIS. While in some *in vivo* and *in vitro* studies suggest that thyroid signaling is associated with decreased GSIS (Lenzen et al., 1974; Ximenes et al., 2007), others have shown an increase in GSIS and cell survival in the INS-1 832/13 cells and rat pancreatic islets following thyroid hormone exposure, primarily by activating the PI3K/Akt pathway (Falzacappa et al., 2007; Falzacappa et al., 2010). However, further research is needed to address the role of thyroid hormone signaling in glucose homeostasis in general, and in pancreatic β -cell function in particular.

1.6 The Role of the PI3K-Akt Pathway in Pancreatic β -cell Function

The PI3-Akt pathway plays a major role in many cellular processes, including cell survival, growth and metabolism. In the context of diabetes and glucose homeostasis, this pathway is involved in insulin signaling and insulin action, which facilitates glucose entry into the tissues from the bloodstream, thus keeping blood glucose levels in check. Insulin binds to the insulin receptor, a tyrosine kinase receptor, which initiates a phosphorylation cascade of many proteins, including insulin receptor substrate 1 (IRS1) and 2 (IRS2), leading to the activation of downstream signaling proteins PI3K, PDK1/2, and Akt (Guo et al., 2014). It is Akt (or protein kinase B) activation that leads to translocation of glucose transporters to the plasma membrane and increased glucose transport inside the cell (Guo et al., 2014).

Although the role of this pathway in insulin signaling is well established, its role in insulin secretion is controversial, with conflicting reports on the role of the pathway in GSIS. Downregulation of Akt activity specifically in β -cells led to glucose intolerance due to impaired

insulin secretion in mice (Bernal-Mizrachi et al., 2014). Akt activation was also positively implicated in a study looking at the effect of adiponectin on β -cell function, where pre-incubation of cells with PI3K inhibitor wortmannin decreased insulin gene expression and GSIS (Wijesekara et al., 2010). Overexpression of dominant negative Akt decreased GSIS, whether overexpression of constitutively active Akt increased GSIS in the INS-1 cell line (Le Bacquer et al., 2013). Akt activation has been implicated to play a role in insulin granule exocytosis, thus increasing GSIS (Bernal-Mizrachi et al., 2004; Cheng et al., 2012). Conversely, a study from Ayoagi et al. reported that acute pharmacological inhibition of Akt led to an increase in insulin secretion by way of increasing insulin granule fusion (Ayoagi et al., 2012). Furthermore, other studies have reported that pharmacological inhibition of PI3K increases GSIS, suggesting that the activation of this pathway suppresses insulin secretion (Eto et al., 2002; Kolic et al., 2013; Zawalich et al., 2002). Thus, the role of the PI3K-Akt pathway in insulin secretion is not clear and further studies are required to determine how activation or downregulation of the pathway affects GSIS.

1.7 INS-1 832/13 Cell Line as a Pancreatic β -cell Model

Pancreatic β -cells are a key component in maintaining glucose homeostasis and are part of the islets of Langerhans, which also contain α -cells that secrete glucagon, PP cells that secrete pancreatic polypeptide, and γ -cells that secrete somatostatin (Hohmeier and Newgard, 2004). β -cells can be used to study the effects of different agents and potential new drugs on insulin secretion and the underlying mechanisms, and are an important tool in identifying new therapeutics and risk agents for type 2 diabetes. Due to their utility in diabetes research, β -cells are constantly in high demand. However, the availability of human pancreatic islets for research is very limited and the alternative of murine pancreatic islets comes with added costs and complications for the researcher: murine colony maintenance, cumbersome isolation procedures, and the finite life in culture of primary islets. Because of these challenges, pancreatic β -cell lines from a variety of sources have been developed with the goal of having a readily available model that mimics the native β -cell. The ideal model is one that is as close to the native cell as possible:

not only expressing high insulin content and having the ability to secrete insulin in response to a glucose challenge, but also expressing key genes and enzymes responsible for normal β -cell function (Hohmeier and Newgard, 2004). Most of the established β -cell lines have originated from animal insulinoma tumors induced by irradiation or the expression of an oncogene (Hohmeier and Newgard, 2004). The INS-1 parental cell line was first established from x-ray radiation induced rat insulinoma, with relatively high insulin content, and no expression of the other pancreatic endocrine hormones: glucagon, somatostatin, or pancreatic polypeptide (Asfari et al., 1992), thus showing phenotypical features of differentiated β -cells. Furthermore, these cells responded to glucose stimulation within the physiological range, which prompted a 2-4-fold increase in insulin secretion (Asfari et al., 1992).

One of the main challenges with the clonal β -cell models is that after subsequent passages, their insulin content decreases, and their ability to secrete insulin in response to a glucose challenge is severely impaired, thus causing a change in phenotype (Hohmeier and Newgard, 2004). In an effort to create a model that is phenotypically stable for a relatively long time in culture conditions, Hohmeier et al. developed various INS-1 subclones by transfecting parental INS-1 cells with a human proinsulin gene. INS-1 832/13 subclone emerged as the one that had the greatest GSIS index, as well as a remarkable phenotypic stability, maintaining the ability to respond to glucose over a span of 7 months or about 66 generations in culture (Hohmeier et al., 2000).

Native β -cells respond by secreting insulin only when glucose concentration is higher than the physiological range. This ensures that the cells don't constantly secrete insulin in response to minor increases in glucose concentrations, or when the glucose concentration is low, which would eventually cause hypoglycemia. They achieve this via their characteristic glucose sensing mechanisms, which involve glucose transporter GLUT-2 and glucokinase, a subtype of hexokinase that phosphorylates glucose upon entry into the β -cell (Fu et al., 2014). Glucokinase has a lower affinity for glucose (with a K_m of 6mM) compared to other hexokinases, which allows

glucose to be metabolized only at high concentrations (Fu et al., 2014). In different β -cell models, the lack of expression of glucokinase, or expression of hexokinase limits their ability to respond to glucose, particularly within the physiological range. The INS-1 832/13 cells express both GLUT-2 and glucokinase, which is a major advantage of this cell line, and allows it to have a similar glucose response to the native β -cells (Hohmeier and Newgard, 2004).

Based on these characteristics, the INS-1 832/13 cell line is one the most physiologically relevant β -cell models, which makes it very suitable as a tool to test the effects of POPs or other agents of interest on pancreatic β -cell function.

1.8 Introduction to Thymoquinone and its Anti-Diabetic Potential

Thymoquinone (TQ) is the main bioactive component of *Nigella sativa*, a spice plant of the *Ranunculaceae* family that has been used in traditional medicine to treat a variety of diseases, including asthma, hypertension, diabetes, and cancer among others (Ali and Blunden, 2003). Most of the pharmacological properties of the *Nigella sativa* plant come from TQ actions (Ali and Blunden, 2003). TQ was first isolated from the plant by El-Dakhakhny in 1963 and has a structure of a dione conjugated to a benzene ring, to which a methyl and an isopropyl side chains are added in the 2 and 5 positions (Figure 1.1 E) (Ali and Blunden, 2003; El-Dakhakhny, 1963).

Thymoquinone has been shown to have antioxidative properties, as TQ administration for a period of 5 days in mice lowered the activity of antioxidant enzymes superoxide dismutase, catalase, and glutathione peroxidase in the liver (Mansour et al., 2002). Furthermore, this was associated with the ability of TQ to scavenge reactive oxygen species (Mansour et al., 2002). TQ has shown anti-inflammatory properties by acting on different inflammatory markers and transcription factors. Nuclear-factor-kappa B (NF- κ B) is a transcription factor that regulates the expression of about 400 genes, including inflammatory cytokines and its activation has been associated with oxidative stress, inflammation, and a myriad of diseases, including diabetes (Ahn and Aggarwal, 2005). TQ has been shown to inhibit the activation of NF- κ B (Chehl et al., 2009; Sethi et al., 2008), as well as to reduce inflammatory cytokine levels in mice (El Gazzar et al.,

2006). This compound has shown promise in ameliorating dyslipidemia, and has been shown to decrease the levels of triglycerides and total cholesterol and low-density lipoprotein (LDL) cholesterol (Alenzi et al., 2010; Asgary et al., 2015; Badary et al., 2000). Since many of the type 2 diabetes pathophysiologies are characterized by increasing levels of reactive oxygen species, pro-inflammatory markers, and dyslipidemia (Lumeng and Saltiel., 2011; Mooradian, 2009; Yan, 2014), these findings highlight the potential antidiabetic effects of TQ.

Evidence for the beneficial effects of TQ in maintaining glucose homeostasis and ameliorating diabetic symptoms comes from several studies in murine models of type 2 diabetes. In streptozotocin (STZ)-induced diabetic rats, TQ improved glucose tolerance, hyperglycemia, decreased the activities of hepatic gluconeogenic enzymes, increased the activities of hepatic glycolytic enzymes, and decreased the levels of glycated hemoglobin (Pari and Sankaranarayanan, 2009). TQ was found to decrease the activity of glycogen phosphorylase, an enzyme that catalyzes the breakdown of liver glycogen in order to release glucose into the bloodstream and contributes to increased hepatic glucose production and eventual hyperglycemia in type 2 diabetes (El-Ameen et al., 2015). In a similar study using the STZ-induced diabetic rats, TQ administration lowered hyperglycemia, increased plasma insulin content, and increased total pancreatic insulin levels (Sankaranarayanan and Pari, 2011). In another study using the same model, TQ administration over a 30-day period lowered hyperglycemia, increased serum insulin concentration, and decreased oxidative stress by restoring the levels of the enzyme superoxide dismutase in the tissues (Abdelmeguid et al., 2010). Furthermore, these changes were more apparent with increased study duration (Abdelmeguid et al., 2010). In STZ-induced diabetic hamsters, TQ administration for 4 weeks decreased total glycated hemoglobin, hepatic glucose production, and blood glucose (Fararh et al., 2005). One of the possible mechanisms by which TQ could ameliorate the diabetic phenotype in the STZ models is the reduction of oxidative stress and inflammation. A study by El-Mahmoudy et al. reported that TQ administration decreased nitric oxide (NO) production, a free radical that can

contribute to oxidative stress and diabetes, and prevented the induction of diabetes after STZ administration (El-Mahmoudy et al., 2005). The same group reported that TQ lowered serum levels of pro-inflammatory cytokines interleukin 1 beta (IL-1 β) and tumor necrosis factor alpha (TNF- α) in STZ-induced diabetic rats (El-Mahmoudy et al., 2005). In rats rendered diabetic by high-fructose diet (HFD) feeding, TQ administration ameliorated hyperglycemia, insulin resistance, dyslipidemia, and increased levels of antioxidant enzymes catalase and superoxide dismutase in a dose-dependent manner (Prabhakar et al., 2015). In rats rendered insulin-resistant and hyperglycemic by high-fat high-cholesterol feeding, TQ lowered fasting blood glucose, improved insulin sensitivity, improved the lipid profile, and decreased pro-inflammatory markers TNF- α and interleukin 10 (IL-10) (Awad et al., 2016).

Since TQ has been shown to decrease inflammatory markers and oxidative stress, researchers have been interested in studying the direct effects of TQ on pancreatic β -cell function. Pancreatic β -cells have very low levels of antioxidant enzymes, making them more prone to oxidative stress, which is elevated in type 2 diabetes, and can result in β -cell death (Montane et al., 2014). Reduction of oxidative stress by TQ may protect β -cells in diabetic conditions, which can lead to improved β -cell function and overall improvements in glucose homeostasis. TQ has been shown to improve streptozotocin-induced β -cell damage, with pancreatic islets showing normal morphology even after STZ treatment in diabetic rats (Abdelmeguid et al., 2010). The increase observed in serum insulin levels after TQ treatment in STZ-induced diabetic rats could be a result of improved β -cell function and consequently increased insulin secretion (El-Mahmoudy et al., 2005; Sankaranarayanan and Pari, 2011). However, few studies have been conducted on the direct effects of TQ on GSIS. *Nigella sativa* extract enhanced GSIS in pancreatic islets in a concentration-dependent manner (Rchid et al., 2004). In INS-1 cells, *Nigella sativa* extract increased GSIS, but the same effect was not observed with TQ (Chandra et al., 2009). In INS-1 832/13 cells, TQ was shown to normalize defective GSIS due to chronic high glucose exposure via inhibition of acetyl CoA carboxylase (ACC) and enhanced oxidation of

glucose and fatty acids (Gray et al., 2016). The same study showed that TQ lowers the NADH/NAD⁺ ratio, leading to more NAD⁺ being available for glucose oxidation, which can potentiate GSIS (Gray et al., 2016).

In humans, *Nigella sativa* oil has been shown to reduce fasting blood glucose and glycated hemoglobin levels in patients with type 2 diabetes (Heshmati et al., 2015; Kaatabi et al., 2015). TQ also improved oxidative stress in patients with type 2 diabetes by reducing the levels of lipid peroxidation markers and elevating the levels of SOD, glutathione, and total oxidant capacity (Kaatabi et al., 2015). Lastly, in a clinical trial, *Nigella sativa* oil enhanced the ability of metformin to decrease fasting and postprandial glucose levels in patients with metabolic syndrome (Najmi et al., 2008)

Taken together, these studies demonstrate the potential of TQ to regulate glucose homeostasis by acting on key peripheral metabolic tissues, as well as by potentially having a direct effect on pancreatic β -cell function; however, the detailed mechanisms of anti-diabetic actions of TQ warrant further investigation.

1.9 Objective, Hypotheses, and Aims

One of the objectives of this work is to evaluate the effect of BDE-47, BDE-85, PFOS, and PFNA on GSIS using the pancreatic β -cell line INS-1 832/13, and the potential mechanisms associated with this effect. Another objective of the work is to evaluate the antidiabetic effects of Thymoquinone, the main bioactive component of plant *Nigella sativa*, in the diet-induced obesity (DIO) mouse model of type 2 diabetes. We hypothesized that the selected POPs will increase *in vitro* GSIS and that the mechanisms by which these POPs affect GSIS depend on thyroid hormone receptor and Akt activation. Secondly, we hypothesized that Thymoquinone will ameliorate hyperglycemia, insulin resistance, tissue metabolic imbalances, lipid profile, inflammation, and weight gain in the diet-induced obesity (DIO) mouse model of type 2 diabetes. Lastly, because TQ has been reported to decrease NADH/NAD⁺ ratio (Gray et al., 2016), thus

increasing NAD⁺, we hypothesized that the anti-diabetic effects of TQ are mediated by activation of NAD⁺- dependent targets, SIRT-1 and AMPK.

We will test these hypotheses by executing the following specific aims:

Specific Aim 1: Examine the effect of selected POPs on glucose-stimulated insulin secretion (GSIS) in INS-1 832/13 pancreatic β -cell line. Cells will be exposed to selected POPs during a chronic 48-hour pre-treatment, as well as during a 1-hour acute treatment, and insulin will be measured by an ELISA kit. Compounds that modify GSIS will be selected for mechanistic studies in Specific Aim 2.

Specific Aim 2: Evaluate the role of thyroid receptor (TR) and Akt in modulation of GSIS by selected POP compounds. GSIS will be performed with the selected compounds in the presence or absence of thyroid receptor agonist (T3) & antagonist (1-850); as well as in the presence or absence of wortmannin, a specific inhibitor of PI3K upstream of Akt. Insulin secretion will be measured by an Elisa kit and phosphorylation (activation) of Akt will be measured by western blotting.

Specific Aim 3: Evaluate the antidiabetic effects of TQ in the DIO mouse model of type 2 diabetes. DIO mice will be administered TQ by oral gavage and glucose homeostasis will be assessed by the following techniques: glucose tolerance by a glucose tolerance test (GTT), insulin sensitivity by insulin tolerance test (ITT), fasting blood glucose will be measured as part of the GTT and ITT. Effect of TQ on lipid profile will be evaluated by measurement of total tissue triglycerides and serum cholesterol, and the effect of TQ on tissue metabolomics will be evaluated by GC/MS. To evaluate whether the antidiabetic effects of TQ are mediated by activating SIRT-1 and AMPK pathways, tissue protein levels of activated (phosphorylated) SIRT-1 and AMPK α will be measured by western blot. To evaluate whether the effects of TQ on insulin sensitivity are dependent on SIRT-1 and AMPK activation, insulin-resistant HepG2 cells will be exposed to TQ in the presence or absence of SIRT-1 and AMPK α pharmacological inhibitors and activators.

1.10 Significance and Impact

The results of this study should serve to initially (1) provide direct evidence for the role of the selected POPs in pancreatic β -cell function, (2) describe the mechanisms by which they act to affect β -cell function, and (3) to establish the antidiabetic role of TQ and the potential molecular mechanisms involved. This study should serve to identify specific agents and mechanisms that can contribute to the development of type 2 diabetes, reinforcing that environmental pollutants can play a role in human health and disease, and particularly in metabolic diseases. The findings of the study could also provide the basis for TQ to be further developed as a treatment option for type 2 diabetes.

1.11 References

- Abdelmeguid, N. E., Fakhoury, R., Kamal, S. M., & Al Wafai, R. J. (2010). Effects of Nigella sativa and thymoquinone on biochemical and subcellular changes in pancreatic β - cells of streptozotocin- induced diabetic rats. *Journal of diabetes*, 2(4), 256-266.
- Ahn, K. S., & Aggarwal, B. B. (2005). Transcription Factor NF- κ B: A Sensor for Smoke and Stress Signals. *Annals of the new York Academy of Sciences*, 1056(1), 21
- Airaksinen, R., Rantakokko, P., Eriksson, J. G., Blomstedt, P., Kajantie, E., & Kiviranta, H. (2011). Association between type 2 diabetes and exposure to persistent organic pollutants. *Diabetes Care*, 34(9), 1972-1979.
- Alenzi, F. Q., El-Bolkiny, Y. E. S., & Salem, M. L. (2010). Protective effects of Nigella sativa oil and thymoquinone against toxicity induced by the anticancer drug cyclophosphamide. *British journal of biomedical science*, 67(1), 20-28.
- Ali, B. H., & Blunden, G. (2003). Pharmacological and toxicological properties of Nigella sativa. *Phytotherapy Research*, 17(4), 299-305.
- Aoyagi, K., Ohara-Imaizumi, M., Nishiwaki, C., Nakamichi, Y., Ueki, K., Kadowaki, T., & Nagamatsu, S. (2012). Acute inhibition of PI3K-PDK1-Akt pathway potentiates insulin secretion through upregulation of newcomer granule fusions in pancreatic β -cells. *PloS one*, 7(10), e47381.
- Asfari, M., Janjic, D., Meda, P., Li, G., Halban, P. A., & Wollheim, C. B. (1992). Establishment of 2-mercaptoethanol-dependent differentiated insulin-secreting cell lines. *Endocrinology*, 130(1), 167-178.
- Asgary, S., Sahebkar, A., & Goli-Malekabadi, N. (2015). Ameliorative effects of Nigella sativa on dyslipidemia. *Journal of endocrinological investigation*, 38(10), 1039-1046.

- Awad, A. S., Al Haleem, E. N. A., El-Bakly, W. M., & Sherief, M. A. (2016). Thymoquinone alleviates nonalcoholic fatty liver disease in rats via suppression of oxidative stress, inflammation, apoptosis. *Naunyn-Schmiedeberg's archives of pharmacology*, 389(4), 381-391.
- Badary, O. A., Abdel-Naim, A. B., Abdel-Wahab, M. H., & Hamada, F. M. (2000). The influence of thymoquinone on doxorubicin-induced hyperlipidemic nephropathy in rats. *Toxicology*, 143(3), 219-226.
- Bernal-Mizrachi, E., Fatrai, S., Johnson, J. D., Ohsugi, M., Otani, K., Han, Z., ... & Permutt, M. A. (2004). Defective insulin secretion and increased susceptibility to experimental diabetes are induced by reduced Akt activity in pancreatic islet β cells. *Journal of Clinical Investigation*, 114(7), 928.
- Betts, K. S. (2008). Unwelcome guest: PBDEs in indoor dust. *Environmental health perspectives*, 116(5), A202.
- Blanco, J., Mulero, M., Domingo, J. L., & Sanchez, D. J. (2013). Perinatal exposure to BDE-99 causes decreased protein levels of cyclin D1 via GSK3 β activation and increased ROS production in rat pup livers. *toxicological sciences*, 137(2), 491-498.
- Bloom, M. S., Kannan, K., Spliethoff, H. M., Tao, L., Aldous, K. M., & Vena, J. E. (2010). Exploratory assessment of perfluorinated compounds and human thyroid function. *Physiology & behavior*, 99(2), 240-245.
- Calafat, A. M., Kuklennyik, Z., Caudill, S. P., Reidy, J. A., & Needham, L. L. (2006). Perfluorochemicals in pooled serum samples from United States residents in 2001 and 2002. *Environmental science & technology*, 40(7), 2128-2134.
- Calafat, A. M., Wong, L. Y., Kuklennyik, Z., Reidy, J. A., & Needham, L. L. (2007). Polyfluoroalkyl chemicals in the US population: data from the National Health and Nutrition Examination Survey (NHANES) 2003–2004 and comparisons with NHANES 1999–2000. *Environmental health perspectives*, 115(11), 1596.
- Centers for Disease Control and Prevention. (2016). Long term trends in diabetes. *Atlanta, GA: US Department of Health and Human Services, 2016.*
- Chandra, S., Murthy, S. N., Mondal, D., & Agrawal, K. C. (2009). Therapeutic effects of *Nigella sativa* on chronic HAART-induced hyperinsulinemia in rats This article is one of a selection of papers from the NATO Advanced Research Workshop on Translational Knowledge for Heart Health (published in part 2 of a 2-part Special Issue). *Canadian journal of physiology and pharmacology*, 87(4), 300-309.
- Chehl, N., Chipitsyna, G., Gong, Q., Yeo, C. J., & Arafat, H. A. (2009). Anti-inflammatory effects of the *Nigella sativa* seed extract, thymoquinone, in pancreatic cancer cells. *HPB*, 11(5), 373-381.
- Cheng, K. K., Lam, K. S., Wu, D., Wang, Y., Sweeney, G., Hoo, R. L., ... & Xu, A. (2012). APPL1 potentiates insulin secretion in pancreatic β cells by enhancing protein kinase Akt-dependent expression of SNARE proteins in mice. *Proceedings of the National Academy of Sciences*, 109(23), 8919-8924.

- Covaci, A., Voorspoels, S., Roosens, L., Jacobs, W., Blust, R., & Neels, H. (2008). Polybrominated diphenyl ethers (PBDEs) and polychlorinated biphenyls (PCBs) in human liver and adipose tissue samples from Belgium. *Chemosphere*, 73(2), 170-175.
- Egeghy, P. P., & Lorber, M. (2011). An assessment of the exposure of Americans to perfluorooctane sulfonate: a comparison of estimated intake with values inferred from NHANES data. *Journal of Exposure Science and Environmental Epidemiology*, 21(2), 150-168.
- El Gazzar, M., El Mezayen, R., Nicolls, M. R., Marecki, J. C., & Dreskin, S. C. (2006). Downregulation of leukotriene biosynthesis by thymoquinone attenuates airway inflammation in a mouse model of allergic asthma. *Biochimica et Biophysica Acta (BBA)-General Subjects*, 1760(7), 1088-1095.
- El-Ameen, N. M. H., Taha, M. M. E., Abdelwahab, S. I., Khalid, A., Elfatih, F., Kamel, M. A., & Sheikh, B. Y. (2015). Anti-diabetic properties of thymoquinone is unassociated with glycogen phosphorylase inhibition. *Pharmacognosy Journal*, 7(6).
- El-Dakhakhny, M. (1963). Studies on the chemical constitution of Egyptian. *Nigella sativa*, 465-70.
- El-Mahmoudy, A., Shimizu, Y., Shiina, T., Matsuyama, H., El-Sayed, M., & Takewaki, T. (2005). Successful abrogation by thymoquinone against induction of diabetes mellitus with streptozotocin via nitric oxide inhibitory mechanism. *International immunopharmacology*, 5(1), 195-207.
- El-Mahmoudy, A., Shimizu, Y., Shiina, T., Matsuyama, H., Nikami, H., & Takewaki, T. (2005). Macrophage-derived cytokine and nitric oxide profiles in type I and type II diabetes mellitus: effect of thymoquinone. *Acta diabetologica*, 42(1), 23-30.
- Eriksen, K. T., Raaschou-Nielsen, O., McLaughlin, J. K., Lipworth, L., Tjønneland, A., Overvad, K., & Sørensen, M. (2013). Association between plasma PFOA and PFOS levels and total cholesterol in a middle-aged Danish population. *PloS one*, 8(2), e56969.
- Erion, M. D., Cable, E. E., Ito, B. R., Jiang, H., Fujitaki, J. M., Finn, P. D., ... & Linemeyer, D. L. (2007). Targeting thyroid hormone receptor- β agonists to the liver reduces cholesterol and triglycerides and improves the therapeutic index. *Proceedings of the National Academy of Sciences*, 104(39), 15490-15495.
- Eto, K., Yamashita, T., Tsubamoto, Y., Terauchi, Y., Hirose, K., Kubota, N., ... & Tobe, K. (2002). Phosphatidylinositol 3-kinase suppresses glucose-stimulated insulin secretion by affecting post-cytosolic [Ca²⁺] elevation signals. *Diabetes*, 51(1), 87-97.
- Falzacappa, C. V., Petrucci, E., Patriarca, V., Michienzi, S., Stigliano, A., Brunetti, E., ... & Misiti, S. (2007). Thyroid hormone receptor TR β 1 mediates Akt activation by T3 in pancreatic β cells. *Journal of molecular endocrinology*, 38(2), 221-233.
- Fang, X., Gao, G., Xue, H., Zhang, X., & Wang, H. (2012). Exposure of perfluorononanoic acid suppresses the hepatic insulin signal pathway and increases serum glucose in rats. *Toxicology*, 294(2), 109-115.

- Fararh, K. M., Shimizu, Y., Shiina, T., Nikami, H., Ghanem, M. M., & Takewaki, T. (2005). Thymoquinone reduces hepatic glucose production in diabetic hamsters. *Research in veterinary science*, 79(3), 219-223.
- Fisher, M., Arbuckle, T. E., Wade, M., & Haines, D. A. (2013). Do perfluoroalkyl substances affect metabolic function and plasma lipids? Analysis of the 2007–2009, Canadian Health Measures Survey (CHMS) Cycle 1. *Environmental research*, 121, 95-103.
- Fletcher, T., Galloway, T. S., Melzer, D., Holcroft, P., Cipelli, R., Pilling, L. C., ... & Harries, L. W. (2013). Associations between PFOA, PFOS and changes in the expression of genes involved in cholesterol metabolism in humans. *Environment international*, 57, 2-10.
- Fu, Z., R Gilbert, E., & Liu, D. (2013). Regulation of insulin synthesis and secretion and pancreatic Beta-cell dysfunction in diabetes. *Current diabetes reviews*, 9(1), 25-53.
- Gilliland, F. D., & Mandel, J. S. (1993). Mortality among employees of a perfluorooctanoic acid production plant. *Journal of Occupational and Environmental Medicine*, 35(9), 950-954.
- Gleason, J. A., Post, G. B., & Fagliano, J. A. (2015). Associations of perfluorinated chemical serum concentrations and biomarkers of liver function and uric acid in the US population (NHANES), 2007–2010. *Environmental research*, 136, 8-14.
- Gray, J. P., Burgos, D. Z., Yuan, T., Seeram, N., Rebar, R., Follmer, R., & Heart, E. A. (2016). Thymoquinone, a bioactive component of *Nigella sativa*, normalizes insulin secretion from pancreatic β -cells under glucose overload via regulation of malonyl-CoA. *American Journal of Physiology-Endocrinology and Metabolism*, 310(6), E394-E404.
- Guo, S. (2014). Insulin signaling, resistance, and metabolic syndrome: insights from mouse models into disease mechanisms. *Journal of Endocrinology*, 220(2), T1-T23.
- Han, W. (2009). PFOS related actions in China. In *International workshop on managing perfluorinated chemicals and transitioning to safer alternatives* (pp. 12-13).
- Harvey, C. B., & Williams, G. R. (2002). Mechanism of thyroid hormone action. *Thyroid*, 12(6), 441-446.
- Heshmati, J., Namazi, N., Memarzadeh, M. R., Taghizadeh, M., & Kolehdooz, F. (2015). *Nigella sativa* oil affects glucose metabolism and lipid concentrations in patients with type 2 diabetes: A randomized, double-blind, placebo-controlled trial. *Food Research International*, 70, 87-93.
- Hohmeier, H. E., & Newgard, C. B. (2004). Cell lines derived from pancreatic islets. *Molecular and cellular endocrinology*, 228(1), 121-128.
- Hohmeier, H. E., Mulder, H., Chen, G., Henkel-Rieger, R., Prentki, M., & Newgard, C. B. (2000). Isolation of INS-1-derived cell lines with robust ATP-sensitive K⁺ channel-dependent and-independent glucose-stimulated insulin secretion. *Diabetes*, 49(3), 424-430.
- Johnson-Restrepo, B., Kannan, K., Rapaport, D. P., & Rodan, B. D. (2005). Polybrominated diphenyl ethers and polychlorinated biphenyls in human adipose tissue from New York. *Environmental science & technology*, 39(14), 5177-5182.

- Kaatabi, H., Bamosa, A. O., Badar, A., Al-Elq, A., Abou-Hozafa, B., Lebda, F., ... & Al-Almaie, S. (2015). *Nigella sativa* improves glycemic control and ameliorates oxidative stress in patients with type 2 diabetes mellitus: Placebo controlled participant blinded clinical trial. *PLoS one*, *10*(2), e0113486.
- Kannan, K., Corsolini, S., Falandysz, J., Fillmann, G., Kumar, K. S., Loganathan, B. G., ... & Aldous, K. M. (2004). Perfluorooctanesulfonate and related fluorochemicals in human blood from several countries. *Environmental science & technology*, *38*(17), 4489-4495.
- Karnes, C., Winqvist, A., & Steenland, K. (2014). Incidence of type II diabetes in a cohort with substantial exposure to perfluorooctanoic acid. *Environmental research*, *128*, 78-83.
- Kärrman, A., Domingo, J. L., Llebaria, X., Nadal, M., Bigas, E., van Bavel, B., & Lindström, G. (2010). Biomonitoring perfluorinated compounds in Catalonia, Spain: concentrations and trends in human liver and milk samples. *Environmental Science and Pollution Research*, *17*(3), 750-758.
- Kolic, J., Spigelman, A. F., Plummer, G., Leung, E., Hajmrle, C., Kin, T., ... & MacDonald, P. E. (2013). Distinct and opposing roles for the phosphatidylinositol 3-OH kinase catalytic subunits p110 α and p110 β in the regulation of insulin secretion from rodent and human beta cells. *Diabetologia*, *56*(6), 1339-1349.
- Le Bacquer, O., Queniat, G., Gmyr, V., Kerr-Conte, J., Lefebvre, B., & Pattou, F. (2013). mTORC1 and mTORC2 regulate insulin secretion through Akt in INS-1 cells. *Journal of Endocrinology*, *216*(1), 21-29.
- Lee, D. H., Lee, I. K., Song, K., Steffes, M., Toscano, W., Baker, B. A., & Jacobs, D. R. (2006). A strong dose-response relation between serum concentrations of persistent organic pollutants and diabetes results from the National Health and Examination Survey 1999–2002. *Diabetes Care*, *29*(7), 1638-1644.
- Lenzen, S., Panten, U., & Hasselblatt, A. (1975). Thyroxine treatment and insulin secretion in the rat. *Diabetologia*, *11*(1), 49-55.
- Lim, J. S., Lee, D. H., & Jacobs, D. R. (2008). Association of brominated flame retardants with diabetes and metabolic syndrome in the US population, 2003–2004. *Diabetes care*, *31*(9), 1802-1807.
- Lin, C. Y., Chen, P. C., Lin, Y. C., & Lin, L. Y. (2009). Association among serum perfluoroalkyl chemicals, glucose homeostasis, and metabolic syndrome in adolescents and adults. *Diabetes care*, *32*(4), 702-707.
- Lind, L., Zethelius, B., Salihovic, S., van Bavel, B., & Lind, P. M. (2014). Circulating levels of perfluoroalkyl substances and prevalent diabetes in the elderly. *Diabetologia*, *57*(3), 473-479.
- Lumeng, C. N., & Saltiel, A. R. (2011). Inflammatory links between obesity and metabolic disease. *The Journal of clinical investigation*, *121*(6), 2111.
- Lv, Z., Li, G., Li, Y., Ying, C., Chen, J., Chen, T., ... & Shu, B. (2013). Glucose and lipid homeostasis in adult rat is impaired by early- life exposure to perfluorooctane sulfonate. *Environmental toxicology*, *28*(9), 532-542.

- Maestri, L., Negri, S., Ferrari, M., Ghittori, S., Fabris, F., Danesino, P., & Imbriani, M. (2006). Determination of perfluorooctanoic acid and perfluorooctanesulfonate in human tissues by liquid chromatography/single quadrupole mass spectrometry. *Rapid Communications in Mass Spectrometry*, 20(18), 2728-2734.
- Mansour, M. A., Nagi, M. N., El- Khatib, A. S., & Al- Bekairi, A. M. (2002). Effects of thymoquinone on antioxidant enzyme activities, lipid peroxidation and DT- diaphorase in different tissues of mice: a possible mechanism of action. *Cell biochemistry and function*, 20(2), 143-151.
- Meironyté Guvenius, D., Bergman, Å., & Noren, K. (2001). Polybrominated diphenyl ethers in Swedish human liver and adipose tissue. *Archives of environmental contamination and toxicology*, 40(4), 564-570.
- Montane, J., Cadavez, L., & Novials, A. (2014). Stress and the inflammatory process: a major cause of pancreatic cell death in type 2 diabetes. *Diabetes, metabolic syndrome and obesity: targets and therapy*, 7, 25.
- Mooradian, A. D. (2009). Dyslipidemia in type 2 diabetes mellitus. *Nature Reviews. Endocrinology*, 5(3), 150.
- Mullur, R., Liu, Y. Y., & Brent, G. A. (2014). Thyroid hormone regulation of metabolism. *Physiological reviews*, 94(2), 355-382.
- Najmi, A., Nasiruddin, M., Khan, R. A., & Haque, S. F. (2008). Effect of Nigella sativa oil on various clinical and biochemical parameters of insulin resistance syndrome. *International journal of diabetes in developing countries*, 28(1), 11.
- Nash, J. T., Szabo, D. T., & Carey, G. B. (2013). Polybrominated diphenyl ethers alter hepatic phosphoenolpyruvate carboxykinase enzyme kinetics in male Wistar rats: implications for lipid and glucose metabolism. *Journal of Toxicology and Environmental Health, Part A*, 76(2), 142-156.
- Nelson, J. W., Hatch, E. E., & Webster, T. F. (2010). Exposure to polyfluoroalkyl chemicals and cholesterol, body weight, and insulin resistance in the general US population. *Environmental health perspectives*, 118(2), 197.
- Nelson, J. W., Hatch, E. E., & Webster, T. F. (2010). Exposure to polyfluoroalkyl chemicals and cholesterol, body weight, and insulin resistance in the general US population. *Environmental health perspectives*, 118(2), 197.
- Olsen, G. W., Hansen, K. J., Stevenson, L. A., Burris, J. M., & Mandel, J. H. (2003). Human donor liver and serum concentrations of perfluorooctanesulfonate and other perfluorochemicals. *Environmental science & technology*, 37(5), 888-891.
- Olsen, G. W., Burris, J. M., Ehresman, D. J., Froehlich, J. W., Seacat, A. M., Butenhoff, J. L., & Zobel, L. R. (2007). Half-life of serum elimination of perfluorooctanesulfonate, perfluorohexanesulfonate, and perfluorooctanoate in retired fluorochemical production workers. *Environmental health perspectives*, 115(9), 1298.

- Pari, L., & Sankaranarayanan, C. (2009). Beneficial effects of thymoquinone on hepatic key enzymes in streptozotocin–nicotinamide induced diabetic rats. *Life sciences*, 85(23), 830-834.
- Prabhakar, P., Reeta, K. H., Maulik, S. K., Dinda, A. K., & Gupta, Y. K. (2015). Protective effect of thymoquinone against high-fructose diet-induced metabolic syndrome in rats. *European journal of nutrition*, 54(7), 1117-1127.
- Ren, X. M., & Guo, L. H. (2013). Molecular toxicology of polybrominated diphenyl ethers: nuclear hormone receptor mediated pathways. *Environmental Science: Processes & Impacts*, 15(4), 702-708.
- Rotander, A., Toms, L. M. L., Aylward, L., Kay, M., & Mueller, J. F. (2015). Elevated levels of PFOS and PFHxS in firefighters exposed to aqueous film forming foam (AFFF). *Environment international*, 82, 28-34.
- Sankaranarayanan, C., & Pari, L. (2011). Thymoquinone ameliorates chemical induced oxidative stress and β -cell damage in experimental hyperglycemic rats. *Chemico-biological interactions*, 190(2), 148-154.
- Schechter, A., Pavuk, M., Pöpke, O., Ryan, J. J., Birnbaum, L., & Rosen, R. (2003). Polybrominated diphenyl ethers (PBDEs) in US mothers' milk. *Environmental health perspectives*, 111(14), 1723.
- Schussler, G. C. (2000). The thyroxine-binding proteins. *Thyroid*, 10(2), 141-149.
- Sethi, G., Ahn, K. S., & Aggarwal, B. B. (2008). Targeting nuclear factor- κ B activation pathway by thymoquinone: role in suppression of antiapoptotic gene products and enhancement of apoptosis. *Molecular cancer research*, 6(6), 1059-1070.
- She, J., Holden, A., Sharp, M., Tanner, M., Williams-Derry, C., & Hooper, K. (2007). Polybrominated diphenyl ethers (PBDEs) and polychlorinated biphenyls (PCBs) in breast milk from the Pacific Northwest. *Chemosphere*, 67(9), S307-S317.
- She, J., Petreas, M., Winkler, J., Visita, P., McKinney, M., & Kopec, D. (2002). PBDEs in the San Francisco Bay Area: measurements in harbor seal blubber and human breast adipose tissue. *Chemosphere*, 46(5), 697-707.
- Shoemaker, T., Kono, T., Mariash, C., & Evans-Molina, C. (2012). Thyroid hormone analogues for the treatment of metabolic disorders: new potential for unmet clinical needs?. *Endocrine Practice*, 18(6), 954-964.
- Sjödin, A., Jones, R. S., Focant, J. F., Lapeza, C., Wang, R. Y., McGahee 3rd, E. E., ... & Patterson Jr, D. G. (2004). Retrospective time-trend study of polybrominated diphenyl ether and polybrominated and polychlorinated biphenyl levels in human serum from the United States. *Environmental health perspectives*, 112(6), 654.
- Stapleton, H. M., Sjödin, A., Jones, R. S., Niehüser, S., Zhang, Y., & Patterson Jr, D. G. (2008). Serum levels of polybrominated diphenyl ethers (PBDEs) in foam recyclers and carpet installers working in the United States. *Environmental science & technology*, 42(9), 3453-3458.

Stein, C. R., Savitz, D. A., & Dougan, M. (2009). Serum levels of perfluorooctanoic acid and perfluorooctane sulfonate and pregnancy outcome. *American journal of epidemiology*, 170(7), 837-846.

Tao, L., Kannan, K., Wong, C. M., Arcaro, K. F., & Butenhoff, J. L. (2008). Perfluorinated compounds in human milk from Massachusetts, USA. *Environmental science & technology*, 42(8), 3096-3101.

Tao, L., Ma, J., Kunisue, T., Libelo, E. L., Tanabe, S., & Kannan, K. (2008). Perfluorinated compounds in human breast milk from several Asian countries, and in infant formula and dairy milk from the United States. *Environmental science & technology*, 42(22), 8597-8602.

Timmermann, C. A. G., Rossing, L. I., Grøntved, A., Ried-Larsen, M., Dalgård, C., Andersen, L. B., ... & Jensen, T. K. (2014). Adiposity and glycemic control in children exposed to perfluorinated compounds. *The Journal of Clinical Endocrinology & Metabolism*, 99(4), E608-E614.

Tung, E. W., Boudreau, A., Wade, M. G., & Atlas, E. (2014). Induction of adipocyte differentiation by polybrominated diphenyl ethers (PBDEs) in 3T3-L1 cells. *PloS one*, 9(4), e94583.

US Environmental Protection Agency. Technical Fact Sheet—Polybrominated Diphenyl Ethers (PBDEs) and Polybrominated Biphenyls (PBBs). <http://www2.epa.gov/fedfac/technical-fact-sheet-polybrominated-diphenyl-ethers-pbdes-and-polybrominated-biphenyls-pbbs>. Published January 2014. Accessed July 18, 2017

Verga Falzacappa, C., Mangialardo, C., Raffa, S., Mancuso, A., Piergrossi, P., Moriggi, G., ... & Toscano, V. (2010). The thyroid hormone T3 improves function and survival of rat pancreatic islets during in vitro culture. *Islets*, 2(2), 96-103.

Wijesekara, N., Krishnamurthy, M., Bhattacharjee, A., Suhail, A., Sweeney, G., & Wheeler, M. B. (2010). Adiponectin-induced ERK and Akt phosphorylation protects against pancreatic beta cell apoptosis and increases insulin gene expression and secretion. *Journal of Biological Chemistry*, 285(44), 33623-33631.

Ximenes, H. M., Lortz, S., Jörns, A., & Lenzen, S. (2007). Triiodothyronine (T₃)-mediated toxicity and induction of apoptosis in insulin-producing INS-1 cells. *Life sciences*, 80(22), 2045-2050.

Xu, W., Wang, X., & Cai, Z. (2013). Analytical chemistry of the persistent organic pollutants identified in the Stockholm Convention: A review. *Analytica chimica acta*, 790, 1-13.

Yamamoto, J., Yamane, T., Oishi, Y., & Kobayashi-Hattori, K. (2015). Perfluorooctanoic acid binds to peroxisome proliferator-activated receptor γ and promotes adipocyte differentiation in 3T3-L1 adipocytes. *Bioscience, biotechnology, and biochemistry*, 79(4), 636-639.

Yan, L. J. (2014). Pathogenesis of chronic hyperglycemia: from reductive stress to oxidative stress. *Journal of diabetes research*, 2014.

Zawalich, W. S., Tesz, G. J., & Zawalich, K. C. (2002). Inhibitors of phosphatidylinositol 3-kinase amplify insulin release from islets of lean but not obese mice. *Journal of Endocrinology*, 174(2), 247-258.

Zhang, Z., Li, S., Liu, L., Wang, L., Xiao, X., Sun, Z., ... & Xu, Q. (2016). Environmental exposure to BDE47 is associated with increased diabetes prevalence: Evidence from community-based case-control studies and an animal experiment. *Scientific reports*, 6.

1.12 Tables and Figures

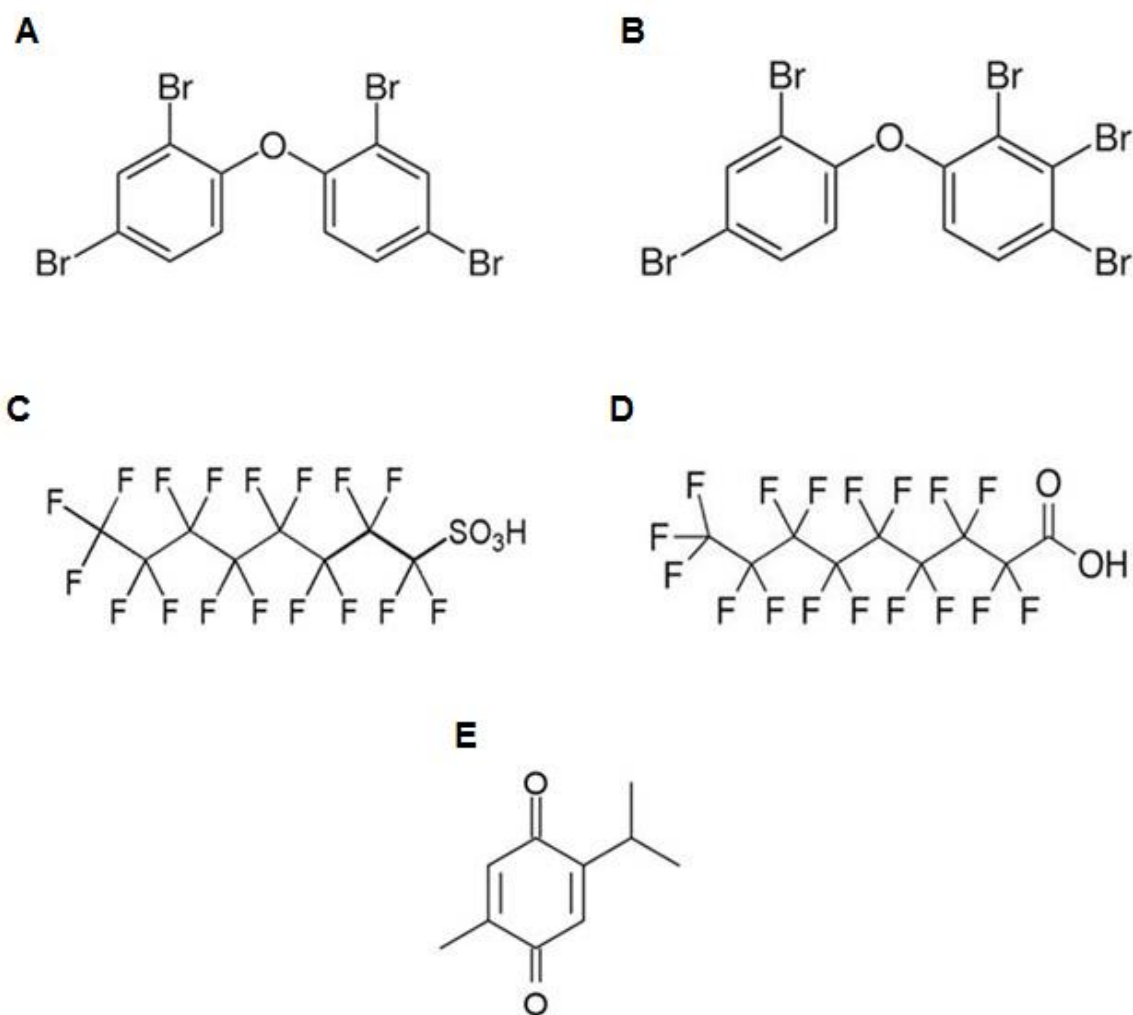


Figure 1.1 Illustration of chemical structures. Chemical structures of BDE-47 (A), BDE-85 (B), PFOS (C), PFNA (D), and thymoquinone (E).

CHAPTER TWO:

EFFECTS OF SELECTED POPs ON INSULIN SECRETION

2.1 The Importance of Identifying Potential Agents that Contribute to β -cell Dysfunction

Pancreatic β -cells are one of the key components in maintaining glucose homeostasis. They are encapsulated within the pancreatic islets, which are robust structures that in addition to beta cells, also contain glucagon producing alpha cells, somatostatin producing delta cells, and pancreatic polypeptide producing gamma cells (Steiner et al., 2010). Pancreatic islets are highly vascularized, which allows for their glucose-sensing capability (Steiner et al., 2010). β -cells secrete insulin in response to elevated blood glucose levels (e.g. following a meal), which helps re-establish normoglycemia by promoting glucose uptake and utilization by insulin-sensitive peripheral tissues (Kahn et al., 2014). Insulin also suppresses hepatic gluconeogenesis as a signal that the body doesn't need more glucose, which helps establish normoglycemia (Muoio and Newgard, 2008). In non-diabetic individuals, there is cross-talk between pancreatic beta cells and insulin-sensitive tissues (most importantly liver, skeletal muscle, and adipose tissue) that allows for adequate insulin secretion (Kahn et al., 2006; Kahn et al., 2014). Failure of this communication continuum can lead to the emergence of type 2 diabetes, although the mechanisms by which this occurs are not clear. One traditional view is that insulin resistance (or the inability of insulin to enter and/or exert its metabolic functions in target tissues) causes overproduction of insulin from β -cells to compensate for this resistance, which eventually leads to β -cell failure and hyperglycemia (Kahn et al., 2014). This view is supported by observations that in early diabetes, there is increased β -cell mass and hyperinsulinemia (Kahn et al., 2006; Fu et al., 2013). This increased β -cell function, on the other hand, may cause hyperinsulinemia, which can worsen insulin resistance (Shanik et al., 2008). Another view is that insulin secretion and

insulin sensitivity are in a continuum (Kahn et al., 2014); however, it is widely accepted that β -cell failure is a critical step in the emergence of hyperglycemia (Kahn et al., 2006; Kahn et al., 2014; Muoio and Newgard, 2008; Fu et al., 2013). Thus, any deviation from normal β -cell function (e.g. β -cell failure or overstimulation) has very important implications in glucose homeostasis and development of type 2 diabetes. Because of this, it is crucial to identify potential factors that can alter pancreatic β -cell function. In the current work, we examined the direct role of environmental pollutants, PFOS, PFNA, BDE-47, and BDE-85 in pancreatic β -cell function using the INS-1 832/13 insulin-producing cells.

2.2 Hypothesis

Exposure of INS-1 832/13 cells to PFOS, PFNA, BDE-47, or BDE-85 will increase glucose-stimulated insulin secretion compared to vehicle control treated cells.

2.3 Methods

2.3.1 INS-1 832/13 Cell Culture and Maintenance

INS-1 832/13 cells (passages 51-60), provided by Dr. Christopher Newgard (Duke University School of Medicine) were cultured in RPMI-1640 glucose-free medium supplemented with 11 mmol/l glucose, 10% fetal bovine serum, 1mmol/l sodium pyruvate, 5mmol/l HEPES, 2g/L sodium bicarbonate, 2mmol/l L-glutamine, 50 μ mol/l 2-mercaptoethanol, 10000 U/ml penicillin, and 10 mg/ml streptomycin (Karandrea et al., 2017). Cells were maintained at 37°C in a humidified incubator with 5% CO₂. Cells were subcultured when confluency was around 80% and medium was replaced every 3 days.

2.3.2 Glucose-stimulated Insulin Secretion (GSIS)

INS-1 832/13 cells grown to confluency in 24 well plates, were washed 3 times with and pre-incubated in Krebs Ringer Buffer (KRB) (120 mM NaCl, 25 mM HEPES, 4.6 mM KCl, 1 mM MgSO₄, 0.15 mM Na₂HPO₄, 0.4 mM KH₂PO₄, 5 mM NaHCO₃, 2 mM CaCl₂) containing 3 mmol/l glucose at 37°C for 2 h; followed by a static 1 h incubation at 37°C in KRB containing 3 or 16 mmol/l glucose. KRB buffer was collected and centrifuged at 5000 x g for 3 min at 4°C to pellet

out any cells. For acute GSIS, compounds were present only during the 1hr static incubation phase. Insulin secreted in buffer was measured by an ELISA kit (Alpco Diagnostics, Salem, NH). All insulin secretion data shown in this study were normalized to the total protein content, measured by the Micro-BCA Protein Assay kit (Pierce, Rockford, IL). For chronic pre-treatment, cells were exposed to indicated concentrations of BDE-47 and BDE-85 in complete growth media for 48 hours, after which cells were washed and preincubated in KRB buffer containing 3 mmol/l glucose and static incubation was performed as described above (compounds not present during the 2 hr pre-incubation or static 1hr glucose stimulation). For all insulin secretion experiments, controls cells were treated with vehicle (DMSO) at 0.1% concentration. Acute vs. chronic pre-treatment exposure design for GSIS is illustrated in Figure 2.1.

2.3.3 Cell Viability

Cell viability was measured by the reduction of Cell Titer Blue (Promega, Madison, WI) according to the manufacturer's protocol. Cells were plated in 96-well plates and treated with indicated concentrations of compounds for 48 hours in culture medium, after which Cell Titer Blue (10% in growth medium) was added to wells and the increase in fluorescence (560 nm excitation, 590 nm emission) was measured using a SpectraMax M5 multi-mode microplate reader (Molecular Devices, Sunnyvale, CA). IC_{50} was calculated using a least squares fit with variable slope using GraphPad Prism (version 6.07).

2.3.4 Chemicals

BDE-47 and BDE-85 were purchased from AccuStandard (New Haven, CT). PFOS and PFNA were purchased from Sigma (St. Louis, MO). Stock solutions (25 mM for BDE-47 and BDE-85; 100 mM for PFOS and PFNA) of BDE-47, BDE-85, PFOS, and PFNA were prepared in dimethyl sulfoxide (DMSO) and were added directly to the culture medium and/or KRB buffer to achieve the indicated concentrations.

2.3.5 Statistical Analysis

Data are expressed as means \pm SEM and are representative from at least three independent experiments performed in quadruplicates or octuplets (for cell viability only). Significance was determined for multiple comparisons using one or two-way analysis of variance (ANOVA) followed by Sidak post-hoc analysis (Abdi, 2007). A p-value of ≤ 0.05 was considered significant. All analyses were conducted using the GraphPad Prism (version 6.07) statistical program software.

2.4 Results

2.4.1 Concentration-response Curves for Cell Viability After 48-hour Exposure to PFOS, PFNA, BDE-47 or BDE-85

Due to the absence of prior studies on the effect of PFOS, PFNA, BDE-47, and BDE-85 on INS-1 832/13 cell viability, we performed concentration-response curves during a 48-hour exposure with each respective compound. Furthermore, it is important to choose concentrations of compounds that don't cause cell death, which could be a confounding factor for GSIS, particularly during the 48-hour chronic pre-treatment exposure. Based on prior studies about *in-vitro* toxicity of each of the four compounds in different cell lines (Hu and Hu, 2009; Jin et al., 2010; Kleszczyński et al., 2007; Yan et al., 2011), we chose the following concentrations for our viability studies: PFOS and PFNA (0, 50, 100, 150, 200, 250, 300, 350, 400, 450, 500, and 600 μ M); and for BDE-47 and BDE-85 (0, 25, 50, 75, 100, 125, 150, 175, 200, 225, 250 μ M). We were able to observe a concentration-dependent decrease in cell viability in the chosen concentration ranges for each compound (Figure 2.2). PFOS and PFNA had similar IC₅₀ values (394.9 μ M and 370.7 μ M respectively), as did BDE-47 and BDE-85 (108.50 μ M and 111.5 μ M respectively). These results corroborate prior studies and our IC₅₀ values are within the range reported for these four compounds (Hu and Hu, 2009; Jin et al., 2010; Kleszczyński et al., 2007; Yan *et al.*, 2011), albeit tested in different cell lines and with different exposure times in these prior studies.

2.4.2 PFOS Does Not Affect GSIS During Chronic Pre-treatment and Acute Exposure

Chronic pre-treatment GSIS with 10 μM PFOS did not affect insulin secretion compared to vehicle control (Figure 2.3 A). During an acute GSIS, exposure to 10, 25, and 50 μM PFOS did not significantly alter insulin secretion compared to vehicle control, although there was a trend towards increased insulin secretion particularly at the 25 μM concentration, which did not reach statistical significance (Figure 2.3 B). No changes were observed between groups in basal (3 mM) glucose conditions compared to vehicle control (Figure 2.3 A and B)

2.4.3 PFNA Does Not Affect GSIS During Chronic Pre-treatment and Acute Exposure

Chronic pre-treatment GSIS with 10 μM PFNA did not affect insulin secretion compared to vehicle control (Figure 2.4 A). During an acute GSIS, exposure to 10, 25, and 50 μM PFNA did not significantly alter insulin secretion compared to vehicle control, although there was a trend towards increased insulin secretion, which did not reach statistical significance (Figure 2.4 B). No changes were observed between groups in basal (3 mM) glucose conditions compared to vehicle control (Figure 2.4 A and B)

2.4.4 BDE-47 Does Not affect GSIS During Chronic Pre-treatment; Increases Acute GSIS

Chronic pre-treatment GSIS with 10 μM BDE-47 did not affect insulin secretion compared to vehicle control (Figure 2.5 A). Acute GSIS with 5 and 10 μM BDE-47 caused a significant increase in insulin secretion, with no change at the 1 μM concentration (Figure 2.5 B). Higher concentrations of BDE-47 (25 and 50 μM) also significantly increased insulin secretion during an acute GSIS (Figure 2.7 A), with the maximal response occurring at 25 μM . No changes were observed between groups in basal (3 mM) glucose conditions compared to vehicle control (Figure 2.5 A and B, Figure 2.7 A).

2.4.5 BDE-85 Does Not Affect GSIS During Chronic Pre-treatment; Increases Acute GSIS

Chronic pre-treatment GSIS with 10 μM BDE-85 did not affect insulin secretion compared to vehicle control (Figure 2.6 A). Acute GSIS with 1, 5, 10 μM BDE-85 caused a significant increase in insulin secretion compared to vehicle controls (Figure 2.6 B). Higher concentrations of BDE-85 (25 and 50 μM) also significantly increased insulin secretion during an acute GSIS (Figure 2.7 B), with the maximal response occurring at 25 μM . No changes were observed between groups in basal (3 mM) glucose conditions compared to vehicle control (Figure 2.6 A and B, Figure 2.7 B).

2.5 Discussion

Epidemiological and animal studies suggest a potential role of PBDEs and PFCs in contributing to the development of type 2 diabetes (Airaksinen et al., 2011; Fang et al., 2012; Lin et al., 2009; Zhang et al., 2016; Timmerman et al., 2014). However, the precise mechanisms are not known. In the present study, we investigated the role of PFOS, PFNA, BDE-47, and BDE-85 in pancreatic β -cell function. We found that BDE-47 and BDE-85 increased acute GSIS, and there was a trend towards increased GSIS during acute incubation with PFOS and PFNA which was not statistically significant. Neither compound increased GSIS during chronic-pretreatment. This suggests that the effect of BDE-47 and BDE-85 on GSIS is not likely due to potential changes in expression of metabolic enzymes or transcription factors involved in GSIS, but rather could be due to acute actions, such as increasing insulin granule exocytosis. Due to the fact that PFOS and PFNA did not elicit a significant increase in GSIS compared to controls, we chose to examine only the potential mechanisms of GSIS potentiation by BDE-47 and BDE-85 in our subsequent work described in chapter three.

GSIS is initiated when glucose enters the β -cell and gets metabolized (glycolysis), which leads to an increase in ATP/ADP ratio, closure of K_{ATP} channels, membrane depolarization, opening of voltage-gated Ca^{2+} channels, calcium entry, and the eventual calcium-induced insulin

granule exocytosis (Rorsman et al., 2000). It is widely accepted that glucose induces a biphasic release of insulin from β -cells, with the first phase being a rapid response involving the change in energy described above, and the second phase where the signal is amplified leading to more insulin secretion over time (Rorsman et al., 2000; Henquin et al., 2002). Insulin secretagogues, or compounds that increase insulin secretion, are classified into nutrient (e.g. glucose, GLP-1, GIP-1) and non-nutrient (e.g. KCl, sulfonylureas) secretagogues, with only the former believed to induce the biphasic insulin secretion (Rorsman et al., 2000). Non-nutrient secretagogues can increase insulin secretion even during low glucose concentrations by closing K_{ATP} channels (Proks et al., 2002). Other environmental pollutants that are similar in structure to PBDEs, such as polychlorinated biphenyls (PCBs) have been shown to increase insulin release from RINm5F cells by increasing intracellular calcium stores (Fischer et al., 1996; Fischer et al., 1999). These studies have suggested that PCBs act in similar fashion to insulin secretagogues to increase intracellular calcium stores and consequently insulin secretion. It is possible that BDE-47 and BDE-85 may act via this pathway to increase insulin secretion. As we observed, during low glucose concentrations at basal conditions (3 mM), BDE-47 and BDE-85 did not increase insulin secretion, suggesting that their effects are dependent on glucose stimulation. Thus, it is unlikely that these compounds act as non-nutrient secretagogues to independently close K_{ATP} channels. It is possible that BDE-47 and BDE-85 potentiate GSIS by other unknown pathways that may increase insulin granule exocytosis independent of increasing intracellular calcium levels.

The increase in GSIS observed with the exposure to these compounds can have important potential implications in long-term β -cell function and glucose homeostasis. Exposure to POPs, such as BDE-47 and BDE-85, coupled with a nutrient-rich diet, may cause insulin oversecretion, which can lead to β -cell exhaustion and failure. Furthermore, insulin oversecretion may cause hyperinsulinemia, which can lead to desensitization of insulin receptors in peripheral tissues and insulin resistance (Fu et al., 2013; Grill and Björklund, 2002).

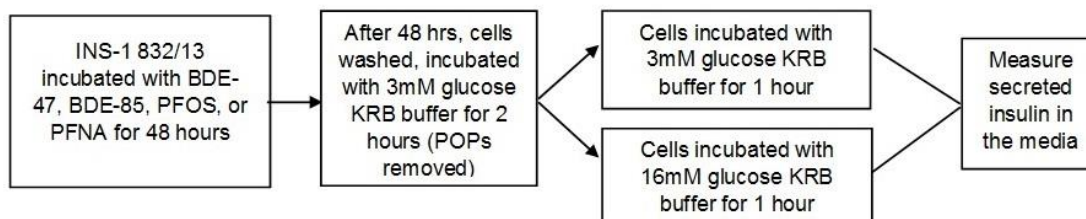
2.6 References

- Abdi, H. (2007). Bonferroni and Šidák corrections for multiple comparisons. *Encyclopedia of measurement and statistics*, 3, 103-107.
- Airaksinen, R., Rantakokko, P., Eriksson, J. G., Blomstedt, P., Kajantie, E., & Kiviranta, H. (2011). Association between type 2 diabetes and exposure to persistent organic pollutants. *Diabetes care*, 34(9), 1972-1979.
- Fang, X., Gao, G., Xue, H., Zhang, X., & Wang, H. (2012). Exposure of perfluorononanoic acid suppresses the hepatic insulin signal pathway and increases serum glucose in rats. *Toxicology*, 294(2), 109-115.
- Fischer, L. J., Wagner, M. A., & Madhukar, B. V. (1999). Potential involvement of calcium, CaM kinase II, and MAP kinases in PCB-stimulated insulin release from RINm5F cells. *Toxicology and applied pharmacology*, 159(3), 194-203.
- Fischer, L. J., Zhou, H. R., & Wagner, M. A. (1996). Polychlorinated biphenyls release insulin from RINm5F cells. *Life sciences*, 59(24), 2041-2049.
- Fu, Z., R Gilbert, E., & Liu, D. (2013). Regulation of insulin synthesis and secretion and pancreatic Beta-cell dysfunction in diabetes. *Current diabetes reviews*, 9(1), 25-53.
- Grill, V., & Björklund, A. (2002). Type 2 Diabetes—Effect of Compensatory Oversecretion as a Reason for β -Cell Collapse. *Journal of Diabetes Research*, 3(3), 153-158.
- Henquin, J. C., Ishiyama, N., Nenquin, M., Ravier, M. A., & Jonas, J. C. (2002). Signals and pools underlying biphasic insulin secretion. *Diabetes*, 51(suppl 1), S60-S67.
- Hu, X. Z., & Hu, D. C. (2009). Effects of perfluorooctanoate and perfluorooctane sulfonate exposure on hepatoma Hep G2 cells. *Archives of toxicology*, 83(9), 851-861.
- Jin, S., Yang, F., Hui, Y., Xu, Y., Lu, Y., & Liu, J. (2010). Cytotoxicity and apoptosis induction on RTG-2 cells of 2, 2', 4, 4'-tetrabromodiphenyl ether (BDE-47) and decabrominated diphenyl ether (BDE-209). *Toxicology in Vitro*, 24(4), 1190-1196.
- Kahn, S. E., Cooper, M. E., & Del Prato, S. (2014). Pathophysiology and treatment of type 2 diabetes: perspectives on the past, present, and future. *The Lancet*, 383(9922), 1068-1083.
- Kahn, S. E., Hull, R. L., & Utzschneider, K. M. (2006). Mechanisms linking obesity to insulin resistance and type 2 diabetes. *Nature*, 444(7121), 840-846.
- Karandrea, S., Yin, H., Liang, X., & Heart, E. A. (2017). BDE-47 and BDE-85 stimulate insulin secretion in INS-1 832/13 pancreatic β -cells through the thyroid receptor and Akt. *Environmental Toxicology and Pharmacology*, 56, 29-34.
- Kleszczyński, K., Gardzielewski, P., Mulkiewicz, E., Stepnowski, P., & Składanowski, A. C. (2007). Analysis of structure–cytotoxicity in vitro relationship (SAR) for perfluorinated carboxylic acids. *Toxicology in vitro*, 21(6), 1206-1211.

- Lin, C. Y., Chen, P. C., Lin, Y. C., & Lin, L. Y. (2009). Association among serum perfluoroalkyl chemicals, glucose homeostasis, and metabolic syndrome in adolescents and adults. *Diabetes care*, 32(4), 702-707.
- Muoio, D. M., & Newgard, C. B. (2008). Molecular and metabolic mechanisms of insulin resistance and β -cell failure in type 2 diabetes. *Nature reviews Molecular cell biology*, 9(3), 193-205.
- Proks, P., Reimann, F., Green, N., Gribble, F., & Ashcroft, F. (2002). Sulfonylurea stimulation of insulin secretion. *Diabetes*, 51(suppl 3), S368-S376.
- Rorsman, P., Eliasson, L., Renström, E., Gromada, J., Barg, S., & Göpel, S. (2000). The cell physiology of biphasic insulin secretion. *Physiology*, 15(2), 72-77.
- Shanik, M. H., Xu, Y., Škrha, J., Dankner, R., Zick, Y., & Roth, J. (2008). Insulin resistance and hyperinsulinemia. *Diabetes care*, 31(Supplement 2), S262-S268.
- Steiner, D. J., Kim, A., Miller, K., & Hara, M. (2010). Pancreatic islet plasticity: interspecies comparison of islet architecture and composition. *Islets*, 2(3), 135-145.
- Timmermann, C. A. G., Rossing, L. I., Grøntved, A., Ried-Larsen, M., Dalgård, C., Andersen, L. B., ... & Jensen, T. K. (2014). Adiposity and glycemic control in children exposed to perfluorinated compounds. *The Journal of Clinical Endocrinology & Metabolism*, 99(4), E608-E614.
- Yan, C., Huang, D., & Zhang, Y. (2011). The involvement of ROS overproduction and mitochondrial dysfunction in PBDE-47-induced apoptosis on Jurkat cells. *Experimental and toxicologic pathology*, 63(5), 413-417.
- Zhang, Z., Li, S., Liu, L., Wang, L., Xiao, X., Sun, Z., ... & Xu, Q. (2016). Environmental exposure to BDE47 is associated with increased diabetes prevalence: Evidence from community-based case-control studies and an animal experiment. *Scientific reports*, 6, 27854.

2.7 Tables and Figures

A.



B.

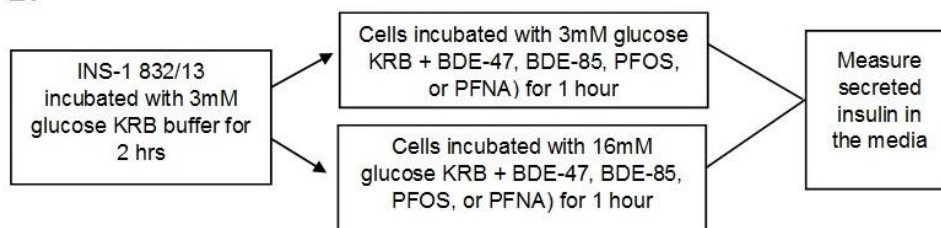


Figure 2.1 Experimental design workflow to test the effects of selected POPs on GSIS. INS-1 832-13 cells will be chronically pre-treated with BDE-47, BDE-85, PFOS, or PFNA for 48-hours in growth medium, after which GSIS will be conducted in the absence of compounds (A). Exposure of INS-1 832-13 cells to BDE-47, BDE-85, PFOS, or PFNA will occur during GSIS in either 3mM or 16 mM glucose KRB buffer during a 1 hour acute treatment (B).

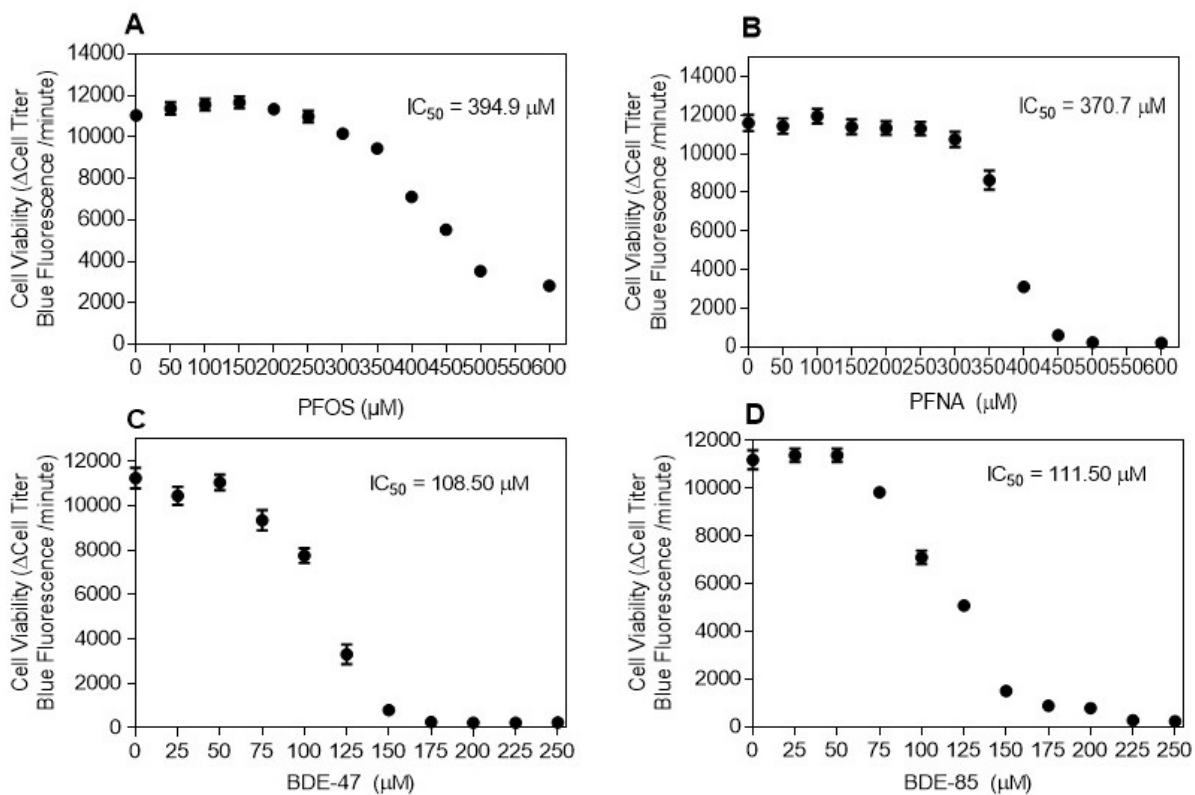


Figure 2.2 PFOS, PFNA, BDE-47, and BDE-85 affect INS-1 832/13 cell viability. Cell viability studies in INS-1 832/13 cells treated with PFOS, $IC_{50} = 394.90 \mu M$ (A), PFNA, $IC_{50} = 370.70 \mu M$ (B), BDE-47, $IC_{50} = 108.50 \mu M$ (C), and BDE-85, $IC_{50} = 111.50 \mu M$ (D) for 48 hours. Data are means \pm SEM from three independent experiments performed in octuplets ($n = 3$).

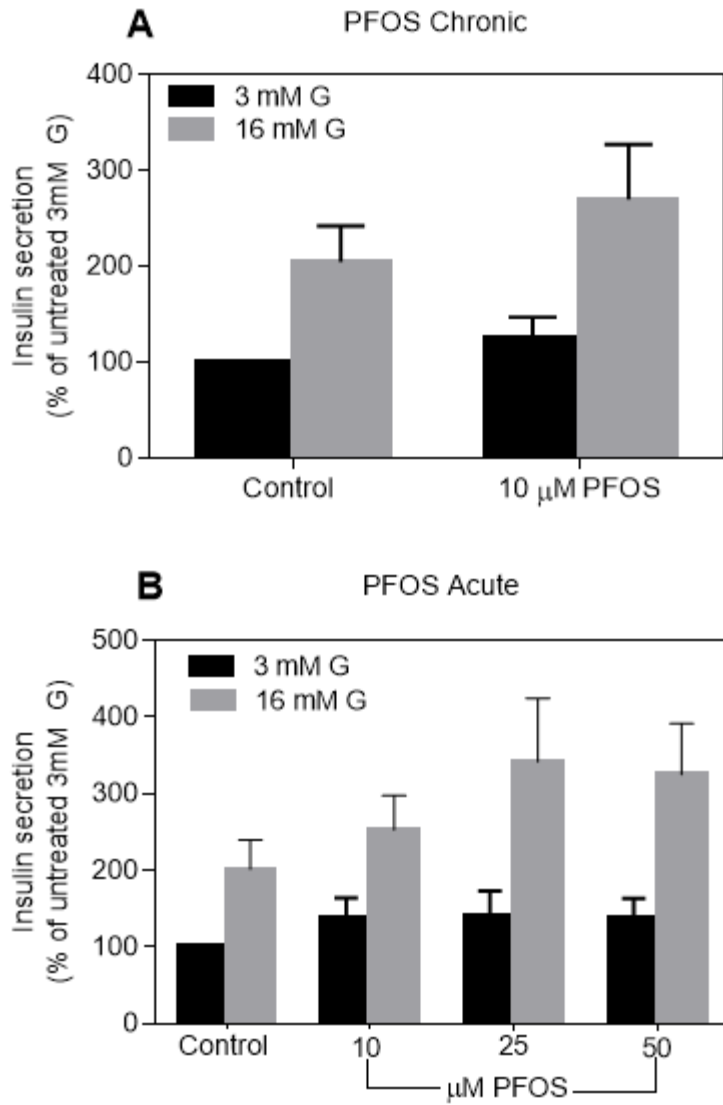


Figure 2.3. Chronic pre-treatment and acute exposure to PFOS does not affect GSIS. GSIS in INS-1 832/13 cells incubated with 10 μ M PFOS during chronic pre-treatment exposure (A) and 10, 25, or 50 μ M PFOS during an acute (B) exposure. No significant differences were noted in the groups compared to vehicle controls using two-way ANOVA followed by Sidak post-test. 3 mM G = 3mM glucose, 16 mM G = 16mM glucose. Data are means \pm SEM from three independent experiments performed in quadruplicates (n = 3).

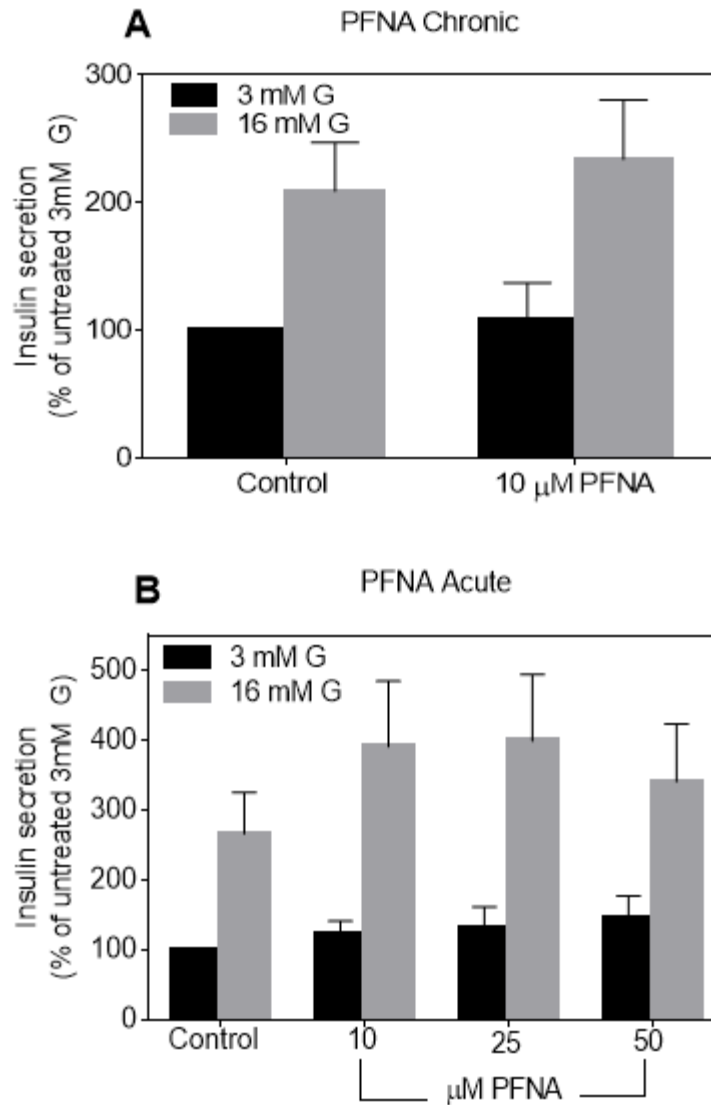


Figure 2.4 Chronic pre-treatment and acute exposure to PFNA does not affect GSIS. GSIS in INS-1 832/13 cells incubated with 10 μ M PFNA during chronic pre-treatment exposure (A) and 10, 25, or 50 μ M PFNA during an acute (B) exposure. No significant differences were noted in the groups compared to vehicle controls using two-way ANOVA followed by Sidak post-test. 3 mM G = 3mM glucose, 16 mM G = 16 mM glucose. Data are means \pm SEM from three independent experiments performed in quadruplicates (n = 3).

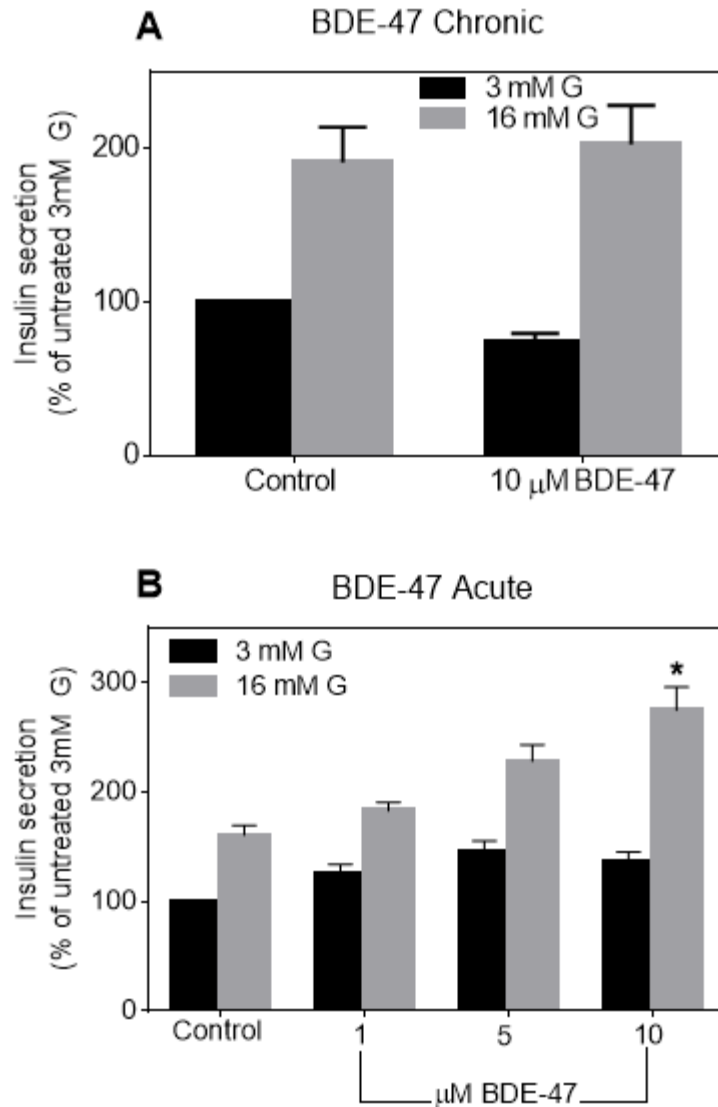


Figure 2.5 BDE-47 potentiates GSIS during acute exposure but not during chronic pre-treatment. GSIS in INS-1 832/13 cells incubated with 10 μ M BDE-47 during chronic pre-treatment (A), and 1, 5, or 10 μ M BDE-47 during an acute (B) exposure. No significant differences were noted in the 10 μ M BDE-47 group compared to vehicle control (A). No significant differences in the 1 and 5 μ M BDE-47 groups compared to vehicle control, 10 μ M BDE-47 significantly increased GSIS compared to control (B). * $p < 0.05$ when compared to 16 mM G vehicle control using two-way ANOVA followed by Sidak post-test. 3 mM G = 3mM glucose, 16 mM G = 16mM glucose. Data are means \pm SEM from three independent experiments performed in quadruplicates (n = 3).

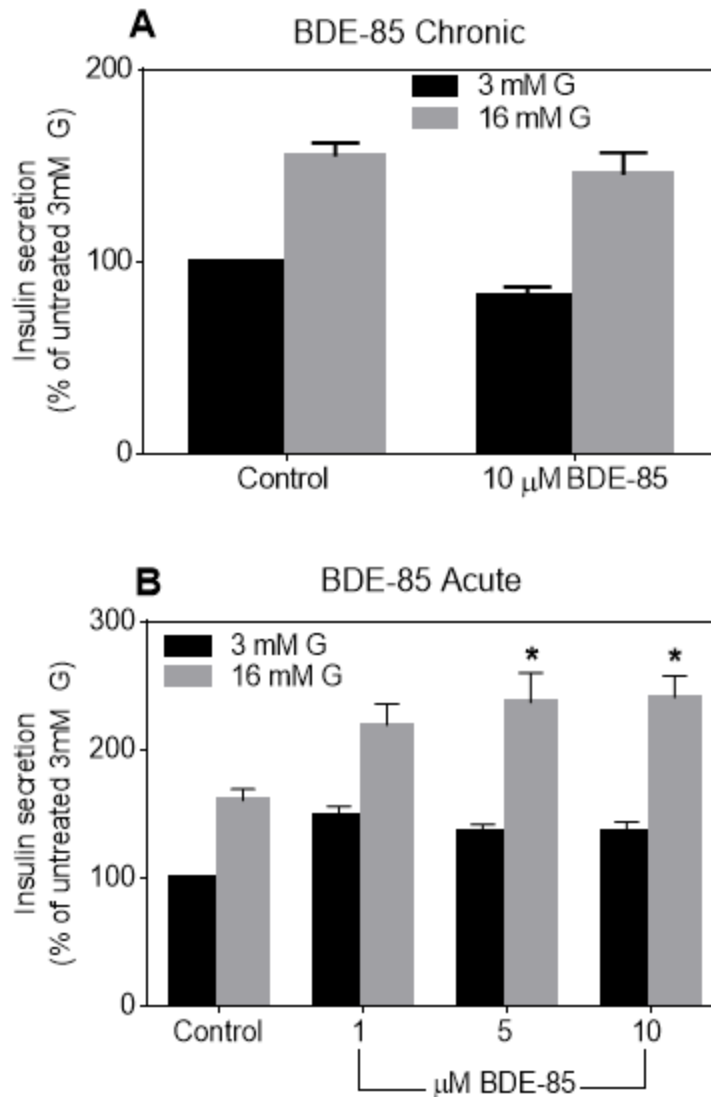


Figure 2.6 BDE-85 potentiates GSIS during acute exposure but not during chronic pre-treatment. GSIS in INS-1 832/13 cells incubated with 10 μ M BDE-85 during chronic pre-treatment (A), and 1, 5, or 10 μ M BDE-85 during an acute (B) exposure. No significant differences were noted in the 10 μ M BDE-85 group compared to vehicle control (A). No significant differences in the 1 μ M BDE-47 group compared to vehicle control, 5 and 10 μ M BDE-47 significantly increased GSIS compared to control (B). * $p < 0.05$ when compared to 16 mM G vehicle control using two-way ANOVA followed by Sidak post-test. 3 mM G = 3mM glucose, 16 mM G = 16mM glucose. Data are means \pm SEM from three independent experiments performed in quadruplicates (n = 3).

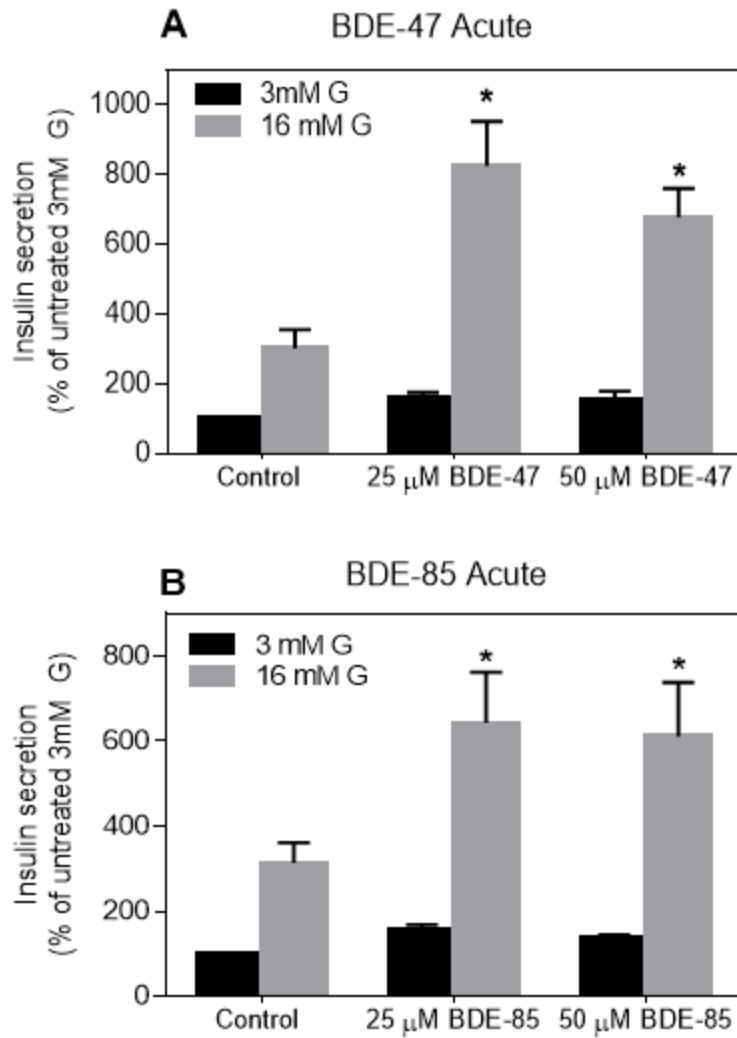


Figure 2.7 High concentrations of BDE-47 and BDE-85 potentiate acute GSIS. GSIS in INS-1 832/13 cells incubated with 25 or 50 μ M BDE-47 (A) and BDE-85 (B) during an acute exposure. * $p < 0.05$ when compared with 16mM G vehicle control using two-way ANOVA followed by Sidak post-test. 3 mM G = 3mM glucose, 16 mM G = 16mM glucose. Data are means \pm SEM from three independent experiments performed in quadruplicates ($n = 3$).

CHAPTER THREE:

POTENTIAL MECHANISMS FOR BDE-47 AND BDE-85-MEDIATED INCREASE IN GSIS

3.1 Polybrominated Diphenyl Ethers and Thyroid Hormone Receptor

PBDEs have structural similarities with thyroid hormones and may disrupt thyroid hormone signaling by binding to thyroid receptor and mimicking thyroid hormones (Ren and Guo, 2013). One of the ways that PBDEs interfere with normal thyroid hormone signaling is by interfering with thyroid hormone transport proteins, such as transthyretin. A study measuring the effect of BDE-47 on plasma levels of thyroxine (T4) in rats found that it leads to decreased circulating thyroxine (Hallgren and Darnerud, 2002). This result was confirmed by other studies reporting a decrease in plasma thyroid hormones after BDE-47 exposure in both mice and rats (Hallgren et al., 2001; Richardson et al., 2007). Furthermore, these studies established that the decrease in thyroid hormone concentration was not due to inhibiting thyroid hormone production, but rather decreasing the expression and activity of one of the major T4 carriers, transthyretin (Hallgren et al., 2001; Hallgren and Darnerud, 2002; Richardson et al., 2007). In addition to decreasing plasma T4 levels, dietary exposure to BDE-47 has been reported to alter the expression levels of thyroid hormone receptor in the brains of male and female minnows; revealing that these effects are consistent even in non-mammalian species (Lema et al., 2008). Furthermore, direct binding and affinity to transthyretin has been shown in competitive *in vitro* assays for BDE-47 and some of its hydroxylated metabolites (Cao et al., 2010; Hamers et al., 2008; Morgado et al., 2007).

Another way that PBDEs disrupt thyroid hormone signaling is by directly binding to the thyroid receptor. Several studies have measured via *in vitro* assays whether different PBDE congeners bind directly to the thyroid hormone receptor. A study using chinese hamster ovary (CHO) cells showed that BDE-85, but not BDE-47 inhibited T3 binding to thyroid receptor alpha

1 (TR α 1), acting as a weak agonist (Nakamura et al., 2013). BDE-47 decreased mRNA and protein levels of TR α 1 and TR β 1 isoforms in HepG2 cells (Hu et al., 2014). Several PBDE congeners showed thyroid hormone-like activity in the absence of thyroid hormone, and potentiated T3-dependent cell proliferation in the rat pituitary tumor cell line GH3 in the absence of T3, showing TR agonistic activity (Hamers et al., 2006). Another study reported weak TR agonistic activities for several PBDE congeners, which was not statistically significant, and reported strong T3 antagonistic effects for BDE-206 using the GH3 screen mentioned above (Schriks et al., 2006). In addition, hydroxylated metabolites of BDE-47 have been shown to bind to the thyroid receptor and inhibit T3 binding (Kitamura et al., 2008). In another study, hydroxylated metabolites of BDE-47 were shown to have TR agonistic activity and enhance T3-dependent GH3 cell proliferation (Ren et al., 2013). From these studies, there are contradicting effects on the role of PBDEs and their metabolites on the thyroid receptor, as both agonistic and antagonistic activities have been reported. Some of them are due to the use of different cell lines for evaluating whether PBDEs directly bind to the TR and only recently studies have taken a more integrative approach for evaluating this relationship (Ren et al., 2013).

In human studies, PBDE exposure has been associated with thyroid hormone signaling parameters, however conflicting results have been reported. In a study looking at the associations between PBDE levels and thyroid hormones in a healthy adult population in North America, several PBDEs (including BDE-47) were associated with decreased serum T4 levels, which is similar to what is observed in animal studies (Makey et al., 2016). This study also reported that PBDEs were not associated with T3 or thyroid stimulating hormone (TSH), suggesting that PBDE exposure doesn't affect the hypothalamus-pituitary-thyroid axis, which controls thyroid hormone production and homeostasis (Makey et al., 2016). In a population of Great Lakes fishermen, which can be exposed to higher PBDE levels since the fish species in these lakes have been reported to be high in PBDE content (Luross et al., 2002), it was found that PBDEs were not associated with thyroid hormones (Bloom et al., 2008). BDE-47, BDE-85 and the other PBDE

congeners were not associated with T4, T3, or TSH levels in this study. However, studies in humans have also reported a positive association between BDE-47 and T4 levels, with T3 shown to be negatively associated with T3 and TSH (Turyk et al., 2008).

Taken together, the studies in cells, animals, and humans show that PBDEs can affect thyroid hormone balance by a variety of mechanisms, such as thyroid hormone transport disruption, mimicking thyroid hormone effects, and potentially acting as agonists and antagonists to alter thyroid signaling at the level of the thyroid receptor. Since thyroid hormone signaling is important in normal development and metabolism, imbalance of such pathways may interfere not only with growth, but also have important metabolic effects (Mullur et al., 2014).

3.2 Polybrominated Diphenyl Ethers and Akt Activation

In addition to interfering with thyroid hormone homeostasis, PBDEs have been shown to activate the PI3K-Akt pathway. Activation of this pathway has implications in cell growth and proliferation, as well as insulin signaling (Guo et al., 2014) and insulin secretion from pancreatic β -cells (Bernal-Mizrachi et al., 2014). Since upregulation and constant activation of the PI3-Akt pathway is related to uncontrolled cell growth, most of the studies evaluating the effects of PBDEs on this pathway have been done in cancer cell lines. BDE-47 activated Akt during an acute incubation in human neuroblastoma SH-SY5Y cells, and the effects of BDE-47 on cell migration were significantly reduced by treatment with the PI3K-Akt inhibitor LY294002 (Tian et al., 2016). Effects of BDE-99 on inducing epithelial to mesenchymal transition (EMT) in the human colon carcinoma cell line HCT-116 were blocked by PI3K-Akt inhibitor LY294002, suggesting that BDE-99 activates this pathway in HCT-116 cells (Wang et al., 2015). In the human hepatoma cell line HepG2, low concentrations of BDE-47 exposure for a period of 24-72 hours increased Akt phosphorylation (Wang et al., 2012). Akt phosphorylation was also increased in a study exposing HepG2 cells to BDE-47 for 3 and 24 hours, with a significant increase only after the 24-hour exposure (Khalil et al., 2017). The hydroxylated metabolite of BDE-47, 6-OH-BDE-47 was shown to induce EMT in lung cancer cells via upregulation of the PI3K-Akt pathway (Qu et al., 2015).

However, in animal studies results have been ambiguous. In mice with liver-specific phosphatase and tensin homolog (PTEN) protein deletion, a negative regulator of PI3K-Akt signaling (Gupta and Dey, 2012), BDE-47 had no effect on Akt activation in the liver (McIntyre et al., 2015). In rat testes, BDE-47 treatment increased PTEN activation and decreased Akt phosphorylation in a dose-dependent manner (Zhang et al., 2013). A study evaluating the differences in gene expression after BDE-47 exposure in the marine medaka, a potential model for investigating the effects of POP on marine fish, found that several genes associated with the activation of PI3K-Akt pathway were overexpressed in livers of both male and female animals (Yu et al., 2013). Developmental exposure to BDE-47 has been shown to increase liver Akt activation in CD-1 mice offspring at postnatal day (PND) 21 (Khalil et al., 2017).

The results of the highlighted studies demonstrate that PBDEs, and particularly BDE-47 have the potential to interfere with the PI3K-Akt pathway and affect cell growth, insulin signaling, and pancreatic β -cell function among other functions. These metabolic effects can be in addition to the disruption of thyroid hormone homeostasis by PBDEs. Since it has been reported that thyroid hormone can activate Akt in pancreatic β -cells (Falzacappa et al., 2007), it is possible that BDE-47 and BDE-85, by acting as thyroid hormone mimics, increase GSIS by acting through TR and Akt.

3.3 Hypothesis

BDE-47 and BDE-85 increase acute glucose-stimulated insulin secretion (GSIS) in INS-1 832/13 cells through the thyroid hormone receptor and Akt activation.

3.4 Methods

3.4.1 INS-1 832/13 Cell Culture and Maintenance

INS-1 832/13 cells (passages 51-60), provided by Dr. Christopher Newgard (Duke University School of Medicine) were cultured in RPMI-1640 glucose-free medium supplemented with 11 mmol/l glucose, 10% fetal bovine serum, 1mmol/l sodium pyruvate, 5mmol/l HEPES, 2g/L sodium bicarbonate, 2mmol/l L-glutamine, 50 μ mol/l 2-mercaptoethanol, 10000 U/ml penicillin,

and 10 mg/ml streptomycin. Cells were maintained at 37°C in a humidified incubator with 5% CO₂. Cells were subcultured when confluency was around 80% and medium was replaced every 3 days.

3.4.2 Chemicals

BDE-47 and BDE-85 were purchased from AccuStandard (New Haven, CT). Thyroid hormone T3 (3,3',5-Triiodo-L-thyronine) was purchased from Alfa Aesar (Lancashire, United Kingdom). Thyroid hormone receptor antagonist 1-850 was purchased from EMD Millipore (Darmstadt, Germany). Wortmannin was purchased from Acros Organics (Geel, Belgium). Stock solutions of BDE-47, BDE-85, T3, 1-850, and wortmannin were prepared in dimethyl sulfoxide (DMSO) and were added directly to the culture medium and/or KRB buffer to achieve the indicated concentrations. All other chemicals were purchased from Sigma (St. Louis, MO) unless otherwise specified.

3.4.3 Glucose-stimulated Insulin Secretion

INS-1 832/13 cells grown to confluency in 24-well plates, were washed 3 times with and preincubated in KRB buffer containing 3 mmol/l glucose at 37°C for 2 h. Following a static 1 h incubation at 37°C in KRB (Krebs Ringer Buffer) containing 3 or 16 mmol/l glucose, KRB buffer was collected and centrifuged at 5000 x g for 3 min at 4°C to pellet out any cells. Insulin secreted in buffer was measured by an ELISA kit (Alpco Diagnostics, Salem, NH). All insulin secretion data shown in this study were normalized to the total protein content, measured by the Micro-BCA Protein Assay kit (Pierce, Rockford, IL). For antagonist experiments, after 2 hr preincubation with 3 mmol/l glucose KRB, cells were preincubated with antagonists or vehicle control (DMSO) at indicated concentrations for 30 min in 3 mmol/l glucose KRB, washed once with 3 mmol/l glucose KRB, followed by static 1 h incubation at 37°C in KRB buffer containing 16 mmol/l glucose (Karandrea et al., 2017). For chronic pre-treatment, cells were exposed to indicated concentrations of T3 in complete growth media for 48 hours, after which cells were washed and

preincubated in KRB buffer containing 3 mmol/l glucose and static incubation was performed as described above (compounds not present during the static incubation phase). For all insulin secretion experiments, controls cells were treated with vehicle (DMSO) at 0.1% concentration.

3.4.4 Western Blot Analysis

INS-1 832/13 cells were grown to confluence in 6-well plates, washed two times in serum-free growth media, and incubated for 30 min at 37°C in serum-free growth media containing BDE-47, BDE-85, T3, or vehicle control. After exposure, cells were solubilized in RIPA lysis buffer (Pierce, Rockford, IL). Protein content was determined using a BCA Protein Assay Kit (Pierce, Rockford, IL) and SDS samples were prepared. Equal amount of protein (100 µg per lane) were electrophoretically separated on SDS-polyacrylamide gel, followed by blotting onto PVDF membrane. Following the transfer, membranes were blocked with TBST (10 mmol/l Tris-HCl pH 7.4, 150 mmol/l NaCl, and 0.1% Tween 20) containing 5% nonfat dry milk (blocking buffer) and incubated with the primary antibodies (diluted in blocking buffer overnight at 4°C) against Akt (Cell Signaling, cat. #9272), p-Akt (Cell Signaling, cat. #9271), and β-actin (Cell Signaling, cat. #4970). Membranes were incubated with goat anti-rabbit immunoglobulin (IgG) secondary antibody (Santa Cruz, cat. #sc-2030) for 1 h at room temperature, and washed 5 times. Proteins were detected by using enhanced chemiluminescence.

3.4.5 Reverse Transcription and Quantitative Real-time RT-PCR (qRT-PCR)

INS-1 832/13 cells were grown to confluence in 6-well plates, washed two times in serum-free growth media, and incubated for 1 or 12 hours at 37°C in serum-free growth media containing BDE-47, BDE-85, T3, inhibitors or vehicle control (0.1 % DMSO) as indicated. Total RNA was prepared using the TRIzol reagent according to the manufacturer's protocol (Invitrogen, Carlsbad, CA) and single-strand cDNA was synthesized from the RNA using a Maxime RT PreMix kit (iNtRON Biotechnology, Seongnam, South Korea). qRT-PCR amplifications were performed using rEVALution 2x qPCR Master Mix (Empirical Bioscience, Grand Rapids, MI) in an MyIQ2 Real-Time PCR Detection System (Bio-Rad, Richmond, CA) following manufacturer's protocol.

To determine the specificity of amplification, melting curve analysis was applied to all final PCR products. The relative amount of target mRNA was calculated by the comparative threshold cycle method by normalizing target mRNA threshold cycle to those for glyceraldehyde-3-phosphate dehydrogenase (GAPDH). The primers were purchased from Integrated DNA Technologies (Coralville, IA) and were as follows: rat TR α (NM_031134) forward 5'-CCTGGATGATACGGAAGTG-3', reverse 5'-AGTGCGGAATGTTGTGTT-3'; rat TR β (NM_012672) forward 5'-ATCATCACACCAGCAATCA-3', reverse 5'-GTCCGTCACCTTCATCAG-3'; rat GAPDH (NM_017008) forward 5'-GACATGCCGCCTGGAGAAAC-3', reverse 5'-AGCCCAGGATGCCCTTTAGT-3'.

3.4.6 Statistical Analysis

Data are expressed as means \pm SEM and are representative of at least three independent experiments. Significance was determined for multiple comparisons using two-way analysis of variance (ANOVA) followed by Sidak post-hoc analysis (Abdi). A p-value of ≤ 0.05 was considered significant. All analyses were conducted using the GraphPad Prism (version 6.07) statistical program software.

3.5 Results

3.5.1 BDE-47 and BDE-85 Do Not Affect TR Expression

There are two major genes of the thyroid receptor (TR), alpha and beta, which generate several isoforms (TR α 1, TR α 2, TR β 1, and TR β 2) that are expressed in different tissues (Zinke et al., 2003). Out of these isoforms, TR α 2 does not bind T3, thus it doesn't act as a transcription factor for thyroid hormone-mediated gene activation, but can have non-genomic effects (Zinke et al., 2003). During development, TR α is expressed first, followed by TR β (Mullur et al., 2014). In pancreatic islets, several studies have shown TR expression, however there is little consensus about which isoform is the predominant one. A study showed that TR α 1 and TR β 1 were expressed in the mouse pancreatic islets, with the TR α 1 localized in the glucagon producing alpha cells within the islet, however the localization of the TR β 1 was not determined (Zinke et al., 2003).

In rat islets, it was found that during development, TR α and TR β are expressed in β -cells, with TR β being the major isoform during adulthood (Aguayo-Mazzucato et al., 2013).

In β -cell clonal models, expression of both TR α and TR β isoforms have been reported. TR α was expressed in the mouse insulinoma-derived MIN6 cells (Takahashi et al., 2014). In the RIN5F cells, a rat insulinoma-derived β -cell, TR α is expressed, however the expression of other isoforms was not measured in this study (Furuya et al., 2010). In the INS-1 832/13 cell line, Shoemaker et al. reported that both TR α and TR β were expressed, with TR β expression being higher. In our study, we measured the mRNA expression of TR α and TR β in INS-1 832/13 cells and found that TR α , but not the TR β isoform is expressed (Figure 3.1 A). To test whether BDE-47 or BDE-85 exposure affected the mRNA expression of TR α , INS-1 832/13 cells, grown to confluence in 6-well plates, were exposed to 10 or 25 μ M BDE-47 or BDE-85 for 1 or 12 hours in serum-free media, and mRNA levels were measured as in section 3.4.5. BDE-47 and BDE-85 did not change TR α mRNA expression during all exposure windows (Figure 3.1 B and C). In parallel experiments, INS-1 832/13 cells were treated with 5 μ M T3, and T3 exposure did not induce changes in TR α expression (Figure 3.1 B and C).

3.5.2 Thyroid Hormone Increases GSIS

Thyroid hormone (T3) increased GSIS during chronic pre-treatment at the 5 μ M concentration, with no change for the 0.1 μ M concentration under the same conditions (Figure 3.2 A). During acute GSIS, thyroid hormone increased insulin secretion in a concentration-dependent manner for the concentrations of 0.1, 1, 5, and 100 μ M (Figure 3.2 B). In addition to increasing insulin secretion at the high glucose (16 mM) concentration, T3 increased insulin secretion at the basal (3 mM) glucose conditions at the 5 μ M concentration during chronic pre-treatment (Figure 3.2 A) and at the 5 and 100 μ M concentrations during acute exposure (Figure 3.2 B).

3.5.3 Combined Effects of Thyroid Hormone and BDE-47/85 on GSIS

During an acute GSIS, BDE-47 and BDE-85 increased insulin secretion compared to vehicle control at the 10 μM concentration as previously observed (Figure 3.3). This concentration (10 μM) for BDE-47 and BDE-85 was chosen since it was the lowest observed concentration that consistently increases insulin secretion during acute GSIS. Furthermore, as expected, T3 alone increased acute GSIS at the 5 and 100 μM concentrations (Figure 3.3). When cells were treated with both BDE-47 or 85 and T3, there was an additional increase in insulin secretion during an acute GSIS (Figure 3.3). For cells treated in combination with 10 μM BDE-47 or BDE-85 and 5 or 100 μM T3, insulin secretion was increased compared to either compound or T3 alone (Figure 3.3). As previously observed, T3 increased insulin secretion during basal glucose conditions (3mM) at the 100 μM concentration, as well as in combination with 10 μM BDE-47 or 10 μM BDE-85 (Figure 3.3)

3.5.4 Thyroid Receptor Antagonist Decreases T3-mediated GSIS Potentiation

To validate the actions of the thyroid receptor antagonist 1-850 in the INS-1 832/13 cells, we tested whether this antagonist would decrease the potentiation of GSIS after T3 treatment during an acute incubation. Cells were starved for 2 hours in low glucose (3 mM) KRB buffer and after pre-incubated for 30 mins with either vehicle control or different concentrations of 1-850 (5, 10, or 20 μM). After pre-incubation, cells were incubated for 1 hour with either T3 (1 μM) or vehicle control in high glucose (16 mM) KRB buffer (antagonist not present during this stimulatory phase), and insulin secretion was measured. As expected, treatment with 1 μM T3 alone significantly increased GSIS compared to vehicle control (Figure 3.4). There was a concentration-dependent decrease in T3-potentiation of GSIS after pre-incubation with 1-850 (Figure 3.4). GSIS in pre-treated groups with 5 or 10 μM 1-850 followed by T3 exposure was still significantly higher than vehicle treated control alone (Figure 3.4). Pre-treatment with 20 μM 1-850 followed by T3 significantly decreased GSIS compared to T3 alone (Figure 3.4). Pre-treatment with antagonist

alone (at 5, 10, and 20 μM) did not significantly alter GSIS compared to vehicle control (Figure 3.4).

3.5.5 BDE-47 and BDE-85 Effect on GSIS is Mediated by TR

Since thyroid hormone administration increased acute GSIS and co-administration with thyroid hormone in the presence of BDE-47 and BDE-85 caused an increase in this response, we set out to determine whether the effects of these two compounds on GSIS are mediated by their actions on thyroid hormone receptor. To evaluate the role of thyroid receptor (TR), we pre-treated the cells with thyroid receptor antagonist 1-850 for 30 minutes, and performed an acute GSIS (as described in Methods). Pre-treatment with TR antagonist caused a decrease in insulin secretion from INS-1 832/13 cells treated with 10 μM BDE-47 or 10 μM BDE-85 compared to compound alone; and with no significant increase compared to untreated control (Figure 3.5)

3.5.6 BDE-47 and BDE-85 Activate Akt in INS-1 832/13 cells

Recently, it has been suggested that thyroid hormone can have important implications in pancreatic β -cell growth and function by activating Akt (Falzacappa et al., 2007; Falzacappa et al., 2010). To evaluate whether thyroid hormone, BDE-47, and BDE-85 active Akt in INS-1 832/13 cells during an acute incubation, cells were treated for 30 minutes and levels of total and phosphorylated (activated) Akt were measured by Western Blot. Both BDE-47 and BDE-85 (at 10 μM concentration) activate Akt during an acute incubation at both low (3 mM) and high (16 mM) glucose compared to vehicle control (Figure 3.6 A). High glucose treatment in the absence of compounds did not increase phosphorylated Akt (Figure 3.6 A). The 10 μM concentration was chosen since it was shown to increase GSIS after acute exposure to both compounds, although lower and higher concentrations were also shown to activate Akt at the normal (11 mM) glucose condition (Figure 3.6 B).

3.5.7 Effect of BDE-47 and BDE-85 on Insulin Secretion is Dependent on Akt Activation

To evaluate whether the activation of Akt plays a role in BDE-47 and BDE-85-mediated increase in GSIS, we tested whether pharmacological inhibition of PI3K, an upstream activator of Akt (Sargis, 2014; Guo, 2014), would affect this response. A 30-min pre-treatment with PI3K inhibitor, wortmannin, followed by a static one hour GSIS, caused a decrease in insulin secretion when cells were treated with BDE-47 or BDE-85 compared to compounds alone (Figure 3.8). The concentration of wortmannin (50nM) was chosen from a previous study showing that this concentration effectively blocked Akt phosphorylation while not affecting insulin secretion (Collier et al., 2004). This was also confirmed in our work, where we show that wortmannin by itself didn't affect GSIS (Figure 3.8), but effectively inhibited BDE-47 and BDE-85-induced Akt activation (Figure 3.7).

3.6 Discussion

BDE-47 and BDE-85 are similar to thyroid hormones in structure and have been shown to disrupt thyroid hormone signaling (Ren and Guo, 2013; Richardson et al., 2008; Blanco et al., 2014). Thyroid hormone is important in development, but also in metabolic rate and weight management (Casals-Casas and Desvergne, 2011). It acts by binding to the thyroid hormone receptor (TR) in various tissues, including the pancreatic β -cell; however, its direct role in β -cell function remains controversial (Shoemaker et al., 2012). While some *in vitro* and *in vivo* studies suggested that thyroid signaling is associated with decreased GSIS (Ximenes et al., 2007; Lenzen et al., 1975); others have shown an increase in GSIS and cell survival in the INS-1 832/13 cells following thyroid hormone treatment (Falzacappa et al, 2007; Falzacappa et al., 2010). Our own data show an increase in insulin secretion in INS-1 832/13 cells during an acute incubation with thyroid hormone (T3), suggesting an important role for the thyroid hormone signaling in GSIS. Furthermore, there was an additional increase in acute GSIS with co-treatment of T3 and BDE-47 or BDE-85. Based on these observations, we tested whether these compounds might act via

the thyroid receptor to increase insulin secretion. Pharmacological inhibition of the thyroid receptor (TR) by the specific antagonist 1-850 led to a decrease in BDE-47 and BDE-85-mediated GSIS. This suggests that the potentiating effects of these compounds on GSIS are mediated via the TR. It is unlikely that the TR antagonist has off-target effects due to its specificity and pre-treatment with the antagonist alone did not affect GSIS. In this study, we reported expression of TR α and no expression of TR β at the mRNA level, however we did not check the protein expression of these TR isoforms in the INS-1 832/13 cell line. Although we observed our effects with TR antagonist 1-850, an antagonist to both isoforms, further studies are required to confirm their expression in the INS-1 832/13 cell line and consequently the role of TR in BDE-47 and BDE-85-mediated potentiation of GSIS.

Thyroid hormone has been shown to have a beneficial effect on pancreatic β -cell growth and function by activating Akt (Falzacappa et al, 2007; Falzacappa et al., 2010). Although the role of Akt in the insulin signaling pathway is well established (reviewed in Guo, 2014), its role in insulin secretion is controversial. Downregulation of Akt activity specifically in β -cells led to glucose intolerance due to impaired insulin secretion in mice (Bernal-Mizrachi et al., 2004). Akt activation has been implicated to play an important role in increasing insulin granule exocytosis (Bernal-Mizrachi et al., 2004; Cheng et al., 2012). Conversely, Akt inhibition has been shown to potentiate insulin secretion and increase insulin granule fusion (Aoyagi et al., 2012). Since BDE-47 and BDE-85 activate Akt during an acute incubation (Figure 4A and B), we were interested to determine whether this activation played a role in their potentiation of GSIS. Treatment with PI3K inhibitor wortmannin inhibited BDE-47 and BDE-85-induced GSIS, suggesting that Akt activation plays a role. In contrast, PI3K inhibition in the absence of compounds didn't affect GSIS, suggesting that this pathway might be involved in insulin secretion only when activated. However, the role of Akt in GSIS and the specific mechanisms involved require further characterization.

Thyroid hormone and BDE compounds both potentiate GSIS, but we also observed significant differences in their actions on pancreatic β -cell function. The potentiation of GSIS from

BDE-47 and BDE-85 occurred only during acute exposure, with no changes in the chronic pre-treatment exposure. T3, on the other hand, in addition to potentiating GSIS during acute exposure, had the same effect during chronic pre-treatment. Furthermore, in addition to increasing insulin secretion in high glucose (16 mM) conditions, T3 did so also during basal glucose conditions (3 mM), a phenomenon not observed with either BDE-47 or BDE-85. This suggests that T3 might influence insulin secretion by additional mechanisms, potentially by activating targets implicated in glucose-independent insulin secretion such as protein kinase alpha (PKA) or protein kinase C (PKC) and consequently upregulate expression of important genes involved in β -cell mass and function (reviewed in Komatsu et al., 2013). However, further studies are required to establish if the role of T3 in insulin secretion is mediated by these pathways.

This study shows for the first time that BDE-47 and BDE-85 increase GSIS in pancreatic β -cells and that this effect is mediated by the thyroid receptor and Akt. Further studies are required to determine the specific mechanisms by which Akt activation by BDE-47 and BDE-85 can lead to increased GSIS; or whether other mechanisms in addition to the one proposed are involved. Additionally, this study provides evidence that these two compounds have a direct role in pancreatic β -cell function. It is possible that exposure to BDE-47 and BDE-85 can cause β -cells to overproduce insulin. This excess insulin could lead to hyperinsulinemia, which can cause insulin resistance, one of the hallmarks of type 2 diabetes (Nolan et al., 2015). These potential long-term implications need to be further assessed in physiologically relevant animal models of type 2 diabetes and in epidemiological studies.

3.7 References

Abdi, H. (2007). Bonferroni and Šidák corrections for multiple comparisons. *Encyclopedia of measurement and statistics*, 3, 103-107.

Aguayo-Mazzucato, C., Zavacki, A. M., Marinelarena, A., Hollister-Lock, J., El Khattabi, I., Marsili, A., ... & Bonner-Weir, S. (2013). Thyroid hormone promotes postnatal rat pancreatic β -cell development and glucose-responsive insulin secretion through MAFA. *Diabetes*, 62(5), 1569-1580.

- Aoyagi, K., Ohara-Imaizumi, M., Nishiwaki, C., Nakamichi, Y., Ueki, K., Kadowaki, T., & Nagamatsu, S. (2012). Acute inhibition of PI3K-PDK1-Akt pathway potentiates insulin secretion through upregulation of newcomer granule fusions in pancreatic β -cells. *PLoS one*, 7(10), e47381.
- Bernal-Mizrachi, E., Fatrai, S., Johnson, J. D., Ohsugi, M., Otani, K., Han, Z., ... & Permutt, M. A. (2004). Defective insulin secretion and increased susceptibility to experimental diabetes are induced by reduced Akt activity in pancreatic islet β cells. *Journal of Clinical Investigation*, 114(7), 928.
- Blanco, J., Mulero, M., Domingo, J. L., & Sanchez, D. J. (2013). Perinatal exposure to BDE-99 causes decreased protein levels of cyclin D1 via GSK3 β activation and increased ROS production in rat pup livers. *toxicological sciences*, 137(2), 491-498.
- Bloom, M., Spliethoff, H., Vena, J., Shaver, S., Addink, R., & Eadon, G. (2008). Environmental exposure to PBDEs and thyroid function among New York anglers. *Environmental toxicology and pharmacology*, 25(3), 386-392.
- Cao, J., Lin, Y., Guo, L. H., Zhang, A. Q., Wei, Y., & Yang, Y. (2010). Structure-based investigation on the binding interaction of hydroxylated polybrominated diphenyl ethers with thyroxine transport proteins. *Toxicology*, 277(1), 20-28.
- Casals-Casas, C., & Desvergne, B. (2011). Endocrine disruptors: from endocrine to metabolic disruption. *Annual review of physiology*, 73, 135-162.
- Cheng, K. K., Lam, K. S., Wu, D., Wang, Y., Sweeney, G., Hoo, R. L., ... & Xu, A. (2012). APPL1 potentiates insulin secretion in pancreatic β cells by enhancing protein kinase Akt-dependent expression of SNARE proteins in mice. *Proceedings of the National Academy of Sciences*, 109(23), 8919-8924.
- Collier, J. J., White, S. M., Dick, G. M., & Scott, D. K. (2004). Phosphatidylinositol 3-kinase inhibitors reveal a unique mechanism of enhancing insulin secretion in 832/13 rat insulinoma cells. *Biochemical and biophysical research communications*, 324(3), 1018-1023.
- Falzacappa, C. V., Petrucci, E., Patriarca, V., Michienzi, S., Stigliano, A., Brunetti, E., ... & Misiti, S. (2007). Thyroid hormone receptor TR β 1 mediates Akt activation by T3 in pancreatic β cells. *Journal of molecular endocrinology*, 38(2), 221-233.
- Furuya, F., Shimura, H., Yamashita, S., Endo, T., & Kobayashi, T. (2010). Liganded thyroid hormone receptor- α enhances proliferation of pancreatic β -cells. *Journal of Biological Chemistry*, 285(32), 24477-24486.
- Guo, S. (2014). Insulin signaling, resistance, and metabolic syndrome: insights from mouse models into disease mechanisms. *Journal of Endocrinology*, 220(2), T1-T23.
- Gupta, A., & Dey, C. S. (2012). PTEN, a widely known negative regulator of insulin/PI3K signaling, positively regulates neuronal insulin resistance. *Molecular biology of the cell*, 23(19), 3882-3898.
- Hallgren, S., & Darnerud, P. O. (2002). Polybrominated diphenyl ethers (PBDEs), polychlorinated biphenyls (PCBs) and chlorinated paraffins (CPs) in rats—testing interactions and mechanisms for thyroid hormone effects. *Toxicology*, 177(2), 227-243.
- Hallgren, S., Sinjari, T., Håkansson, H., & Darnerud, P. (2001). Effects of polybrominated diphenyl ethers (PBDEs) and polychlorinated biphenyls (PCBs) on thyroid hormone and vitamin A levels in rats and mice. *Archives of toxicology*, 75(4), 200-208.

- Hamers, T., Kamstra, J. H., Sonneveld, E., Murk, A. J., Kester, M. H., Andersson, P. L., ... & Brouwer, A. (2006). In vitro profiling of the endocrine-disrupting potency of brominated flame retardants. *Toxicological Sciences*, 92(1), 157-173.
- Hamers, T., Kamstra, J. H., Sonneveld, E., Murk, A. J., Visser, T. J., Van Velzen, M. J., ... & Bergman, Å. (2008). Biotransformation of brominated flame retardants into potentially endocrine-disrupting metabolites, with special attention to 2, 2', 4, 4'- tetrabromodiphenyl ether (BDE- 47). *Molecular nutrition & food research*, 52(2), 284-298.
- Hu, X., Zhang, J., Jiang, Y., Lei, Y., Lu, L., Zhou, J., ... & Tao, G. (2014). Effect on metabolic enzymes and thyroid receptors induced by BDE-47 by activation the pregnane X receptor in HepG2, a human hepatoma cell line. *Toxicology in Vitro*, 28(8), 1377-1385.
- Karandrea, S., Yin, H., Liang, X., & Heart, E. A. (2017). BDE-47 and BDE-85 stimulate insulin secretion in INS-1 832/13 pancreatic β -cells through the thyroid receptor and Akt. *Environmental Toxicology and Pharmacology*, 56, 29-34.
- Khalil, A., Parker, M., Mpanga, R., Cevik, S. E., Thorburn, C., & Suvorov, A. (2017). Developmental Exposure to 2, 2', 4, 4'-Tetrabromodiphenyl Ether Induces Long-Lasting Changes in Liver Metabolism in Male Mice. *Journal of the Endocrine Society*, 1(4), 323-344.
- Kitamura, S., Shinohara, S., Iwase, E., Sugihara, K., Uramaru, N., Shigematsu, H., ... & Ohta, S. (2008). Affinity for thyroid hormone and estrogen receptors of hydroxylated polybrominated diphenyl ethers. *Journal of health science*, 54(5), 607-614.
- Komatsu, M., Takei, M., Ishii, H., & Sato, Y. (2013). Glucose-stimulated insulin secretion: A newer perspective. *Journal of diabetes investigation*, 4(6), 511-516.
- Lema, S. C., Dickey, J. T., Schultz, I. R., & Swanson, P. (2008). Dietary Exposure to 2, 2', 4, 4'-tetrabromodiphenyl ether (PBDE-47) alters thyroid status and thyroid hormone-regulated gene transcription in the pituitary and brain. *Environmental health perspectives*, 116(12), 1694.
- Lenzen, S., Panten, U., & Hasselblatt, A. (1975). Thyroxine treatment and insulin secretion in the rat. *Diabetologia*, 11(1), 49-55.
- Luross, J. M., Alaei, M., Sergeant, D. B., Cannon, C. M., Whittle, D. M., Solomon, K. R., & Muir, D. C. (2002). Spatial distribution of polybrominated diphenyl ethers and polybrominated biphenyls in lake trout from the Laurentian Great Lakes. *Chemosphere*, 46(5), 665-672.
- Makey, C. M., McClean, M. D., Braverman, L. E., Pearce, E. N., He, X. M., Sjödin, A., ... & Webster, T. F. (2016). Polybrominated diphenyl ether exposure and thyroid function tests in North American adults. *Environmental health perspectives*, 124(4), 420.
- McIntyre, R. L., Kenerson, H. L., Subramanian, S., Wang, S. A., Kazami, M., Stapleton, H. M., & Yeung, R. S. (2015). Polybrominated diphenyl ether congener, BDE-47, impairs insulin sensitivity in mice with liver-specific Pten deficiency. *BMC obesity*, 2(1), 3.
- Morgado, I., Hamers, T., Van der Ven, L., & Power, D. M. (2007). Disruption of thyroid hormone binding to sea bream recombinant transthyretin by ioxinyl and polybrominated diphenyl ethers. *Chemosphere*, 69(1), 155-163.
- Mullur, R., Liu, Y. Y., & Brent, G. A. (2014). Thyroid hormone regulation of metabolism. *Physiological reviews*, 94(2), 355-382.

- Nakamura, N., Matsubara, K., Sanoh, S., Ohta, S., Uramaru, N., Kitamura, S., ... & Fujimoto, N. (2013). Cell type-dependent agonist/antagonist activities of polybrominated diphenyl ethers. *Toxicology letters*, 223(2), 192-197.
- Nolan, C. J., Ruderman, N. B., Kahn, S. E., Pedersen, O., & Prentki, M. (2015). Insulin resistance as a physiological defense against metabolic stress: implications for the management of subsets of type 2 diabetes. *Diabetes*, 64(3), 673-686.
- Qu, B. L., Yu, W., Huang, Y. R., Cai, B. N., Du, L. H., & Liu, F. (2015). 6-OH-BDE-47 promotes human lung cancer cells epithelial mesenchymal transition via the AKT/Snail signal pathway. *Environmental toxicology and pharmacology*, 39(1), 271-279.
- Ren, X. M., & Guo, L. H. (2013). Molecular toxicology of polybrominated diphenyl ethers: nuclear hormone receptor mediated pathways. *Environmental Science: Processes & Impacts*, 15(4), 702-708.
- Ren, X. M., Guo, L. H., Gao, Y., Zhang, B. T., & Wan, B. (2013). Hydroxylated polybrominated diphenyl ethers exhibit different activities on thyroid hormone receptors depending on their degree of bromination. *Toxicology and applied pharmacology*, 268(3), 256-263.
- Richardson, V. M., Staskal, D. F., Ross, D. G., Diliberto, J. J., DeVito, M. J., & Birnbaum, L. S. (2008). Possible mechanisms of thyroid hormone disruption in mice by BDE 47, a major polybrominated diphenyl ether congener. *Toxicology and applied pharmacology*, 226(3), 244-250.
- Schriks, M., Vrabie, C. M., Gutleb, A. C., Faassen, E. J., Rietjens, I. M., & Murk, A. J. (2006). T-screen to quantify functional potentiating, antagonistic and thyroid hormone-like activities of poly halogenated aromatic hydrocarbons (PHAHs). *Toxicology in vitro*, 20(4), 490-498.
- Shoemaker, T., Kono, T., Mariash, C., & Evans-Molina, C. (2012). Thyroid hormone analogues for the treatment of metabolic disorders: new potential for unmet clinical needs?. *Endocrine Practice*, 18(6), 954-964.
- Takahashi, K., Furuya, F., Shimura, H., Kaneshige, M., & Kobayashi, T. (2014). Impaired oxidative endoplasmic reticulum stress response caused by deficiency of thyroid hormone receptor α . *Journal of Biological Chemistry*, 289(18), 12485-12493.
- Tian, P. C., Wang, H. L., Chen, G. H., Luo, Q., Chen, Z., Wang, Y., & Liu, Y. F. (2016). 2, 2', 4, 4'-Tetrabromodiphenyl ether promotes human neuroblastoma SH-SY5Y cells migration via the GPER/PI3K/Akt signal pathway. *Human & experimental toxicology*, 35(2), 124-134.
- Turyk, M. E., Persky, V. W., Imm, P., Knobeloch, L., Chatterton Jr, R., & Anderson, H. A. (2008). Hormone disruption by PBDEs in adult male sport fish consumers. *Environmental health perspectives*, 116(12), 1635.
- Verga Falzacappa, C., Mangialardo, C., Raffa, S., Mancuso, A., Piergrossi, P., Moriggi, G., ... & Toscano, V. (2010). The thyroid hormone T3 improves function and survival of rat pancreatic islets during in vitro culture. *Islets*, 2(2), 96-103.
- Wang, F., Ruan, X. J., & Zhang, H. Y. (2015). BDE-99 (2, 2', 4, 4', 5-pentabromodiphenyl ether) triggers epithelial-mesenchymal transition in colorectal cancer cells via PI3K/Akt/Snail signaling pathway. *Tumori*, 101(2), 238-245.

Wang, L., Zou, W., Zhong, Y., An, J., Zhang, X., Wu, M., & Yu, Z. (2012). The hormesis effect of BDE-47 in HepG 2 cells and the potential molecular mechanism. *Toxicology letters*, 209(2), 193-201.

Ximenes, H. M., Lortz, S., Jörns, A., & Lenzen, S. (2007). Triiodothyronine (T₃)-mediated toxicity and induction of apoptosis in insulin-producing INS-1 cells. *Life sciences*, 80(22), 2045-2050.

Yu, W. K., Shi, Y. F., Fong, C. C., Chen, Y., Van De Merwe, J. P., Chan, A. K., ... & Wu, R. S. (2013). Gender-specific transcriptional profiling of marine medaka (*Oryzias melastigma*) liver upon BDE-47 exposure. *Comparative Biochemistry and Physiology Part D: Genomics and Proteomics*, 8(3), 255-262.

Zhang, Z., Zhang, X., Sun, Z., Dong, H., Qiu, L., Gu, J., ... & Wang, S. L. (2013). Cytochrome P450 3A1 mediates 2, 2', 4, 4'-tetrabromodiphenyl ether-induced reduction of spermatogenesis in adult rats. *PloS one*, 8(6), e66301.

Zinke, A., Schmoll, D., Zachmann, M., Schmoll, J., Junker, H., Grempler, R., ... & Walther, R. (2003). Expression of thyroid hormone receptor isoform $\alpha 1$ in pancreatic islets. *Experimental and clinical endocrinology & diabetes*, 111(04), 198-202

3.8 Tables and Figures

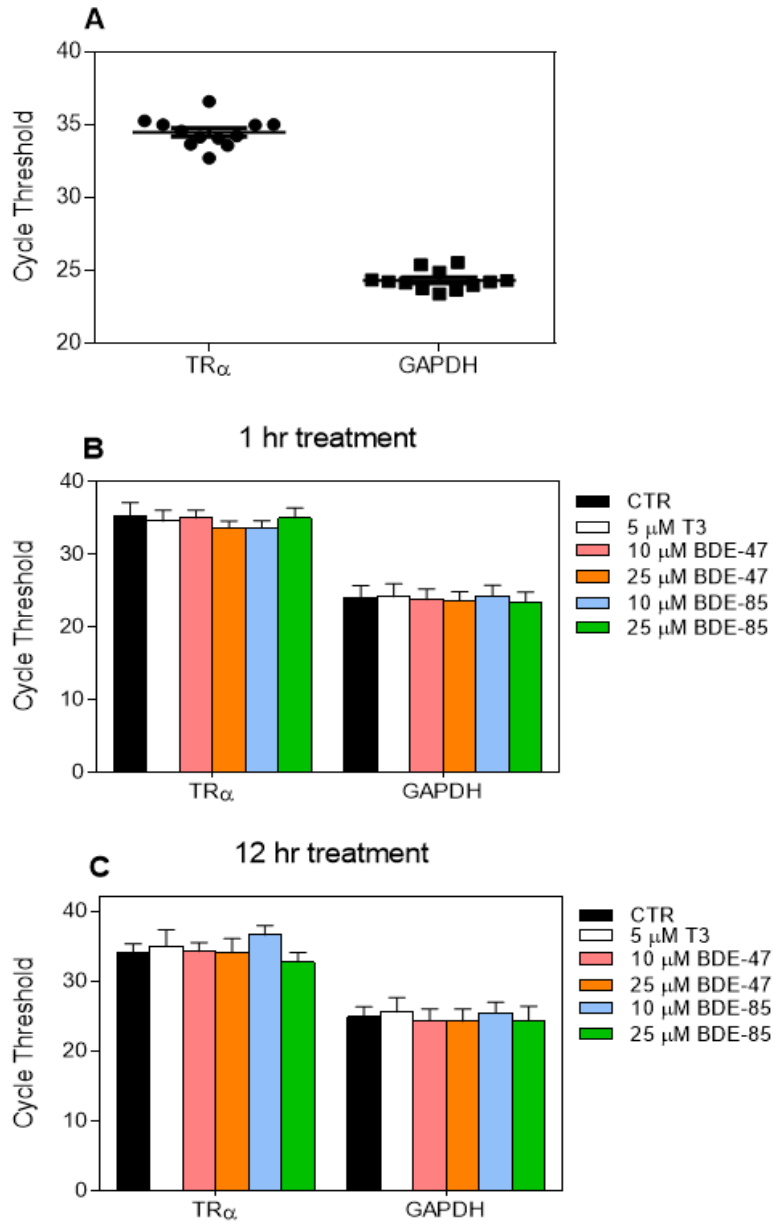


Figure 3.1 BDE-47 and BDE-85 do not affect thyroid receptor α expression. Expression of TR α and GAPDH in INS-1 832/13 cells (A). Expression of TR α and GAPDH after a 1 hour treatment in serum-free media with vehicle control, 5 μ M T3, 10 or 25 μ M BDE-47 or BDE-85 (B). Expression of TR α and GAPDH after a 12-hour treatment in serum-free media with vehicle control, 5 μ M T3, 10 or 25 μ M BDE-47 or BDE-85 (C). No significant differences were noted in all groups compared to vehicle control using two-way ANOVA followed by Sidak post-test. GAPDH = Glyceraldehyde 3-phosphate dehydrogenase. Data are means \pm SEM from three independent experiments (n = 3).

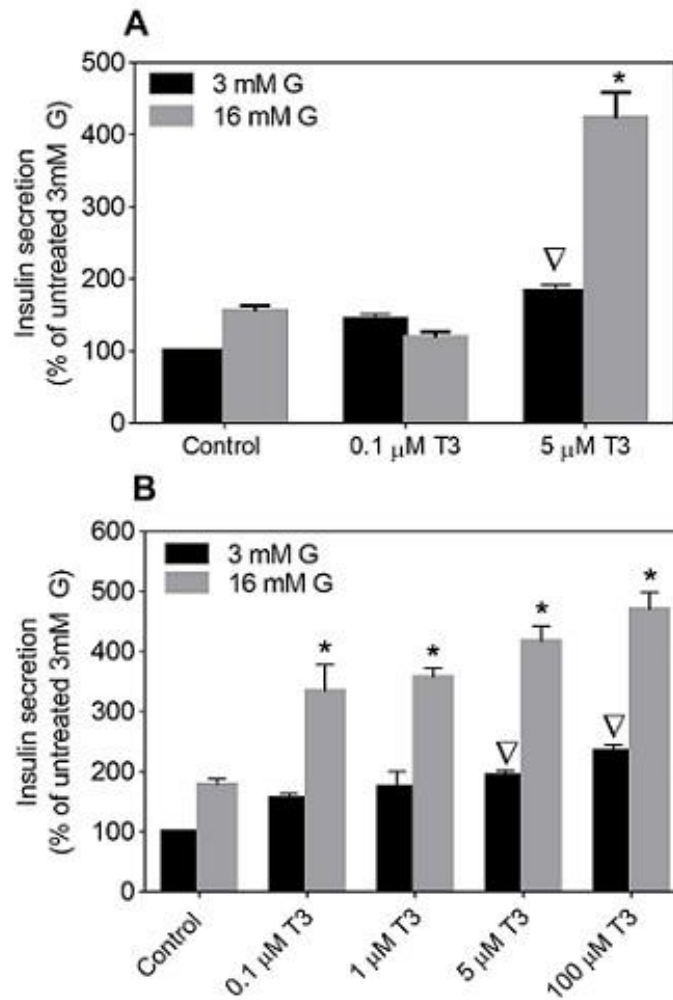


Figure 3.2 Thyroid hormone increases GSIS during chronic pre-treatment and acute exposure. GSIS in INS-1 832/13 cells incubated with 0.1 and 5 μ M T3 during chronic pre-treatment exposure (A). GSIS in INS-1 832/13 incubated with 0.1, 1, 5, or 100 μ M T3 during an acute exposure(B). * p <0.05 when compared with control 16mM G, ∇p <0.05 when compared with control 3mM G using two-way ANOVA followed by Sidak post-test. 3mM glucose, 16 mM G = 16mM glucose. Data are means \pm SEM from three independent experiments performed in quadruplicates (n = 3).

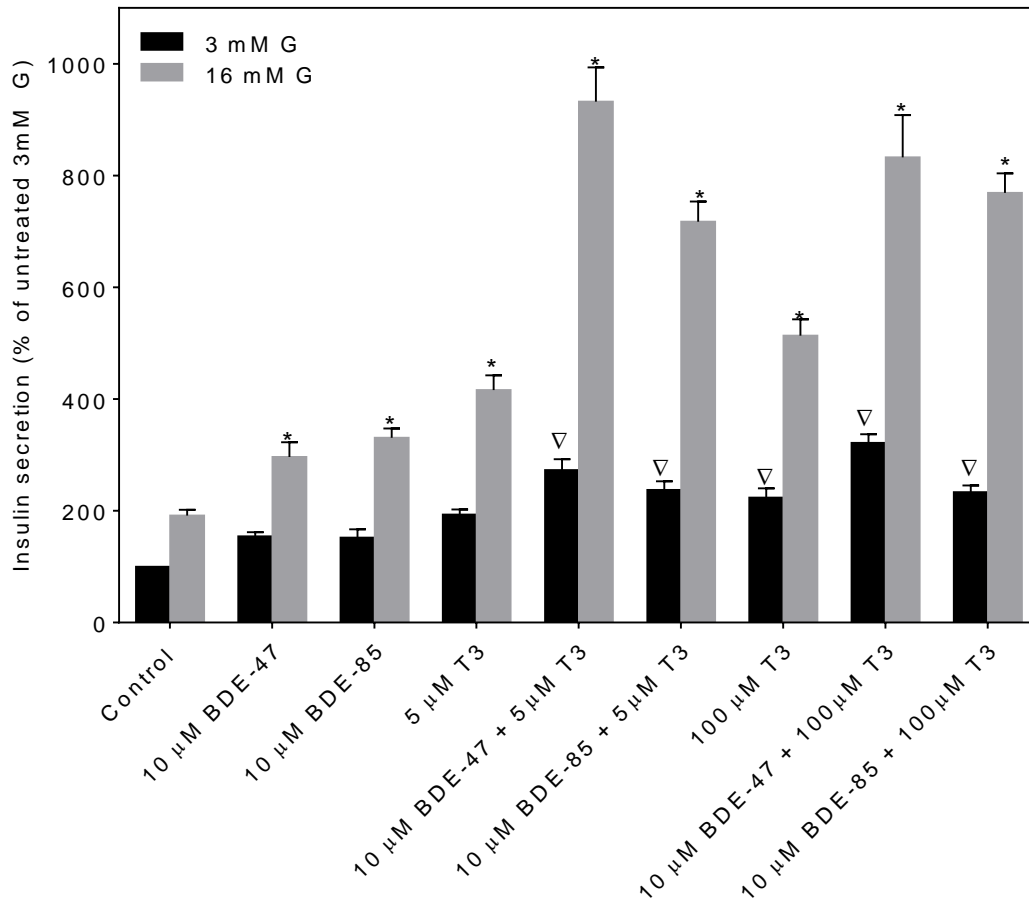


Figure 3.3 Co-treatment with BDE-47 or BDE-85 and thyroid hormone potentiates GSIS compared to single treatment. GSIS in INS-1 832/13 cells treated with T3 alone (5 or 100 μM), BDE-47 alone (10 μM), BDE-85 alone (10 μM), T3 + BDE-47 (5 μM or 100 μM T3 + 10 μM BDE-47), or T3 + BDE-85 (5 μM or 100 μM T3 + 10 μM BDE-85) during an acute exposure. * $p < 0.05$ when compared with control 16mM G, $\nabla p < 0.05$ when compared with control 3mM G using two-way ANOVA followed by Sidak post-test. 3mM G = 3mM glucose, 16mM G = 16mM glucose. Data are means \pm SEM from three independent experiments performed in quadruplicates ($n = 3$).

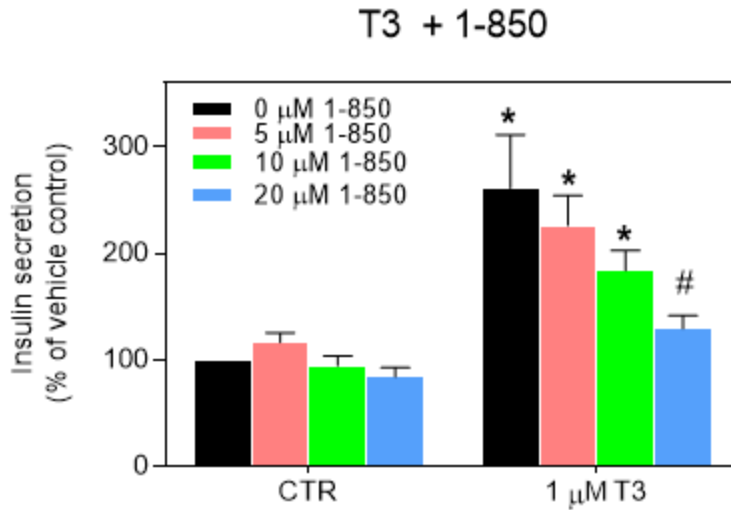


Figure 3.4 Thyroid receptor antagonist 1-850 decreases GSIS potentiation by T3. INS-1 832/13 cells were pre-incubated for 2 hours in 3mM glucose KRB buffer, followed by a 30 pre-incubation with TR antagonist 1-850 (5, 10, or 20 μ M) or vehicle in 3mM glucose KRB, washed once with 3mM glucose KRB, and acute GSIS was done in 16mM glucose KRB for 1 hour with T3 (1 μ M) or vehicle control. * $p \leq 0.05$ when compared with vehicle control. # $p \leq 0.05$ when compared with 1 μ M T3 alone using two-way ANOVA followed by Sidak post-test. Data are means \pm SEM from three independent experiments performed in quadruplicates (n = 3).

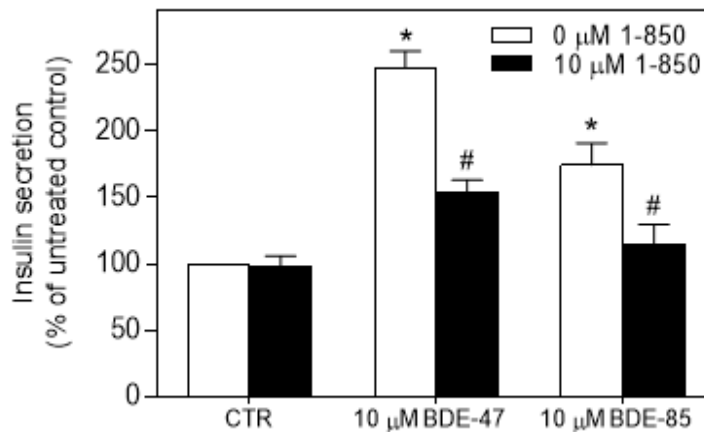


Figure 3.5 Thyroid Receptor Antagonist 1-850 decreases GSIS potentiation by BDE-47 and BDE-85. INS-1 832/13 cells were pre-incubated for 2 hours in 3mM glucose KRB buffer, followed by a 30 pre-incubation with TR antagonist 1-850 (10 μ M) or vehicle in 3mM glucose KRB, washed once with 3mM glucose KRB, and acute GSIS was done in 16mM glucose KRB for 1 hour with BDE-47 (10 μ M), BDE-85 (10 μ M), or vehicle control. * $p \leq 0.05$ when compared with vehicle control. # $p \leq 0.05$ when compared with BDE-47 or BDE-85 alone using two-way ANOVA followed by Sidak post-test. Data are means \pm SEM from three independent experiments performed in quadruplicates (n = 3).

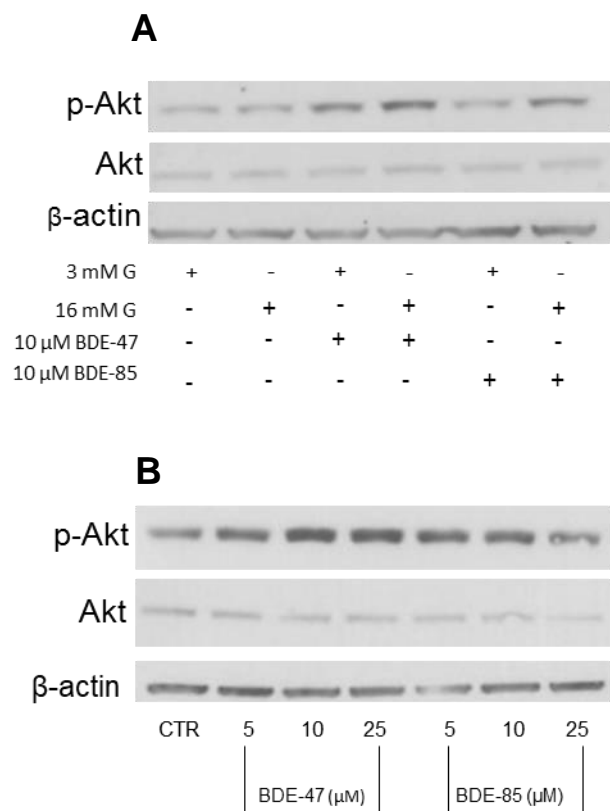


Figure 3.6 BDE-47 and BDE-85 activate Akt during an acute exposure. INS-1 832/13 cells were exposed to 10 μM BDE-47 or BDE-85 for 30 mins in serum-free media containing 3 mM or 16 mM glucose and Akt, p-Akt, and β-actin protein were measured as described in methods (A). INS-1 832/13 cells exposed to 5, 10, or 25 μM BDE-47 or BDE-85 for 30 mins in serum-free media containing 11 mM glucose and Akt, p-Akt, and β-actin protein were measured as described in methods (B). G: glucose. Western blot images are representative of three independent experiments (n=3).

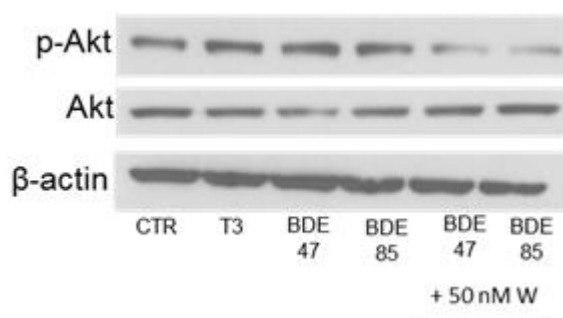


Figure 3.7 Wortmannin inhibits BDE-47 and BDE-85-mediated Akt activation. INS-1 832/13 cells exposed to wortmannin (50 nM) or vehicle for 30 mins, followed by incubation with BDE-47 (10 μM), BDE-85 (10 μM), or vehicle for 30 mins in serum-free 11 mM glucose media and Akt, p-Akt, and β-actin protein were measured as described in methods. W: wortmannin. Western blot image is representative of three independent experiments (n=3).

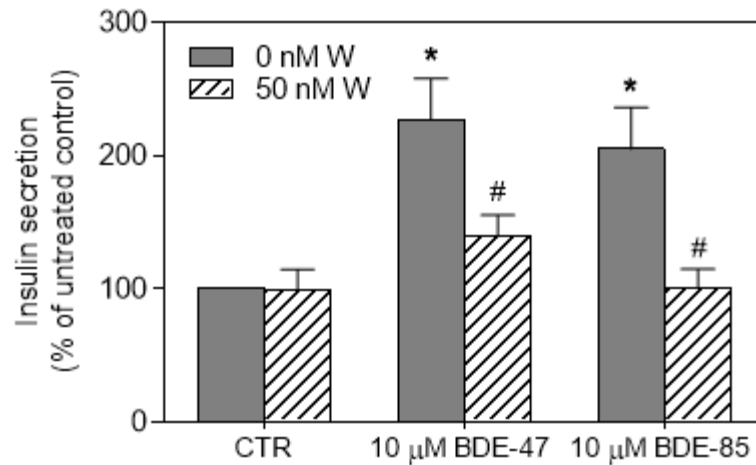


Figure 3.8 Effect of PI3K inhibitor wortmannin on BDE-47 and BDE-85-mediated GSIS potentiation. Cells were pre-incubated for 2 hours in 3mM glucose KRB buffer, followed by a 30 pre-incubation with wortmannin or vehicle in 3mM glucose KRB, washed once with 3mM glucose KRB, acute GSIS was done in 16 mM glucose KRB for 1 hour with BDE-47 (10 μM), BDE-85 (10 μM), or vehicle control. Data are means ± SEM from three independent experiments performed in quadruplicate. * $p \leq 0.05$ when compared with vehicle control. # $p \leq 0.05$ when compared with BDE-47 or BDE-85 alone using two-way ANOVA followed by Sidak post-test. Data are means ± SEM from three independent experiments performed in quadruplicates (n = 3).

CHAPTER FOUR:
ANTI-DIABETIC EFFECTS OF THYMOQUINONE IN THE DIET-INDUCED OBESITY (DIO)
MOUSE MODEL OF TYPE 2 DIABETES

4.1 Prevalence and Overall Impact of Type 2 Diabetes

Type 2 Diabetes Mellitus (T2DM) is a metabolic disorder characterized by chronic hyperglycemia, which develops as a consequence of peripheral insulin resistance and defective insulin secretion from pancreatic β -cells (ADA, 2014). In addition to hyperglycemia, common symptoms of T2DM include polydipsia, polyphagia, and polyuria (ADA, 2014). 29.1 million people have diabetes in the US with 1.7 million new cases reported in 2012. In the US, most patients (90-95%) diagnosed with diabetes have type 2 diabetes and only 5% have type 1 (CDC, 2014). Type 2 diabetes prevalence has increased exponentially in the last two decades in the United States (CDC, 2016). As of 2012, 9.3% of the US population has diabetes, and the numbers are projected to be on the rise, with as many as 7.2 million undiagnosed cases. Diabetes can lead to major complications, including blindness, heart disease, stroke, kidney failure, while causing about 240,000 deaths/year, making it the 7th leading cause of death in the US. Annually, diabetes related medical care costs the US economy \$245 billion, up from \$174 billion in 2007 (CDC, 2014). There are an estimated 86 million people in the US with prediabetes, a state where blood glucose levels are above normal but fall just below diagnostic criteria, making these individuals prone to developing type 2 diabetes (Dall et al., 2014). In addition, prediabetes healthcare costs are estimated at \$25 billion annually (Dall et al., 2014). Furthermore, 85% of people with type 2 diabetes are also overweight or obese, which exacerbates the impacts of the disease.

It is now believed that type 2 diabetes is a multifactorial disease, where contributions from many factors such as lifestyle, environment, and genetics can lead to its development. Thus, it is critical to identify new risk factors and potential treatments to design effective interventions to

minimize the impacts of this disease. One of the goals of this study is to evaluate the anti-diabetogenic effects of Thymoquinone and assess its potential in treating type 2 diabetes, as well as to demonstrate the possible mechanisms by which Thymoquinone ameliorates hyperglycemia and other metabolic imbalances related to type 2 diabetes.

4.2 Current Treatments for Type 2 Diabetes

Type 2 diabetes is commonly referred to as a disease of high blood sugar. There are many factors that contribute to this end result and the chronology of these events is still being debated in the scientific community. One of the main contributors to hyperglycemia is insulin resistance in target tissues, most importantly skeletal muscle, liver, and adipose tissue. If insulin fails to exert its actions in these tissues, it would translate to less glucose uptake and consequently increased blood glucose. Insulin resistance causes hyperinsulinemia, one of the hallmarks of the disease. Furthermore, since most type 2 diabetics are also overweight or obese, it can contribute to the insulin resistant state. Initially, the pancreatic β -cells tend to compensate for this insulin resistance by increasing in size and secreting more insulin (Kahn et al., 2006). Eventually, this can lead to β -cell failure and decreased insulin production, which can exacerbate the phenotype (Fu et al., 2013; Kahn et al., 2006). Lack of insulin production or insulin action leads to the failure of insulin to suppress hepatic gluconeogenesis and to counteract the actions of glucagon-producing alpha cells in the islets, both of which contribute to increasing blood sugar (Inzucchi et al., 2012). Although traditionally type 2 diabetes is referred to as non-insulin dependent, most type 2 diabetics will end up needing exogenous insulin to treat the disease.

Treatments for type 2 diabetes are aimed at improving one or more of these pathophysiological defects. Metformin is a drug that is used as a first line of defense since it has minimal side effects and doesn't cause hypoglycemia. It is an AMPK activator and it decreases hepatic glucose production (Inzucchi et al., 2012). Due to its activation of AMPK, an important metabolic regulator, metformin has been associated with additional beneficial effects, such as increasing fatty acid oxidation and improving oxidative stress and inflammation associated with

type 2 diabetes and obesity (Rojas and Gomez, 2013). Although initially metformin is very effective in blood glucose control, its effects decrease over time, and most patients end up needing a second form of therapy in addition (Rojas and Gomez, 2013).

One of the critical components of glucose homeostasis is adequate and proper insulin secretion from pancreatic β -cells. There are many drugs on the market aimed to improve this function in type 2 diabetics. Sulfonylureas and glinides are two classes of drugs that increase insulin secretion by closing K_{ATP} channels on β -cell membranes, leading to depolarization, calcium entry and insulin granule exocytosis (Inzucchi et al., 2012). Some of the disadvantages of these drugs include risk of hypoglycemia and weight gain due to adipogenic actions of excess insulin (Dimitriadis et al., 2011; Inzucchi et al., 2012). Incretins are gut hormones that are released in the bloodstream after eating and have been shown to increase insulin secretion (Kim and Egan, 2008). They do so by a variety of mechanisms, such as stimulation of the cAMP-PKA pathway, K_{ATP} channel closure, and increased intracellular Ca^{2+} in the β -cells (Kim and Egan, 2008). Because of this important role, incretin mimics or agents that prevent the breakdown of endogenous incretins are being used to augment insulin secretion (Inzucchi et al., 2012; Kim and Egan, 2008). In patients with inadequate insulin secretion, exogenous insulin administration is recommended. Exogenous insulin comes in a variety of forms with different actions (e.g. short vs. long acting), mimics the endogenous counterpart and lowers blood glucose and suppresses liver glucose production (Inzucchi et al., 2012). However, patients must closely monitor their blood glucose and calculate the amount of insulin being injected to minimize the risk of hypoglycemia. In addition, one of the challenges of this therapy is the rising cost of insulin worldwide (Sorli and Heile, 2014).

Another important pathophysiology of type 2 diabetes is insulin resistance, with many treatment options available to target and improve insulin action in key peripheral tissues. One such drug class are thiazolidinediones (TZDs), which are peroxisome proliferator receptor gamma (PPAR γ) activators, which improve insulin sensitivity in skeletal muscle (Inzucchi et al., 2012).

However, TZDs are associated with weight gain, which can counteract their beneficial effect on insulin signaling (Inzucchi et al., 2012). Some of the other commonly prescribed options include agents that slow down the breakdown of glucose in the gut, delaying an immediate spike in blood glucose after a meal and helping patients in administering hyperglycemia (Fonseca et al., 2010; Van de Laar et al., 2006). It is important to note that one of the first recommended strategies for managing diabetes is a change in life habits, such as increased exercise coupled with a low-carbohydrate diet, which should always be recommended either as single therapy or in combination depending on the current health and advancement of type 2 diabetes. However, the challenges of adhering to these lifestyle changes can minimize their positive impacts.

Even with these existing therapies, there is a need to develop new and more effective ones that can be used alone or in combination with the existing options to improve treatment of type 2 diabetes. One of the aims of this study is to provide more evidence for the anti-diabetic role of Thymoquinone, which can be developed as a type 2 diabetes therapeutic in the near future.

4.3 Diet-induced Obesity (DIO) Mouse Model of Type 2 Diabetes

To study new potential treatments for type 2 diabetes, it is necessary to use animal models to not only to study the related pathophysiologies, but also the possible mechanisms of action. Thus, an adequate animal model of the disease would need to display some of the most important phenotypic abnormalities of type 2 diabetes: hyperglycemia, hyperinsulinemia, and insulin resistance. In humans, the development of the disease occurs in a progression and is the result of many factors including lifestyle and genetic predisposition. An animal model of type 2 diabetes that mimics the disease progression including these causative factors is closer to being a relevant physiological model.

One animal model of type 2 diabetes is the Diet Induced Obesity (DIO) mouse. The DIO mice belong to the C57/BL6J strain and when fed a high fat diet (HFD), they become obese, and are otherwise lean when fed a low fat diet (Reuter, 2007). In addition to obesity, these mice show a progression towards the diabetic phenotype while on the HFD, becoming hyperglycemic, insulin

resistant, and hyperinsulinemic (Reuter, 2007; Surwit et al., 1988). Furthermore, their pancreatic β -cell function is impaired (Lee et al., 1995; Wencel et al., 1995). Additionally, they show a genetic predisposition to developing type 2 diabetes under HFD that is strain-specific for the C57/BL6J strain, as mice from other backgrounds (such as C/J and C57BL/KsJ) do not develop this phenotype under HFD (Reuter, 2007). With comparison to other genetic models or models rendered diabetic by streptozotocin injection, DIO mice have an advantage because they show a less severe phenotype that develops over time, thus better mimicking the pathophysiology of type 2 diabetes in humans (King, 2012). Additionally, in these models, diabetes is caused by genetic mutations (such as in the leptin or leptin receptor genes) that are very rare in human T2D (Kim et al., 2009), whereas the genetic susceptibility to T2D in DIO mice is broader and viewed as polygenic or multifactorial, which is closer to the human condition. Due to these characteristics, the DIO mice are a physiologically relevant model of both diabetes and obesity and have been vastly utilized in the research of new therapeutics for these diseases (Reuter et al., 2007). Furthermore, this model has been extensively used to test the effects of various natural products on diabetes and metabolic disorders (Choi et al., 2016; Hamza et al., 2012; Kim et al., 2009; Ouchfoun et al., 2016; Winters et al., 2003; Yang et al., 2010). Thus, we believe that the DIO mouse is a very suitable model to study the effects of Thymoquinone on glucose homeostasis, dyslipidemia, and inflammation in type 2 diabetes.

4.4 Hypothesis

Thymoquinone will ameliorate hyperglycemia, insulin resistance, tissue metabolic imbalances, lipid profile, inflammation, and weight gain in the diet-induced obesity (DIO) mouse model of type 2 diabetes. Because TQ has been reported to decrease NADH/NAD⁺ ratio (Gray et al., 2016), thus increasing NAD⁺, we also hypothesize that the anti-diabetic effects of TQ are mediated by activation of NAD⁺- dependent targets, SIRT-1 and AMPK.

4.5 Methods

4.5.1 Mouse Colony Maintenance and Ethical Statement

Male C57BL/6J mice (6 weeks of age) were purchased from Jackson Laboratories (Bar Harbor, ME) and housed (4 animals per cage) in a USF Animal Facility; room was maintained at a constant temperature (25°C) in a light:dark 12:12-h schedule. Food and water was available *ad libitum*. Body weight was monitored on a weekly basis. Mice were pair fed either control low fat diet, LFD (10% fat cal, Research Diets, New Brunswick, NJ) or high fat diet, HFD (45% fat cal, Research Diets, New Brunswick, NJ). Mice were separated in the following groups: LFD, LFD+TQ, HFD, HFD+TQ. TQ (dissolved in canola oil) was administered daily by oral gavage at 20 mg/kg body weight, respectively, for the duration of the study. Vehicle only (canola oil) was administered to control groups (LFD and HFD). The dose of TQ was chosen because it was shown to lower blood glucose (Pari and Sankaranarayanan, 2009), albeit in a non-physiological rodent model of diabetes. The chosen dose is well below toxic doses established for oral administration in mice (Al-Ali et al., 2008). As expected, TQ was well tolerated, and TQ administration did not affect the overall health of the animals in the study. After 24 weeks, animals were euthanized with isoflurane, tissues and serum collected, and either used immediately or were snap frozen in liquid nitrogen and stored in -80°C until further use. All animal procedures were performed in accordance with and approved by the Institutional Animal Care and Use Committee (IACUC) of the University of South Florida.

4.5.2 HepG2 Cell Culture and Treatment

HepG2 cells were obtained from American Tissue Culture Collection (ATCC) and were cultured in DMEM containing 1 g/L glucose and L-glutamine, and supplemented with 10% fetal bovine serum, 3.4 g/L sodium bicarbonate, 10000 U/mL penicillin, and 10 mg/mL streptomycin. Cells were maintained at 37°C in a humidified incubator with 5% CO₂. Cells were subcultured when confluency was around 80% using 0.25% Trypsin-EDTA and the suspension was passed 3 times through an 18-gauge needle to aid in cell dispersion and avoid cell clustering.

Cells were made insulin resistant by treatment with 20mM glucose for 18 hours, as previously described (Zhu et al., 2017). Following high glucose treatment, cells were starved for 2 hours in serum-free media, prior to treatment with the respective compounds for 24 hours. For inhibitor treatment, cells were pre-incubated with the inhibitors for 30 mins, and the inhibitors were also present during the 24-hour incubation period. To measure insulin signaling, insulin was added during the last 30 minutes. Vehicle-treated cells (0.5% DMSO) in normal (5.5 mM) and high (20 mM) glucose conditions served as controls.

4.5.3 Chemicals

Human recombinant insulin, resveratrol, and AICAR were purchased from Tocris Bioscience (Bristol, UK). Nicotinamide was purchased from Acros Organics (Geel, Belgium) and Compound C was purchased from EMD Millipore (Billerica, MA). All other chemicals and reagents were purchased from Sigma (St Louis, MO) unless specified otherwise. Stock solutions of thymoquinone, resveratrol, AICAR, Nicotinamide, and Compound C were prepared in DMSO and added to culture medium to achieve the indicated concentrations.

4.5.4 Oral Glucose Tolerance Tests (OGTT) and Insulin Tolerance Tests (ITT)

Mice were anesthetized with ketamine (80 mg/kg body weight). Oral glucose and insulin tolerance tests were performed following a 6 hr fast. Mice were oral gavaged with 2 mg/kg/bw glucose (OGTT), or injected intraperitoneally with 0.5 IU insulin/kg/bw (ITT). Blood was obtained at 0, 15, 30, 60, 90, 120 and 180 minutes post-glucose or insulin administration from the tail vein and blood glucose was measured with a glucometer (Bayer Contour).

4.5.5 Serum Collection

Whole blood was collected via cardiac puncture. After collection, blood was allowed to clot in room temperature for 30 minutes. Clot was removed by centrifuging at 2000 x g for 10 minutes, the resultant supernatant (serum) was collected and frozen at -80°C until further analysis.

4.5.6 Tissue Collection and Storage

At the end of the experiment, animals were euthanized; soleus muscle and liver were collected from mice in each group. To maximize the experimental efforts, each tissue was appropriately divided into three tubes: tissue collected for protein, metabolomics (GC-MS), or RNA analysis. Tissues for RNA analysis were collected in RNAlater (Sigma, St Louis, MO). All tissues were immediately snap-frozen in liquid nitrogen and stored at -80°C until further analysis.

4.5.7 Serum Cholesterol Content Measurement

Total cholesterol, HDL, and LDL/VLDL content was determined from serum samples using the HDL and LDL/VLDL Cholesterol Assay Kit (abcam, Cambridge, MA) according to the manufacturer's protocols.

4.5.8 Serum Measurements of Insulin, Resistin, and MCP-1

Serum levels of insulin, resistin and MCP-1 were determined by Ocean Ridge Biosciences (Deerfield Beach, FL) using a Luminex multiplex protein profiling assay (Luminex Corp., Austin, TX) per the manufacturer's protocols.

4.5.9 Western Blot Analysis

Liver and soleus muscle tissues were solubilized in RIPA lysis buffer (Pierce, Rockford, IL) using Fast Prep 24G system (MP Biosciences, Santa Ana, CA). After exposure, HepG2 cells were solubilized in RIPA lysis buffer. Protein content was determined using a BCA Protein Assay Kit (Pierce, Rockford, IL) and SDS samples were prepared. Equal amount of protein (100 µg per lane) were electrophoretically separated on SDS-polyacrylamide gel, followed by blotting onto PVDF membrane. Following the transfer, membranes were blocked with TBST (10 mmol/l Tris-HCl pH 7.4, 150 mmol/l NaCl, and 0.1% Tween 20) containing 5% nonfat dry milk (blocking buffer) and incubated with the primary antibodies (diluted in blocking buffer overnight at 4°C) against SIRT-1 (Cell Signaling, cat. #9475), p-SIRT-1 (Cell Signaling, cat. #2314), Akt (Cell Signaling, cat. #9272), p-Akt (Cell Signaling, cat. #9271), AMPK α (Cell Signaling, cat. #5831), p-AMPK α (Cell Signaling, cat. #2535), NQO1 (Santa Cruz, cat. #sc-16464), β -actin (Cell Signaling, cat.

#4970), and β -tubulin (Cell Signaling, cat. #2146). Membranes were incubated with goat anti-rabbit immunoglobulin (IgG) secondary antibody (Santa Cruz, cat. #sc-2030) for 1 h at room temperature, and washed 5 times. Proteins were detected by using enhanced chemiluminescence.

4.5.10 Reverse Transcription and Quantitative Real-time RT-PCR (qRT-PCR)

The tissue samples stored in RNAlater (Invitrogen, Carlsbad, CA) were homogenized by using the FastPrep 24G instrument (MP Biosciences, Santa Ana, CA). Total RNA was prepared using the TRIzol reagent according to the manufacturer's protocol (Invitrogen, Carlsbad, CA) and single-strand cDNA was synthesized from the RNA in a reaction mixture containing optimum blend of oligo(dT) primers and iScript reverse transcriptase (Bio-Rad, Richmond, CA). qRT-PCR amplifications were performed using rEVALution 2x qPCR Master Mix (Empirical Bioscience, Grand Rapids, MI) in an MyIQ2 Real-Time PCR Detection System (Bio-Rad, Richmond, CA) following manufacturer's protocol. To determine the specificity of amplification, melting curve analysis was applied to all final PCR products. The relative amount of target mRNA was calculated by the comparative threshold cycle method by normalizing target mRNA threshold cycle to those for glyceraldehyde-3-phosphate dehydrogenase (GAPDH). The primers used for analysis were as follows: NQO1: sense primer, 5'-AGGATGGGAGGTA CT CGAATC-3', anti-sense primer, 5'-AGGCGTCCTTCCTTATATGCTA-3'; GAPDH: sense primer, 5'-CTTCACCACCATGGAGAAGGC-3', anti-sense primer, 5'-GGCATGGACTGTGGTCATGAG-3'.

4.5.11 Metabolomics Analysis (GC/MS)

INS-1 832/13 cells, and frozen liver and soleus muscle samples were sent to the University of Utah Metabolomics core for Gas Chromatography Mass Spectrometry (GC/MS) analysis and were analyzed according to an in-house protocol. The levels of 80, 97, and 102 different metabolites were measured respectively in cells, liver, and soleus muscle and statistically relevant results from the appropriate control groups were reported.

4.5.12 Tissue Triglyceride Content Measurements

Triglyceride content was determined in liver and soleus muscle RIPA buffer lysates (lysates as described above) using the Triglyceride kit (Pointe Scientific, Canton, MI) according to the manufacturer's protocols.

4.5.13 Tissue NADH/NAD⁺ Measurement

Adenine nucleotides were measured in liver and soleus muscle using the NAD/NADH assay kit as per the manufacturer's protocol (Abcam, Cat #65348, Cambridge, UK).

4.5.14 Statistical Analysis

Data are expressed as means \pm SEM and are results from at least three independent experiments. Significance was determined for multiple comparisons using one-way or two-way analysis of variance (ANOVA) followed by Sidak or Holm-Sidak multiple comparisons tests (Neter et al., 1996; Wright, 1992) for planned comparisons (as mentioned in each figure) or independent t-test as indicated. A p-value of ≤ 0.05 was considered significant.

4.6 Results

4.6.1 C57/BL6J Mice Became Diabetic and Obese Following High Fat Diet Administration

The Diet Induced Obesity (DIO) mice develop obesity, hyperinsulinemia, glucose intolerance and insulin resistance when fed a high fat diet, making them a suitable model to study type 2 diabetes pathophysiology. The emergence of the obese phenotype is confirmed in our study, where after HFD administration, C57/BL6J mice weight gain was significant from week 8 until the end of the study compared to the LFD counterparts (Figure 4.1A). Mean weight of HFD mice was 36 grams compared to 29 grams for LFD during the same period, and this difference became much more apparent by the last week of the study.

HFD mice became hyperglycemic (as demonstrated by fasting blood glucose) and hyperinsulinemic (Figure 4.1 B and C). Furthermore, they displayed decreased glucose tolerance

and insulin sensitivity as shown by the OGTT and ITT tests (Figure 4.2 A and B). These results are in agreement with prior studies showing the emergence of the diabetic and obese phenotype in C57/BL6J mice fed a HFD compared to their LFD counterparts (Reuter, 2007; Surwit et al., 1988).

4.6.2 Thymoquinone Ameliorates Weight Gain and Lowers Fasting Blood Glucose in DIO Mice

TQ treatment led to a mild amelioration of the weight gain in HFD group compared to HFD alone, with the decrease being significant only during weeks 22 and 23 of the study, and no differences were observed in the LFD with TQ (Figure 4.1 A). TQ administration lowered fasting blood glucose in HFD mice compared to HFD alone (Figure 4.1 B). No differences were seen in the LFD groups with TQ administration (Figure 4.1 B).

4.6.3 Thymoquinone Ameliorates Hyperinsulinemia, Improves Glucose Tolerance and Insulin Sensitivity in DIO Mice

One of the distinct pathophysiologies of type 2 diabetes is hyperinsulinemia, which we observe in DIO mice after HFD regimen. TQ treatment decreased the hyperinsulinemia as measured by serum insulin levels in DIO mice compared to HFD alone, with no change in the LFD group (Figure 4.1 C).

Glucose tolerance tests (GTTs) measure the ability of the body to normalize blood glucose levels after a bolus glucose challenge. GTTs are done to assess pancreatic response (insulin secretion) and insulin action (sensitivity) during and after the glucose challenge (Ayala et al., 2010). As a result, animals with impaired β -cell function or with insulin resistance will clear glucose at a slower rate than non-impaired animals. Indeed, the blood glucose spike that we saw in DIO mice treated with TQ is significantly lower than that of HFD mice after 15, 30, and 60-minutes post-glucose bolus (Figure 4.2 B)

Similar to GTTs, insulin tolerance tests measure the ability of the body to normalize blood glucose levels after a bolus insulin challenge and indicates a whole-body response to insulin

(Ayala et al., 2010). Thus, in animals with insulin resistance, the decrease in blood glucose is smaller compared to animals with normal insulin sensitivity. TQ treatment in DIO mice caused a more rapid decrease in blood glucose at 15 and 30-minutes post-injection compared to HFD mice, improving their insulin sensitivity (Figure 4.2 B).

4.6.4 Thymoquinone Lowers Serum Levels of Resistin and MCP-1 in DIO Mice

Type 2 diabetes is associated with increased inflammation, which can contribute to insulin resistance and is shown to be detrimental to many tissues including pancreatic β -cells (Dula et al., 2010; Lumeng and Saltiel, 2011). Resistin, a hormone secreted by adipocytes, impairs glucose tolerance and insulin sensitivity in mice (Steppan et al., 2001) and has been associated with insulin resistance in humans (Rodriguez et al., 2016; Santilli et al., 2016). Monocyte chemoattractant protein-1 (MCP-1) is a pro-inflammatory chemokine that can induce insulin resistance (Tateya et al., 2010) and circulating levels of this chemokine are increased in patients with type 2 diabetes (Nomura et al., 2000; Piemonti et al., 2009; Zietz et al., 2005). TQ lowered serum levels of resistin in DIO mice (Figure 4.3 A). There was a trend to lower the MCP-1 levels, however, this didn't reach statistical significance in HFD animals ($p = 0.06$), although TQ decreased MCP-1 in LFD animals (Figure 4.3 B).

4.6.5 Thymoquinone Normalizes Lipid Profile in DIO Mice

Elevated levels of triglycerides, together with decreased HDL and increased LDL cholesterol levels are the key identifiers of diabetic dyslipidemia, which can exacerbate insulin resistance (Mooradian et al., 2009). Consistent with previously reported data demonstrating TQ-dependent increase in fatty acid oxidation (Gray et al., 2016), and observed increased peripheral insulin sensitivity in this study (as shown by the improvement of the ITT in DIO mice, Figure 4.2 B), TQ ameliorated HFD-dependent increase in liver triglyceride levels (Figure 4.4 A). There was a trend to lower HFD-dependent muscle triglyceride content, however this did not reach statistical significance (Figure 4.4 B). There was also a trend to decrease serum cholesterol level, albeit statistically not significant (Figure 4.5 A). However, TQ significantly decreased the levels of LDL

cholesterol in the serum of HFD animals (Figure 4.5 C), with no effect on the HDL levels (Figure 4.5 B). This effect was selective to the HFD diet, as LFD animals did not demonstrate changes in their HDL or LDL/VLDL cholesterol in response to TQ regimen. We saw similar trends when analyzing serum glycerol and three relevant fatty acids: palmitic acid, oleic acid, and stearic acid. GC/MS analysis showed that serum levels of these metabolites were decreased in DIO mice treated with TQ compared to HFD alone (Table 4.1), however this didn't reach statistical significance.

4.6.6 Thymoquinone Activates SIRT-1 and AMPK α in Insulin-sensitive Tissues

The lowered tissue triglyceride levels following TQ administration argues for the TQ-dependent activation of the oxidative pathways (and consequent oxidation, rather than deposition of metabolic substrates). NADH/NAD⁺ ratio is important determinant of metabolic flux (Wu et al., 2016), and a prior study reported that TQ lowers NADH/NAD⁺ ratio in pancreatic β -cells exposed to glucose overload (Gray et al., 2016). Since NADH/NAD⁺ ratio is known to regulate SIRT-1 pathway, we analyzed effect of TQ feeding on this pathway in the liver and soleus muscle of TQ-treated compared to control mice. Liver and soleus muscle from mice treated with TQ had enhanced phosphorylated (activated) SIRT-1 in both LFD and HFD groups (Figure 4.7 A-D). In the liver, TQ enhanced AMPK α phosphorylation as well as phosphorylation of Akt (protein kinase B), a key member of insulin signaling pathway (reviewed in Tanti and Jager, 2009) (Figure 4.8 A and B).

4.6.7 Thymoquinone Lowers NADH/NAD⁺ Ratio in Liver and Soleus Muscle

To determine whether the increase in SIRT-1 activation in liver and soleus muscle is due to the increase in NAD⁺ in these tissues, we examined the NADH/NAD⁺ ratio. In liver, we saw an increase in this ratio in DIO mice (Figure 4.6 A), which agrees with prior studies reporting an increase in NADH with obesity and type 2 diabetes (Wu et al., 2016). However, we did not observe this in soleus muscle, as we saw no change in this ratio compared to lean mice (Figure 4.6 B). In both liver and solus muscle, we saw a decrease in the NADH/NAD⁺ ratio in TQ-treated

DIO mice compared to HFD alone (Figures 4.6 A and B). This result is in agreement with a prior study by Gray et al., showing that TQ lowers the NADH/NAD⁺ ratio in INS-1 832/13 cells chronically exposed to high glucose concentrations.

4.6.8 Thymoquinone Improves Insulin Resistance via SIRT-1 Activation in HepG2 Cells

To evaluate the mechanistic actions behind TQ-induced insulin sensitivity, we used the HepG2 cell line, a widely used *in vitro* model of insulin resistance to assess whether this action is SIRT-1-dependent. HepG2 cells were made insulin resistant as described above, which was confirmed by decreased p-Akt protein after high glucose treatment (Figure 4.9 A and B). TQ increased p-Akt in high-glucose treated cells, restoring these levels to that of the control cells (Figure 4.9 A and B). This shows that TQ improves insulin resistance in similar fashion to what we see in livers of DIO mice. This action showed to be SIRT-1-dependent, as pre-treatment of insulin resistant cells with SIRT-1 inhibitor nicotinamide in the presence of TQ, significantly decreases p-Akt protein and TQ-induced insulin sensitivity (Figure 4.9 A and B). Furthermore, treatment with resveratrol (a SIRT-1 activator) and AICAR (an AMPK α activator) increased insulin sensitivity, although this trend was not statistically significant (Figure 4.9 A and B). Pre-treatment with compound C (AMPK α inhibitor) or compound C and nicotinamide in the presence of TQ decreased insulin sensitivity compared to TQ treatment alone, albeit statistically insignificant (Figure 4.9 A and B).

TQ treatment showed similar trends to the *in vivo* experiments in increasing phosphorylation of SIRT-1 and AMPK α in insulin-resistant cells, which was not significant (Figure 4.10 A-D). Trends were also observed in increased p-SIRT-1 and p-AMPK α with resveratrol and AICAR in the presence of TQ (Figure 4.10 A-D), as well as a decrease in phosphorylation of SIRT-1 with nicotinamide or compound C in the presence of TQ after high glucose treatment (Figure 4.10 A and B). Pre-treatment with compound C and combined pre-treatment with compound C and nicotinamide significantly decreased p-AMPK α in the presence of TQ compared to TQ

treatment alone (Figure 4.10 C and D). Taken together, these results provide additional support about the role of TQ in improving insulin resistance, as well as show that this action is likely mediated by SIRT-1 activation.

4.6.9 Thymoquinone Does Not Induce Oxidative Stress

TQ applied in this study was within the physiologically relevant diet-derived levels. However, non-physiologically high and toxic levels of quinones are known to generate excessive levels of reactive oxygen intermediates via quinone-dependent redox cycling, and this causes induction of the NAD(P)H-dependent Quinone Oxidoreductase 1 (NQO1). NQO1 is a phase 2 detoxification enzyme induced in response to oxidative stress, which expression is regulated by the Keap1/Nrf2/ARE pathway (Dinkova-Kostova and Talalay, 2010; Gray et al., 2016), and NQO1 alone has been shown to regulate NADH/NAD⁺ ratio (Gaikwad et al., 2001; Gray et al., 2016). To ascertain that applied doses of TQ were physiologically low and not inductive of NQO1 and/or oxidative stress, mRNA and protein levels of NQO1 were measured in liver and muscle. Levels of NQO1 were not elevated in any of these tissues, confirming that applied doses, while effective in regulating the cellular redox status, do not activate the Keap1/Nrf2/ARE pathway and do not increase oxidative stress (Figure 4.11 A-D). This further supports our hypothesis that TQ-dependent re-oxidation of NADH and consequent decrease of the NADH/NAD⁺ ratio is the main mechanism to activate SIRT-1/AMPK pathway and promote fuel oxidation rather than deposition, which leads to the observed changes in normalization of glucose homeostasis in DIO mice following TQ administration.

4.6.10 Thymoquinone Lowers Levels of TCA Cycle Anaplerotic Intermediates in INS-1 832/13 Cells but Not in the DIO Mice

Western style diets have contributed to the rise in obesity and diabetes in the last two decades. Obesity is closely associated with type 2 diabetes, as most type 2 diabetics are either overweight or obese. Obesity can increase insulin resistance in the metabolically relevant tissues. One proposed mechanism is that obesity increases anaplerotic (storage promoting) intermediates

of the TCA cycle, leading to a decrease in fuel mobilization by the insulin sensitive periphery, which can exacerbate insulin resistance (Muio and Newgard, 2008). Due to the protective effect on β -cells under hyperglycemia and nutrient overload via enhanced glucose and fatty acid oxidation observed *in vitro* (Gray et al., 2016), we hypothesized that TQ may decrease the levels of TCA cycle anaplerotic intermediates. To mimic the HFD (or nutrient overload) state in cells, INS-1 832/13 cells were exposed to high glucose (25 mM) chronically for 72 hours in the presence or absence of TQ. Cells in growth media (containing 11 mM glucose) served as controls. After 72 hours, cells were collected and the levels of TCA cycle intermediates were analyzed by GC/MS. There was an increase in TCA cycle anaplerotic intermediates with high glucose treatment (Table 4.2). Treatment with TQ decreased the levels of citric acid, aconitate, isocitric acid, and malic acid in high glucose-treated cells, suggesting that TQ might be beneficial in decreasing the storage-promoting functions of the TCA cycle.

To evaluate whether a similar action was taking effect *in vivo*, livers and soleus muscle from DIO and LFD mice treated with TQ or vehicle were analyzed for the levels of TCA cycle intermediates. However, in liver and soleus muscle, we did not see any expected trends either in the increase of anaplerotic intermediates with HFD administration, or the decrease of them after TQ treatment in DIO mice (Tables 4.3 and 4.4). Significant changes in the liver included decreases in fumaric acid, malic acid, and aspartic acid with in DIO mice compared to lean (LFD) (Table 4.3). In soleus muscle, there was an increase in pyruvic acid with HFD administration, as well as a decrease in 2-ketoglutaric acid in DIO mice after TQ administration (Table 4.4) There were no significant changes in the other TCA cycle intermediates in liver and soleus muscle when comparing LFD with HFD, and HFD with HFD + TQ (Tables 4.3 and 4.4).

4.7 Discussion

This is one of the first *in vivo* studies, to our knowledge, aimed to comprehensively evaluate the effect of thymoquinone (TQ), a bioactive component of the *Nigella sativa* plant, on whole body glucose homeostasis using a physiologically-relevant mouse model of type 2

diabetes. In our published *in vitro* study, we have reported that both *Nigella sativa* extract (NSE) of high thymoquinone (TQ) content, as well as TQ alone, decreased NADH/NAD⁺ ratio and stimulated glucose and fatty acid oxidation in pancreatic β -cells, and this action was accompanied by the restoration of the glucose-stimulated insulin secretion (GSIS) in cells exposed to glucose overload (Gray et al., 2016). Here we have expanded our studies to an *in vivo* model with focus on the TQ effect on the insulin sensitive peripheral tissues, and evaluated the action of TQ on glucose homeostasis in Diet Induced Obesity (DIO) mice.

After 24 weeks of HFD, C57/BL6J mice became obese and diabetic, as demonstrated by their increased body weight (Figure 4.1 A), elevated fasting blood glucose (Figure 4.1 B), insulin (Figure 4.1 C) and impaired OGTT and ITT (Figure 4.2). While TQ treatment improved all these parameters in HFD animals, TQ had no significant effect on weight, fasting blood glucose and insulin, or OGTT /ITT in animals treated with LFD, suggesting that TQ primarily affects DIO metabolism by increasing oxidation of diet-derived fatty acid surplus. However, it is still possible that TQ treatment beyond the 24 weeks could lead to observed changes in physiological parameters in the LFD group as well, and further studies are required to address this issue. Bioavailability of TQ after an oral administration can be a limiting factor on TQ actions. Although such studies have been very limited in mice, studies with other animal models have shown that TQ is rapidly eliminated and slowly absorbed (Alkharfy et al., 2015; Elmowafy et al., 2016). Therefore, further studies are required to address the bioavailability of TQ after oral administration in mice to properly determine a relevant dose and exposure window, particularly in physiologically relevant mouse models of type 2 diabetes.

Metabolism is governed by the oxidation status of nicotinamide adenine dinucleotide, represented by the ratio between its reduced and oxidized forms (NADH/NAD⁺) (Wu et al., 2016). During glycolysis NAD⁺ is reduced to NADH, which needs to be re-oxidized back to NAD⁺ (Wu et al., 2016). In chronic hyperglycemic conditions, such as in type 2 diabetes, there can be NADH overproduction due to the fact that mitochondrial shuttles are unable to efficiently re-oxidize

NADH, which leads to the condition known as reductive stress (Ido et al., 2007; Wu et al., 2016). This leads to increased pressure on mitochondrial complex I, the primary site of NADH recycling, which in turn causes the formation of superoxide (Ido et al., 2007; Wu et al., 2016) and enhanced oxidative stress, known to be detrimental to insulin sensitivity and insulin secretion and exacerbate the diabetic phenotype (Luo et al., 2015; Yan, 2014). NADH excess inhibits glycolytic and TCA cycle enzymes (glyceraldehyde 3-phosphate dehydrogenase, pyruvate dehydrogenase, isocitrate dehydrogenase, α -ketoglutarate dehydrogenase, malate dehydrogenase), leading to the impairment of glucose oxidation and TCA cycle oxidative pathways (Wu et al., 2016; Yan, 2014). TQ has been shown to regulate oxidation level of adenine nucleotides (Gray et al., 2016). Due to its conjugated double bond system, TQ is able to re-oxidize NADH in the process of NAD(P)-dependent redox cycling (Khader et al., 2009), and thus decrease the NADH/NAD⁺ ratio, as shown by our group (Gray et al., 2016). Furthermore, in this study we also demonstrate that TQ treatment leads to a decrease in the NADH/NAD⁺ ratio in liver and skeletal muscle in HFD mice (Figure 4.6). Regeneration of NAD⁺ from TQ can thus increase glucose and fatty acid oxidation and ameliorate diabetic dyslipidemia. Diabetic dyslipidemia is characterized by high plasma triglyceride concentration, low HDL cholesterol and elevated non-HDL cholesterol (Mooradian, 2009). The main cause of this phenotype is the increased free fatty acid release from insulin-resistant adipose tissue in type 2 diabetes (Krauss and Siri, 2009; Taskinen, 2003). The influx of free fatty acids in the liver can promote triglyceride synthesis, increasing the production of non-HDL (LDL, VLDL) cholesterol to transfer lipids to tissues and decreasing HDL cholesterol levels, which transfer lipids back to liver for degradation (Mooradian, 2009). Indeed, our data demonstrating that TQ treatment decreased serum LDL/VLDL levels (while not affecting HDL levels) and tissue level of triglycerides (Figures 4.4 and 4.5) in HFD mice are consistent with TQ antidiabetic action and effect on lipid homeostasis. TQ-dependent decrease in triglyceride and LDL/VLDL levels correlated with improved insulin signaling and insulin sensitivity judged by enhanced phosphorylation of Akt (Figure 4.8). Akt activation is consistent with the observed

improvement in insulin sensitivity seen with the insulin tolerance test (Figure 2B). These results are in accordance with our previously reported *in vitro* results (Gray et al., 2016) that TQ increases glucose and fatty acid oxidation, which can lead to enhanced fuel oxidation by peripheral tissues, weight loss and increased insulin sensitivity.

In addition to serving as a regulator of metabolic flux and substrate for metabolic processes, NAD⁺ can activate sirtuin 1 (SIRT-1) and consequently SIRT-1-dependent pathways (Kitada and Koya, 2015). SIRT-1 is a class III histone deacetylase, where NAD⁺ functions as a substrate for SIRT-1 deacetylation of target proteins (Kitada and Koya, 2015). SIRT-1 has been implicated directly in critical aspects of glucose homeostasis, such as increasing insulin secretion and insulin sensitivity, and lowering the inflammation and oxidative stress associated with diabetes and obesity (Bordone et al., 2005; Karandrea et al., 2017; Kitada and Koya, 2015; Sun et al., 2007; Zhang, 2007). Enhanced production of NAD⁺ via TQ-dependent redox cycling is consistent with increased level of SIRT-1 phosphorylation in liver and muscle (Figure 4.7 A-D). It has been previously shown that SIRT-1 can activate AMPK (AMP-activated protein kinase) by de-acetylating and activating serine-threonine liver kinase B1 (LKB1), an upstream activator of AMPK (Ruderman et al., 2010). AMPK is activated when cellular energy levels are low (e.g. high AMP/ATP ratio), and has been shown to enhance fatty acid oxidation, glycolysis, stimulate glucose uptake in skeletal muscle, and inhibit cholesterol synthesis (Coughlan et al., 2014). We saw increased phosphorylated AMPK α protein in the liver of both LFD and HFD animals treated with TQ (Figure 4.8), suggesting that TQ can activate AMPK-dependent pathways. Due to similarities in their action on different processes, such as cellular metabolism and inflammation, it has been suggested that AMPK and SIRT-1 are involved in a cycle where they regulate each other (Ruderman et al., 2010). Whether TQ administration activates AMPK indirectly via SIRT-1, or directly via alteration of parameters different from NADH/NAD⁺ ratio, warrants further investigation. To mechanistically explore whether the increase in insulin sensitivity with TQ treatment is SIRT-1-dependent, we used the HepG2 cell line as a model of insulin resistance. TQ

treatment reversed insulin resistance after 24 hours, shown by the increase in phosphorylated Akt (Figure 4.9). Pre-treatment with SIRT-1 inhibitor nicotinamide suppressed this TQ effect on insulin signaling, suggesting that it is likely SIRT-1-dependent. Pre-treatment with AMPK α inhibitor compound C also inhibited the effect of TQ, albeit statistically insignificant. Furthermore, there was an improvement in insulin resistance after treatment with SIRT-1 and AMPK activators, suggesting a positive role of these pathways in insulin signaling.

Diabetes and obesity are associated with tissue inflammation, which can exacerbate insulin resistance. Adipose-derived pro-inflammatory markers such as resistin and chemokines (MCP-1) can exacerbate insulin resistance by activating c-Jun N-terminal (JNK) kinases and NF- κ B transcription factors, which can promote serine phosphorylation (inhibition) of insulin receptor substrate-1 (IRS-1), a key component of insulin signaling (Shoelson et al., 2006). SIRT-1 has been shown to inhibit NF- κ B activity, and therefore suppress the inflammatory process (Yoshizaki et al., 2010). Indeed, TQ treatment decreased serum levels of the pro-inflammatory marker resistin (Figure 4.3 A). Lower resistin levels are consistent with observed increase in the insulin sensitivity in HFD animals (Figure 4.2 B). Since resistin has been shown to increase LDL levels (Rashid, 2013), lowering of this marker is also consistent with the observed decreases in serum LDL cholesterol (Figure 4.5 C).

Taken together, our study shows that TQ administration improves glucose tolerance and insulin sensitivity in the diet-induced obesity (DIO) mouse model of type 2 diabetes. Furthermore, TQ treatment has the potential to ameliorate inflammation, altered lipid profile, and weight gain associated with the diabetic and obese state. These anti-diabetic effects of TQ may be mediated by activating SIRT-1 and AMPK pathways, as shown from this study. Our results add to the existing evidence supporting the role of TQ as a natural therapeutic for the treatment of type 2 diabetes, however, further studies are necessary to establish the potential of TQ to treat type 2 diabetes in humans.

4.8 References

- Al-Ali, A., Alkhawajah, A. A., Randhawa, M. A., & Shaikh, N. A. (2008). Oral and intraperitoneal LD50 of thymoquinone, an active principle of *Nigella sativa*, in mice and rats. *J Ayub Med Coll Abbottabad*, *20*(2), 25-27.
- Alkharfy, K. M., Ahmad, A., Khan, R. M., & Al-Shagha, W. M. (2015). Pharmacokinetic plasma behaviors of intravenous and oral bioavailability of thymoquinone in a rabbit model. *European journal of drug metabolism and pharmacokinetics*, *40*(3), 319-323.
- American Diabetes Association. (2014). Diagnosis and classification of diabetes mellitus. *Diabetes care*, *37*(Supplement 1), S81-S90.
- Ayala, J. E., Samuel, V. T., Morton, G. J., Obici, S., Croniger, C. M., Shulman, G. I., ... & McGuinness, O. P. (2010). Standard operating procedures for describing and performing metabolic tests of glucose homeostasis in mice. *Disease models & mechanisms*, *3*(9-10), 525-534.
- Centers for Disease Control and Prevention. (2014). National diabetes statistics report: estimates of diabetes and its burden in the United States, 2014. *Atlanta, GA: US Department of Health and Human Services, 2014*.
- Centers for Disease Control and Prevention. (2016). Long term trends in diabetes. *Atlanta, GA: US Department of Health and Human Services, 2016*.
- Choi, J. Y., Kim, Y. J., Ryu, R., Cho, S. J., Kwon, E. Y., & Choi, M. S. (2016). Effect of Green Tea Extract on Systemic Metabolic Homeostasis in Diet-Induced Obese Mice Determined via RNA-Seq Transcriptome Profiles. *Nutrients*, *8*(10), 640.
- Dall, T. M., Yang, W., Halder, P., Pang, B., Massoudi, M., Wintfeld, N., ... & Hogan, P. F. (2014). The economic burden of elevated blood glucose levels in 2012: diagnosed and undiagnosed diabetes, gestational diabetes mellitus, and prediabetes. *Diabetes care*, *37*(12), 3172-3179.
- Dimitriadis, G., Mitrou, P., Lambadiari, V., Maratou, E., & Raptis, S. A. (2011). Insulin effects in muscle and adipose tissue. *Diabetes research and clinical practice*, *93*, S52-S59.
- Dinkova-Kostova, A. T., & Talalay, P. (2010). NAD (P) H: quinone acceptor oxidoreductase 1 (NQO1), a multifunctional antioxidant enzyme and exceptionally versatile cytoprotector. *Archives of biochemistry and biophysics*, *501*(1), 116-123.
- Dula, S. B., Jecmenica, M., Wu, R., Jahanshahi, P., Verrilli, G. M., Carter, J. D., ... & Nunemaker, C. S. (2010). Evidence that low-grade systemic inflammation can induce islet dysfunction as measured by impaired calcium handling. *Cell calcium*, *48*(2), 133-142.
- Elmowafy, M., Samy, A., Raslan, M. A., Salama, A., Said, R. A., Abdelaziz, A. E., ... & Viitala, T. (2016). Enhancement of bioavailability and pharmacodynamic effects of thymoquinone via nanostructured lipid carrier (NLC) formulation. *AAPS PharmSciTech*, *17*(3), 663-672.
- Fonseca, V. A., Handelsman, Y., & Staels, B. (2010). Colesevelam lowers glucose and lipid levels in type 2 diabetes: the clinical evidence. *Diabetes, Obesity and Metabolism*, *12*(5), 384-392.

Fu, Z., R Gilbert, E., & Liu, D. (2013). Regulation of insulin synthesis and secretion and pancreatic Beta-cell dysfunction in diabetes. *Current diabetes reviews*, 9(1), 25-53.

Gaikwad, A., Long, D. J., Stringer, J. L., & Jaiswal, A. K. (2001). In vivo role of NAD (P) H: quinone oxidoreductase 1 (NQO1) in the regulation of intracellular redox state and accumulation of abdominal adipose tissue. *Journal of Biological Chemistry*, 276(25), 22559-22564.

Gray, J. P., Burgos, D. Z., Yuan, T., Seeram, N., Rebar, R., Follmer, R., & Heart, E. A. (2016). Thymoquinone, a bioactive component of *Nigella sativa*, normalizes insulin secretion from pancreatic β -cells under glucose overload via regulation of malonyl-CoA. *American Journal of Physiology-Endocrinology and Metabolism*, 310(6), E394-E404.

Gray, J. P., Karandrea, S., Burgos, D. Z., Jaiswal, A. A., & Heart, E. A. (2016). NAD (P) H-dependent quinone oxidoreductase 1 (NQO1) and cytochrome P450 oxidoreductase (CYP450OR) differentially regulate menadione-mediated alterations in redox status, survival and metabolism in pancreatic β -cells. *Toxicology letters*, 262, 1-11.

Hamza, N., Berke, B., Cheze, C., Le Garrec, R., Umar, A., Agli, A. N., ... & Moore, N. (2012). Preventive and curative effect of *Trigonella foenum-graecum* L. seeds in C57BL/6J models of type 2 diabetes induced by high-fat diet. *Journal of ethnopharmacology*, 142(2), 516-522.

Ido, Y. (2007). Pyridine nucleotide redox abnormalities in diabetes. *Antioxidants & redox signaling*, 9(7), 931-942.

Inzucchi, S. E., Bergenstal, R. M., Buse, J. B., Diamant, M., Ferrannini, E., Nauck, M., ... & Matthews, D. R. (2012). Management of hyperglycaemia in type 2 diabetes: a patient-centered approach. Position statement of the American Diabetes Association (ADA) and the European Association for the Study of Diabetes (EASD). *Diabetologia*, 55(6), 1577-1596.

Kahn, S. E., Cooper, M. E., & Del Prato, S. (2014). Pathophysiology and treatment of type 2 diabetes: perspectives on the past, present, and future. *The Lancet*, 383(9922), 1068-1083.

Kahn, S. E., Hull, R. L., & Utzschneider, K. M. (2006). Mechanisms linking obesity to insulin resistance and type 2 diabetes. *Nature*, 444(7121), 840.

Karandrea, S., Yin, H., Liang, X., Slitt, A. L., & Heart, E. A. (2017). Thymoquinone ameliorates diabetic phenotype in Diet-Induced Obesity mice via activation of SIRT-1-dependent pathways. *PloS one*, 12(9), e0185374.

Khader, M., Bresgen, N., & Eckl, P. M. (2009). In vitro toxicological properties of thymoquinone. *Food and Chemical Toxicology*, 47(1), 129-133.

Kim, K., Kim, H., Kwon, J., Lee, S., Kong, H., Im, S. A., ... & Park, Y. I. (2009). Hypoglycemic and hypolipidemic effects of processed Aloe vera gel in a mouse model of non-insulin-dependent diabetes mellitus. *Phytomedicine*, 16(9), 856-863.

Kim, W., & Egan, J. M. (2008). The role of incretins in glucose homeostasis and diabetes treatment. *Pharmacological reviews*, 60(4), 470-512.

King, A. J. (2012). The use of animal models in diabetes research. *British journal of pharmacology*, 166(3), 877-894.

- Kitada, M., & Koya, D. (2013). SIRT1 in type 2 diabetes: mechanisms and therapeutic potential. *Diabetes & metabolism journal*, 37(5), 315-325.
- Krauss, R. M., & Siri, P. W. (2004). Dyslipidemia in type 2 diabetes. *Medical Clinics*, 88(4), 897-909.
- Lee, S. K., Opara, E. C., Surwit, R. S., Feinglos, M. N., & Akwari, O. E. (1995). Defective glucose-stimulated insulin release from perfused islets of C57BL/6J mice. *Pancreas*, 11(2), 206-211.
- Lumeng, C. N., & Saltiel, A. R. (2011). Inflammatory links between obesity and metabolic disease. *The Journal of clinical investigation*, 121(6), 2111.
- Mooradian, A. D. (2009). Dyslipidemia in type 2 diabetes mellitus. *Nature clinical practice Endocrinology & metabolism*, 5(3), 150-159.
- Neter, J., Kutner, M. H., Nachtsheim, C. J., & Wasserman, W. (1996). *Applied linear statistical models* (Vol. 4, p. 318). Chicago: Irwin.
- Nomura, S., Shouzu, A., Omoto, S., Nishikawa, M., & Fukuhara, S. (2000). Significance of chemokines and activated platelets in patients with diabetes. *Clinical & Experimental Immunology*, 121(3), 437-443.
- Ouchfoun, M., Eid, H. M., Musallam, L., Brault, A., Li, S., Vallerand, D., ... & Haddad, P. S. (2016). Labrador tea (*Rhododendron groenlandicum*) attenuates insulin resistance in a diet-induced obesity mouse model. *European journal of nutrition*, 55(3), 941-954.
- Piemonti, L., Calori, G., Lattuada, G., Mercalli, A., Ragogna, F., Garancini, M. P., ... & Perseghin, G. (2009). Association between plasma monocyte chemoattractant protein-1 concentration and cardiovascular disease mortality in middle-aged diabetic and nondiabetic individuals. *Diabetes care*, 32(11), 2105-2110.
- Rashid, S. (2013). Mechanisms by which elevated resistin levels accelerate atherosclerotic cardiovascular disease. *Rheumatol Curr Res*, 3(1), 1-6.
- Reuter, T. Y. (2007). Diet-induced models for obesity and type 2 diabetes. *Drug discovery today: disease models*, 4(1), 3-8.
- Rodríguez, I. M., García, J. O., Sánchez, J. J. A., González, D. A., Coello, S. D., Díaz, B. B., ... & de León, A. C. (2016). Lipid and inflammatory biomarker profiles in early insulin resistance. *Acta diabetologica*, 53(6), 905-913.
- Rojas, L. B. A., & Gomes, M. B. (2013). Metformin: an old but still the best treatment for type 2 diabetes. *Diabetology & metabolic syndrome*, 5(1), 6.
- Ruderman, N. B., Xu, X. J., Nelson, L., Cacicedo, J. M., Saha, A. K., Lan, F., & Ido, Y. (2010). AMPK and SIRT1: a long-standing partnership?. *American Journal of Physiology-Endocrinology and Metabolism*, 298(4), E751-E760.

- Santilli, F., Liani, R., Di Fulvio, P., Formoso, G., Simeone, P., Tripaldi, R., ... & Davi, G. (2016). Increased circulating resistin is associated with insulin resistance, oxidative stress and platelet activation in type 2 diabetes mellitus. *Thrombosis and haemostasis*, 116(6), 1089-1099.
- Shoelson, S. E., Lee, J., & Goldfine, A. B. (2006). Inflammation and insulin resistance. *Journal of Clinical Investigation*, 116(7), 1793.
- Sorli, C., & Heile, M. K. (2014). Identifying and meeting the challenges of insulin therapy in type 2 diabetes. *Journal of multidisciplinary healthcare*, 7, 267.
- Steppan, C. M., Bailey, S. T., Bhat, S., & Brown, E. J. (2001). The hormone resistin links obesity to diabetes. *Nature*, 409(6818), 307.
- Surwit, R. S., Kuhn, C. M., Cochrane, C., McCubbin, J. A., & Feinglos, M. N. (1988). Diet-induced type II diabetes in C57BL/6J mice. *Diabetes*, 37(9), 1163-1167.
- Tanti, J. F., & Jager, J. (2009). Cellular mechanisms of insulin resistance: role of stress-regulated serine kinases and insulin receptor substrates (IRS) serine phosphorylation. *Current opinion in pharmacology*, 9(6), 753-762.
- Tateya, S., Tamori, Y., Kawaguchi, T., Kanda, H., & Kasuga, M. (2010). An increase in the circulating concentration of monocyte chemoattractant protein-1 elicits systemic insulin resistance irrespective of adipose tissue inflammation in mice. *Endocrinology*, 151(3), 971-979.
- Van de Laar, F. A., Lucassen, P. L., Akkermans, R. P., Van de Lisdonk, E. H., & De Grauw, W. J. (2006). Alpha-glucosidase inhibitors for people with impaired glucose tolerance or impaired fasting blood glucose. *The Cochrane Library*.
- Wencel, H. E., Smothers, C., Opara, E. C., Kuhn, C. M., Feinglos, M. N., & Surwit, R. S. (1995). Impaired second phase insulin response of diabetes-prone C57BL/6J mouse islets. *Physiology & behavior*, 57(6), 1215-1220.
- Winters, W. D., Huo, Y. S., & Yao, D. L. (2003). Inhibition of the progression of type 2 diabetes in the C57BL/6J mouse model by an anti-diabetes herbal formula. *Phytotherapy Research*, 17(6), 591-598.
- Wright, S. P. (1992). Adjusted p-values for simultaneous inference. *Biometrics*, 1005-1013.
- Wu, J., Jin, Z., Zheng, H., & Yan, L. J. (2016). Sources and implications of NADH/NAD⁺ redox imbalance in diabetes and its complications. *Diabetes, metabolic syndrome and obesity: targets and therapy*, 9, 145.
- Yan, L. J. (2014). Pathogenesis of chronic hyperglycemia: from reductive stress to oxidative stress. *Journal of diabetes research*, 2014.
- Yang, J. H., Lim, H. S., & Heo, Y. R. (2010). Sasa borealis leaves extract improves insulin resistance by modulating inflammatory cytokine secretion in high fat diet-induced obese C57/BL6J mice. *Nutrition research and practice*, 4(2), 99-105.

Zhang, J. (2007). The direct involvement of SirT1 in insulin-induced insulin receptor substrate-2 tyrosine phosphorylation. *Journal of Biological Chemistry*, 282(47), 34356-34364.

Zhu, D., Zhang, N., Zhou, X., Zhang, M., Liu, Z., & Liu, X. (2017). Cichoric acid regulates the hepatic glucose homeostasis via AMPK pathway and activates the antioxidant response in high glucose-induced hepatocyte injury. *RSC Advances*, 7(3), 1363-1375.

Zietz, B., Büchler, C., Herfarth, H., Müller-Ladner, U., Spiegel, D., Schölmerich, J., & Schäffler, A. (2005). Caucasian patients with type 2 diabetes mellitus have elevated levels of monocyte chemoattractant protein-1 that are not influenced by the-2518 A→ G promoter polymorphism. *Diabetes, Obesity and Metabolism*, 7(5), 570-578.

4.9 Tables and Figures

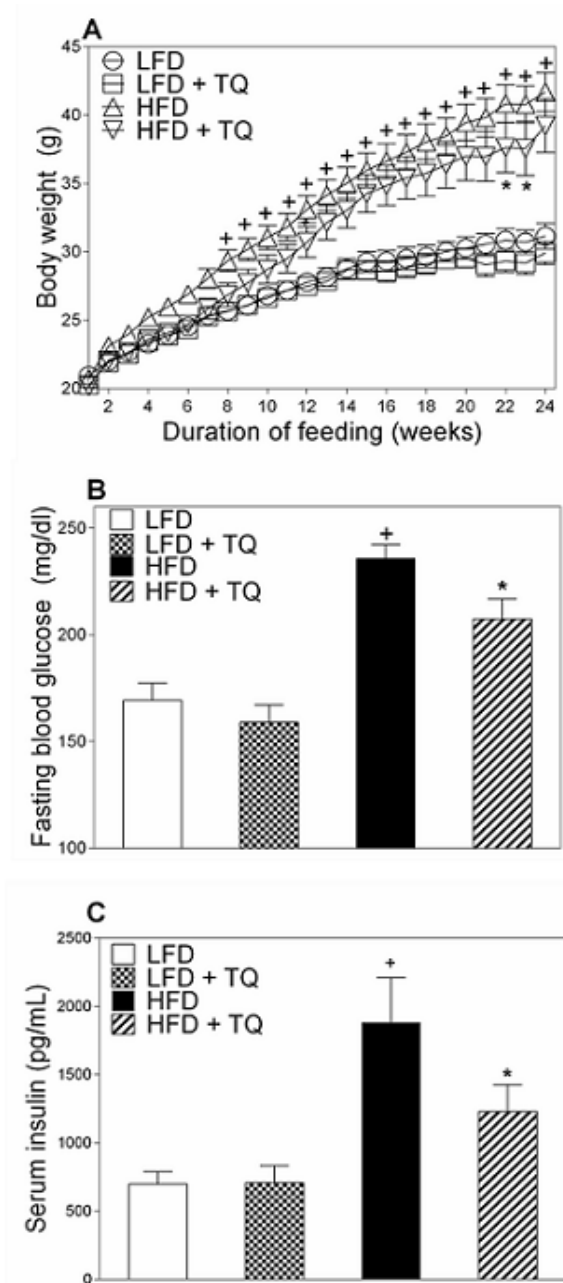


Figure 4.1 TQ ameliorates weight gain, lowers fasting blood glucose and insulin in DIO mice. (A) Effect of TQ on body weight (B) Effect of TQ treatment on fasting blood glucose after a 6 hour fast. (C) Effect of TQ on serum insulin. Total body weight was measured weekly for the duration of the study. $p < 0.05$ when comparing HFD and LFD (+), and HFD and HFD+TQ (*), using a one-way ANOVA followed by Sidak post-test (A and B) or independent t-test (C). Results are means \pm SEM ($n = 10-12$ mice per treatment group). LFD: low fat diet, HFD: high fat diet, TQ: thymoquinone.

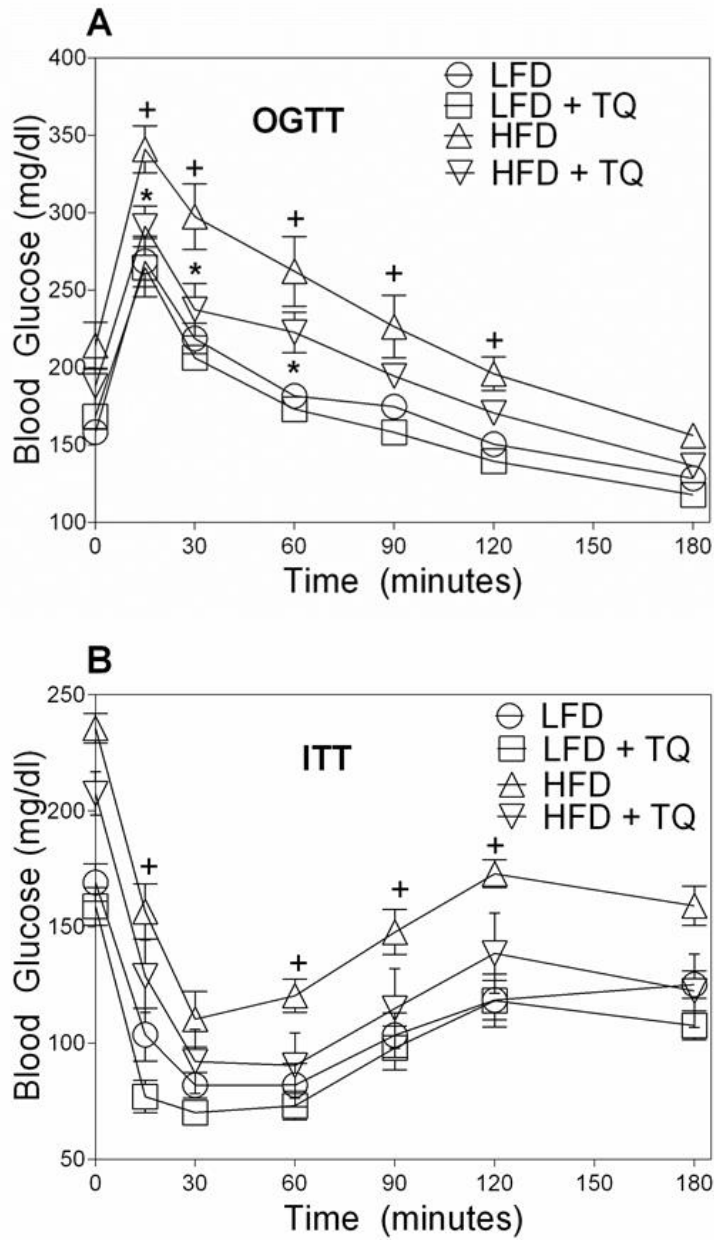


Figure 4.2 TQ improves glucose tolerance and insulin sensitivity. (A) Blood glucose levels in response to oral glucose tolerance test (OGTT). (B) Blood glucose levels in response to insulin tolerance test (ITT). $p < 0.05$ when comparing HFD and LFD (+), and HFD and HFD+TQ (*), using a two-way ANOVA followed by Holm-Sidak post-test. Results are means \pm SEM ($n = 10-12$ mice per treatment group). LFD: low fat diet, HFD: high fat diet, TQ: thymoquinone.

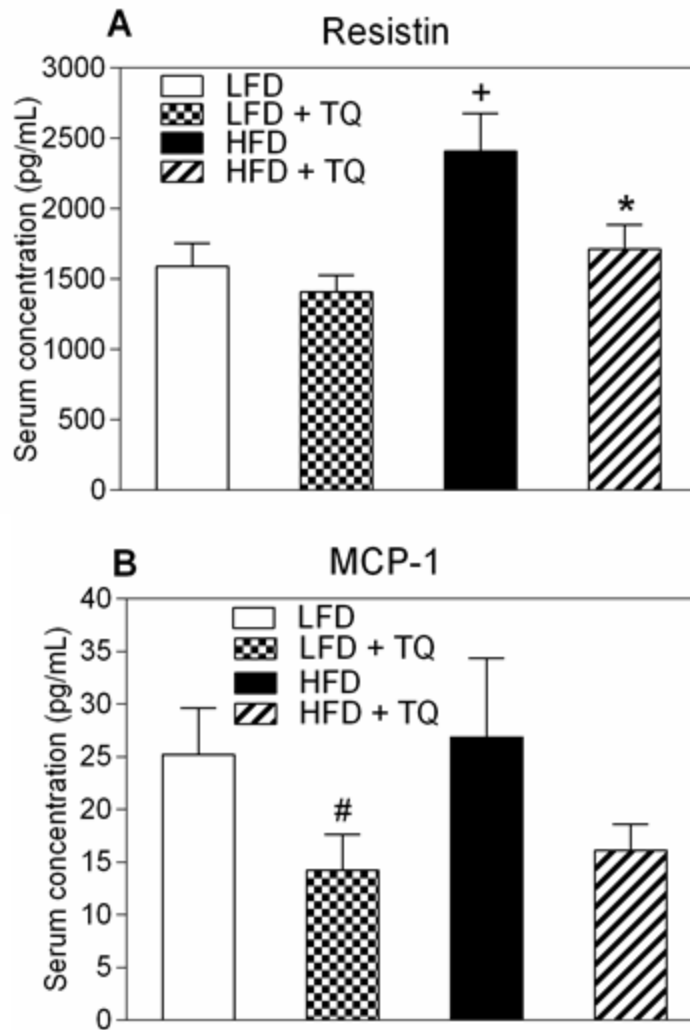


Figure 4.3 Effects of TQ on serum resistin and MCP-1. (A) Resistin serum concentration. (B) MCP-1 serum concentration. $p \leq 0.05$ when comparing (+) HFD and LFD, (*) HFD + TQ and HFD, and (#) LFD and LFD + TQ using independent t-tests. Results are means \pm SEM (n = 10-12 mice per treatment group). LFD: low fat diet, HFD: high fat diet, TQ: thymoquinone, MCP-1: monocyte chemotactic protein 1.

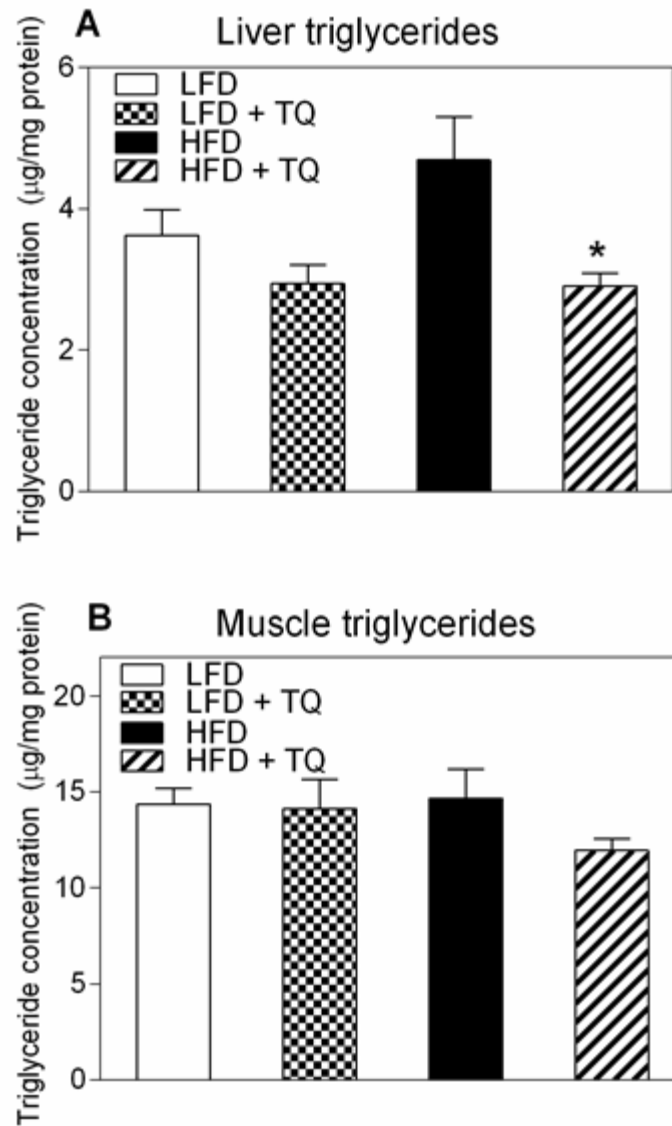


Figure 4.4 Effects of TQ on triglyceride content in liver and muscle. (A) Triglyceride concentration in liver. (B) Triglyceride concentration in soleus muscle. (*) $p < 0.05$ when comparing HFD + TQ and HFD using a one-way ANOVA followed by Sidak post-test. Results are means \pm SEM (n=8-12 mice per treatment group). LFD: low fat diet, HFD: high fat diet, TQ: thymoquinone.

Table 4.1 Effect of TQ on serum glycerol and fatty acids. Results expressed as means \pm SEM (n= 10-12 mice per treatment group). Means within the same row with different superscripts differ, $p \leq 0.05$ as determined by using a one-way ANOVA followed by Sidak post-test. a,b = LFD vs. HFD only; a,c = LFD vs. LFD + TQ only. TQ = Thymoquinone, LFD = low fat diet, HFD = high fat diet

Metabolite	Treatment			
	LFD	LFD + TQ	HFD	HFD + TQ
Glycerol	844.7 \pm 70.1 ^a	1282 \pm 101.9 ^c	1348 \pm 124.2 ^b	1186 \pm 47.1
Palmitic Acid	820.3 \pm 26.1	970.4 \pm 61.3	862.7 \pm 53.8	798.7 \pm 23.4
Oleic Acid	2851 \pm 179.8	3335 \pm 195.8	2807 \pm 345.9	2597 \pm 114.5
Stearic Acid	381.9 \pm 15.0	371.9 \pm 22.3	471.2 \pm 25.8	437.5 \pm 21.4

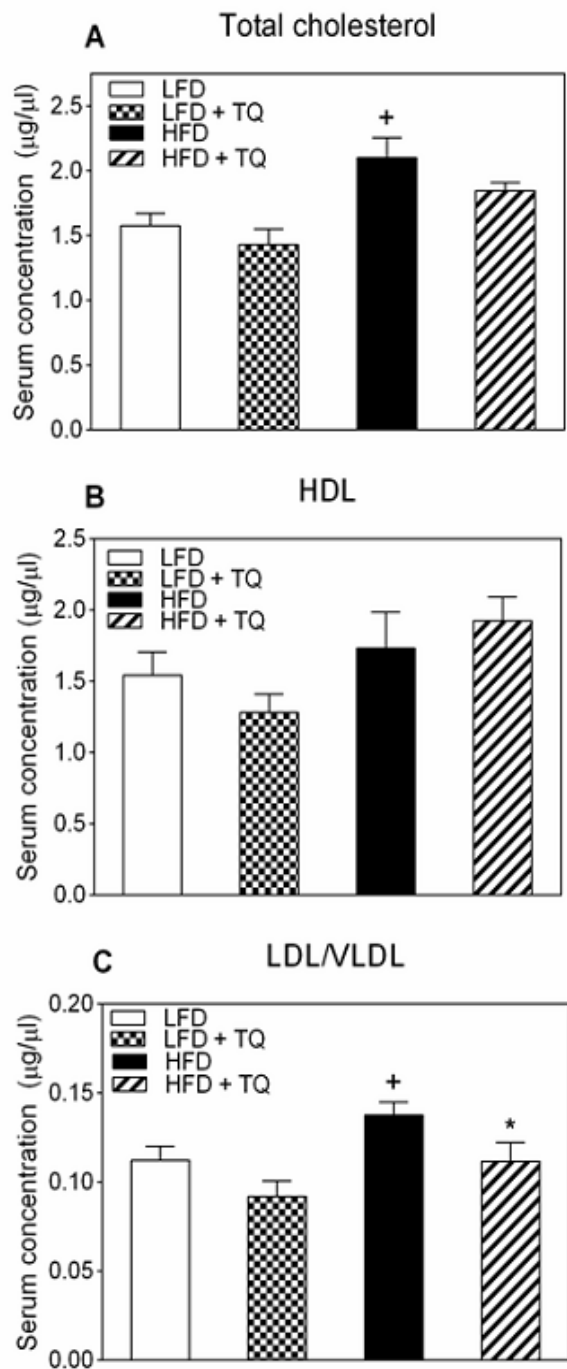


Figure 4.5 Effects of TQ on serum cholesterol. (A) Total cholesterol serum concentration. (B) HDL cholesterol serum concentration. (C) LDL/VLDL cholesterol serum concentration. $p \leq 0.05$ when comparing (+) HFD and LFD, (*) HFD + TQ and HFD using independent t-tests. Results are means \pm SEM ($n=6-7$ mice per treatment group). LFD: low fat diet, HFD: high fat diet, TQ: thymoquinone, LDL: low-density lipoprotein, HDL: high-density lipoprotein, VLDL: very-low-density lipoprotein.

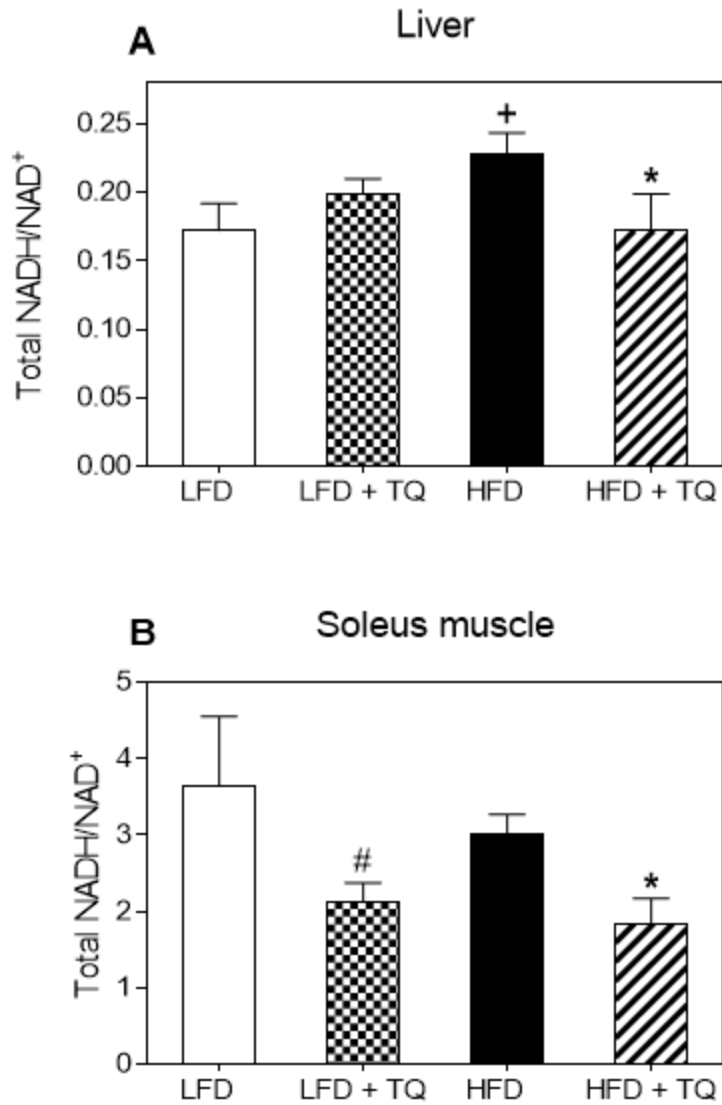


Figure 4.6 TQ decreases NADH/NAD⁺ ratio in liver and soleus muscle. (A) NADH/NAD⁺ ratio in liver. (B) NADH/NAD⁺ ratio in soleus muscle. $p \leq 0.05$ when comparing (+) HFD and LFD, (*) HFD + TQ and HFD, and (#) LFD and LFD + TQ using independent t-tests. Results are means \pm SEM (n = 8-10 mice per treatment group). LFD: low fat diet, HFD: high fat diet, TQ: thymoquinone.

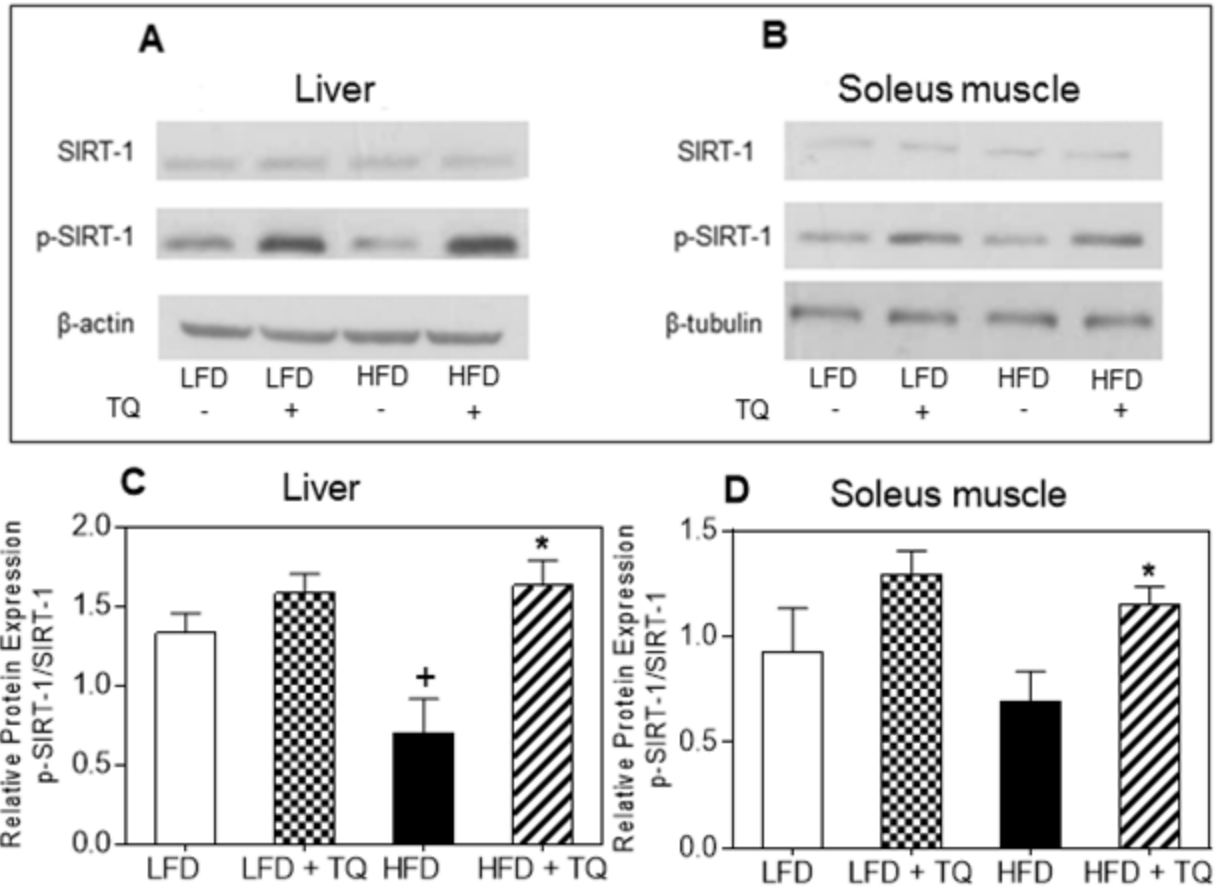


Figure 4.7 TQ activates SIRT-1 in liver and soleus muscle. (A) Western blot images of SIRT-1 and p-SIRT-1 protein in liver. β -actin was used as a loading control. (B) Western blot images of SIRT-1 and p-SIRT-1 protein in soleus muscle. β -tubulin was used as a loading control. Western blot images are representative of combined liver and soleus muscle lysates from $n=10-12$ mice per treatment group. (C and D) Protein band quantification using densitometry from three independent experiments. $p \leq 0.05$ when comparing (+) HFD and LFD and (*) HFD + TQ and HFD using independent t-tests LFD: low fat diet, HFD: high fat diet, TQ: thymoquinone.

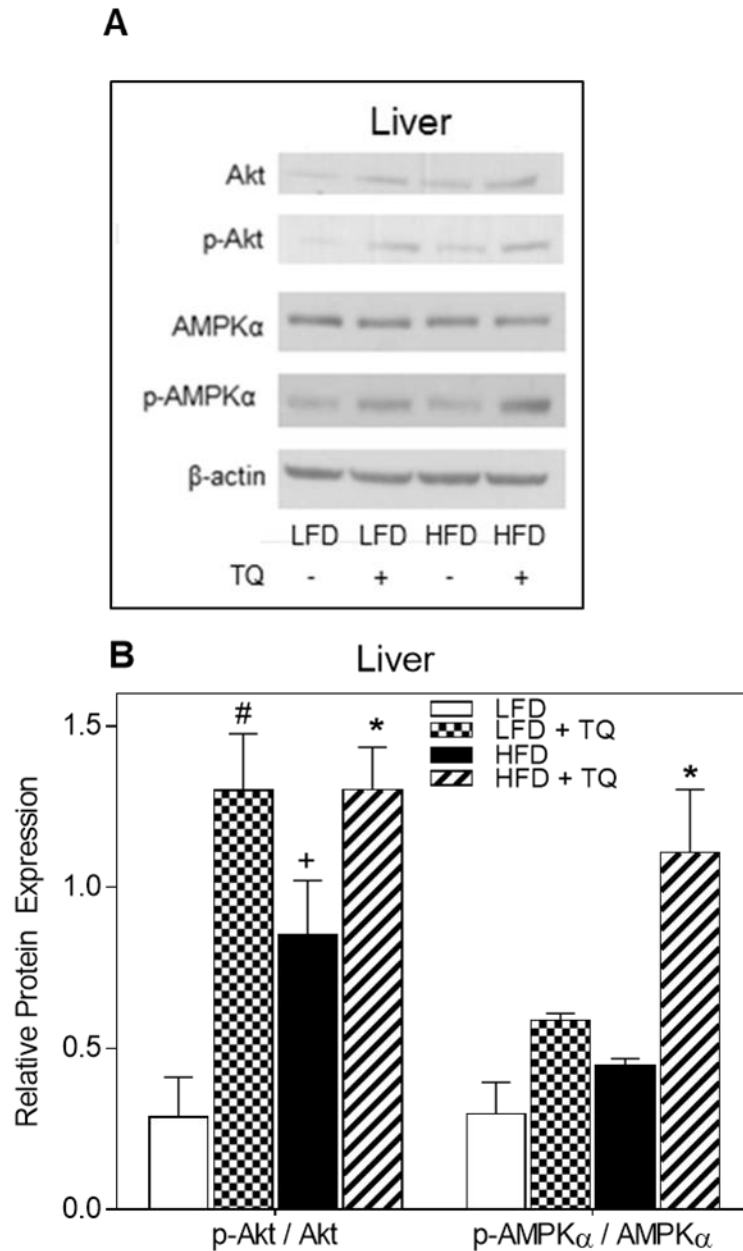


Figure 4.8 TQ activates Akt and AMPK α in liver. (A) Western blot images of Akt, p-Akt, AMPK α and p-AMPK α protein in liver. β -actin was used as a loading control. Western blot images are representative of combined liver lysates from n=10-12 mice per treatment group. (B) Protein band quantification using densitometry from three independent experiments. $p \leq 0.05$ when comparing (+) HFD and LFD, (*) HFD + TQ and HFD, and (#) LFD and LFD + TQ using independent t-tests. LFD: low fat diet, HFD: high fat diet, TQ: thymoquinone.

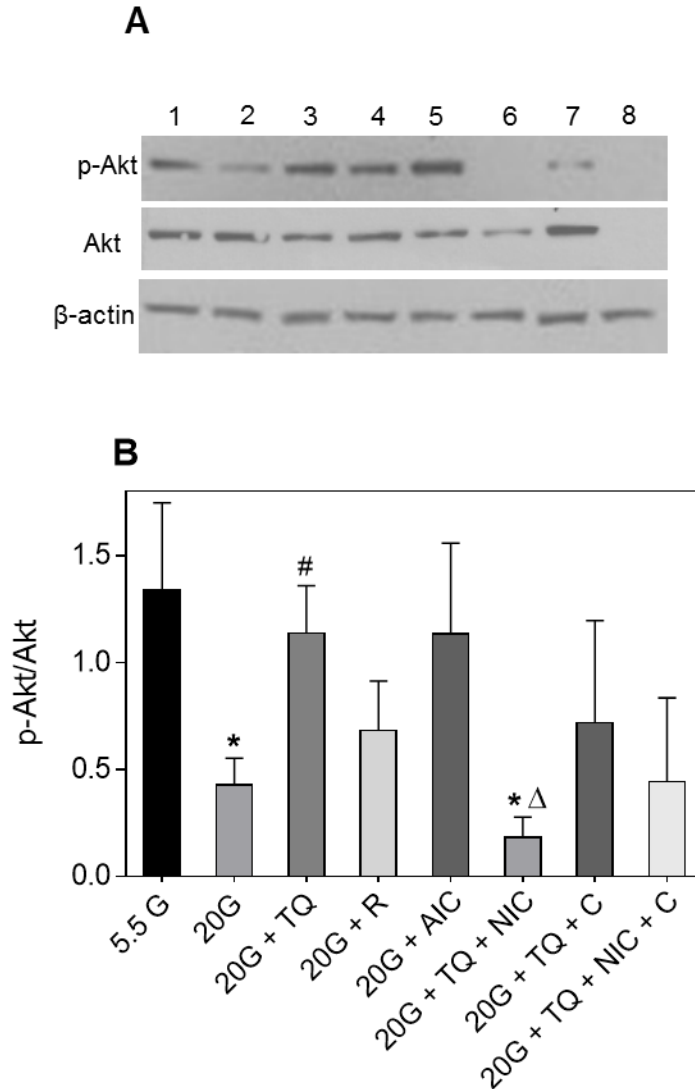


Figure 4.9 TQ improves insulin sensitivity in HepG2 cells via a SIRT-1 dependent mechanism. HepG2 cells were cultured in high (20 mM) glucose or in growth media containing 5.5 mM glucose for 18 hours, starved with serum-free media for 2 hours, then pre-incubated with vehicle control, nicotinamide, compound C, or with nicotinamide and compound C together for 30 mins, followed by incubation with TQ in the presence or absence of nicotinamide and compound C; or with TQ, resveratrol, or AICAR alone for 24 hours in 20mM glucose media. Vehicle-treated cells in 5.5 mM glucose served as control. Insulin was added during the last 30 min. (A) Western blot images of p-Akt, Akt, and β -actin. (B) Protein band quantification using densitometry from three independent experiments ($n=3$). $p \leq 0.05$ where (*) is significantly different from 5.5G, (#) is significantly different from 20G, and (Δ) is significantly different from 20G + TQ using independent t-tests. 5.5 G: 5.5 mM glucose, 20G: 20 mM glucose, TQ: thymoquinone, R: resveratrol, AIC: AICAR, NIC: nicotinamide, C: compound C. 1: 5.5G, 2: 20G, 3: 20G +TQ, 4: 20G + R, 5: 20G + AIC, 6: 20G + TQ + NIC, 7: 20G + TQ + C, 8: 20G + TQ + NIC + C.

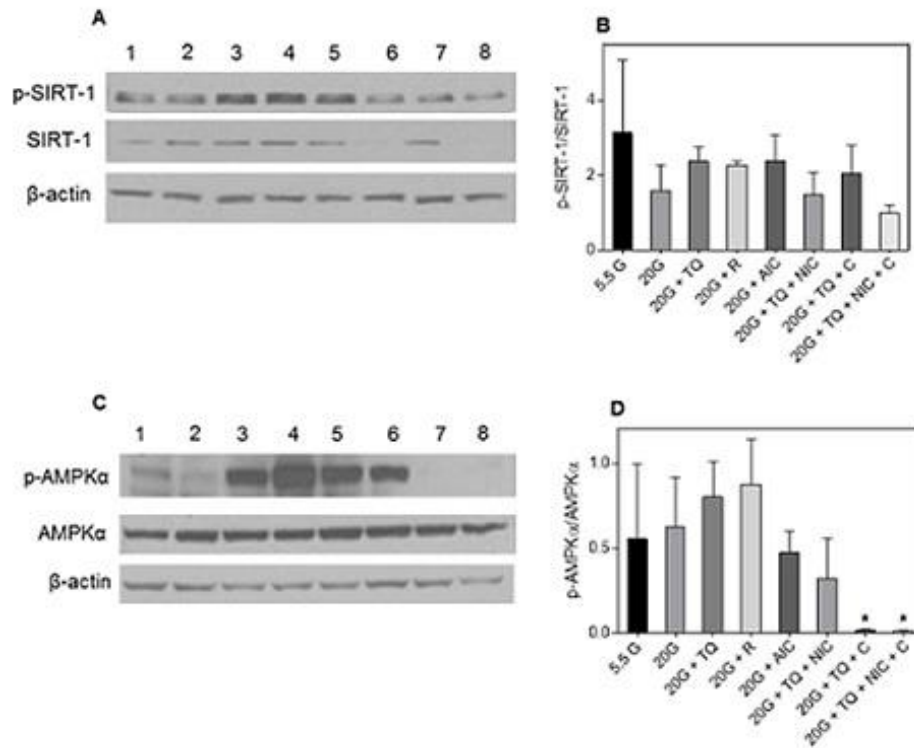


Figure 4.10 Effect of TQ on SIRT-1 and AMPK α activation in HepG2 cells. HepG2 cells were cultured in high (20 mM) glucose or in growth media containing 5.5 mM glucose for 18 hours, starved with serum-free media for 2 hours, then pre-incubated with vehicle control, nicotinamide, compound C, or with nicotinamide and compound C together for 30 mins, followed by incubation with TQ in the presence or absence of nicotinamide and compound C; or with TQ, resveratrol, or AICAR alone for 24 hours in 20mM glucose media. Vehicle-treated cells in 5.5 mM glucose served as control. Insulin was added during the last 30 min. (A) Western blot images of p-SIRT-1, SIRT-1, and β -actin. (C) Western blot images of p-AMPK α , AMPK α , and β -actin. (B and D) Protein band quantification using densitometry from three independent experiments (n=3). $p \leq 0.05$ where (*) is significantly different from 20G + TQ using independent t-tests. 5.5 G: 5.5 mM glucose, 20G: 20 mM glucose, TQ: thymoquinone, R: resveratrol, AIC: AICAR, NIC: nicotinamide, C: compound C. 1: 5.5G, 2: 20G, 3: 20G + TQ, 4: 20G + R, 5: 20G + AIC, 6: 20G + TQ + NIC, 7: 20G + TQ + C, 8: 20G + TQ + NIC + C.

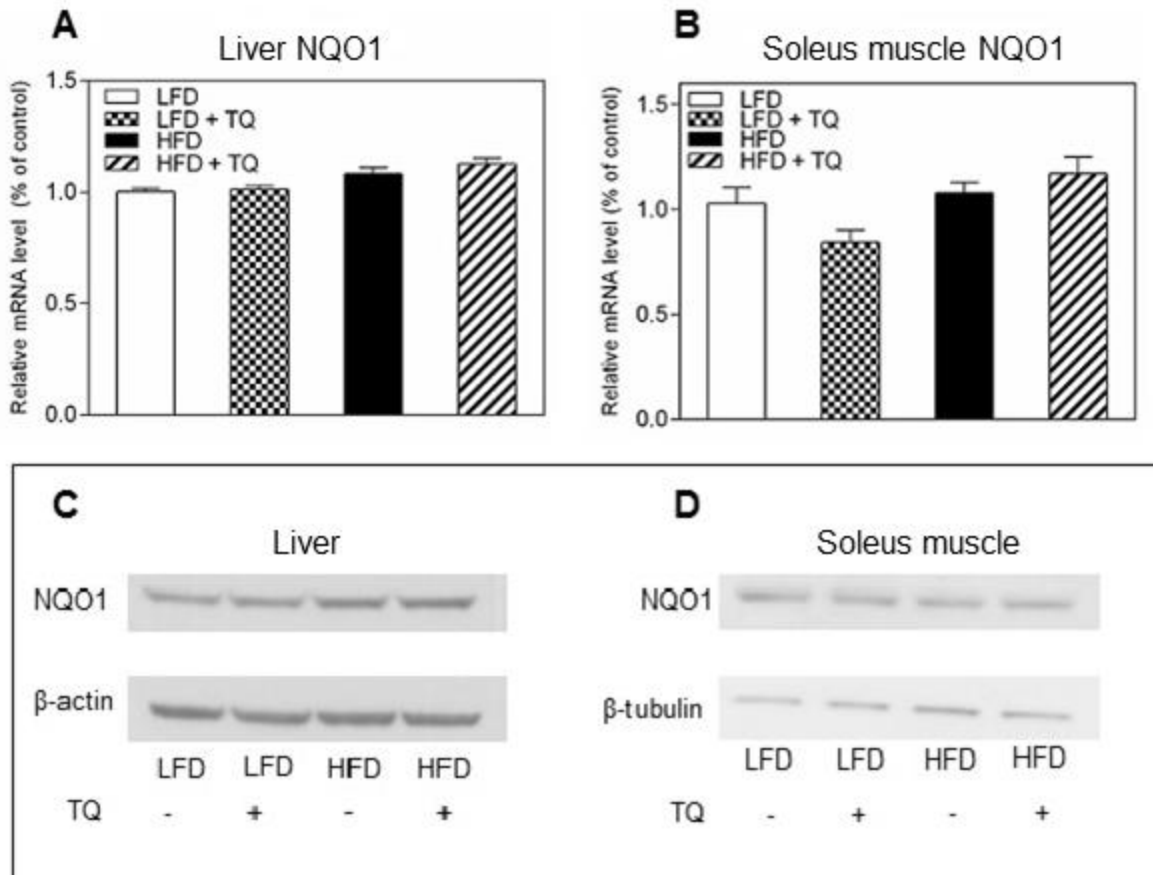


Figure 4.11 Effects of TQ on NQO1 expression. NQO1 mRNA expression in liver (A) and soleus muscle (B). (C) Western blot images of NQO1 and β -actin protein in liver (D) Western blot images of NQO1 protein in soleus muscle. β -tubulin was used as a loading control. Statistical analysis (A and B): one-way ANOVA followed by Sidak post-test ($p \leq 0.05$). qPCR results are means \pm SEM ($n=8-12$ mice per treatment group). Western blot images are representative of combined liver and soleus muscle lysates from $n=10-12$ mice per treatment group. LFD: low fat diet, HFD: high fat diet, TQ: thymoquinone.

Table 4.2. TQ decreases the levels of anaplerotic TCA cycle metabolites in INS-1 832/13 cells exposed to high glucose. Effect of TQ treatment on TCA cycle intermediates following chronic exposure (72 h) of INS 832/13 cells to 11 or 25 mM glucose. Results expressed as means \pm SEM from three independent experiments (n=3). Means within the same row with different superscripts differ (25G vs. 25G + TQ only), $p < 0.05$ when comparing 25G to 25G + TQ using one-way ANOVA followed by Sidak post-tests. 11G = 11mM glucose, 25G = 25mM glucose, TQ = Thymoquinone.

Metabolite	Treatment			
	11G	11G + TQ	25G	25G + TQ
Citric Acid	24.20 \pm 0.97	28.69 \pm 1.21	38.18 \pm 1.36 ^a	26.2 \pm 1.55 ^b
Aconitate	1.28 \pm 0.09	1.38 \pm 0.16	2.18 \pm 0.12 ^a	1.52 \pm 0.11 ^b
Isocitric Acid	6.16 \pm 0.22	6.87 \pm 0.31	10.11 \pm 0.36 ^a	7.29 \pm 0.42 ^b
Malic Acid	83.56 \pm 1.97	91.32 \pm 1.86	156.86 \pm 2.97 ^a	141.28 \pm 5.40 ^b

Table 4.3 Effect of TQ on TCA cycle intermediates in liver. Results expressed as means \pm SEM (n=10-12 mice per treatment group). Means within the same row with different superscripts differ, $p < 0.05$ a,b = LFD vs. HFD only; c,d = HFD vs. HFD + TQ only, a,e = LFD vs. LFD + TQ only. TQ = Thymoquinone, LFD = low fat diet, HFD = high fat diet.

Metabolite	Treatment			
	LFD	LFD + TQ	HFD	HFD + TQ
Pyruvic acid	673.4 \pm 51.90	700.3 \pm 85.47	653.1 \pm 93.72	656.2 \pm 72.94
Citricacid	129.9 \pm 21.48 ^a	221.3 \pm 33.18 ^e	72.15 \pm 5.495 ^b	75.52 \pm 8.924
cis-Aconitic acid	7.577 \pm 1.22	12.81 \pm 2.53	5.145 \pm 0.36	5.466 \pm 0.65
Isocitric acid	10.77 \pm 1.69 ^a	17.56 \pm 3.59	6.181 \pm 0.78 ^b	6.650 \pm 0.62
2-ketoglutaric acid	10.23 \pm 0.75 ^a	15.22 \pm 1.42 ^e	11.19 \pm 1.01	10.43 \pm 0.83
Succinic acid	230.5 \pm 28.46	235.4 \pm 32.90	183.4 \pm 21.08	165.0 \pm 18.34
Fumaric acid	977.6 \pm 146.6 ^a	851.9 \pm 82.34	538.8 \pm 45.18 ^b	567.6 \pm 70.44
Malicacid	611.1 \pm 62.42 ^a	683.6 \pm 55.50	456.8 \pm 29.85 ^b	564.3 \pm 74.77
Aspartic acid	584.6 \pm 43.27 ^a	515.1 \pm 44.42	400.8 \pm 23.08 ^b	419.6 \pm 28.93

Table 4.4 Effect of TQ on TCA cycle intermediates in soleus muscle. Results expressed as means \pm SEM (n=10-12 mice per treatment group). Means within the same row with different superscripts differ, $p < 0.05$ a,b = LFD vs. HFD only; c,d = HFD vs. HFD + TQ only, a,e = LFD vs. LFD + TQ only. TQ = Thymoquinone, LFD = low fat diet, HFD = high fat diet.

Metabolite	Treatment			
	LFD	LFD + TQ	HFD	HFD + TQ
Pyruvic acid	177.6 \pm 19.96 ^a	203.5 \pm 25.68	286.8 \pm 40.97 ^b	222.0 \pm 53.64
Citricacid	249.3 \pm 30.28 ^a	443.3 \pm 45.58 ^e	252.0 \pm 32.28	229.5 \pm 34.51
Isocitric acid	19.86 \pm 2.08 ^a	28.85 \pm 2.23 ^e	20.00 \pm 1.74	19.76 \pm 2.37
2-ketoglutaric acid	4.150 \pm 0.58	4.690 \pm 0.61	5.217 \pm 0.68 ^c	2.782 \pm 0.60 ^d
Succinic acid	1669 \pm 141.1	1420 \pm 69.31	1484 \pm 169.6	1516 \pm 189.1
Fumaric acid	878.8 \pm 54.70	799.7 \pm 61.13	782.2 \pm 101.3	674.0 \pm 59.67
Malicacid	687.7 \pm 34.32	695.5 \pm 45.25	670.3 \pm 57.30	574.2 \pm 35.23
Aspartic acid	1171 \pm 64.00 ^a	1487 \pm 111.9 ^e	1423 \pm 281.9	1160 \pm 125.6

CHAPTER FIVE:

CONCLUSIONS

5.1 Adverse Effects of Selected POPs on Pancreatic β -cell Function

The results presented in this study show the potential of four selected POPs, PFNA, PFOS, BDE-47, and BDE-85 to alter pancreatic β -cell function. Specifically, BDE-47 and BDE-85 increased GSIS in INS-1 832/13 cells during an acute exposure, while a similar trend was observed with PFOS and PFNA that didn't reach statistical significance. Chronic pre-treatment for 48 hours didn't increase GSIS, performed in the absence of compounds, suggesting that both BDE-47 and BDE-85 must be present during glucose stimulation in order to increase insulin secretion. This is confirmed by our results showing that in basal glucose conditions, none of the selected compounds increase insulin secretion, suggesting that their effects on GSIS are likely mediated by potentiating the actions of high glucose on β -cell function during an acute exposure. Mechanistically, it was determined that BDE-47 and BDE-85 act via thyroid hormone receptor to increase GSIS and this response was shown to be Akt-dependent, as pharmacological inhibition of PI3K, an upstream activator of Akt, abolishes this response (Karandrea et al., 2017a). These results confirm prior reports of the role of PBDEs and their metabolites in disrupting thyroid hormone signaling by mimicking the role of thyroid hormones and potentially binding to thyroid receptor (Dong et al., 2014; Ibhazehiebo et al., 2011; Li et al., 2010; Ren et al., 2013; Ren and Guo, 2013). Since thyroid hormones can activate Akt, we hypothesized that BDE-47 and BDE-85 also activate Akt and that this activation plays a role in potentiation of GSIS. Indeed, we found out that BDE-47 and BDE-85 activate Akt and that this pathway plays a role in the effect of BDE-47 and BDE-85 on GSIS. The activation of Akt by several PBDEs has been previously reported, albeit in different cell lines (Qu et al., 2015; Wang et al., 2015; Tian et al., 2016). Furthermore,

activation of Akt has important implications on GSIS, although the effects of the PI3K-Akt pathway have been controversial. It is possible that BDE-47 and BDE-85 act via thyroid receptor to activate Akt, which in turn potentiates GSIS by an unknown mechanism (Figure 5.1). Further studies are required to evaluate the role of Akt in BDE-47/85-mediated potentiation of GSIS in INS-1 832/13 cells and the mechanisms associated with this action.

These results suggest that exposure to BDE-47 and BDE-85 can increase GSIS, which can have detrimental effects to exposed human populations. Since PBDEs can accumulate in the body and humans can be exposed to these compounds in a variety of ways, it is possible that they can cause β -cells to oversecrete insulin, particularly when coupled with a high-calorie and high-carbohydrate diet. The excess insulin may cause hyperinsulinemia, insulin resistance, and possibly β -cell exhaustion and failure, leading to increased blood glucose and emergence of type 2 diabetes. Our work provides a basis for future studies to explore the role of BDE-47, BDE-85 and other PBDEs or classes of POPs in pancreatic β -cell function, glucose homeostasis, and the mechanisms responsible for such metabolic effects.

5.2 Effects of Thymoquinone in the DIO Mouse Model of Type 2 Diabetes

Our work highlights the anti-diabetic effects of Thymoquinone in a physiologically-relevant animal model of type 2 diabetes, such as the DIO mice. Although positive effects on glucose homeostasis have been reported from prior *in vivo* studies, most of them have used animal models rendered diabetic by chemically-induced β -cell death, which doesn't allow for proper evaluation of β -cell function. To our knowledge, this is the first study to report that TQ improves glucose homeostasis parameters, such as glucose intolerance, insulin resistance, and hyperglycemia in diabetic and obese DIO mice. Furthermore, TQ improved low-grade inflammation, dyslipidemia, and decreased the levels of tissue triglycerides in DIO mice compared to controls, suggesting that it has an important role not only in glucose homeostasis, but also potentially ameliorating these conditions that are elevated in type 2 diabetes. TQ decreased NADH/NAD⁺ ratio, leading to more NAD⁺ being available, which can reduce the effects of oxidative

and reductive stress on insulin resistance and hyperglycemia (Wu et al., 2016). Furthermore, increased NAD⁺ can potentiate glucose metabolism in pancreatic β -cells, which can increase GSIS and ameliorate hyperglycemia (Revollo et al., 2007). We show increased SIRT-1 and AMPK α activation in liver and skeletal muscle of DIO mice treated with TQ, which could be a consequence of increased NAD⁺, thus activating SIRT-1 and potentially AMPK. Both SIRT-1 and AMPK have been implicated in ameliorating insulin resistance, oxidative stress and inflammation, as well as increasing GSIS in pancreatic β -cells (Coughlan et al., 2014; Moynihan et al., 2005; Sun et al., 2007; Zhang et al., 2007). TQ improved hepatic insulin sensitivity by increasing Akt phosphorylation (activation), an important component of insulin signaling pathway. This improvement in insulin sensitivity could be due to the lipid lowering effects of TQ, as well as activation of SIRT-1 dependent pathways. Indeed, we showed that in insulin-resistant HepG2 cells, TQ restores insulin sensitivity via a SIRT-1-dependent mechanism. By undergoing quinone-dependent redox cycling, we propose that TQ decreases NADH/NAD⁺ ratio, which in turn activates SIRT-1 and AMPK, leading to improved glucose and fatty acid oxidation and insulin sensitivity, a mechanism shown in Figure 5.2.

Taken together, the results of our study show additional evidence for the anti-diabetic effects of TQ. Furthermore, this study suggests that these effects and in particular the increase in insulin sensitivity, can be due to activation of SIRT-1 and AMPK pathways in DIO mice (Karandrea et al., 2017b). This provides a platform to investigate the specific role of these pathways in TQ-mediated improvement of glucose homeostasis, such as (but not limited to) the use of transgenic mouse models or treatment with agonists and inhibitors of such pathways.

5.3 Future Directions

One immediate future direction as the result of this work is to study the effects of exposure to BDE-47 and BDE-85 on glucose homeostasis in a diabetic susceptible murine model, such as the C57/BL6J mice on a lean background and fed a high fat diet. One purpose of such exposure is to evaluate whether exposure to these compounds alone is sufficient to induce the diabetic

phenotype, or whether they exacerbate the diabetic state in the animals fed a high fat diet. To evaluate their role on glucose homeostasis, glucose tolerance tests (GTTs), insulin tolerance tests (ITTs), fasting blood glucose, and insulin measurements can be performed. Furthermore, to assess whether BDE-47 and BDE-85 increase *in vivo* insulin secretion, hyperglycemic clamp experiments can be used to evaluate pancreatic β -cell function (Ayala et al., 2010). After the duration of the study, pancreatic islets can be collected to study GSIS and evaluate whether these compound increase *ex vivo* insulin secretion. Furthermore, insulin-sensitive tissues such as liver, skeletal muscle, and adipose tissue can be collected to evaluate the degree of insulin resistance by analyzing activation of proteins in the PI3K-Akt pathway. This *in vivo* study will serve to confirm the role of BDE-47 and BDE-85 on insulin secretion, and evaluate whether they cause hyperinsulinemia and insulin resistance as a result of increased pancreatic β -cell function. One important component can be to analyze insulin secretion during the study to determine whether there is an initial increase, followed by a progressive decrease in β -cell function, which can suggest ultimate β -cell exhaustion due to POP exposure. These studies could confirm the role of BDE-47 and BDE-85 in altering β -cell function and their importance in the development of type 2 diabetes, expanding upon the results obtained from INS-1 832/13 cells.

Another important future direction of this study is to evaluate the role of SIRT-1 and AMPK α in TQ-mediated amelioration of diabetic phenotype in DIO mice. Our results with HepG2 human liver cancer cell line suggest that TQ reverses insulin resistance via a SIRT-1 dependent mechanism. Furthermore, AMPK α also was shown to be important in this response. A study using a SIRT1 or AMPK α inhibitors in DIO mice exposed to TQ would provide additional evidence about whether these pathways play a role in the anti-diabetic effects of TQ. Furthermore, to bypass some of the off-target effects of inhibitors, SIRT-1 (Herranz and Serrano, 2010) or AMPK α knock out mice (Viollet et al., 2009) can be used to assess whether the effects of TQ on insulin resistance and glucose homeostasis are dependent on the activation of these pathways.

We showed that TQ improves insulin sensitivity both *in vivo* and *in vitro*, but we did not study the effects of TQ treatment on pancreatic β -cell function in DIO mice. Future experiments measuring *in vivo* GSIS or *ex vivo* pancreatic islet function in DIO mice treated with TQ are needed to establish the role of this compound on β -cell function.

5.4 References

Ayala, J. E., Samuel, V. T., Morton, G. J., Obici, S., Croniger, C. M., Shulman, G. I., ... & McGuinness, O. P. (2010). Standard operating procedures for describing and performing metabolic tests of glucose homeostasis in mice. *Disease models & mechanisms*, 3(9-10), 525-534.

Coughlan, K. A., Valentine, R. J., Ruderman, N. B., & Saha, A. K. (2014). AMPK activation: a therapeutic target for type 2 diabetes?. *Diabetes, metabolic syndrome and obesity: targets and therapy*, 7, 241.

Dong, W., Macaulay, L. J., Kwok, K. W., Hinton, D. E., Ferguson, P. L., & Stapleton, H. M. (2014). The PBDE metabolite 6-OH-BDE 47 affects melanin pigmentation and THR β mRNA expression in the eye of zebrafish embryos. *Endocrine Disruptors*, 2(1), e969072.

Herranz, D., & Serrano, M. (2010). SIRT1: recent lessons from mouse models. *Nature reviews. Cancer*, 10(12), 819.

Ibhazehiebo, K., Iwasaki, T., Kimura-Kuroda, J., Miyazaki, W., Shimokawa, N., & Koibuchi, N. (2011). Disruption of thyroid hormone receptor-mediated transcription and thyroid hormone-induced Purkinje cell dendrite arborization by polybrominated diphenyl ethers. *Environmental health perspectives*, 119(2), 168.

Karandrea, S., Yin, H., Liang, X., & Heart, E. A. (2017a). BDE-47 and BDE-85 stimulate insulin secretion in INS-1 832/13 pancreatic β -cells through the thyroid receptor and Akt. *Environmental Toxicology and Pharmacology*, 56, 29-34.

Karandrea, S., Yin, H., Liang, X., Slitt, A. L., & Heart, E. A. (2017b). Thymoquinone ameliorates diabetic phenotype in Diet-Induced Obesity mice via activation of SIRT-1-dependent pathways. *PloS one*, 12(9), e0185374.

Li, F., Xie, Q., Li, X., Li, N., Chi, P., Chen, J., ... & Hao, C. (2010). Hormone activity of hydroxylated polybrominated diphenyl ethers on human thyroid receptor- β : in vitro and in silico investigations. *Environmental health perspectives*, 118(5), 602.

Moynihan, K. A., Grimm, A. A., Plueger, M. M., Bernal-Mizrachi, E., Ford, E., Cras-Méneur, C., ... & Imai, S. I. (2005). Increased dosage of mammalian Sir2 in pancreatic β cells enhances glucose-stimulated insulin secretion in mice. *Cell metabolism*, 2(2), 105-117.

Qu, B. L., Yu, W., Huang, Y. R., Cai, B. N., Du, L. H., & Liu, F. (2015). 6-OH-BDE-47 promotes human lung cancer cells epithelial mesenchymal transition via the AKT/Snail signal pathway. *Environmental toxicology and pharmacology*, 39(1), 271-279.

Ren, X. M., & Guo, L. H. (2013). Molecular toxicology of polybrominated diphenyl ethers: nuclear hormone receptor mediated pathways. *Environmental Science: Processes & Impacts*, 15(4), 702-708.

Ren, X. M., Guo, L. H., Gao, Y., Zhang, B. T., & Wan, B. (2013). Hydroxylated polybrominated diphenyl ethers exhibit different activities on thyroid hormone receptors depending on their degree of bromination. *Toxicology and applied pharmacology*, 268(3), 256-263.

Revollo, J. R., Körner, A., Mills, K. F., Satoh, A., Wang, T., Garten, A., ... & Milbrandt, J. (2007). Namp1/PBEF/visfatin regulates insulin secretion in β cells as a systemic NAD biosynthetic enzyme. *Cell metabolism*, 6(5), 363-375.

Sun, C., Zhang, F., Ge, X., Yan, T., Chen, X., Shi, X., & Zhai, Q. (2007). SIRT1 improves insulin sensitivity under insulin-resistant conditions by repressing PTP1B. *Cell metabolism*, 6(4), 307-319.

Tian, P. C., Wang, H. L., Chen, G. H., Luo, Q., Chen, Z., Wang, Y., & Liu, Y. F. (2016). 2, 2', 4, 4'-Tetrabromodiphenyl ether promotes human neuroblastoma SH-SY5Y cells migration via the GPER/PI3K/Akt signal pathway. *Human & experimental toxicology*, 35(2), 124-134.

Viollet, B., Ailhaud, Y., Mounier, R., Guigas, B., Zarrinpashneh, E., Horman, S., ... & Foretz, M. (2009). AMPK: Lessons from transgenic and knockout animals. *Frontiers in bioscience (Landmark edition)*, 14, 19.

Wang, F., Ruan, X. J., & Zhang, H. Y. (2015). BDE-99 (2, 2', 4, 4', 5-pentabromodiphenyl ether) triggers epithelial-mesenchymal transition in colorectal cancer cells via PI3K/Akt/Snail signaling pathway. *Tumori*, 101(2), 238-245.

Wu, J., Jin, Z., Zheng, H., & Yan, L. J. (2016). Sources and implications of NADH/NAD⁺ redox imbalance in diabetes and its complications. *Diabetes, metabolic syndrome and obesity: targets and therapy*, 9, 145.

Zhang, J. (2007). The direct involvement of Sirt1 in insulin-induced insulin receptor substrate-2 tyrosine phosphorylation. *Journal of Biological Chemistry*, 282(47), 34356-34364.

5.5 Tables and Figures

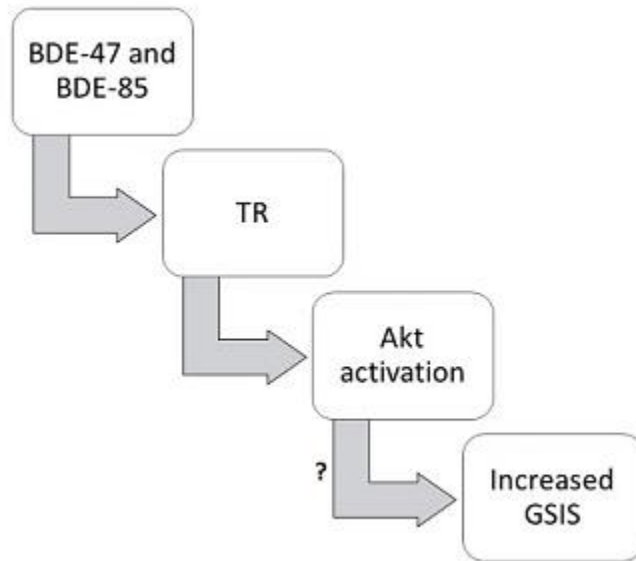


Figure 5.1 Proposed mechanisms for potentiation of GSIS by BDE-47 and BDE-85. BDE-47 and BDE-85 bind to the thyroid receptor (TR), leading to Akt activation, which in turn leads to increased GSIS by an unknown mechanism.

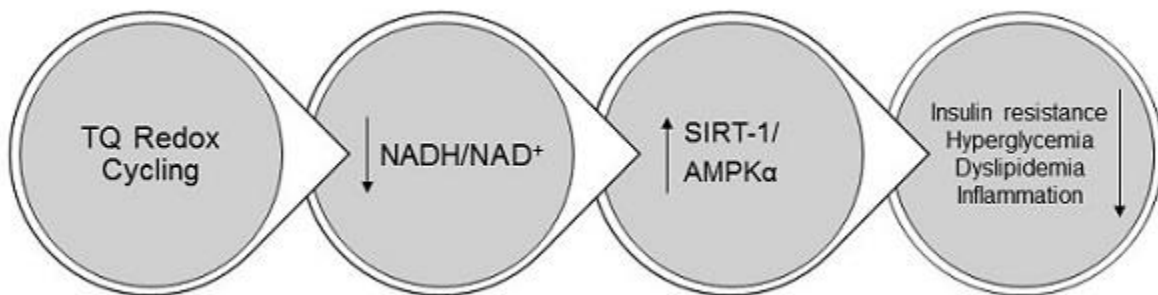


Figure 5.2 Proposed mechanism for anti-diabetic actions of TQ. TQ undergoes redox cycling in metabolically relevant tissues, which leads to a decrease in the NADH/NAD⁺ ratio, activation of SIRT-1 and AMPK α , which leads to decreased insulin resistance, hyperglycemia, dyslipidemia, and inflammation.


APPENDIX A: IACUC APPROVAL FOR ANIMAL RESEARCH



RESEARCH INTEGRITY AND COMPLIANCE INSTITUTIONAL ANIMAL CARE & USE COMMITTEE

MEMORANDUM

TO: Emma Heart,

FROM: 
Farah Moulvi, MSPH, IACUC Coordinator
Institutional Animal Care & Use Committee
Research Integrity & Compliance

DATE: 5/7/2015

PROJECT TITLE: Cytosolic and plasma membrane circuitry of beta cell redox control: role in survival, oxidative defense and insulin secretion
Role of NQO1 and plasma membrane electron transport in pancreatic beta cell redox control and insulin secretion.

FUNDING SOURCE: Natl Insti of Diabetes (NIDDK); American Diabetes Association

IACUC PROTOCOL #: R IS0001255

PROTOCOL STATUS: **APPROVED**

The Institutional Animal Care and Use Committee (IACUC) reviewed your application requesting the use of animals in research for the above-entitled study. The IACUC **APPROVED** your request to use the following animals in your protocol for a one-year period beginning 5/7/2015:

Mouse: C57BL/6 (8-24 weeks/25-45grams/male) 188

Please take note of the following:


- IACUC approval is granted for a one-year period at the end of which, an annual renewal form must be submitted for years two (2) and three (3) of the protocol through the eIACUC system. After three years all continuing studies must be completely re-described in a new electronic application and submitted to IACUC for review.
- All modifications to the IACUC-Approved Protocol must be approved by the IACUC prior to initiating the modification. Modifications can be submitted to the



RESEARCH INTEGRITY AND COMPLIANCE
INSTITUTIONAL ANIMAL CARE & USE COMMITTEE

MEMORANDUM

TO: Emma Heart,

FROM: 
Farah Moulvi, MSPH, IACUC Coordinator
Institutional Animal Care & Use Committee
Research Integrity & Compliance

DATE: 4/25/2017

PROJECT TITLE: Cytosolic and plasma membrane circuitry of beta cell redox control: role in survival, oxidative defense and insulin secretion
Role of NQO1 and plasma membrane electron transport in pancreatic beta cell redox control and insulin secretion.

FUNDING SOURCE: Natl Insti of Diabetes (NIDDK) American Diabetes Association

IACUC PROTOCOL #: R IS00001255

PROTOCOL STATUS: **APPROVED**

Your request for continuation of this study was received and will be reported to the Institutional Animal Care and Use Committee (IACUC). The IACUC acknowledges that this study is currently on going as previously approved. Please be advised that continuation of this study is in effect for a one-year period beginning 5/5/2017:

Please take note of the following:

- IACUC approval is granted for a one-year period at the end of which, an annual renewal form must be submitted for years two (2) and three (3) of the protocol through the eIACUC system. After three years all continuing studies must be completely re-described in a new electronic application and submitted to IACUC for review.
- All modifications to the IACUC-Approved Protocol must be approved by the IACUC prior to initiating the modification. Modifications can be submitted to the IACUC for review and approval as an Amendment or Procedural Change through the eIACUC system. These changes must be within the scope of the original research hypothesis, involve the original species and justified in writing. Any change in the IACUC-approved protocol that does not meet the latter definition is considered a major protocol change and requires the submission of a new application.

APPENDIX B: COPYRIGHT PERMISSIONS

Part of the information in Chapter 2, “Effects of Selected POPs on Insulin Secretion” and in Chapter 3, “Potential Mechanisms for BDE-47 and BDE-85-Mediated Increase in GSIS” has been reproduced with the publisher’s approval for educational purposes only.

Karandrea, S., Yin, H., Liang, X., & Heart, E. A. (2017). BDE-47 and BDE-85 stimulate insulin secretion in INS-1 832/13 pancreatic β -cells through the thyroid receptor and Akt. *Environmental Toxicology and Pharmacology*, 56, 29-34.

**ELSEVIER LICENSE
TERMS AND CONDITIONS**

Sep 18, 2017

This Agreement between University of South Florida -- Shpetim Karandrea ("You") and Elsevier ("Elsevier") consists of your license details and the terms and conditions provided by Elsevier and Copyright Clearance Center.

License Number	4192010824899
License date	Sep 18, 2017
Licensed Content Publisher	Elsevier
Licensed Content Publication	Environmental Toxicology and Pharmacology
Licensed Content Title	BDE-47 and BDE-85 stimulate insulin secretion in INS-1 832/13 pancreatic β -cells through the thyroid receptor and AKT
Licensed Content Author	Shpetim Karandrea,Huquan Yin,Xiaomei Liang,Emma A. Heart
Licensed Content Date	Dec 1, 2017
Licensed Content Volume	56
Licensed Content Issue	n/a
Licensed Content Pages	6
Start Page	29
End Page	34
Type of Use	reuse in a thesis/dissertation
Portion	full article
Format	both print and electronic
Are you the author of this Elsevier article?	Yes
Will you be translating?	No
Title of your thesis/dissertation	Identifying New Treatment Options and Risk Factors for Type 2 Diabetes: The Potential Role of Thymoquinone and Persistent Organic Pollutants
Expected completion date	Oct 2017
Estimated size (number of pages)	120
Requestor Location	University of South Florida 12901 Bruce B. Downs Blvd MDC #8 TAMPA, FL 33612 United States Attn: Shpetim Karandrea
Publisher Tax ID	98-0397604
Total	0.00 USD
Terms and Conditions	

The information in Chapter 4, "Anti-diabetic Effects of Thymoquinone in the Diet-Induced Obesity (DIO) Mouse Model of Type 2 Diabetes" has been legally partially reproduced under the Creative

Commons Attribution (CC BY) license; this publication is available online without any restrictions and can be re-used or reproduced as long as the original source is properly cited.

Karandrea, S., Yin, H., Liang, X., Slitt, A. L., & Heart, E. A. (2017). Thymoquinone ameliorates diabetic phenotype in Diet-Induced Obesity mice via activation of SIRT-1-dependent pathways. *PloS one*, 12(9), e0185374.

10/18/2017

PLOS ONE: accelerating the publication of peer-reviewed science

Licenses and Copyright

The following policy applies to all PLOS journals, unless otherwise noted.

What Can Others Do with My Original Article Content?

PLOS applies the Creative Commons Attribution (CC BY) license to articles and other works we publish. If you submit your paper for publication by PLOS, you agree to have the CC BY license applied to your work. Under this Open Access license, you as the author agree that anyone can reuse your article in whole or part for any purpose, for free, even for commercial purposes. Anyone may copy, distribute, or reuse the content as long as the author and original source are properly cited. This facilitates freedom in re-use and also ensures that PLOS content can be mined without barriers for the needs of research.

APPENDIX C: PUBLISHED MANUSCRIPTS



Research Paper

BDE-47 and BDE-85 stimulate insulin secretion in INS-1 832/13 pancreatic β -cells through the thyroid receptor and Akt

Shpetim Karandrea, Huquan Yin, Xiaomei Liang, Emma A. Heart*

Department of Molecular Pharmacology and Physiology, University of South Florida, Tampa, FL, 33612, United States

ARTICLE INFO

Keywords:

BDE-47
BDE-85
Glucose-stimulated insulin secretion
Thyroid receptor
Thyroid hormone
Akt

ABSTRACT

PBDEs (polybrominated diphenyl ethers) are environmental pollutants that have been linked to the development of type 2 diabetes, however, the precise mechanisms are not clear. Particularly, their direct effect on insulin secretion is unknown. In this study, we show that two PBDE congeners, BDE-47 and BDE-85, potentiate glucose-stimulated insulin secretion (GSIS) in INS-1 832/13 cells. This effect of BDE-47 and BDE-85 on GSIS was dependent on thyroid receptor (TR). Both BDE-47 and BDE-85 (10 μ M) activated Akt during an acute exposure. The activation of Akt by BDE-47 and BDE-85 plays a role in their potentiation of GSIS, as pharmacological inhibition of PI3K, an upstream activator of Akt, significantly lowers GSIS compared to compounds alone. This study shows that BDE-47 and BDE-85 directly act on pancreatic β -cells to stimulate GSIS, and that this effect is mediated by the thyroid receptor (TR) and Akt activation.

1. Introduction

Type 2 diabetes is a metabolic disorder characterized by chronic hyperglycemia, which develops as a consequence of peripheral insulin resistance and defective insulin secretion from pancreatic β -cells (Sargis, 2014). Diabetes prevalence has been on the rise and it can lead to major health complications, which increase the impacts of the disease in our society (Guariguata et al., 2014). A high calorie diet coupled with physical inactivity are known risk factors for the development of type 2 diabetes; however, these alone fail to account for the rapid rise of the disease (Sargis, 2014).

Recent attention has turned to the role of environmental pollutants in the development of metabolic diseases. Persistent organic pollutants (POPs), as their name suggests, are compounds that do not degrade easily and can bioaccumulate in the environment (Manzetti et al., 2014). They are man-made chemicals that are byproducts of various industrial processes (Manzetti et al., 2014). Polybrominated diphenyl ethers (PBDEs) are a class of POPs, and have been extensively used as flame retardants (Airaksinen et al., 2011; Darnerud et al., 2001). BDE-47 (2,2',4,4'-tetrabromodiphenyl ether) and BDE-85 (2,2',3,4,4'-pentabromodiphenyl ether) are two of the congeners in this class (Darnerud et al., 2001; Vagula et al., 2011). Data from epidemiological studies have suggested that PBDEs may be involved in the development of type 2 diabetes (Airaksinen et al., 2011; Lim et al., 2008; Zhang et al., 2016).

PBDEs have been positively associated with diabetes and metabolic syndrome (Lim et al., 2008), although in this study BDE-47 did not reach statistical significance. Data from animal studies show that BDE-47 exposure increases fasting blood glucose in mice (Zhang et al., 2016), whether commercial mixture penta-BDE exposure (containing BDE-47 and BDE-85 among others) increased lipolysis and decreased glucose oxidation in rat adipocytes (Hoppe and Carey, 2007). These findings suggest that exposure to these compounds may lead to changes in glucose and lipid homeostasis and thus contribute to diabetes development.

Limited studies have been done to address the diabetogenic potential of BDE-47 and BDE-85. Although some PBDE studies have focused on BDE-47, as it is one of the most abundant PBDE congeners (Darnerud et al., 2001), there are no studies done on BDE-85. Particularly, the direct effect of these compounds on pancreatic β -cell function remains underassessed. β -cells secrete an appropriate amount of insulin in response to elevated blood glucose levels (such as after a meal), which helps re-establish normoglycemia by promoting glucose uptake and utilization by insulin-sensitive peripheral tissues (Kahn et al., 2014). Altering this normal β -cell function can disrupt glucose homeostasis; inadequate insulin secretion can cause severe hyperglycemia whether oversecretion can possibly lead to hyperinsulinemia, resulting in peripheral insulin resistance and β -cell defects. In order to minimize the impacts of the disease it is important to identify potential risk agents

Abbreviations: GSIS, glucose-stimulated insulin secretion; POP, Persistent organic pollutant; PBDE, poly-brominated diphenyl ether; BDE-47, 2,2',4,4'-tetrabromodiphenyl ether; BDE-85, 2,2',3,4,4'-pentabromodiphenyl ether; TR, thyroid receptor

* Corresponding author at: University of South Florida, Department of Molecular Pharmacology & Physiology, 12901 Bruce B. Downs Blvd MDC 2008, Tampa, FL 33612, United States.
E-mail address: ehheart@health.usf.edu (E.A. Heart).

that can cause β -cell dysfunction. In the present study, we examined whether BDE-47 and BDE-85 exposure alters GSIS in insulin-producing INS-1 832/13 cells, and the potential underlying molecular mechanisms involved.

2. Materials and Methods

2.1. Chemicals

BDE-47 and BDE-85 were purchased from AccuStandard (New Haven, CT). Thyroid hormone T3 (3,3',5-Triiodo-L-thyronine) was purchased from Alfa Aesar (Lancashire, United Kingdom). Thyroid hormone receptor antagonist 1–850 was purchased from EMD Millipore (Darmstadt, Germany). Wortmannin was purchased from Acros Organics (Geel, Belgium). Stock solutions of BDE-47, BDE-85, T3, 1–850, and wortmannin were prepared in dimethyl sulfoxide (DMSO) and were added to the culture medium and/or KRB buffer to achieve the indicated concentrations. Final concentration of DMSO did not exceed 0.1%. All other chemicals were purchased from Sigma (St Louis, MO) unless otherwise specified.

2.2. Cell culture

INS-1 832/13 cells were a kind gift by Dr. Christopher Newgard (Duke University School of Medicine) and were cultured in RPMI-1640 glucose-free medium supplemented with 11 mmol/l glucose, 10% fetal bovine serum, 1 mmol/l sodium pyruvate, 5 mmol/l HEPES, 2 g/l sodium bicarbonate, 2 mmol/l L-glutamine, 50 μ mol/l 2-mercaptoethanol, 10000 U/ml penicillin, and 10 mg/ml streptomycin. Cells were maintained at 37 °C in a humidified incubator with 5% CO₂ and used at passages 51–56.

2.3. Cell viability

Cell viability was measured by the reduction of CellTiter-Blue® (Promega, Madison, WI) according to the manufacturer's protocol. In brief, cells were plated in 96-well plates and treated with indicated concentrations of compounds for 48 h in culture medium, after which CellTiter-Blue® was added to wells and the increase in fluorescence (560 nm excitation, 590 nm emission) was measured using a SpectraMax M5 multi-mode microplate reader (Molecular Devices, Sunnyvale, CA). IC₅₀ was calculated using a least squares fit with variable slope using GraphPad Prism (version 6.07).

2.4. Glucose-stimulated insulin secretion (GSIS)

INS-1 832/13 cells grown to confluency in 24-well plates, were washed 3 times with and pre-incubated in Krebs Ringer Buffer (KRB, 120 mM NaCl, 25 mM HEPES, 4.6 mM KCl, 1 mM MgSO₄, 0.15 mM Na₂HPO₄, 0.4 mM KH₂PO₄, 5 mM NaHCO₃, 2 mM CaCl₂) buffer containing 3 mmol/l glucose at 37 °C for 2 h; followed by a static 1 h incubation at 37 °C in KRB containing 3 (basal) or 16 (stimulating) mmol/l glucose. For acute GSIS, compounds were present only during the 1hr static incubation phase. KRB buffer was collected and centrifuged at 5000 x g for 3 min at 4 °C to pellet out any cells. Insulin released in buffer was measured by an ELISA kit (Alpco Diagnostics, Salem, NH) and data were normalized to the protein content, measured by the Micro-BCA Protein Assay kit (Pierce, Rockford, IL). For antagonist experiments, after a 2 h preincubation with 3 mmol/l glucose KRB, cells were preincubated with antagonists or vehicle control (DMSO) at indicated concentrations for 30 min in 3 mmol/l glucose KRB, washed once with 3 mmol/l glucose KRB, followed by static 1 h incubation at 37 °C in KRB buffer containing 16 mmol/l glucose. For chronic pre-treatment, cells were exposed to indicated concentrations of BDE-47 and BDE-85 for 48 h, after which cells were washed and preincubated in KRB buffer containing 3 mmol/l glucose and static incubation was

performed as described above (compounds not present during the 2 h pre-incubation or static 1 h glucose stimulation). For all insulin secretion experiments, controls cells were treated with vehicle (DMSO) at 0.1% concentration.

2.5. Western blot analysis

INS-1 832/13 cells were grown to confluence in 6-well plates, washed two times in serum-free growth media, and incubated for 30 min at 37 °C in serum-free growth media containing BDE-47, BDE-85, or T3. For inhibitor experiments, cells were preincubated with inhibitor or vehicle control (0.1% DMSO) at indicated concentrations for 30 min in serum-free growth media, washed once, and incubated for 30 min at 37 °C in serum-free media containing BDE-47 or BDE-85. After exposure, cells were solubilized in RIPA lysis buffer (Pierce, Rockford, IL). Protein content was determined using a BCA Protein Assay Kit (Pierce, Rockford, IL) and SDS samples were prepared. Equal amounts of protein were electrophoretically separated on SDS-polyacrylamide gel, followed by blotting onto PVDF membrane. Following the transfer, membranes were blocked with TBST (10 mmol/l Tris-HCl pH 7.4, 150 mmol/l NaCl, and 0.1% Tween 20) containing 5% nonfat dry milk (blocking buffer) and incubated with the primary antibodies diluted in blocking buffer overnight at 4 °C, followed by application of appropriate secondary antibodies for 1 h at room temperature. Proteins were detected by using enhanced chemiluminescence (ECL).

2.6. Reverse transcription and quantitative real-time RT-PCR (qRT-PCR)

INS-1 832/13 cells were grown to confluence in 6-well plates and total RNA was prepared using the TRIzol reagent according to the manufacturer's protocol (Invitrogen, Carlsbad, CA) and single-strand cDNA was synthesized from the RNA using a Maxime RT PreMix kit (iNtRON Biotechnology, Seongnam, South Korea). qRT-PCR amplifications were performed using rEVALution 2x qPCR Master Mix (Empirical Bioscience, Grand Rapids, MI) in an MyIQ2 Real-Time PCR Detection System (Bio-Rad, Richmond, CA) following manufacturer's protocol. To determine the specificity of amplification, melting curve analysis was applied to all final PCR products. The relative amount of target mRNA was calculated by the comparative threshold cycle method by normalizing target mRNA threshold cycle to those for glyceraldehyde-3-phosphate dehydrogenase (GAPDH). The primers were purchased from Integrated DNA Technologies (Coralville, IA) and were as follows: rat TR α (NM_031134) forward 5'-CCTGGATGATACGGAAGTG-3', reverse 5'-AGTGCAGGAATGTTGTGTT-3'; rat TR β (NM_012672) forward 5'-ATCATCACACCAGCAATCA-3', reverse 5'-GTCCGTCACCTTCATCAG-3'; rat GAPDH (NM_017008) forward 5'-GACATGCCGCTGGAGAAAC-3', reverse 5'-AGCCCAGGATGCCCTTTAGT-3'

2.7. Statistical analysis

Data are expressed as means \pm SEM and are results from at least three independent experiments performed in quadruplicate measurements. Significance was determined for multiple comparisons using two-way analysis of variance (ANOVA) followed by Sidak post-hoc analysis (Abdi, 2007). A *p*-value of ≤ 0.05 was considered significant. All analyses were conducted using the GraphPad Prism (version 6.07) statistical program software.

3. Results

To evaluate the role of chronic BDE-47 and BDE-85 exposure on INS-1 832/13 cell function, cells were exposed to different concentrations of compounds for 48 h, and GSIS was measured after the removal of these compounds. Chronic pre-treatment with 10 μ M BDE-47 or BDE-85 didn't affect insulin secretion (Fig. 1A and B). The concentrations used for chronic pre-treatment GSIS did not affect cell viability during

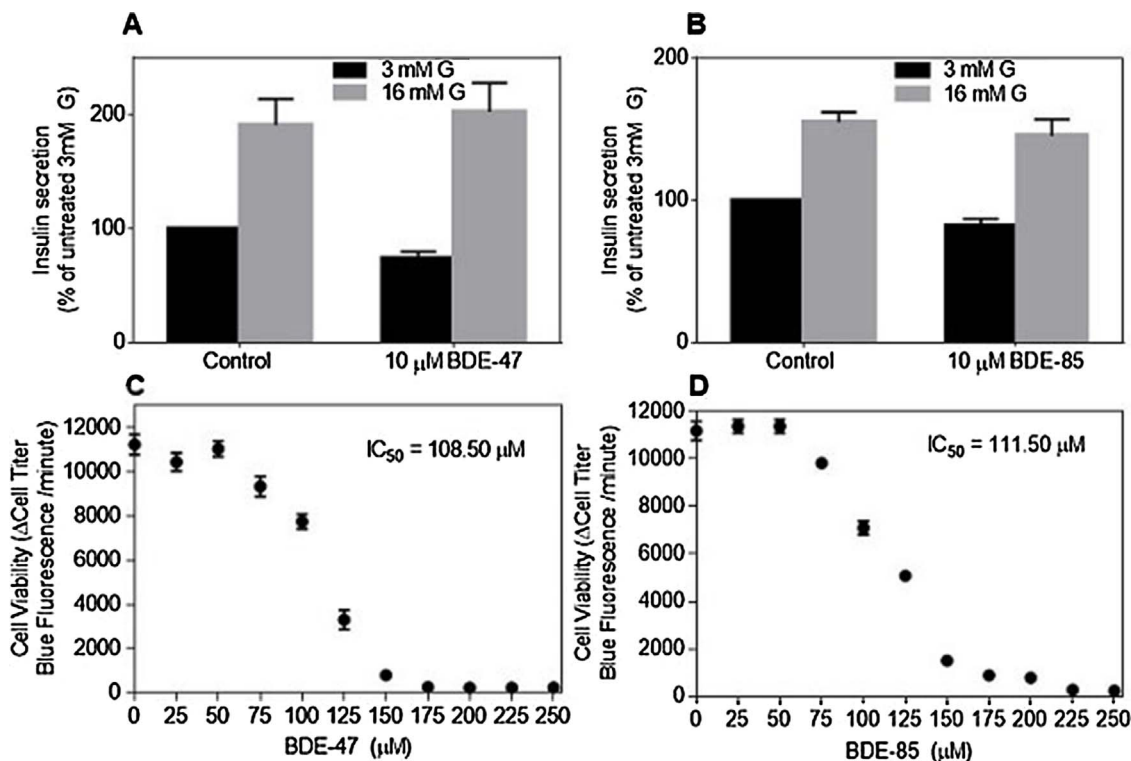


Fig. 1. Effect of chronic BDE-47 and BDE-85 exposure on GSIS and cell viability. INS-1 832/13 cells were pre-treated with BDE-47 (A) or BDE-85 (B) for 48 h and GSIS was assessed (as described in materials and methods). Effect of BDE-47 (C) and BDE-85 (D) on INS-1 832/13 cell viability after 48 h of exposure. 3 mM G = 3 mM glucose, 16 mM G = 16 mM glucose.

the same 48-h exposure period (Fig. 1C and D).

To evaluate whether these compounds have an acute effect on GSIS, we performed a 1 h static incubation in either 3 (low) or 16 mmol/l (high) glucose KRB buffer in the presence of compounds at 1, 5, or 10 μM concentrations. We observed a concentration-dependent increase in GSIS compared to vehicle control for both BDE-47 and BDE-85 during acute exposure. This increase was significant at 5 and 10 μM BDE-85 and 10 μM BDE-47 (Fig. 2A and B).

Since BDE-47 and BDE-85 have structural similarity with thyroid hormones (Ren and Guo, 2013), we investigated whether thyroid hormone signaling has any role in mediating the observed increase in GSIS caused by these compounds. Thyroid hormone (T3) administration increased acute GSIS in a concentration-dependent manner (data not shown). Furthermore, co-administration with T3 (5 μM) in the presence of 10 μM BDE-47 or BDE-85 caused an increase in this response (Fig. 3A). Based on this observation, we set to determine whether the

effects of these two compounds on GSIS are mediated by their actions on the thyroid hormone receptor. To confirm the expression of the thyroid receptor in the INS-1 832/13 cells, we measured the levels of two receptor isoforms (α and β) by qRT-PCR. As shown in Fig. 3B, TRα (but not TRβ) is expressed in this cell line, suggesting a possible role of thyroid hormone signaling in pancreatic β-cell function. To evaluate the role of thyroid receptor (TR) in BDE-mediated potentiation of GSIS, we pre-treated the cells with TR antagonist 1–850 (which inhibits both isoforms of the TR) for 30 min, and performed an acute GSIS (as described in Methods). Pre-treatment with TR antagonist decreased BDE-47 and BDE-85-mediated enhancement of GSIS, while the antagonist alone had no effect on GSIS (Fig. 3C).

Recently, it has been suggested that thyroid hormone can have important implications in pancreatic β-cell growth and function by activating Akt (Falzacappa et al., 2007, 2010). To evaluate whether BDE-47 and BDE-85 activate Akt in INS-1 832/13 cells during an acute

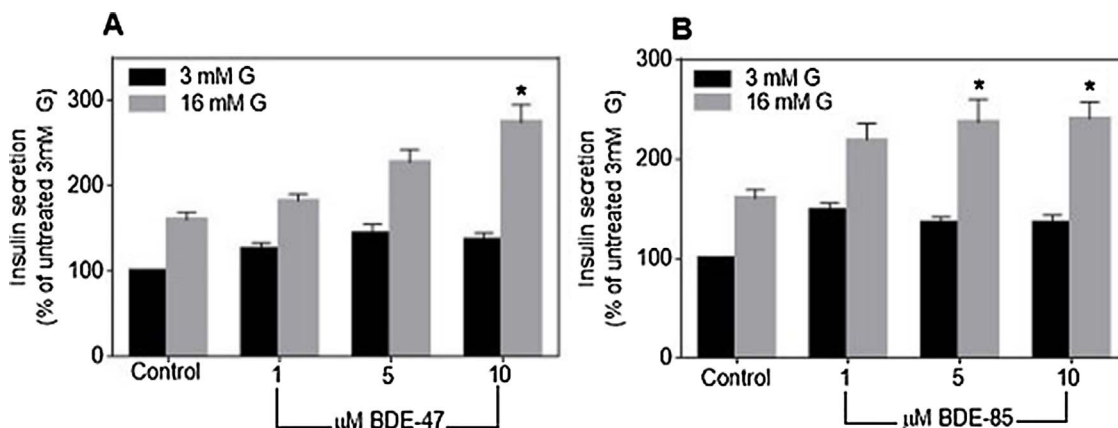


Fig. 2. Effect of BDE-47 and BDE-85 on acute GSIS. Acute GSIS (as described in methods) in INS-1 832/13 cells incubated with 1, 5, or 10 μM BDE-47 (A) or BDE-85 (B). * $p \leq 0.05$ when compared with control 16 mM G. 3 mM G = 3 mM glucose, 16 mM G = 16 mM glucose.

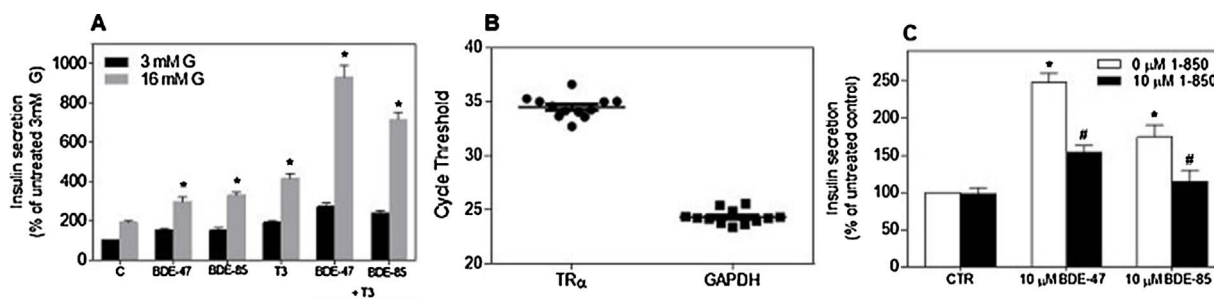


Fig. 3. Effect of BDE-47 and BDE-85 on GSIS is mediated via the thyroid receptor. (A) Acute GSIS in INS-1 832/13 cells treated with 10 μM BDE-47, 10 μM BDE-85, 5 μM T3, or co-treated with BDE-47 or BDE-85 and T3 as indicated. (B) Quantitative real-time polymerase chain reaction (qRT-PCR) showing expression of TRα and GAPDH in INS-1 832/13 cells. (C) INS-1 832/13 cells were pre-incubated with thyroid receptor antagonist 1–850 (10 μM) or vehicle for 30 min, followed by the addition of BDE-47 (10 μM), BDE-85 (10 μM) or vehicle for 1 h and GSIS was measured (as described in methods). 3 mM G = 3 mM glucose, 16 mM G = 16 mM glucose, CTR = vehicle control. * $p \leq 0.05$ when compared with control 16 mM G (A) or vehicle control (B), # $p \leq 0.05$ when compared with compound alone.

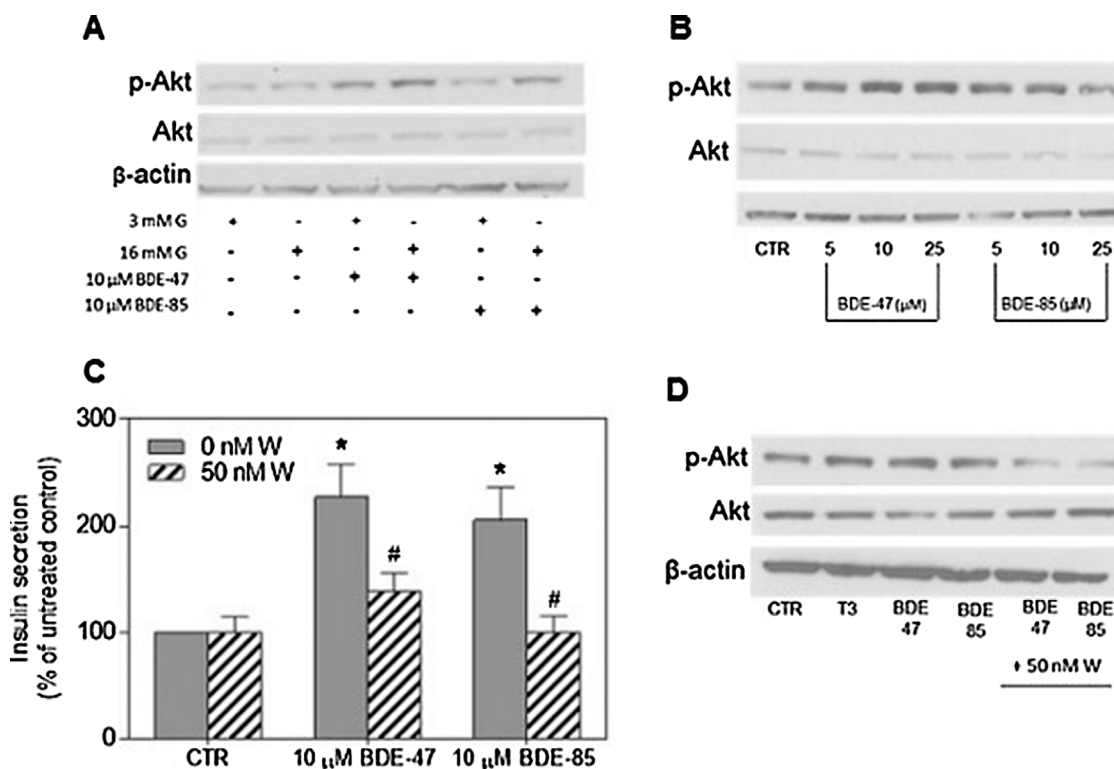


Fig. 4. Effect of BDE-47 and BDE-85 on GSIS is mediated through Akt. (A) Western blot images of *p*-Akt, Akt, and β-actin after 30-min exposure to BDE-47 (10 μM), BDE-85 (10 μM), or vehicle control in either low (3 mM) or high (16 mM) glucose media as described in methods. (B) Western blot images of *p*-Akt, Akt, and β-actin after 30-min exposure to BDE-47 (5, 10, or 25 μM), BDE-85 (5, 10, or 25 μM), or vehicle control in 11 mM glucose media as described in methods. (C) INS-1 832/13 cells were pre-incubated with PI3 K inhibitor, wortmannin (50 nM) or vehicle for 30 min, followed by the addition of BDE-47 (10 μM), BDE-85 (10 μM) or vehicle for 1 h and GSIS was measured (as described in methods). (D) INS-1 832/13 cells were pre-incubated with wortmannin (50 nM) or vehicle for 30 min in 11 mM glucose media, followed by the addition of BDE-47 (10 μM), BDE-85 (10 μM), T3 (5 μM) or vehicle in 11 mM glucose media for 30 min, after which protein levels of *p*-Akt, Akt, and β-actin were measured by western blot. 3 mM G = 3 mM glucose, 16 mM G = 16 mM glucose, W = wortmannin, CTR = vehicle control. * $p \leq 0.05$ when compared with vehicle control, # $p \leq 0.05$ when compared with compound alone.

incubation, cells were treated for 30 min with these compounds and levels of total and phosphorylated (activated) Akt were measured by Western Blot. Both BDE-47 and BDE-85 (at 10 μM concentration) activate Akt during an acute incubation at high (16 mM) glucose compared to vehicle control (Fig. 4A). High glucose treatment in the absence of compounds did not increase phosphorylated Akt (Fig. 4A). The 10 μM concentration was chosen since it was shown to increase GSIS after acute exposure to both compounds, although lower and higher concentrations were also shown to activate Akt at the normal (11 mM) glucose condition (Fig. 4B).

To evaluate whether Akt plays a role in BDE-47 and BDE-85-mediated increase in GSIS, we tested whether pharmacological inhibition of PI3 K, an upstream activator of Akt (Sargis, 2014; Guo, 2014), would affect this response. A 30-min pre-treatment with PI3 K

inhibitor, wortmannin, followed by a static one hour GSIS, caused a decrease in GSIS when cells were treated with BDE-47 or BDE-85 compared to compounds alone (Fig. 4C). The concentration of wortmannin (50 nM) was chosen from a previous study showing that this concentration effectively blocked Akt phosphorylation while not affecting insulin secretion (Collier et al., 2004). Indeed, at this concentration (50 nM), wortmannin didn't affect GSIS (Fig. 4C), but effectively inhibited BDE-47 and BDE-85-induced Akt phosphorylation (Fig. 4D). Furthermore, acute incubation with T3 (5 μM) increased Akt phosphorylation (Fig. 4D) as expected and as previously reported (Falzacappa et al., 2007, 2010).

4. Discussion

Polybrominated diphenyl ethers (PBDEs) such as BDE-47 and BDE-85 are heavily used in various industrial processes. These compounds, once disseminated into the environment, do not degrade easily, and can thus bioaccumulate in the food chain, making their way into our diets. Dietary intake is one of the main routes of exposure; with high estimated intake from food (ng/kg range) in humans previously reported (Manzetti et al., 2014). Furthermore, they can bioaccumulate in various tissues, thus increasing their potential effects (Manzetti et al., 2014; Airaksinen et al., 2011). Epidemiological and animal studies suggest a potential role of PBDEs in contributing to the development of type 2 diabetes (Airaksinen et al., 2011; Hoppe and Carey, 2007; Lim et al., 2008; Zhang et al., 2016). However, the precise mechanisms are not known. In the present study, we have investigated the role of BDE-47 and BDE-85 in pancreatic β -cell function and demonstrate that these two compounds increase acute glucose-stimulated insulin secretion (GSIS). This effect was mediated by the thyroid hormone receptor (TR) and was dependent on Akt activation.

Concentrations as low as 1 μ M affected GSIS, although the maximum increase in insulin secretion was achieved at the 10 μ M concentration for both BDE-47 and BDE-85. This increase happened only during an acute (1 h) static incubation, and no change was observed during a 48 h chronic pre-treatment (compounds absent during GSIS). This suggests that BDE-47 and BDE-85 have a direct effect on β -cell function that is not likely due to potential changes in expression of metabolic enzymes or transcription factors involved in GSIS.

PBDEs are similar to thyroid hormones in structure and have been shown to disrupt thyroid hormone signaling (Blanco et al., 2014; Ren and Guo, 2013; Richardson et al., 2008). Thyroid hormone is important in development, but also in metabolic rate and weight management (Casals-Casas and Desvergne, 2011). It acts by binding to the thyroid hormone receptor (TR) in various tissues, including the pancreatic β -cell; however, its direct role in β -cell function remains controversial (Shoemaker et al., 2012). While some *in vitro* and *in vivo* studies suggested that thyroid signaling is associated with decreased GSIS (Lenzen et al., 1975; Ximenes et al., 2007); others have shown an increase in GSIS and cell survival in the INS-1 832/13 cells following thyroid hormone treatment (Falzacappa et al., 2007, 2010). Our own data show an increase in GSIS in INS-1 832/13 cells during an acute incubation with thyroid hormone, suggesting an important role for the thyroid hormone signaling in GSIS. Furthermore, there was an additional increase in acute GSIS with co-treatment of T3 and BDE-47 or BDE-85. Based on these observations, we tested whether these compounds might act via the thyroid receptor to potentiate GSIS. Pharmacological inhibition of the thyroid receptor (TR) by the specific antagonist 1–850 led to a decrease in BDE-47 and BDE-85-mediated GSIS. This suggests that the potentiating effects of these compounds on GSIS are mediated via the TR. It is unlikely that the TR antagonist has off-target effects due to its specificity and the fact that pre-treatment with the antagonist alone did not affect GSIS.

Thyroid hormone has been shown to have a beneficial effect on pancreatic β -cell growth and function by activating Akt (Falzacappa et al., 2007, 2010). Although the role of Akt in the insulin signaling pathway is well established (Guo, 2014), its role in insulin secretion is controversial. Downregulation of Akt activity specifically in β -cells led to glucose intolerance due to impaired insulin secretion in mice (Bernal-Mizrachi et al., 2004). Akt activation has been implicated to play an important role in increasing insulin granule exocytosis (Bernal-Mizrachi et al., 2004; Cheng et al., 2012). Conversely, Akt inhibition has been shown to potentiate insulin secretion and increase insulin granule fusion (Aoyagi et al., 2012). Since BDE-47 and BDE-85 activate Akt during an acute incubation (Fig. 4A and B), we were interested to determine whether this activation played a role in their potentiation of GSIS. Treatment with PI3 K inhibitor wortmannin inhibited BDE-47 and BDE-85-induced GSIS, suggesting that Akt activation plays a role. In

contrast, PI3 K inhibition in the absence of compounds didn't affect GSIS, suggesting that this pathway might be involved in insulin secretion only when activated. However, the role of Akt in GSIS and the specific mechanisms involved require further characterization. It is unclear whether BDE-47 and BDE-85 bind to thyroid receptor in the nucleus or whether their effects are due to binding cytosolic TR, thus having non-genomic actions. A prior study showed that thyroid hormone activates Akt via a non-genomic mechanism (Falzacappa et al., 2007); however further studies are needed to determine whether BDE-47 and BDE-85 bind to TR and activate Akt via a similar mechanism.

Most of the effects on GSIS for these two compounds were observed at the 10 μ M concentration, which is higher than the nanomolar ranges of concentrations reported in human tissues (Costa et al., 2014; Darnerud et al., 2001). However, given the fact that PBDEs bioaccumulate in various tissues and have estimated half-lives measured in years in humans (Geyer et al., 2004), it is possible that cells in the human body are exposed to similar concentrations of PBDEs *in vivo*. Furthermore, prolonged or chronic exposure to PBDEs even at lower concentrations could cause a similar effect on insulin secretion observed with the acute exposure in our study. Thus, further work is required to adequately assess the relevant concentrations of PBDEs that affect pancreatic β -cell function and glucose homeostasis *in vivo*.

This study shows for the first time that BDE-47 and BDE-85 increase GSIS in pancreatic β -cells and that this effect is possibly mediated by the thyroid receptor and Akt. This provides evidence that exposure to environmental pollutants such as PBDEs can alter pancreatic β -cell function, a key player in glucose homeostasis. Further studies are required to determine the specific mechanisms by which Akt activation by BDE-47 and BDE-85 can lead to increased GSIS; or whether other mechanisms in addition to the one proposed are involved. It is possible that chronic exposure to PBDEs can cause chronic elevated insulin secretion. This excess insulin could lead to hyperinsulinemia, which can cause insulin resistance, one of the hallmarks of type 2 diabetes (Nolan et al., 2015). These potential long-term implications need to be further assessed in physiologically relevant animal models of type 2 diabetes and in epidemiological studies.

Conflict of interest

The authors report no conflicts of interest, financial or otherwise.

Acknowledgements

The work was supported by National Institute of Diabetes and Digestive and Kidney Diseases Grant R01-DK-098747 and American Diabetes Association Grant No. 7-12-BS-073 (E. A. Heart). Shpetim Karandrea was supported by the Graduate Student Success Fellowship (University of South Florida). We are forever indebted to the intellectual input of the late Prof. M. Meow, Prof. L. Dracek, and Prof. K. Rocket for their support.

References

- Abdi, H., 2007. Bonferroni and Šidák corrections for multiple comparisons. *Encyclopedia of Measurement and Statistics*, vol. 3. pp. 103–107.
- Airaksinen, R., Rantakokko, P., Eriksson, J.G., Blomstedt, P., Kajantie, E., Kiviranta, H., 2011. Association between type 2 diabetes and exposure to persistent organic pollutants. *Diabetes Care* 34, 1972–1979.
- Aoyagi, K., Ohara-Imaizumi, M., Nishiwaki, C., Nakamichi, Y., Ueki, K., Kadowaki, T., Nagamatsu, S., 2012. Acute inhibition of PI3K-PDK1-Akt pathway potentiates insulin secretion through upregulation of newcomer granule fusions in pancreatic β -cells. *PLoS One* 7, e47381.
- Bernal-Mizrachi, E., Fatrai, S., Johnson, J.D., Ohsugi, M., Otani, K., Han, Z., Polonsky, K.S., Permutt, M.A., 2004. Defective insulin secretion and increased susceptibility to experimental diabetes are induced by reduced Akt activity in pancreatic islet β cells. *J. Clin. Invest.* 114, 928–936.
- Blanco, J., Mulero, M., Domingo, J.L., Sanchez, D.J., 2014. Perinatal exposure to BDE-99 causes decreased protein levels of cyclin D1 via GSK3 β activation and increased ROS production in rat pup livers. *Toxicol. Sci.* 137, 491–498.

- Casals-Casas, C., Desvergne, B., 2011. Endocrine disruptors: from endocrine to metabolic disruption. *Annu. Rev. Physiol.* 73, 135–162.
- Cheng, K.K., Lam, K.S., Wu, D., Wang, Y., Sweeney, G., Hoo, R.L., Zhang, J., Xu, A., 2012. APPL1 potentiates insulin secretion in pancreatic β cells by enhancing protein kinase Akt-dependent expression of SNARE proteins in mice. *Proc. Natl. Acad. Sci. U. S. A.* 109, 8919–8924.
- Collier, J.J., White, S.M., Dick, G.M., Scott, D.K., 2004. Phosphatidylinositol 3-kinase inhibitors reveal a unique mechanism of enhancing insulin secretion in 832/13 rat insulinoma cells. *Biochem. Biophys. Res. Commun.* 324, 1018–1023.
- Costa, L.G., de Laat, R., Tagliaferri, S., Pellacani, C., 2014. A mechanistic view of polybrominated diphenyl ether (PBDE) developmental neurotoxicity. *Toxicol. Lett.* 230, 282–294.
- Darnerud, P.O., Eriksen, G.S., Jóhannesson, T., Larsen, P.B., Viluksela, M., 2001. Polybrominated diphenyl ethers: occurrence, dietary exposure, and toxicology. *Environ. Health Perspect.* 109, 49–68.
- Falzacappa, C.V., Petrucci, E., Patriarca, V., Michienzi, S., Stigliano, A., Brunetti, E., Toscano, V., Misiti, S., 2007. Thyroid hormone receptor TR β 1 mediates Akt activation by T3 in pancreatic β cells. *J. Mol. Endocrinol.* 38, 221–233.
- Falzacappa, C.V., Mangialardo, C., Raffa, S., Mancuso, A., Piergrossi, P., Moriggi, G., Piro, S., Stigliano, A., Torrissi, M.R., Brunetti, E., Toscano, V., 2010. The thyroid hormone T3 improves function and survival of rat pancreatic islets during in vitro culture. *Islets* 2, 96–103.
- Geyer, H.J., Schramm, K.W., Darnerud, P.O., Aune, M., Feicht, E.A., Fried, K.W., Henkelmann, B., Lenoir, D., Schmid, P., McDonald, T.A., 2004. Terminal elimination half-lives of the brominated flame retardants TBBPA, HBCD, and lower brominated PBDEs in humans. *Organohalogen Compd.* 66, 3867–3872.
- Guariguata, L., Whiting, D.R., Hambleton, I., Beagley, J., Linnenkamp, U., Shaw, J.E., 2014. Global estimates of diabetes prevalence for 2013 and projections for 2035. *Diabetes Res. Clin. Pract.* 103, 137–149.
- Guo, S., 2014. Insulin signaling, resistance, and metabolic syndrome: insights from mouse models into disease mechanisms. *J. Endocrinol.* 220, T1–T23.
- Hoppe, A.A., Carey, G.B., 2007. Polybrominated diphenyl ethers as endocrine disruptors of adipocyte metabolism. *Obesity* 15, 2942–2950.
- Kahn, S.E., Cooper, M.E., Del Prato, S., 2014. Pathophysiology and treatment of type 2 diabetes: perspectives on the past, present, and future. *Lancet* 383, 1068–1083.
- Lenzen, S., Panten, U., Hasselblatt, A., 1975. Thyroxine treatment and insulin secretion in the rat. *Diabetologia* 11, 49–55.
- Lim, J.S., Lee, D.H., Jacobs, D.R., 2008. Association of brominated flame retardants with diabetes and metabolic syndrome in the US population, 2003–2004. *Diabetes Care* 31, 1802–1807.
- Manzetti, S., van der Spoel, E.R., van der Spoel, D., 2014. Chemical properties, environmental fate, and degradation of seven classes of pollutants. *Chem. Res. Toxicol.* 27, 713–737.
- Nolan, C.J., Ruderman, N.B., Kahn, S.E., Pedersen, O., Prentki, M., 2015. Insulin resistance as a physiological defense against metabolic stress: implications for the management of subsets of type 2 diabetes. *Diabetes* 64, 673–686.
- Ren, X.M., Guo, L.H., 2013. Molecular toxicology of polybrominated diphenyl ethers: nuclear hormone receptor mediated pathways. *Environ. Sci. Process Impacts* 15, 702–708.
- Richardson, V.M., Staskal, D.F., Ross, D.G., Diliberto, J.J., DeVito, M.J., Birnbaum, L.S., 2008. Possible mechanisms of thyroid hormone disruption in mice by BDE 47, a major polybrominated diphenyl ether congener. *Toxicol. Appl. Pharmacol.* 226, 244–250.
- Sargis, R.M., 2014. The hijacking of cellular signaling and the diabetes epidemic: mechanisms of environmental disruption of insulin action and glucose homeostasis. *Diabetes Metab. J.* 38, 13–24.
- Shoemaker, T., Kono, T., Mariash, C., Evans-Molina, C., 2012. Thyroid hormone analogues for the treatment of metabolic disorders: new potential for unmet clinical needs? *Endocr. Pract.* 18, 954–964.
- Vagula, M.C., Kubeldis, N., Nelatury, C.F., 2011. Effects of BDE-85 on the oxidative status and nerve conduction in rodents. *Int. J. Toxicol.* 30, 428–434.
- Ximenes, H.M., Lortz, S., Jörnset, A., Lenzen, S., 2007. Triiodothyronine (T3)-mediated toxicity and induction of apoptosis in insulin-producing INS-1 cells. *Life Sci.* 80, 2045–2050.
- Zhang, Z., Li, S., Liu, L., Wang, L., Xiao, X., Sun, Z., Wang, X., Wang, C., Wang, M., Li, L., Xu, Q., 2016. Environmental exposure to BDE47 is associated with increased diabetes prevalence: evidence from community-based case-control studies and an animal experiment. *Sci. Rep.* 6, 27854.

RESEARCH ARTICLE

Thymoquinone ameliorates diabetic phenotype in Diet-Induced Obesity mice via activation of SIRT-1-dependent pathways

Shpetim Karandrea¹, Huquan Yin¹, Xiaomei Liang¹, Angela L. Slitt², Emma A. Heart^{1*}

1 Department of Molecular Pharmacology and Physiology, University of South Florida, Tampa, Florida, United States of America, **2** Department of Pharmaceutical Sciences, University of Rhode Island, Kingston, Rhode Island, United States of America

* eheart@health.usf.edu



OPEN ACCESS

Citation: Karandrea S, Yin H, Liang X, Slitt AL, Heart EA (2017) Thymoquinone ameliorates diabetic phenotype in Diet-Induced Obesity mice via activation of SIRT-1-dependent pathways. PLoS ONE 12(9): e0185374. <https://doi.org/10.1371/journal.pone.0185374>

Editor: Guillermo López Lluch, Universidad Pablo de Olavide, SPAIN

Received: March 2, 2017

Accepted: September 12, 2017

Published: September 26, 2017

Copyright: © 2017 Karandrea et al. This is an open access article distributed under the terms of the [Creative Commons Attribution License](https://creativecommons.org/licenses/by/4.0/), which permits unrestricted use, distribution, and reproduction in any medium, provided the original author and source are credited.

Data Availability Statement: All relevant data are within the paper and its Supporting Information files.

Funding: The work was supported by National Institute of Diabetes and Digestive and Kidney Diseases Grant R01-DK-098747 and American Diabetes Association Grant No. 7-12-BS-073 (E. A. Heart). Shpetim Karandrea was supported by the Graduate Student Success Fellowship (University of South Florida).

Abstract

Thymoquinone, a natural occurring quinone and the main bioactive component of plant *Nigella sativa*, undergoes intracellular redox cycling and re-oxidizes NADH to NAD⁺. TQ administration (20 mg/kg/bw/day) to the Diet-Induced Obesity (DIO) mice reduced their diabetic phenotype by decreasing fasting blood glucose and fasting insulin levels, and improved glucose tolerance and insulin sensitivity as evaluated by oral glucose and insulin tolerance tests (OGTT and ITT). Furthermore, TQ decreased serum cholesterol levels and liver triglycerides, increased protein expression of phosphorylated Akt, decreased serum levels of inflammatory markers resistin and MCP-1, and decreased NADH/NAD⁺ ratio. These changes were paralleled by an increase in phosphorylated SIRT-1 and AMPK α in liver and phosphorylated SIRT-1 in skeletal muscle. TQ also increased insulin sensitivity in insulin-resistant HepG2 cells via a SIRT-1-dependent mechanism. These findings are consistent with the TQ-dependent re-oxidation of NADH to NAD⁺, which stimulates glucose and fatty acid oxidation and activation of SIRT-1-dependent pathways. Taken together, these results demonstrate that TQ ameliorates the diabetic phenotype in the DIO mouse model of type 2 diabetes.

Introduction

Maintenance of glucose homeostasis involves insulin secretion from the pancreatic β -cells in response to a rise in blood glucose, and insulin action in target tissues (predominantly liver, muscle, and adipose tissue) to stimulate glucose entry and utilization, and inhibit hepatic glucose production [1]. Development of type 2 diabetes (T2D) involves both peripheral insulin resistance and pancreatic β -cell dysfunction. Insulin resistance, the inability of peripheral tissues to properly respond to insulin, is initially compensated by a rise in insulin output in order to maintain normoglycemia [1]. However, this compensatory mechanism is impaired in individuals predisposed to T2D, and later results in overt hyperglycemia [2, 3].

Thymoquinone (TQ) is the main bioactive component of *Nigella sativa*, a spice plant of *Ranunculacea* family, and a traditional medicine that has been used to treat diabetes symptoms

Competing interests: The authors have declared that no competing interests exist.

and to lower blood glucose [4]. *Nigella sativa* has been reported to increase both insulin secretion and insulin sensitivity [5, 6]. TQ has been shown to reduce hepatic glucose production [7] and protect β -cells from oxidative stress following streptozotocin (STZ) treatment [8]. However, mechanistic studies and comprehensive evaluation of TQ action under physiological diabetic conditions and models is currently lacking.

TQ belongs to the family of quinones, naturally-derived compounds featuring a conjugated double bond system, which is responsible for their reactivity and intracellular process known as “redox cycling” [9]. Our laboratory has been instrumental in establishing the concept that re-oxidation of NADH back to NAD⁺ via quinone-dependent redox cycling lowers cellular reductive poise and facilitates glucose and fatty acid oxidation, and is necessary for the overall health of the cells [9, 10]. Our group has previously shown that TQ supports redox cycling in pancreatic β -cells, resulting in the reduction of NADH/NAD⁺ ratio and normalization of defective glucose-stimulated insulin secretion (GSIS) under chronically elevated glucose via inhibition of acetyl CoA carboxylase (ACC) and enhanced oxidation of glucose and fatty acids [11].

The oxidation status of nicotinamide adenine dinucleotide, represented by the ratio between its reduced and oxidized forms (NADH/NAD⁺) is a critical determinant of the direction of metabolic flux [12, 13], as NAD⁺ promotes oxidative pathways via activation of TCA cycle enzymes [14]. Furthermore, increased intracellular level of NAD⁺ activates SIRT1-dependent metabolic pathways, which stimulate energy metabolism, enhance life span, and can positively regulate insulin secretion and insulin signaling [14, 15].

Here we evaluated the capacity of TQ to ameliorate the diabetic phenotype in a physiologically relevant rodent model of obesity and diabetes, Diet-Induced Obesity (DIO) mice. We hypothesized that sustained decrease in the NADH/NAD⁺ ratio due to TQ-dependent redox cycling will result in the enhanced fuel oxidation and amplification of NAD⁺-dependent SIRT-1 pathway in metabolic tissues, leading to the enhanced insulin sensitivity and improved glucose homeostasis.

Materials and methods

Chemicals

Human recombinant insulin, resveratrol, and AICAR were purchased from Tocris Bioscience (Bristol, UK). Nicotinamide was purchased from Acros Organics (Geel, Belgium) and Compound C was purchased from EMD Millipore (Billerica, MA). All other chemicals and reagents were purchased from Sigma (St Louis, MO) unless specified otherwise. Stock solutions of thymoquinone, resveratrol, AICAR, Nicotinamide, and Compound C were prepared in DMSO and added to culture medium to achieve the indicated concentrations.

Ethics statement

All procedures were performed in accordance with and approved by the Institutional Animal Care and Use Committee (IACUC) of the University of South Florida.

Animals

Male C57BL/6J mice (6 weeks of age) were purchased from Jackson Laboratories (Bar Harbor, ME) and housed (4 animals per cage) in a USF Animal Facility; room was maintained at a constant temperature (25°C) in a light:dark 12:12-h schedule. Food and water was available *ad libitum*. Body weight was monitored on a weekly basis. Mice were pair fed either control low fat diet, LFD (10% fat cal, Research Diets, New Brunswick, NJ) or high fat diet, HFD (45% fat cal,

Research Diets, New Brunswick, NJ). Mice were separated in the following groups: LFD, LFD +TQ, HFD, HFD+TQ. TQ (dissolved in canola oil) was administered daily by oral gavage at 20 mg/kg body weight for the duration of the study. Vehicle only (canola oil) was administered to control groups (LFD and HFD). The dose of TQ was chosen because it was shown to lower blood glucose [16], albeit in a non-physiological rodent model of diabetes. The chosen dose is well below toxic doses established for oral administration in mice [17]. As expected, TQ was well tolerated, and TQ administration did not affect the overall health of the animals in the study. After 24 weeks, animals were euthanized with isoflurane, tissues and serum collected, and either used immediately or were snap frozen in liquid nitrogen and stored in -80°C until further use.

Cell culture

HepG2 human hepatoma cell line was purchased from American Type Culture Collection (ATCC, Manassas, VA) and cultured in DMEM medium supplemented with 10% FBS, 100 units of penicillin, and 100 $\mu\text{g}/\text{mL}$ streptomycin at 37°C in a humidified incubator with 5% CO_2 . Cells were made insulin resistant by treatment with 20mM glucose for 18 hours, as previously described [18, 19]. Following high glucose treatment, cells were starved for 2 hours in serum-free medium, prior to treatment with the respective compounds for 24 hours. For inhibitor treatment, cells were pre-incubated with the inhibitors for 30 mins, and the inhibitors were also present during the 24-hour incubation period. To measure insulin signaling, insulin was added during the last 30 minutes. Vehicle-treated cells (0.5% DMSO) in normal (5.5 mM) and high (20 mM) glucose conditions served as controls.

OGTT and ITT

For *in vivo* studies, animals were anesthetized with ketamine (80 mg/kg body weight). Oral glucose and insulin tolerance tests were performed following a 6 hr fast. Mice were oral gavaged with 2 mg/kg/bw glucose (OGTT), or injected intraperitoneally with 0.5 IU insulin/kg/bw (ITT). Blood glucose, obtained at 0, 15, 30, 60, 90, 120 and 180 minutes from the tail vein was measured with a glucometer (Bayer Contour).

Cholesterol content

Total cholesterol, HDL, and LDL/VLDL content was determined from serum samples using the HDL and LDL/VLDL Cholesterol Assay Kit (abcam, Cambridge, MA) according to the manufacturer's protocols.

Serum profile

Serum levels of insulin, resistin and MCP-1 were determined by Ocean Ridge Biosciences (Deerfield Beach, FL) using a Luminex multiplex protein profiling assay (Luminex Corp., Austin, TX) according to the manufacturer's protocols.

Western blot analysis

Liver and soleus muscle tissues were solubilized in RIPA lysis buffer (Pierce, Rockford, IL) using Fast Prep 24G system (MP Biosciences, Santa Ana, CA). After exposure, HepG2 cells were solubilized in RIPA lysis buffer. Protein content was determined using a BCA Protein Assay Kit (Pierce, Rockford, IL) and SDS samples were prepared. Equal amount of protein (100 μg per lane) were electrophoretically separated on SDS-polyacrylamide gel, followed by blotting onto PVDF membrane. Following the transfer, membranes were blocked with TBST

(10 mmol/l Tris-HCl pH 7.4, 150 mmol/l NaCl, and 0.1% Tween 20) containing 5% nonfat dry milk (blocking buffer) and incubated with the primary antibodies (diluted in blocking buffer overnight at 4°C) against SIRT-1 (Cell Signaling, cat. #9475), p-SIRT-1 (Cell Signaling, cat. #2314), Akt (Cell Signaling, cat. #9272), p-Akt (Cell Signaling, cat. #9271), AMPK α (Cell Signaling, cat. #5831), p-AMPK α (Cell Signaling, cat. #2535), NQO1 (Santa Cruz, cat. #sc-16464), β -actin (Cell Signaling, cat. #4970), and β -tubulin (Cell Signaling, cat. #2146). Membranes were incubated with goat anti-rabbit immunoglobulin (IgG) secondary antibody (Santa Cruz, cat. #sc-2030) for 1 h at room temperature, and washed 5 times. Proteins were detected by using enhanced chemiluminescence. Semiquantitative analysis of Western blot images were performed using ImageJ.

Triglyceride content

Triglyceride content was determined in liver and soleus muscle RIPA buffer lysates (lysates as described above) using the Triglyceride kit (Pointe Scientific, Canton, MI) according to the manufacturer's protocols.

Metabolomics analysis

Serum levels of glycerol, palmitic acid, oleic acid, and stearic acid were measured by gas chromatography—mass spectrometry (GC/MS) analysis. The GC/MS experiments were performed by the University of Utah Metabolomics Core.

Determination of nucleotides

NADH/NAD⁺ ratio was determined in liver and soleus muscle using the NAD/NADH assay kit as per the manufacturer's protocol (Abcam, Cat #65348, Cambridge, UK).

Quantitative real time RT-PCR

The tissue samples stored in RNAlater (Invitrogen, Carlsbad, CA) were homogenized by using the Fast Prep 24G instrument (MP Biosciences, Santa Ana, CA). Total RNA was prepared using the TRIzol reagent according to the manufacturer's protocol (Invitrogen, Carlsbad, CA) and single-strand cDNA was synthesized from the RNA in a reaction mixture containing optimum blend of oligo(dT) primers and iScript reverse transcriptase (Bio-Rad, Richmond, CA). qRT-PCR amplifications were performed using rEVALution 2x qPCR Master Mix (Empirical Bioscience, Grand Rapids, MI) in an MyIQ2 Real-Time PCR Detection System (Bio-Rad, Richmond, CA) following manufacturer's protocol. To determine the specificity of amplification, melting curve analysis was applied to all final PCR products. The relative amount of target mRNA was calculated by the comparative threshold cycle method by normalizing target mRNA threshold cycle to those for glyceraldehyde-3-phosphate dehydrogenase (GAPDH). The primers used for analysis were as follows: NQO1: sense primer, 5' -AGGATGGGAGGTACTCGAATC-3', anti-sense primer, 5' -AGGCGTCCTTCCTTATATGCTA-3'; GAPDH: sense primer, 5' -CTTCACCACCATGGAGAAGGC-3', anti-sense primer, 5' -GGCATGGACTGTGGTCATGAG-3'.

Statistical analysis

Data are expressed as means \pm SEM. Significance was determined for multiple comparisons using one-way or two-way analysis of variance (ANOVA) followed by Sidak or Holm-Sidak multiple comparisons tests [20, 21] for planned comparisons (as mentioned in each figure) or independent t-test as indicated. A p-value of ≤ 0.05 was considered significant.

Results

The Diet Induced Obesity (DIO) mice develop obesity, hyperinsulinemia, glucose intolerance and insulin resistance when fed a high fat diet, making them a suitable model to study type 2 diabetes pathophysiology [22, 23]. This is confirmed in our study, where after high fat feeding, mice developed a diabetic phenotype as shown by the weight gain (Fig 1A), elevated fasting blood glucose (BG) and insulin levels (Fig 1B and 1C), and impaired oral glucose and insulin tolerance tests (OGTT and ITT) (Fig 2A and 2B). TQ administration was effective in ameliorating these parameters: TQ lowered body weight (Fig 1A), fasting blood glucose and insulin (Fig 1B and 1C, respectively), and improved glucose tolerance and insulin sensitivity, evaluated by OGTT and ITT (Fig 2A and 2B).

Type 2 diabetes is associated with increased inflammation, which can contribute to insulin resistance and is shown to be detrimental to many tissues including pancreatic β -cells [24, 25]. Resistin, a hormone secreted by adipocytes, impairs glucose tolerance and insulin sensitivity in mice [26] and has been associated with insulin resistance in humans [27, 28]. Monocyte chemoattractant protein-1 (MCP-1) is a pro-inflammatory chemokine that can induce insulin resistance [29] and circulating levels of this chemokine are increased in patients with type 2 diabetes [30–32]. TQ lowered serum levels of resistin in DIO mice (Fig 3A). There was a trend to lower the MCP-1 levels, however, this didn't reach statistical significance in HFD animals ($p = 0.06$), although TQ decreased MCP-1 in LFD animals (Fig 3B). These results demonstrate the potential of TQ to alleviate tissue inflammation in diabetes and obesity.

Elevated levels of triglycerides, together with decreased HDL and increased LDL cholesterol levels are the key identifiers of diabetic dyslipidemia, which can exacerbate insulin resistance [33]. Consistent with our previously reported data demonstrating TQ-dependent increase in fatty acid oxidation [11], and observed increased peripheral insulin sensitivity in this study (as shown by the improvement of the ITT in DIO mice, Fig 2B), TQ ameliorated HFD-dependent increase in liver triglyceride levels (Fig 4A). There was a trend to lower HFD-dependent muscle triglyceride content, however this did not reach statistical significance (Fig 4B). We saw similar trends when analyzed serum glycerol and three relevant fatty acids: palmitic acid, oleic acid, and stearic acid. GC/MS analysis of serum levels of these metabolites were decreased compared to HFD alone (Table 1), however this didn't reach statistical significance.

There was also a trend to decrease serum cholesterol level, albeit statistically not significant (Fig 5A). However, TQ significantly decreased the levels of LDL cholesterol in the serum of HFD animals (Fig 5C), with no effect on the HDL levels (Fig 5B). This effect was selective to the HFD diet, as LFD animals did not demonstrate changes in their HDL or LDL/VLDL cholesterol in response to TQ regimen.

The lowered tissue triglyceride levels following TQ administration argues for the TQ-dependent activation of the oxidative pathways (and consequent oxidation, rather than deposition of metabolic substrates). NADH/NAD⁺ ratio is important determinant of metabolic flux [14], and our group previously reported that TQ lowers NADH/NAD⁺ ratio in pancreatic β -cells exposed to glucose overload [11]. To confirm that TQ exerts this effect *in vivo*, we measured NADH/NAD⁺ ratio in liver and skeletal muscle. In liver, there was an increase in this ratio in HFD mice (Fig 6A), which is in agreement with prior studies suggesting an increase in NADH in diabetes and obesity [14]. However, we did not observe this change in skeletal muscle (Fig 6B). In both liver and soleus muscle, TQ lowered the NADH/NAD⁺ ratio in the HFD group compared to HFD alone (Fig 6A and 6B).

Since NADH/NAD⁺ ratio is known to regulate SIRT-1 pathway, we analyzed effect of TQ feeding on this pathway in the liver and soleus muscle of TQ-treated compared to control mice. Liver and soleus muscle from mice treated with TQ had enhanced phosphorylated

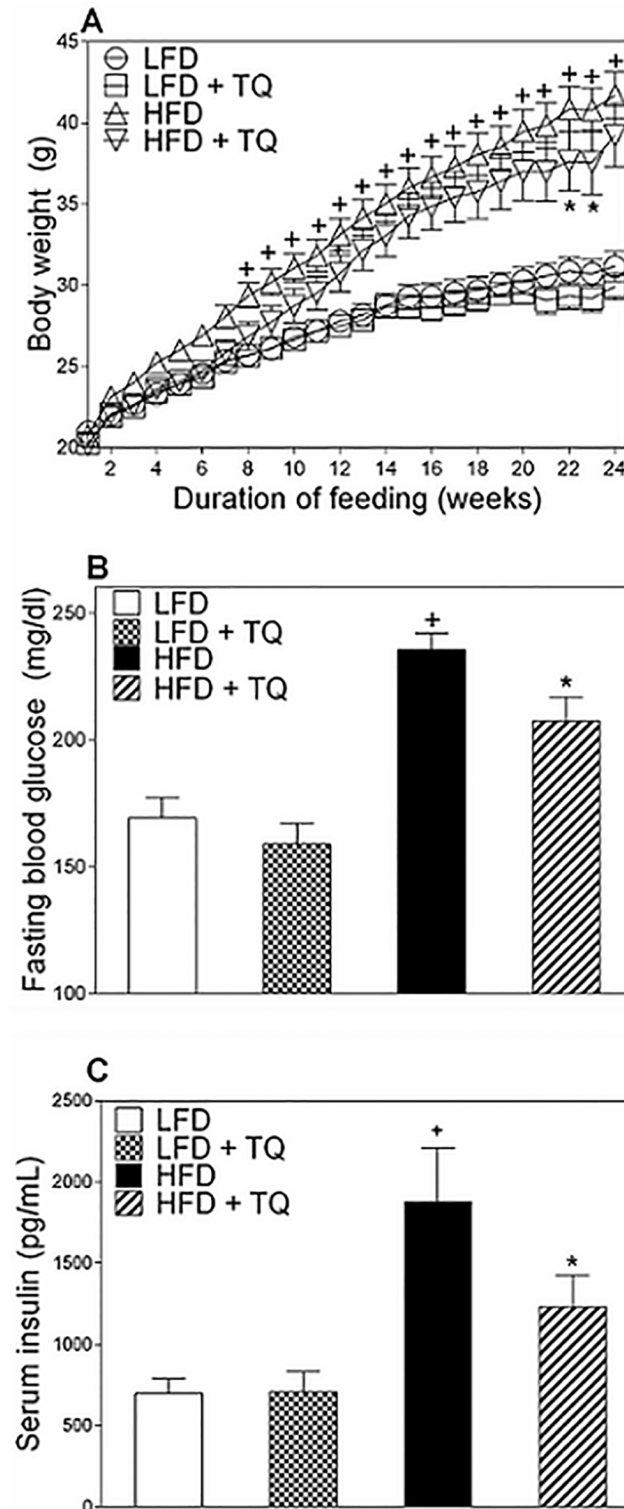


Fig 1. TQ ameliorates weight gain, lowers fasting blood glucose and insulin in DIO mice. (A) Effect of TQ on body weight (B) Effect of TQ treatment on fasting blood glucose after a 6 hour fast. (C) Effect of TQ on serum insulin. Total body weight was measured weekly for the duration of the study. $p < 0.05$ when comparing HFD and LFD (+), and HFD and HFD+TQ (*), using a one-way ANOVA followed by Sidak post-test (A and B) or independent t-test (C). Results are means \pm SEM ($n = 10$ – 12 mice per treatment group). LFD: low fat diet, HFD: high fat diet, TQ: thymoquinone.

<https://doi.org/10.1371/journal.pone.0185374.g001>

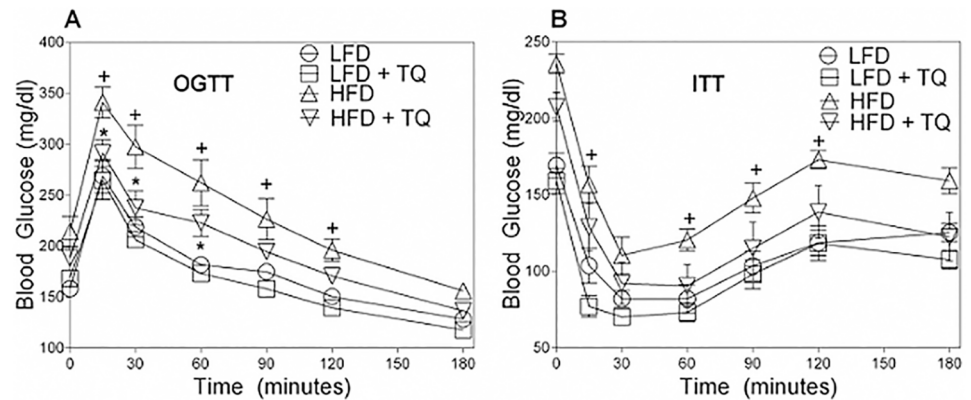


Fig 2. TQ normalizes glucose tolerance and insulin sensitivity. (A) Blood glucose levels in response to oral glucose tolerance test (OGTT). (B) Blood glucose levels in response to insulin tolerance test (ITT). $p < 0.05$ when comparing HFD and LFD (+), and HFD and HFD+TQ (*), using a two-way ANOVA followed by Holm-Sidak post-test. Results are means \pm SEM ($n = 10-12$ mice per treatment group). LFD: low fat diet, HFD: high fat diet, TQ: thymoquinone.

<https://doi.org/10.1371/journal.pone.0185374.g002>

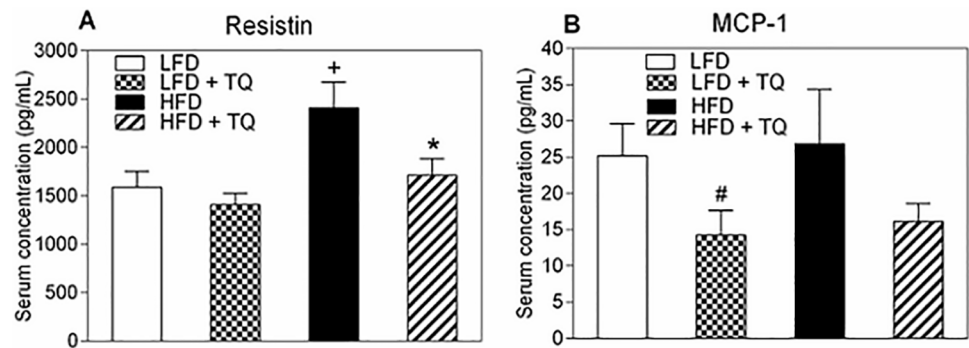


Fig 3. Effects of TQ on serum resistin and MCP-1. (A) Resistin serum concentration. (B) MCP-1 serum concentration. $p < 0.05$ when comparing (+) HFD and LFD, (*) HFD + TQ and HFD, and (#) LFD and LFD + TQ using independent t-tests. Results are means \pm SEM ($n = 10-12$ mice per treatment group). LFD: low fat diet, HFD: high fat diet, TQ: thymoquinone, MCP-1: monocyte chemotactic protein 1.

<https://doi.org/10.1371/journal.pone.0185374.g003>

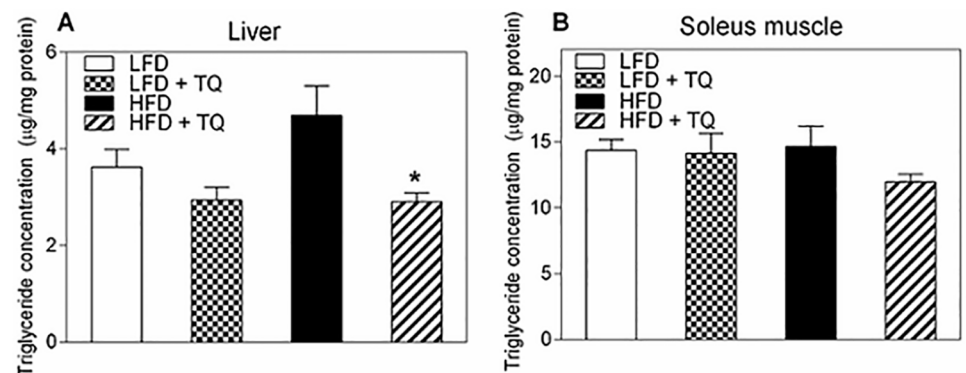


Fig 4. Effects of TQ on triglyceride content in liver and muscle. (A) Triglyceride concentration in liver. (B) Triglyceride concentration in soleus muscle. (*) $p < 0.05$ when comparing HFD + TQ and HFD using a one-way ANOVA followed by Sidak post-test. Results are means \pm SEM ($n = 8-12$ mice per treatment group). LFD: low fat diet, HFD: high fat diet, TQ: thymoquinone.

<https://doi.org/10.1371/journal.pone.0185374.g004>

Table 1. Effect of TQ on serum glycerol and fatty acids.

Metabolite	Treatment			
	LFD	LFD + TQ	HFD	HFD + TQ
Glycerol	844.7 ± 70.1 ^a	1282 ± 101.9 ^c	1348 ± 124.2 ^b	1186 ± 47.1
Palmitic Acid	820.3 ± 26.1	970.4 ± 61.3	862.7 ± 53.8	798.7 ± 23.4
Oleic Acid	2851 ± 179.8	3335 ± 195.8	2807 ± 345.9	2597 ± 114.5
Stearic Acid	381.9 ± 15.0	371.9 ± 22.3	471.2 ± 25.8	437.5 ± 21.4

Results expressed as means ± SEM. n = 10–12 mice/group. Means within the same row with different superscripts differ, p ≤ 0.05 as determined by using a one-way ANOVA followed by Sidak post-test. a, b = LFD vs. HFD only; a, c = LFD vs. LFD + TQ only. TQ = Thymoquinone, LFD = low fat diet, HFD = high fat diet.

<https://doi.org/10.1371/journal.pone.0185374.t001>

(activated) SIRT-1 in both LFD and HFD groups (Fig 7A–7D). We also analyzed the protein expression levels of other SIRT proteins in the liver, and did not see a difference with TQ treatment across groups for SIRT-2, SIRT-3, SIRT-5, SIRT-6, and SIRT-7 (S1 Fig). This could be due to SIRTs 2–7 having a lower deacetylase activity, as SIRT-6 and SIRT-7 have been previously shown to have a lower NAD⁺-deacetylase activity compared to SIRT-1 [34]. In the liver, TQ enhanced AMPKα phosphorylation as well as phosphorylation of Akt (protein kinase B), a key member of insulin signaling pathway [35,36] (Fig 8A and 8B).

To evaluate the mechanistic actions behind TQ-induced insulin sensitivity, we used the HepG2 cell line as an *in vitro* model of insulin resistance to assess whether this action is SIRT-1-dependent. HepG2 cells were made insulin resistant as previously described [18, 19], which was confirmed by decreased p-Akt protein after high glucose treatment (Fig 9A and 9B). TQ increased p-Akt in high-glucose treated cells, restoring these levels to that of the control cells (Fig 9A and 9B). This shows that TQ improves insulin resistance in similar fashion to what we see in livers of DIO mice. This action showed to be SIRT-1-dependent, as pre-treatment of insulin resistant cells with SIRT-1 inhibitor nicotinamide in the presence of TQ, significantly decreases p-Akt protein and TQ-induced insulin sensitivity (Fig 9A and 9B). Furthermore, treatment with SIRT-1 activator resveratrol and AMPKα activator AICAR increased insulin sensitivity, although this trend was not statistically significant (Fig 9A and 9B). Pre-treatment with compound C (AMPKα inhibitor) or compound C and nicotinamide in the presence of TQ decreased insulin sensitivity compared to TQ treatment alone, albeit statistically insignificant (Fig 9A and 9B). TQ treatment showed similar trends to the *in vivo* experiments in increasing phosphorylation of SIRT-1 and AMPKα in insulin-resistant cells (S2A–S2D Fig). Trends were also observed in increased p-SIRT-1 and p-AMPKα with resveratrol and AICAR in the presence of TQ (S2A–S2D Fig), as well as a decrease in phosphorylation of SIRT-1 with nicotinamide or compound C in the presence of TQ after high glucose treatment (S2A and S2B Fig). Pre-treatment with compound C or with compound C and nicotinamide significantly decreased p-AMPKα in the presence of TQ compared to TQ treatment alone (S2C and S2D Fig). Taken together, these results provide additional support about the role of TQ in improving insulin resistance, as well as show that this action is likely mediated by SIRT-1 activation.

TQ applied in this study was within the physiologically relevant diet-derived levels. However, non-physiologically high and toxic levels of quinones is known to generate excessive levels of reactive oxygen intermediates via quinone-dependent redox cycling, and this causes induction of the NAD(P)H-dependent Quinone Oxidoreductase 1 (NQO1). NQO1 is a phase 2 detoxification enzyme induced in response to oxidative stress, which expression is regulated by the Keap1/Nrf2/ARE pathway [10, 37], and NQO1 alone has been show to regulate NADH/

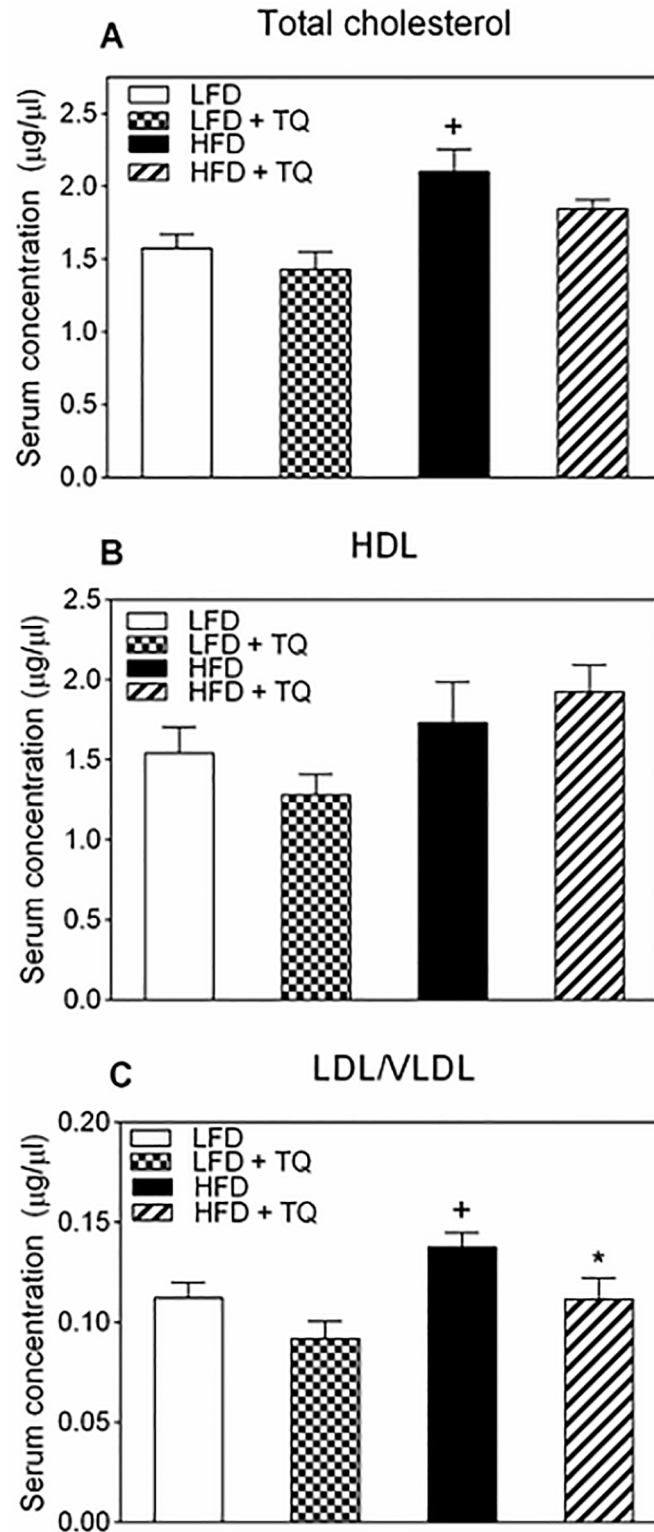


Fig 5. Effects of TQ on serum cholesterol. (A) Total cholesterol serum concentration. (B) HDL cholesterol serum concentration. (C) LDL/VLDL cholesterol serum concentration. $p \leq 0.05$ when comparing (+) HFD and LFD, (*) HFD + TQ and HFD using independent t-tests. Results are means \pm SEM ($n = 6-7$ mice per treatment group). LFD: low fat diet, HFD: high fat diet, TQ: thymoquinone, LDL: low-density lipoprotein, HDL: high-density lipoprotein, VLDL: very-low-density lipoprotein.

<https://doi.org/10.1371/journal.pone.0185374.g005>

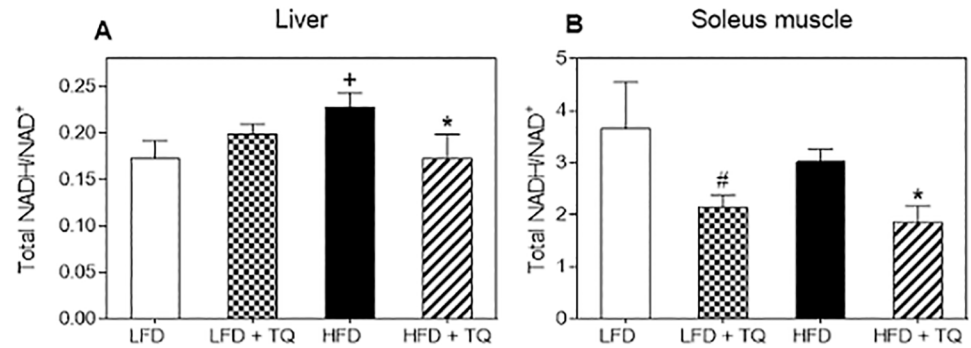


Fig 6. Effects of TQ on NADH/NAD⁺ ratio in liver and soleus muscle. (A) NADH/NAD⁺ ratio in liver. (B) NADH/NAD⁺ ratio in soleus muscle. $p \leq 0.05$ when comparing (+) HFD and LFD, (*) HFD + TQ and HFD, and (#) LFD and LFD + TQ using independent t-tests. Results are means \pm SEM (n = 8–10 mice per treatment group). LFD: low fat diet, HFD: high fat diet, TQ: thymoquinone.

<https://doi.org/10.1371/journal.pone.0185374.g006>

NAD⁺ ratio [10, 38]. To ascertain that applied doses of TQ were physiologically low and not inductive of NQO1 and/or oxidative stress, mRNA and protein levels of NQO1 were measured in liver and muscle. Levels of NQO1 were not elevated in any of these tissues, confirming that applied doses, while effective in regulating the cellular redox, do not activate the Keap1/Nrf2/ARE pathway and do not increase oxidative stress (Fig 10). This further supports our

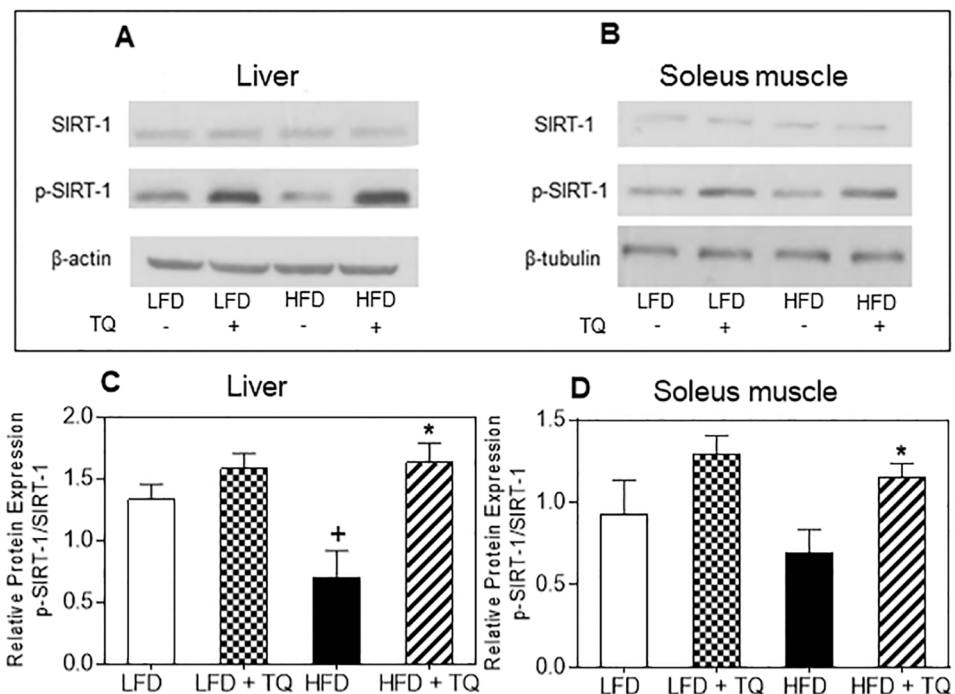


Fig 7. Effects of TQ on SIRT-1 protein expression. (A) Western blot images of SIRT-1 and p-SIRT-1 protein in liver. β -actin was used as a loading control. (B) Western blot images of SIRT-1 and p-SIRT-1 protein in soleus muscle. β -tubulin was used as a loading control. Western blot images are representative of combined liver and soleus muscle lysates from n = 10–12 mice per treatment group. (C and D) Protein band quantification using densitometry from three independent experiments. $p \leq 0.05$ when comparing (+) HFD and LFD and (*) HFD + TQ and HFD using independent t-tests LFD: low fat diet, HFD: high fat diet, TQ: thymoquinone.

<https://doi.org/10.1371/journal.pone.0185374.g007>

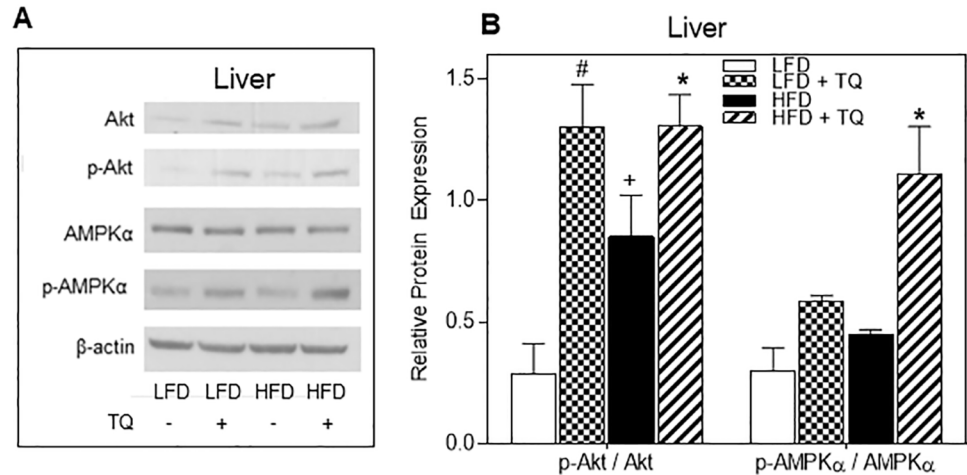


Fig 8. Effects of TQ on Akt and AMPK α protein expression in liver. (A) Western blot images of Akt, p-Akt, AMPK α and p-AMPK α protein in liver. β -actin was used as a loading control. Western blot images are representative of combined liver lysates from n = 10–12 mice per treatment group. (B) Protein band quantification using densitometry from three independent experiments. $p \leq 0.05$ when comparing (+) HFD and LFD, (*) HFD + TQ and HFD, and (#) LFD and LFD + TQ using independent t-tests. LFD: low fat diet, HFD: high fat diet, TQ: thymoquinone.

<https://doi.org/10.1371/journal.pone.0185374.g008>

hypothesis that TQ-dependent re-oxidation of NADH and consequent decrease of the NADH/NAD⁺ ratio is the main mechanism to activate SIRT-1/AMPK pathway and promote fuel oxidation rather than deposition, which leads to the observed changes in normalization of glucose homeostasis in DIO mice following TQ administration.

Discussion and conclusions

This is the first *in vivo* study aimed to comprehensively evaluate the effect of thymoquinone (TQ), a bioactive component of the *Nigella sativa* plant, on whole body glucose homeostasis using a physiologically-relevant mouse model of type 2 diabetes. In our published *in vitro* study, we have reported that both *Nigella sativa* extract (NSE) of high thymoquinone (TQ) content, as well as TQ alone, decreased NADH/NAD⁺ ratio and stimulated glucose and fatty acid oxidation in pancreatic β -cells, and this action was accompanied by the restoration of the glucose-stimulated insulin secretion (GSIS) in cells exposed to glucose overload [11]. Here we have expanded our studies to an *in vivo* model with focus on the TQ effect on the insulin sensitive peripheral tissues, and evaluated the action of TQ on glucose homeostasis in Diet Induced Obesity (DIO) mice.

After 24 weeks of HFD, C57/BLJ mice became obese and diabetic, as demonstrated by their increased body weight (Fig 1A), elevated fasting blood glucose (Fig 1B), insulin (Fig 1C) and impaired OGTT and ITT (Fig 2). While TQ treatment improved all these parameters in HFD animals, TQ had no significant effect on weight, fasting blood glucose and insulin, or OGTT /ITT in animals treated with LFD, suggesting that TQ primarily affects DIO metabolism by increasing oxidation of diet-derived fatty acid surplus. However, it is still possible that TQ treatment beyond the 24 weeks could lead to observed changes in physiological parameters in the LFD group as well, and further studies are required to address this issue. Bioavailability of TQ after an oral administration can be a limiting factor on TQ actions. Although such studies have been very limited in mice, studies with other animal models have shown that TQ is rapidly eliminated and slowly absorbed [39,40]. Therefore, further studies are required to address the bioavailability of TQ after oral administration in mice to properly determine a relevant

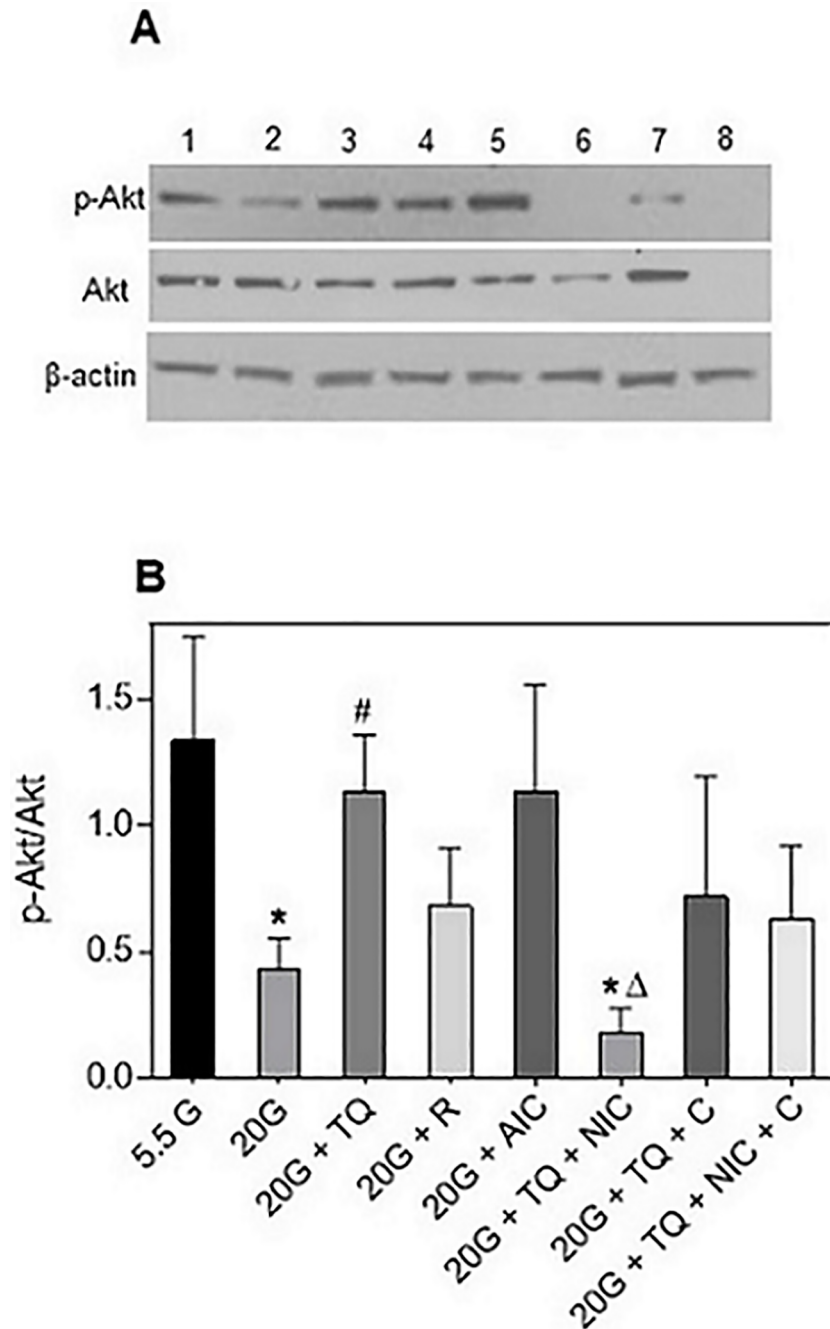


Fig 9. TQ improves insulin sensitivity in HepG2 cells via a SIRT-1 dependent mechanism. HepG2 cells were cultured in high (20 mM) glucose or in growth media containing 5.5 mM glucose for 18 hours, starved with serum-free media for 2 hours, then pre-incubated with vehicle control (0.5% DMSO), nicotinamide (0.5 mM), compound C (20 μ M), or with nicotinamide and compound C together for 30 mins, followed by incubation with TQ (10 μ M) in the presence or absence of nicotinamide and compound C; or with TQ, resveratrol (50 μ M), or AICAR (2 mM) alone for 24 hours in 20mM glucose media. Vehicle-treated cells in 5.5 mM glucose served as control. Insulin (100 nM) was added during the last 30 min. (A) Western blot images of p-Akt, Akt, and β -actin. (B) Protein band quantification using densitometry from three independent experiments. $p \leq 0.05$ where (*) is significantly different from 5.5G, (#) is significantly different from 20G, and (Δ) is significantly different from 20G + TQ using independent t-tests. 5.5 G: 5.5 mM glucose, 20G: 20 mM glucose, TQ: thymoquinone, R: resveratrol, AIC: AICAR, NIC: nicotinamide, C: compound C.

<https://doi.org/10.1371/journal.pone.0185374.g009>

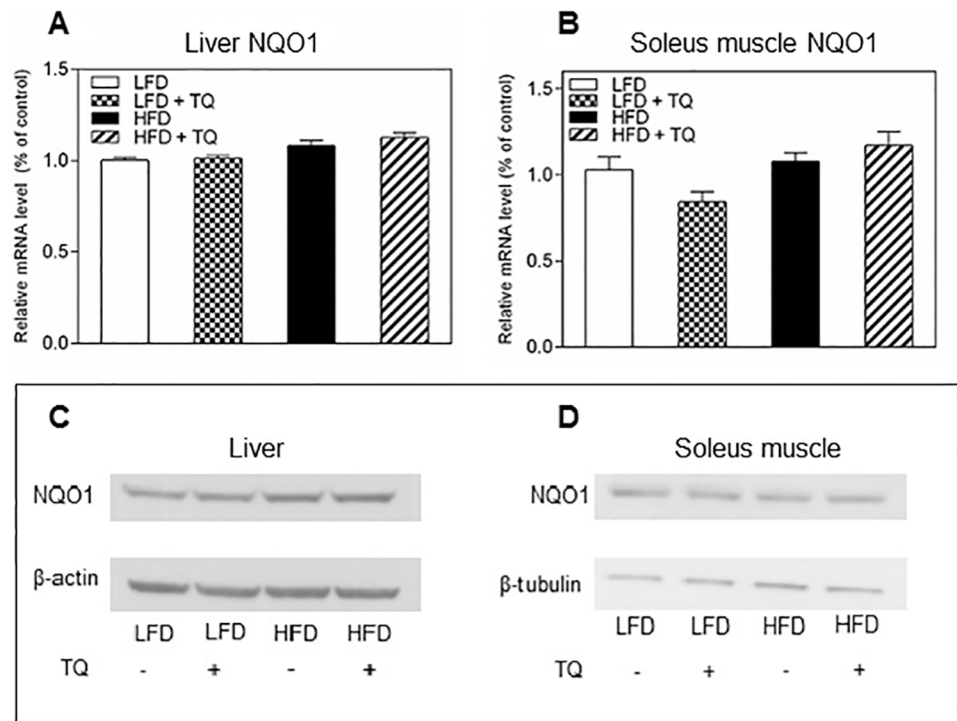


Fig 10. Effects of TQ on NQO1 expression. NQO1 mRNA expression in liver (A) and soleus muscle (B). (C) Western blot images of NQO1 and β -actin protein in liver (D) Western blot images of NQO1 protein in soleus muscle. β -tubulin was used as a loading control. Statistical analysis (A and B): one-way ANOVA followed by Sidak post-test ($p \leq 0.05$). qPCR results are means \pm SEM ($n = 8-12$ mice per treatment group). Western blot images are representative of combined liver and soleus muscle lysates from $n = 10-12$ mice per treatment group. LFD: low fat diet, HFD: high fat diet, TQ: thymoquinone.

<https://doi.org/10.1371/journal.pone.0185374.g010>

dose and exposure window, particularly in physiologically relevant mouse models of type 2 diabetes.

Metabolism is governed by the oxidation status of nicotinamide adenine dinucleotide, represented by the ratio between its reduced and oxidized forms ($NADH/NAD^+$) [14]. During glycolysis NAD^+ is reduced to $NADH$, which needs to be re-oxidized back to NAD^+ [14]. In chronic hyperglycemic conditions, such as in type 2 diabetes, there can be $NADH$ overproduction due to the fact that mitochondrial shuttles are unable to efficiently re-oxidize $NADH$, which leads to the condition known as reductive stress [14, 41]. This leads to increased pressure on mitochondrial complex I, the primary site of $NADH$ recycling, which in turn causes the formation of superoxide [14, 42] and enhanced oxidative stress, known to be detrimental to insulin sensitivity and insulin secretion and exacerbate the diabetic phenotype [43]. $NADH$ excess inhibits glycolytic and TCA cycle enzymes (glyceraldehyde 3-phosphate dehydrogenase, pyruvate dehydrogenase, isocitrate dehydrogenase, α -ketoglutarate dehydrogenase, malate dehydrogenase), leading to the impairment of glucose oxidation and TCA cycle oxidative pathways [14, 43]. TQ has been shown to regulate oxidation level of adenine nucleotides [11]. Due to its conjugated double bond system, TQ is able to re-oxidize $NADH$ in the process of $NAD(P)$ -dependent redox cycling [44], and thus decrease the $NADH/NAD^+$ ratio, as shown by our group [11]. Furthermore, in this study we also demonstrate that TQ treatment leads to a decrease in the $NADH/NAD^+$ ratio in liver and skeletal muscle in HFD mice (Fig 6). Regeneration of NAD^+ from TQ can thus increase glucose and fatty acid oxidation and ameliorate diabetic dyslipidemia. Diabetic dyslipidemia is characterized by high plasma triglyceride

concentration, low HDL cholesterol and elevated non-HDL cholesterol [33]. The main cause of this phenotype is the increased free fatty acid release from insulin-resistant adipose tissue in type 2 diabetes [45, 46]. The influx of free fatty acids in the liver can promote triglyceride synthesis, which increases the production of non-HDL (LDL, VLDL) cholesterol to transfer lipids to tissues and decreases HDL cholesterol levels, which transfers lipids back to liver for degradation [33]. Indeed, our data demonstrating that TQ treatment decreased serum LDL/VLDL levels (while not affecting HDL levels) and tissue level of triglycerides (Figs 4 and 5) in HFD mice are consistent with TQ antidiabetic action and effect on lipid homeostasis. TQ-dependent decrease in triglyceride and LDL/VLDL levels correlated with improved insulin signaling and insulin sensitivity judged by enhanced phosphorylation of Akt (Fig 8). Akt activation is consistent with the observed improvement in insulin sensitivity seen with the insulin tolerance test (Fig 2B). These results are in accordance with our previously reported *in vitro* results [11] that TQ increases glucose and fatty acid oxidation, which can lead to enhanced fuel oxidation by peripheral tissues, weight loss and increased insulin sensitivity.

In addition to serving as a regulator of metabolic flux and substrate for metabolic processes, NAD^+ can activate sirtuin 1 (SIRT-1) and consequently SIRT-1-dependent pathways [15]. SIRT-1 is a class III histone deacetylase, where NAD^+ functions as a substrate for SIRT-1 deacetylation of target proteins [15]. SIRT-1 has been implicated directly in critical aspects of glucose homeostasis, such as increasing insulin secretion and insulin sensitivity, and lowering the inflammation and oxidative stress associated with diabetes and obesity [15, 47–49]. Enhanced production of NAD^+ via TQ-dependent redox cycling is consistent with increased level of SIRT-1 phosphorylation in liver and muscle (Fig 7A–7D). It has been previously shown that SIRT-1 can activate AMPK (AMP-activated protein kinase) by de-acetylating and activating serine-threonine liver kinase B1 (LKB1), an upstream activator of AMPK [50]. AMPK is activated when cellular energy levels are low (e.g. high AMP/ATP ratio), and has been shown to enhance fatty acid oxidation, glycolysis, stimulate glucose uptake in skeletal muscle, and inhibit cholesterol synthesis [51]. We saw increased phosphorylated AMPK α protein in the liver of both LFD and HFD animals treated with TQ (Fig 8), suggesting that TQ can activate AMPK-dependent pathways. Due to similarities in their action on different processes, such as cellular metabolism and inflammation, it has been suggested that AMPK and SIRT-1 are involved in a cycle where they regulate each other [50]. Whether TQ administration activates AMPK indirectly via SIRT-1, or directly via alteration of parameters different from NADH/ NAD^+ ratio, warrants further investigation. To mechanistically explore whether the increase in insulin sensitivity with TQ treatment is SIRT-1-dependent, we used the HepG2 cell line as a model of insulin resistance. TQ treatment reversed insulin resistance after 24 hours, shown by the increase in phosphorylated Akt (Fig 9). Pre-treatment with SIRT-1 inhibitor nicotinamide suppressed this TQ effect on insulin signaling, suggesting that it is likely SIRT-1-dependent. Pre-treatment with AMPK α inhibitor compound C also inhibited the effect of TQ, albeit statistically insignificant. Furthermore, there was an improvement in insulin resistance after treatment with SIRT-1 and AMPK activators, suggesting a positive role of these pathways in insulin signaling.

Diabetes and obesity are associated with tissue inflammation, which can exacerbate insulin resistance. Adipose-derived pro-inflammatory markers such as resistin and chemokines (MCP-1) can exacerbate insulin resistance by activating c-Jun N-terminal (JNK) kinases and NF- κ B transcription factors, which can promote serine phosphorylation (inhibition) of insulin receptor substrate-1 (IRS-1), a key component of insulin signaling [52]. SIRT-1 has been shown to inhibit NF- κ B activity, and therefore suppress the inflammatory process [53]. Indeed, TQ treatment decreased serum levels of the pro-inflammatory marker resistin

(Fig 3A). Lower resistin levels are consistent with observed increase in the insulin sensitivity in HFD animals (Fig 2B). Since resistin has been shown to increase LDL levels [54], lowering of this marker is also consistent with the observed decreases in serum LDL cholesterol (Fig 5C).

Taken together, our study shows that TQ administration improves glucose tolerance and insulin sensitivity in the diet-induced obesity (DIO) mouse model of type 2 diabetes. Furthermore, TQ treatment has the potential to ameliorate inflammation, altered lipid profile, and weight gain associated with the diabetic and obese state. These anti-diabetic effects of TQ may be mediated by activating SIRT-1 and AMPK pathways, as shown from this study. Our results add to the existing evidence supporting the role of TQ as a natural therapeutic for the treatment of type 2 diabetes, however, further studies are necessary to establish the potential of TQ to treat type 2 diabetes in humans.

Supporting information

S1 Fig. Effect of TQ on expression of other SIRT proteins. Western blot images showing protein expression of SIRT-2, SIRT-3, SIRT-5, SIRT-6, SIRT-7, and β -actin in liver. LFD: low fat diet, HFD: high fat diet, TQ: thymoquinone. (TIF)

S2 Fig. Effect of TQ on SIRT-1 and AMPK α activation in HepG2 cells. HepG2 cells were cultured in high (20 mM) glucose or in growth media containing 5.5 mM glucose for 18 hours, starved with serum-free media for 2 hours, then pre-incubated with vehicle control (0.5% DMSO), nicotinamide (0.5 mM), compound C (20 μ M), or with nicotinamide and compound C together for 30 mins, followed by incubation with TQ (10 μ M) in the presence or absence of nicotinamide and compound C; or with TQ, resveratrol (50 μ M), or AICAR (2 mM) alone for 24 hours in 20mM glucose media. Vehicle-treated cells in 5.5 mM glucose served as control. Insulin (100 nM) was added during the last 30 min. (A) Western blot images of p-SIRT-1, SIRT-1, and β -actin. (C) Western blot images of p-AMPK α , AMPK α , and β -actin. (B and D) Protein band quantification using densitometry from three independent experiments. $p \leq 0.05$ where (*) is significantly different from 20G + TQ using independent t-tests. 5.5 G: 5.5 mM glucose, 20G: 20 mM glucose, TQ: thymoquinone, R: resveratrol, AIC: AICAR, NIC: nicotinamide, C: compound C. (TIF)

S1 File. Data for Fig 1. GraphPad file with corresponding data for Fig 1. (PZFX)

S2 File. Data for Fig 2. GraphPad file with corresponding data for Fig 2. (PZFX)

S3 File. Data for Fig 3. GraphPad file with corresponding data for Fig 3. (PZFX)

S4 File. Data for Fig 4. GraphPad file with corresponding data for Fig 4. (PZFX)

S5 File. Data for Fig 5. GraphPad file with corresponding data for Fig 5. (PZFX)

S6 File. Data for Fig 6. GraphPad file with corresponding data for Fig 6. (PZFX)

S7 File. Data for Figs 7 and 8. GraphPad file with corresponding data for Fig 7 (panels C and D) and Fig 8 (panel B).

(PZFX)

S8 File. Data for Fig 9. GraphPad file with corresponding data for Fig 9 (panel B).

(PZFX)

S9 File. Data for Fig 10. GraphPad file with corresponding data for Fig 10 (panels A and B).

(PZF)

Acknowledgments

We are forever indebted to the intellectual input of the late Prof. M. Meow, Prof. L. Dracek, and Prof. K. Rocket for their relentless support in the preparation of this manuscript.

Author Contributions

Conceptualization: Shpetim Karandrea, Angela L. Slitt, Emma A. Heart.

Data curation: Shpetim Karandrea, Huquan Yin.

Formal analysis: Shpetim Karandrea, Huquan Yin, Emma A. Heart.

Funding acquisition: Emma A. Heart.

Investigation: Shpetim Karandrea, Emma A. Heart.

Methodology: Shpetim Karandrea, Huquan Yin, Xiaomei Liang.

Project administration: Shpetim Karandrea, Angela L. Slitt.

Resources: Shpetim Karandrea, Emma A. Heart.

Supervision: Shpetim Karandrea, Angela L. Slitt, Emma A. Heart.

Validation: Shpetim Karandrea.

Visualization: Shpetim Karandrea.

Writing – original draft: Shpetim Karandrea.

Writing – review & editing: Shpetim Karandrea, Emma A. Heart.

References

1. Kahn SE, Cooper ME, Del Prato S (2014) Pathophysiology and treatment of type 2 diabetes: perspectives on the past, present, and future. *Lancet* 383: 1068–1083. [https://doi.org/10.1016/S0140-6736\(13\)62154-6](https://doi.org/10.1016/S0140-6736(13)62154-6) PMID: 24315620
2. Bergman RN (2005) Minimal model: perspective from 2005. *Horm Res* 64: 8–15. <https://doi.org/10.1159/000089312> PMID: 16439839
3. Fu Z, Gilbert ER, Liu D (2013) Regulation of insulin synthesis and secretion and pancreatic Beta-cell dysfunction in diabetes. *Curr Diabetes Rev* 9: 25–53. PMID: 22974359
4. Ali BH, Blunden G (2003) Pharmacological and toxicological properties of *Nigella sativa*. *Phytother Res* 17: 299–305. <https://doi.org/10.1002/ptr.1309> PMID: 12722128
5. Le PM, Benhaddou-Andaloussi A, Elimadi A, Settaf A, Cherrah Y, Haddad PS (2004) The petroleum ether extract of *Nigella sativa* exerts lipid-lowering and insulin-sensitizing actions in the rat. *J Ethnopharmacol* 94: 251–259. <https://doi.org/10.1016/j.jep.2004.04.030> PMID: 15325727
6. Rchid H, Chevassus H, Nmila R, Guiral C, Petit P, Chokaïri M, et al. (2004) *Nigella sativa* seed extracts enhance glucose-induced insulin release from rat-isolated Langerhans islets. *Fundam Clin Pharmacol* 18: 525–529. <https://doi.org/10.1111/j.1472-8206.2004.00275.x> PMID: 15482373

7. Fararh KM, Shimizu Y, Shiina T, Nikami H, Ghanem MM, Takewaki T (2005) Thymoquinone reduces hepatic glucose production in diabetic hamsters. *Res Vet Sci* 79: 219–223. <https://doi.org/10.1016/j.rvsc.2005.01.001> PMID: 16054891
8. Sankaranarayanan C, Pari L (2011) Thymoquinone ameliorates chemical induced oxidative stress and β -cell damage in experimental hyperglycemic rats. *Chem Biol Interact* 190: 148–154. <https://doi.org/10.1016/j.cbi.2011.02.029> PMID: 21382363
9. Heart E, Palo M, Womack T, Smith PJ, Gray JP (2012) The level of menadione redox-cycling in pancreatic beta-cells is proportional to the glucose concentration: role of NADH and consequences for insulin secretion. *Toxicol Appl Pharmacol* 258: 216–25. <https://doi.org/10.1016/j.taap.2011.11.002> PMID: 22115979
10. Gray JP, Karandrea S, Burgos DZ, Jaiswal AA, Heart EA (2016) NAD(P)H-dependent quinone oxidoreductase 1 (NQO1) and cytochrome P450 oxidoreductase (CYP450OR) differentially regulate menadione-mediated alterations in redox status, survival and metabolism in pancreatic β -cells. *Toxicol Lett* 262: 1–11. <https://doi.org/10.1016/j.toxlet.2016.08.021> PMID: 27558805
11. Gray JP, Burgos DZ, Yuan T, Seeram N, Rebar R, Follmer R, et al. (2016) Thymoquinone, a bioactive component of *Nigella sativa*, normalizes insulin secretion from pancreatic β -cells under glucose overload via regulation of malonyl-CoA. *Am J Physiol Endocrinol Metab* 310: E394–E404. <https://doi.org/10.1152/ajpendo.00250.2015> PMID: 26786775
12. Berger F, Ramirez-Hernandez MH, Ziegler M (2004) The new life of a centenarian: signaling functions of NAD (P). *Trends Biochem Sci* 29: 111–118. <https://doi.org/10.1016/j.tibs.2004.01.007> PMID: 15003268
13. Pollak N, Dölle C, Ziegler M (2007) The power to reduce: pyridine nucleotides—small molecules with a multitude of functions. *Biochem J* 402: 205–218. <https://doi.org/10.1042/BJ20061638> PMID: 17295611
14. Wu J, Jin Z, Zheng H, Yan LJ (2016) Sources and implications of NADH/NAD⁺ redox imbalance in diabetes and its complications. *Diabetes Metab Syndr Obes* 9: 145–153. <https://doi.org/10.2147/DMSO.S106087> PMID: 27274295
15. Kitada M, Koya D (2013) SIRT1 in type 2 diabetes: mechanisms and therapeutic potential. *Diabetes Metab J* 37: 315–325. <https://doi.org/10.4093/dmj.2013.37.5.315> PMID: 24199159
16. Pari L, Sankaranarayanan C (2009) Beneficial effects of thymoquinone on hepatic key enzymes in streptozotocin—nicotinamide induced diabetic rats. *Life Sci* 85: 830–834. <https://doi.org/10.1016/j.lfs.2009.10.021> PMID: 19903489
17. Al-Ali A, Alkhwajah AA, Randhawa MA, Shaikh NA (2008) Oral and intraperitoneal LD50 of thymoquinone, an active principle of *Nigella sativa*, in mice and rats. *J Ayub Med Coll Abbottabad*, 20: 25–27. PMID: 19385451
18. Zhu D, Wang Y, Du Q, Liu Z, Liu X (2015) Cichoric acid reverses insulin resistance and suppresses inflammatory responses in the glucosamine-induced HepG2 cells. *J Agric Food Chem* 63: 10903–10913. <https://doi.org/10.1021/acs.jafc.5b04533> PMID: 26592089
19. Zhu D, Zhang N, Zhou X, Zhang M, Liu Z, Liu X (2017) Cichoric acid regulates the hepatic glucose homeostasis via AMPK pathway and activates the antioxidant response in high glucose-induced hepatocyte injury. *RSC Adv*, 7: 1363–1375.
20. Neter J, Kutner MH, Nachtsheim CJ, Wasserman W (1996) In: *Applied linear statistical models*, edited by Neter J. Chicago, IL: Irwin; 1992.
21. Wright SP (1992) Adjusted p-values for simultaneous inference. *Biometrics* 48: 1005–1013. <https://doi.org/10.2307/2532694>
22. Petro AE, Cotter J, Cooper DA, Peters JC, Surwit SJ, Surwit RS (2004) Fat, carbohydrate, and calories in the development of diabetes and obesity in the C57BL/6J mouse. *Metabolism* 53: 454–457. PMID: 15045691
23. Srinivasan K, Ramarao P (2007) Animal models in type 2 diabetes research: an overview. *Indian J Med Res* 125: 451–472. PMID: 17496368
24. Dula SB, Jecmenica M, Wu R, Jahanshahi P, Verrilli GM, Carter JD, et al. (2010) Evidence that low-grade systemic inflammation can induce islet dysfunction as measured by impaired calcium handling. *Cell Calcium* 48: 133–142. <https://doi.org/10.1016/j.ceca.2010.07.007> PMID: 20800281
25. Lumeng CN, Saltiel AR (2011) Inflammatory links between obesity and metabolic disease. *J Clin Invest* 121: 2111–2117. <https://doi.org/10.1172/JCI57132> PMID: 21633179
26. Stepan CM, Bailey ST, Bhat S, Brown EJ, Banerjee RR, Wright CM, et al. (2001) The hormone resistin links obesity to diabetes. *Nature* 409: 307–312. <https://doi.org/10.1038/35053000> PMID: 11201732
27. Rodríguez IM, García JO, Sánchez JJA, González DA, Coello SD, Díaz BB, et al. (2016) Lipid and inflammatory biomarker profiles in early insulin resistance. *Acta Diabetol* 1–9. <https://doi.org/10.1007/s00592-016-0885-6> PMID: 27432443

28. Santilli F, Liani R, Di Fulvio P, Formoso G, Simeone P, Tripaldi R, et al. (2016) Increased circulating resistin is associated with insulin resistance, oxidative stress and platelet activation in type 2 diabetes mellitus. *Thromb Haemost* 116: 1089–1099. <https://doi.org/10.1160/TH16-06-0471> PMID: 27709225
29. Tateya S, Tamori Y, Kawaguchi T, Kanda H, Kasuga M (2010) An increase in the circulating concentration of monocyte chemoattractant protein-1 elicits systemic insulin resistance irrespective of adipose tissue inflammation in mice. *Endocrinology* 151: 971–979. <https://doi.org/10.1210/en.2009-0926> PMID: 20056828
30. Nomura S, Shouzu A, Omoto S, Nishikawa M, Fukuhara S (2000) Significance of chemokines and activated platelets in patients with diabetes. *Clin Exp Immunol* 121: 437–443. <https://doi.org/10.1046/j.1365-2249.2000.01324.x> PMID: 10971508
31. Piemonti L, Calori G, Lattuada G, Mercalli A, Ragogna F, Garancini MP, et al. (2009) Association between plasma monocyte chemoattractant protein-1 concentration and cardiovascular disease mortality in middle-aged diabetic and nondiabetic individuals. *Diabetes Care* 32: 2105–2110. <https://doi.org/10.2337/dc09-0763> PMID: 19641159
32. Zietz B, Büchler C, Herfarth H, Müller-Ladner U, Spiegel D, Schölmerich J, Schäffler A (2005) Caucasian patients with type 2 diabetes mellitus have elevated levels of monocyte chemoattractant protein-1 that are not influenced by the $-2518 A \rightarrow G$ promoter polymorphism. *Diabetes Obes Metab* 7: 570–578. <https://doi.org/10.1111/j.1463-1326.2004.00436.x> PMID: 16050950
33. Mooradian AD (2009) Dyslipidemia in type 2 diabetes mellitus. *Nat Clin Pract Endocrinol Metab* 5: 150–159. <https://doi.org/10.1038/ncpendmet1066> PMID: 19229235
34. Michishita E, Park JY, Burneskis JM, Barrett JC, Horikawa I (2005) Evolutionarily conserved and non-conserved cellular localizations and functions of human SIRT proteins. *Mol Biol Cell* 16: 4623–4635. <https://doi.org/10.1091/mbc.E05-01-0033> PMID: 16079181
35. Muoio DM, Newgard CB (2008) Molecular and metabolic mechanisms of insulin resistance and β -cell failure in type 2 diabetes. *Nat Rev Mol Cell Biol* 9: 193–205. <https://doi.org/10.1038/nrm2327>
36. Tanti JF, Jager J (2009) Cellular mechanisms of insulin resistance: role of stress-regulated serine kinases and insulin receptor substrates (IRS) serine phosphorylation. *Curr Opin Pharmacol* 9: 753–762. <https://doi.org/10.1016/j.coph.2009.07.004> PMID: 19683471
37. Dinkova-Kostova AT, Talalay P (2010) NAD(P)H:quinone acceptor oxidoreductase 1 (NQO1), a multifunctional antioxidant enzyme and exceptionally versatile cytoprotector. *Arch Biochem Biophys* 501: 116–123. <https://doi.org/10.1016/j.abb.2010.03.019> PMID: 20361926
38. Gaikwad A, Long DJ, Stringer JL, Jaiswal AK (2001) In vivo role of NAD(P)H: quinone oxidoreductase 1 (NQO1) in the regulation of intracellular redox state and accumulation of abdominal adipose tissue. *J Biol Chem* 276: 22559–22564. <https://doi.org/10.1074/jbc.M101053200> PMID: 11309386
39. Alkharfy KM, Ahmad A, Khan RM, Al-Shagha WM (2015) Pharmacokinetic plasma behaviors of intravenous and oral bioavailability of thymoquinone in a rabbit model. *Eur J Drug Metab Pharmacokinet* 40: 319–323. <https://doi.org/10.1007/s13318-014-0207-8> PMID: 24924310
40. Elmowafy M, Samy A, Raslan MA, Salama A, Said RA, Abdelaziz AE, El-Eraky W, El Awdan S, Viitala T (2016) Enhancement of bioavailability and pharmacodynamic effects of thymoquinone via nanostructured lipid carrier (NLC) formulation. *AAPS PharmSciTech*, 17: 663–672. <https://doi.org/10.1208/s12249-015-0391-0> PMID: 26304932
41. Ido Y (2007) Pyridine nucleotide redox abnormalities in diabetes. *Antioxid Redox Signal* 9: 931–942. <https://doi.org/10.1089/ars.2007.1630> PMID: 17508915
42. Yan LJ (2014) Pathogenesis of chronic hyperglycemia: from reductive stress to oxidative stress. *J Diabetes Res* <https://doi.org/10.1155/2014/137919> PMID: 25019091
43. Luo X, Li R, Yan LJ (2015) Roles of pyruvate, NADH, and mitochondrial complex I in redox balance and imbalance in β cell function and dysfunction. *J Diabetes Res*. <https://doi.org/10.1155/2015/512618> PMID: 26568959
44. Khader M, Bresgen N, Eckl PM (2009) In vitro toxicological properties of thymoquinone. *Food Chem Toxicol* 47: 129–133. <https://doi.org/10.1016/j.fct.2008.10.019> PMID: 19010375
45. Krauss RM, Siri PW (2004) Dyslipidemia in type 2 diabetes. *Med Clin North Am* 88: 897–909. <https://doi.org/10.1016/j.mcna.2004.04.004> PMID: 15308384
46. Taskinen MR (2003) Diabetic dyslipidaemia: from basic research to clinical practice. *Diabetologia* 46: 733–749. <https://doi.org/10.1007/s00125-003-1111-y> PMID: 12774165
47. Bordone L, Motta MC, Picard F, Robinson A, Jhala US, Apfeld J, et al. (2005) Sirt1 regulates insulin secretion by repressing UCP2 in pancreatic β cells. *PLoS Biol* 4: e31. <https://doi.org/10.1371/journal.pbio.0040031> PMID: 16366736

48. Sun C, Zhang F, Ge X, Yan T, Chen X, Shi X, et al. (2007) SIRT1 improves insulin sensitivity under insulin-resistant conditions by repressing PTP1B. *Cell Metab* 6: 307–319. <https://doi.org/10.1016/j.cmet.2007.08.014> PMID: 17908559
49. Zhang J (2007) The direct involvement of SirT1 in insulin-induced insulin receptor substrate-2 tyrosine phosphorylation. *J Biol Chem* 282: 34356–34364. <https://doi.org/10.1074/jbc.M706644200> PMID: 17901049
50. Ruderman NB, Xu XJ, Nelson L, Cacicedo JM, Saha AK, Lan F, et al. (2010) AMPK and SIRT1: a long-standing partnership? *Am J Physiol Endocrinol Metab* 298: E751–E760. <https://doi.org/10.1152/ajpendo.00745.2009> PMID: 20103737
51. Coughlan KA, Valentine RJ, Ruderman NB, Saha AK (2014) AMPK activation: a therapeutic target for type 2 diabetes? *Diabetes Metab Syndr Obes* 7: 241–253. <https://doi.org/10.2147/DMSO.S43731> PMID: 25018645
52. Shoelson SE, Lee J, Goldfine AB (2006) Inflammation and insulin resistance. *J Clin Invest* 116: 1793–1801. <https://doi.org/10.1172/JCI29069> PMID: 16823477
53. Yoshizaki T, Schenk S, Imamura T, Babendure JL, Sonoda N, Bae EJ, et al. (2010) SIRT1 inhibits inflammatory pathways in macrophages and modulates insulin sensitivity. *Am J Physiol Endocrinol Metab* 298: E419–E428. <https://doi.org/10.1152/ajpendo.00417.2009> PMID: 19996381
54. Rashid S (2013) Mechanisms by which elevated resistin levels accelerate atherosclerotic cardiovascular disease. *Rheumatol Curr Res* 3: 115. <https://doi.org/10.4172/2161-1149.1000115>